UNIVERSITA' DEGLI STUDI DI MILANO

Department of Pharmaceutical Sciences

Doctoral School in Pharmaceutical Sciences

PhD – Cycle the 36th

INTEGRATED AND SUSTAINABLE STRATEGY FOR THE INVESTIGATION AND VALORIZATION OF EXTRA VIRGIN OLIVE OIL EXTRACTS AND BY-PRODUCTS

Sector CHIM/10 – Food chemistry

Dr. Martina BARTOLOMEI

Matr. R12818

Faculty advisor: Prof. Carmen Lammi

PhD coordinator: Prof. Giulio Vistoli

ACADEMIC YEAR
2022/2023

Aim of the thesis

Aim of the thesis

Motivations and outlines of the PhD thesis

Nutrition allows to ensure the intake of energy and nutrients that guarantee growth, development, and good health. The attention in human nutrition and the consumption of foods that can improve health or prevent the onset of disease has grown significantly. A group of essential components of the human diet are the bioactive molecules present in plant foods. Among them, polyphenols have received considerable attention from the scientific community for their potential protective role against several complex diseases. Between naturally polyphenol-rich foods, extra virgin olive oil (EVOO) is especially studied and characterized. In addition to their antioxidant power, they shown a cardioprotective role, considering their ability to protection of low-density lipoproteins (LDL) against oxidative stress, to reduce the triglycerides and to maintain the normal blood high density lipoproteins (HDL) cholesterol concentrations. The promising beneficial effects of olive oil polyphenols are heavily affected by the degree of bioavailability of these molecules. Furthermore, polyphenol metabolism studies focus on the absorption of single compounds and not on assessing the behavior of a complex mixture. For example, it is known that some polyphenols present in olive oil, such as hydroxytyrosol and tyrosol, are well absorbed and metabolized leading to the formation of metabolites with different biological activities and bioavailability.

In the field of nutrition, protein hydrolysates derived from foods are increasingly used. Hydrolyzed proteins are suggested to reduce the risk that consuming proteins in their original form could trigger allergies (such as allergy to milk) and are more tolerated at the gastrointestinal level. Hydrolysates may contain bioactive peptides, which are protein fragments showing beneficial effects on human health i.e. antioxidant, hypocholesterolemic, anticoagulant, antimicrobial, hypotensive, anti-inflammatory, antitumor activity. Given the constant growth of the population and the excessive consumption of resources, the demand for low-cost proteins and peptides, obtained by considering environmental sustainability, is rapidly increasing. In addition to the population, the production of waste has grown rapidly with consequent damage to the ecosystem. Therefore, a recycling/reuse outlook is needed to allow for the decrease of the quantity of waste generated and the related socio-economic costs. The introduction of the circular economy which aims to recover materials directly from waste and by-products to re-enter then in a new production cycle could be a solution to the problem. In the Mediterranean area, olives and olive oil by-products have a substantial

consequence for the environment. Olive and olive oil by-products such as pomace, leaves, stones and oil vegetation water can be fostered.

Based on these considerations, the aim of my PhD thesis was to assess the antioxidant activity and intestinal trans-epithelial transport of extra virgin olive oil phenolic extract using *in vitro* and cellular techniques. Furthermore, a purpose of my thesis was the use of sustainable strategies that allow the valorization of by-products of the olive and oil supply chain to obtain products with high added value. To achieve this objective, the hypocholesterolemic properties of olive-vegetation water polyphenols complex was evaluated using biochemical and cellular tools. Additionally, the protein from olive seeds by-product were extracted, deeply characterized, and use to obtain protein hydrolysates by enzymatic reactions. These hydrolysates were further investigated using multidisciplinary approaches involving peptidomic techniques to profile the peptide sequences and *in vitro* and cellular techniques to assess their bioactivities.

The thesis includes three parts:

Part I introduces the state of the art about olive oil composition, production, and valorization of EVOO extracts and by-products. **Chapter 1** reports olive oil composition and production. Numerous works of literature highlight the health benefits of its consumption and a more sustainable olive oil production involves eco-friendly agricultural practices, efficient management of resources and waste, thus helping to ensure a healthy source of oil while respecting the environment. **Chapter 2** states the biological properties, absorption mechanisms and bioavailability of olive polyphenols. **Chapter 3** explains the production, bioactivity, and bioavailability of by-products peptides.

Part II presents my scientific contributions in the PhD period, which contains two cases, including the assessment of the antioxidant effect and intestinal transepithelial transport of EVOO extracts, in addition to the assessment of hypocholesterolemic properties of olive by-products polyphenolic complex derived from olive oil vegetation water (**Case I**) and the characterization and investigation of olive seed peptides bioactivities and intestinal transepithelial transport (**Case II**).

Case I: EVOO and OVW polyphenolic extracts

Chapter 4 focus on the trans-epithelial transport and biological activity assessment of BUO, an EVOO phenolic extract obtain from a Tuscany oil, cultivar *Frantoio*. This work demonstrated: i) the characterization of its antioxidant properties, both *in vitro* at

the cellular level in human hepatic HepG2 and human intestinal Caco-2 cells; ii) the intestinal transport of the different phenolic components of the phytocomplex; iii) the *in vitro* and cellular modulation of dipeptidyl peptidase 4 activity. The results allowed to gain further knowledge on the molecular mechanisms underlying the beneficial effects of the polyphenols contained in EVOO and they suggest a role played not only by single phenolic compounds, but by the entire pool of secoiridoids molecules. Furthermore, the results demonstrated that Ole derivatives are selectively transported by differentiated Caco-2 cells. **Chapter 5** focuses on the characterization of the cholesterol-lowering properties of a polyphenolic phytocomplex, obtained in collaboration with an olive oil company, derived from the olive oil vegetation water. This work assessed: i) the modulation of LDLR and PCSK9 pathways *in vitro*, at cellular level and *in vivo*; ii) the direct antioxidant activity; iii) the lipid profiles modulation in western diet-fed mice. The findings showed that the phytocomplex could be used as a novel ingredient in functional foods and/or nutraceuticals intended to prevent cardiovascular disease.

Case II: olive seed peptides

Chapter 6 focus on the extraction and characterization of proteins for *Olea europaea* L. seeds to produce two protein hydrolysates using alcalase and papain enzymes. This work evaluated: i) the peptidomic analysis of medium- and short-sized peptides present in the hydrolysates and *in silico* assessment of their potential bioactivities; ii) the characterization of the antioxidant properties *in vitro* and at cellular levels in HepG2 and Caco-2 cells; iii) the DPP-IV inhibitory activity and stimulation of release and stability of GLP-1 hormone; iv) the dual hypocholesterolemic activity inhibiting the activity of HMGCoAR and impairing the PPI of PCSK9/LDLR and modulation of the LDLR pathway; v) the intestinal transport by differentiated human intestinal Caco-2 cells. Based on these results, olive seed hydrolysates may represent new ingredients with antioxidant and anti-diabetic properties for the development of nutraceuticals and functional foods for the prevention of metabolic syndrome onset, promoting the principles of environmental sustainability.

Part I.

State of the art

CHAPTER 1

1. Introduction

1.1 Olea europaea

Olive europaea belongs to the family of Oleaceae and is a small evergreen tree, with a height between 3 and 12 meters. It is a slow growing plant, with dark green leaves on the upper side and silvery underneath, they are about 5-6 cm long and 1-1.5 cm wide at the middle [1]. It is possible to find *Olea europaea* in nature as a spontaneous element of the vegetation, but it is also an important crop and for this reason it constitutes an economically relevant species of Mediterranean agriculture. Nowadays, the olive tree is mainly used for oil and fruit production, nonetheless it's used to produce therapeutic and cosmetic products. The wild form of the olive tree (*Olea europea subspecies europea var. sylvestris*) is the ancestor of the cultivated olive tree (*subspecies europea var. europea*) [2]. The plant is native to the Mediterranean coasts, particularly in Italy, Spain, France, Greece, and Turkey. 95% of the total olive fields cultivated worldwide are in the Mediterranean basin, where the olive cultivation areas cover a total of 12,000 hectares of land [3]. Two significant factors influencing olive tree productivity are flowering and fruit set. Olive flowers are distinguished by both hermaphroditic flowers and male flowers on the same plant, a condition called andromonoecy. The production of staminate flowers, which are unable to produce fruit, rather than hermaphrodites is one of the major reasons limiting fruit set in olive tree. Depending on the available resources, the plant activates an adaptive mechanism that allows it to balance the fruit load through flowering and fruit setting [4,5]. High productivity is guaranteed by a high number of flower buds and a sufficient rate of good quality flowers. Environmental factors such as the availability of water and the winter cold also affect productivity. Olive trees have a two years cycle, therefore a generous olive harvest one year is followed by a scarcity the next [6]. The most worthwhile trees, such as those with high fruit set, larger fruit and higher oil content were selected by vegetative propagation for their domestication. The widespread diffusion of olive growing has resulted in a mixture of feral and wild forms in many Mediterranean habitats [7].

Figure 1. Olive tree, fruits, and flowers.

Worldwide there are more than 2000 olive tree *cultivars*. A *cultivar* is a type of cultivated plant that has been selected for interesting traits that are retained by vegetative propagation. The complete name of an olive tree includes the botanical Latin scientific name continued by a *cultivar* epithet, generally in the language of the country where the olive tree was first selected and cultivated, e.g. *Olea europaea sativa* cultivar Moraiolo. Wild subspecies are called *oleaster* and do not have further *cultivar* specification. Obtaining new olive varieties through genetic methods (crosses, mutagens, etc.) is complex as the existing olive genetic heritage is stable and it is for this reason that very ancient *cultivars* are still cultivated today. To date, all the *cultivars* have not yet been identified, but progress is being made thanks to the use of molecular biology. **Table 1** shows some of the most common *cultivars* in the three major growing countries.

Country	Olive Oil production (tonnes)	N° cultivars	Cultivars
Spain	1 232 246,95	262	*Picual, Cornicabra, Hojiblanca, Manzanilla de Sevilla, Arbequina, Morisca de Badajoz, Empeltre, Manzanilla Cacereña, Lechin de Sevilla, Picudo*
Italy	500 285,10	538	*Coratina, Ogliarola salentina, Cellina di Nardò, Carolea, Frantoio, Leccino, Ogliarola barese, Moraiolo, Bosana, Cima di Mola*
Greece	326 664,93	52	*Koroneiki, Kalamata, Mastoidis*

Table 1. Olive tree *cultivars*. The three major olive-producing countries in the table are listed according to the quantities of olive oil produced calculated as the average of the 2001-2021 period. Data processed from FAO sources (http://faostat.fao.org/site/339/default.aspx) and the *World Catalogue of Olive Varieties* by the International Olive Council.

1.1.1 Olive Drupe

The olive is a drupe, botanically like other stone fruits. The drupe presents three pericarp sections structure including of an outer epicarp called *exocarp* or skin, a pulpy

mesocarp, which represents the 70-80% of the weight, and a hard, stony *endocarp* which surrounds the seed (Figure 2). Compared to other drupes it contains way less sugar (2-5%) content and an elevated concentration of oil [8]. Depending on the *cultivar* and growing conditions, drupe size and shape differ significantly, with a weight at physiological maturity changing from 1.5 to 4.5 g and generally falls between 3 and 10 g. The principal components of olive flesh are water (60-75%) and lipids (10-25%). The fruit additionally includes appreciable amounts of flavonoids and anthocyanins [9].

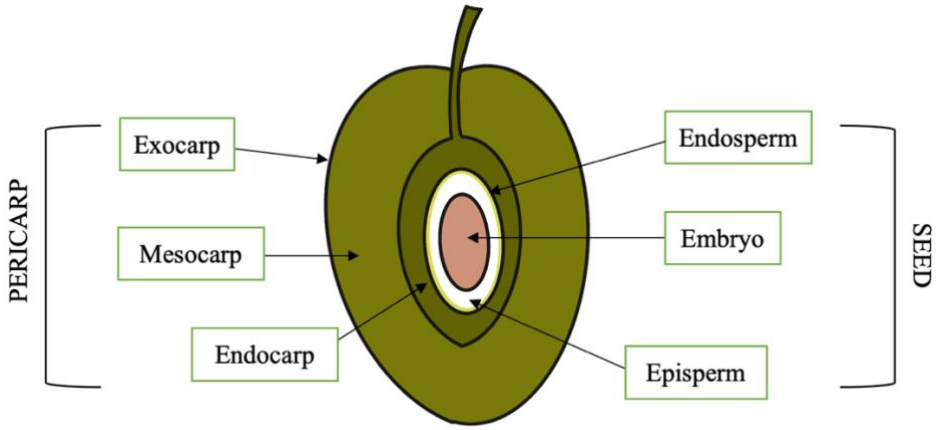

Figure 2. Structure of olive drupe.

Olive fruit growth lasts for 4-5 months and from fertilization to full black ripening, five stages of fruit development are observed: (i) fertilization and fruit set, from flowering to about 30 days after, when cells divide rapidly to support embryo's growth, (ii) seed development, a stage of intense cell division and enlargement that primarily involves growth and development of the endocarp, (iii) seed hardening, when the endocarp cells stop dividing and become sclerified, (iv) mesocarp development, mainly delineated by the expansion of pre-existing flesh cells, and oil accumulation, and (v) ripening, when the fruit changes from dark lime green to lighter green/purple and gets a softener texture. Indeed, the ripening is linked with significant changes in the cell wall structure that cause a texture changes and loss of firmness due to enzymatic degradation of cell wall. Chemically, the ripening of the olive is associated with a sugar content reduction in the fruit and with the accumulation of various aromatic compounds, in particular alcohols and terpenes [10,11]. The potential amount of oil accumulated in the fruit at the time of harvesting is determined by the variety but presents a strong variability depending on the growing conditions, age, climate, locality, and fruit load [12]. Economically, the optimal time for oil production is at the end of the oil accumulation period, when the

olive pulp has an ideal fatty acid balance, both from the dietary and oxidative stability point of view, as well as the highest antiradical power due to the high amounts of total phenols and tocopherols. A late harvest can support fruit loss and a reduction in quality, without a significant gain in oil quality [13].

1.2 Olive Oil

Within the drupe, the oil is found mainly in the mesocarp within vacuoles. Since the mesocarp represents about 70%-80% of the total weight of the drupe, olive oil essentially originates from the coalescence of vacuolar oil droplets. Olives contain 20% oil which is extracted by mechanical crushing combined with heat and/or solvent. Olive oils are classified according to a specific scale. The best oil is the product of the first crushing, where is applied a mechanical process and is avoided the heating phase; for this reason, it is as known as “cold crushed oil”. Each subsequent crushing produces lower quality oil, which generally needs to be refined to improve its flavor and storage capacity. The oil produced from the first crushing is called "Extra Virgin" olive oil (EVOO) and is obtained from ripe olives with low acidity (up to 0.8%), contains fewer impurities and does not require refining. The nutritional properties are also preserved. Even the "Virgin" olive oil (VOO) is obtained from the first crushing, but a hot process is employed. Finally, the "Refined" olive oil (ROO) is obtained by refining VOO and “Olive Oil” is the oil consisting of a blend of ROO and VOO [14–16]. Olive oil can also be extracted from the paste obtained after the first crushing (pomace) using a solvent. To protect its quality, each batch of oil produced and sold in Europe must comply with strict parameters established by the European Community (EUR-Lex, Regulation 2568/91, https://eur-lex.europa.eu/eli/reg/1991/2568/oj). The composition of the oil can change depending on the extraction method and the *cultivar*, but it can be divided into a saponifiable (98% of total weight) and unsaponifiable fraction (at least 1% of total weight) [17].

1.2.1 Saponifiable Fraction

The saponifiable fraction is formed predominantly by oleic acid (ω-9, 63-83%) and other saturated and unsaturated acids including palmitic acid (7-17%), stearic acid (1.5-5%), arachidic acid (0-0.6%), palmitoleic acid (0.3-3%), linoleic acid (ω-6, 3-14%) and α-linolenic acid (ω-3, less than 1.5%) (Figure 3). Because the level of saturated fatty acid content is generally below 10%, olive oil meets current dietary advice in terms of

minimal saturated fatty acid intake. The presence of elevated quantity of MUFAs provides oxidative resistance to olive oil, contributing to its antioxidant properties, high stability, and a long shelf life. For this reason, the elevated content of MUFAs was considered the major responsible for the protective effects of EVOO. Oleic acid reduces the formation of pro-inflammatory molecules making cells less susceptible to oxidation [17–19]. Additionally, its lipid profile and high ω6/ω3 ratio have been associated with the prevention of autoimmune, thrombotic and inflammatory diseases [20,21].

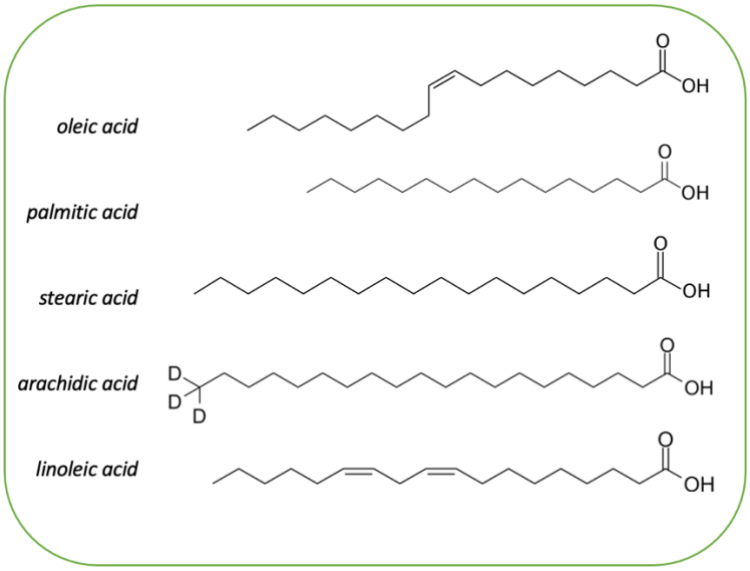

Figure 3. Major monounsaturated, polyunsaturated, and saturated fatty acids in olive oil.

1.2.2 Unsaponifiable Fraction

Even if the unsaponifiable portion represents only 1% of the oil composition, it is strongly responsible for the beneficial effect of olive oil. The 30-50% of the total weight of the unsaponifiable fraction is composed of hydrocarbons and squalene is the most abundant. Squalene possesses antioxidant properties by acting as singlet oxygen scavenger and protect cells from lipid peroxidation [22–24]. Squalene has anticancer activity and is active against several types of cancer. Experimental studies on rodents have shown that it can inhibit chemically induced skin, colon and lung tumorigenesis [25]. Another class of active molecules that are found in the unsaponifiable fraction are tocopherols and α-tocopherol is the most abundant isoform in EVOO (90%-95%). Tocopherols inhibit oxidation of cell membranes and exert radical scavenging activity [26]. Moreover, tocopherol has an major role regarding cardiovascular disorders, since it is capable of decrease the aggregation processes of platelets, with consequential reduction of emboli, plaques and thrombi in the arteries [27]. Phytosterols are a relevant

component of the unsaponifiable fraction of olive oil known for their ability to lower the low density lipoprotein (LDL) cholesterol reducing the onset of cardiovascular disease [28,29]. The most representative sterol in olive oil is β-sitosterol (75-90% of total sterols), which is being studied for its antioxidant and anticarcinogenic capacities [30,31]. Finally, one of the most studied elements of the unsaponifiable fraction are phenolic compounds, which guarantee the EVOO high antioxidant potential.

1.3 Olive oil production

The oldest traces of olive oil were found in Haifa (Israel), and date back to the 5th millennium BC [32,33]. The first techniques for producing and preserving olive oil were created by the Greeks and Romans: techniques that have remained unchanged for centuries. The diffusion of the plant is mainly due to these two populations who exported it during the expansion of their empires [34]. The oil extracted from the fruits of this plant was in fact used in ancient times for various purposes such as religious ones, during rituals, for lighting with oil lamps, for cosmetic and medical applications. Olives were found in Egyptian tombs (2000 years BC) where they represent eternal life and fertility, they are mentioned in Greek legends in which the goddess Athena produces the olive plant to obtain possession of the city of Athens and the olive leaves crown the heads of Greek and Roman victorious athletes, generals, and sovereign. The first to cultivate the olive tree not only for the fruit, but also to extract oil to use as a condiment in the diet were the Romans. Olive oil thus became one of the hubs of the Roman economy, as demonstrated by the existence of the "arca olearia" a sort of olive oil commodity exchange [35]. Nowadays, olive oil is mainly produced in the Mediterranean basin where the greatest climatic conditions are found for the development of the plant. More than 3.3 million olive growers are present in the Mediterranean regions, where in fact 97% of the total olive oil is produced. The average annual production is over 3 million tons of olive oil and Spain is the largest producer [36,37]. Currently olive oil is mainly produced using a traditional pressing process, to maintain its natural organoleptic characteristics, and with two- and three-phase centrifugation systems according to the European Commission Regulation No. 1513/2001. Initially the olives are washed, to avoid the accumulation of vegetable waste and to remove any foreign bodies such as residues of soil or sand, and then crushed to allow the release of the oil from the mesocarp obtaining a homogeneous paste. This is one of the most crucial steps that influences EVOO chemical profile. In fact, phenolic

compounds are generated and transformed by a number of activatable enzymes during the crushing of olives [38]. The next step is the malaxation where, from the paste generated during the crushing, the oil is separated. During this step further notable changes occur in the chemical composition of the oil and determines the quality and composition of the final product. In details, a stainless-steel apparatus consisting of a semicylindrical vat with a horizontal shaft, rotating arms, and variously shaped and sized blades is used to malax olive paste. Following this steps, different techniques can be applied to extract oil from the solids and fruit-water such as pressing and centrifugation [39,40]. The centrifugation can occur applying the combination of two different systems: horizontal centrifugation (three- and two-phase decanter) and vertical centrifugation. Precisely, while the horizontal centrifugation using three-phase decanter demands warm water addition to dilute the olive paste to facilitate the separation, the two-phase decanter uses "no-water" centrifugation to separate the oily phase from malaxed pastes [41]. Therefore, the balance between the volume of water added and a good separation phase determines the optimum strategy to decrease the loss of phenolic compounds during both horizontal and vertical centrifugation. Due to the low lipophilic behavior of the phenolic structures, which resulted in a low concentration in EVOO, the most significant losses of the various phenolic groups contained in olive paste occur in the aqueous phase and solid phase (wet pomace). On the other hand, a low phenolic content in some EVOOs might enhance their sensory appeal and therefore it is a desired step [42]. This enormous production has a significant environmental impact due to the generation of high quantities of organic waste that may have a significant effect on land and water environments considering of their high phytotoxicity. The vast number of byproducts have been documented in the literature based on extraction, filtration, and storage methods.

1.3.1 Circular economy in olive oil industry

In the last decade, besides to the concept of sustainability, that of the circular economy has spread which, in addition to improving the efficiency of resources and the recovery of materials, encourages the development of new industrial processes for more efficient use and redevelopment/valorization of materials and products. Sustainability in the production process can improve water resource management, promote eco-friendly agricultural practices, and preserve biodiversity. Investing in the sustainability of olive oil is crucial to ensuring its long-term availability. Indeed, regarding the production of

olive oil, pesticide, fertilizer and water usage are impactful components of the pharming phase; by-products as olive pomace (OP), olive mill wastewater known as olive vegetation-water (OVW) and olive stones (OS) are generated during olive oil processing; wood, leaves and branches are produced during olive pruning [32]. The most abundant liquid by-product is OVW while the solid one is OP, however, the use of modern two-phase processing method without the addition of water, generate a new by-product that consists of a mixture of solid and liquid waste. Finally, cakes obtained after EVOO filtration and storage make up additional solid olive oil by-products [43]. According to estimates, pruning results in 25 kg of by-products per tree per year, and for every 100 kg of treated olives, the olive oil industry generates 35 kg of solid waste and 1001 kg of liquid waste [44]. Current waste management causes economic and environmental damage. However, olive waste and by-products can be valorized into new and higher value-added products, to achieve more sustainable and profitable production in the olive oil sector, encouraging the implementation of "Transforming our world: the Agenda 2030 for sustainable development". Furthermore, the transition from the linear to the circular economy requires a permanent structural change through multiple production cycles, representing a new opportunity also for seasonal sectors such as olive oil production generating a constant profit [45]. Currently, by-products and biomass are mainly used to produce energy or compost. This "recovery" represents 80% of the total by-product use. The residual biomass obtained after the pruning phase (leaves and branches) is used only in small amounts to directly generate electrical or thermal energy, while it is primarily transformed into pellets for industrial or domestic heating [46–48]. The direct combustion of biomass to generate electricity is an already consolidated sector and the use of OSs as biofuel for heating is fully widespread [49]. As for OVW and OP pre-treatments are necessary to reduce their phytotoxic power [50]. The OVW is a dark liquid which contain olive pulp and oil, mucilage, pectin, and more suspended molecules within a stable emulsion [51]. As might be expected, the chemical composition varies based on olive *cultivars*, growth methods, harvesting time, and particularly the technology employed in oil extraction, however it exhibits a range of distinct characteristics, including elevated levels of organic pollutants, acidic pH, elevated electrical conductivity, and high phenolic content [52,53]. Notably, OVW are the most pollutant and phytotoxic by-products, since during the extraction nearly all the phenolic content of the olive fruit (~98%) stays in the olive mill by-products. Indeed, the elevated phenolic nature of OVW and its organic contents make it extremely

resistant to biodegradation. In fact, the disposal or composting of OVW presents a high management cost for mills. Nevertheless, if the target compounds are correctly recovered from this by-product, it will not only help the olive oil producers financially, but it will also be beneficial to the environment since the waters can be used as fertilizers or compost [54,55]. Finally, OVW can be treated in anaerobic digesters to produce biogas (mainly methane) through a process called anaerobic digestion. This biogas can be used for energy production or as a fuel [56]. Olive pulp, peel, stone, and water constitute the OP. Depending on characteristics such moisture, phenolic composition, and oil content OP can be referred as crude, fresh, or dry OP. Moreover, it is possible to distinguish between the OP that comes from the two- or three-phase extraction process by looking at the higher moisture and lower oil content: after the application of the two-stage system OP moisture reaches up to 70%, which are significantly higher than those derived from the three-stage system, with moisture values of 45% in the residue. Nowadays, OP is employed in multiple applications, such as biofuel production, feedstock in biorefineries, for soil amendment as an organic fertilizer or soil conditioner or in the production of olive oil applying solvent extraction [57,58].

1.3.2 *Recovery of Active Ingredients*

From waste and by-products, it is also possible to obtain ingredients with high added value that can be used in the pharmaceutical, nutraceutical and cosmetic fields. The main bioactive compounds recovered from olive by-products are polyphenols and phenolic acids, phytosterols, triterpenoids and flavonoids. In-depth research has reported the presence of polyphenols and other antioxidant compounds in all olive oil by-products, of which olive leaves are the main source. Olive leaves are very abundant and economical waste rich in secoiridoids (oleacein and oleuropein) [59] and in oleanolic acid, a triterpenoid compound known for its anti-inflammatory, hepatoprotective and antiviral properties [60]. Olive leaf extracts are marketed as a natural medicine with numerous health benefits due to the high content of these bioactive compounds, particularly oleuropein. Particular emphasis is placed on the antioxidant activity of the extract and the corresponding health benefits such as cardioprotective, antimicrobial and hypoglycemic properties [61,62]. Large quantities of polyphenols, in particular tyrosol and hydroxytyrosol, are also recovered from OVW. The waters are also rich in fatty acids, carotenoids, tocopherols, and represent a rich

source of bioactive compounds with high added value [63]. In fact, due to their high phytotoxicity, the use of OVW in the agricultural sector is limited while purified extracts that have antioxidant, anti-inflammatory, antiproliferative and neuroprotective activities are already being applied [63]. Even in the OP the most precious fraction is the polyphenolic one, but it also contains fatty acids, vitamin E and phenolic compounds [64]. Currently, various techniques are to isolate and concentrate the polyphenols present in these by-products. The most used techniques are: solvent extraction; solid-liquid extraction were OP is mixed with a liquid solvent to allow the polyphenols to transfer from the solid matrix to the liquid phase; supercritical fluid extraction were supercritical CO_2 is used as a solvent under specific temperature and pressure conditions; ultrasound-assisted extraction in which high-frequency ultrasound waves are used to disrupt the cell walls of the olive by-products, enhancing the release of polyphenols into the solvent; enzyme-assisted extraction were enzymes are employed to break down the cell walls of the olive pomace, facilitating the release of polyphenol. Once extracted, the polyphenols are typically concentrated and purified through techniques such as evaporation, filtration, or chromatography. The choice of extraction method depends on factors like efficiency, cost, environmental impact, and the intended application of the extracted polyphenols [65–67].

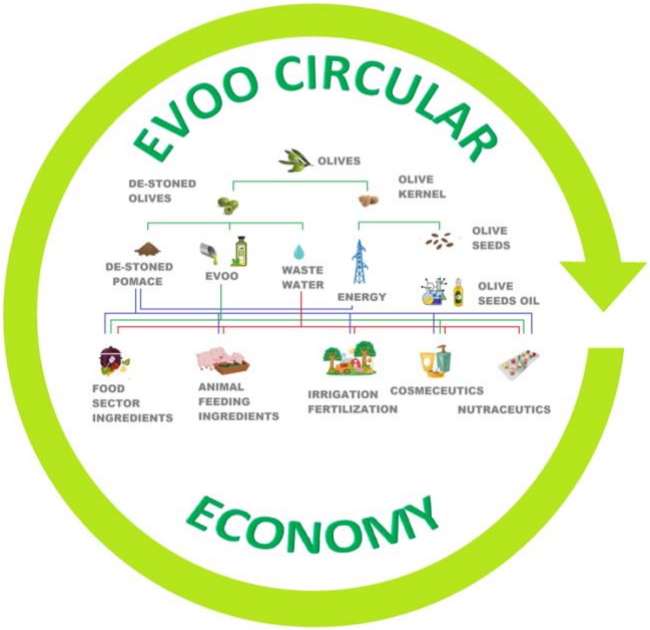

Figure 4. Circular economy: reuse of by-products from EVOO production. Figure from Mallamaci *et al.* [68].

1.3.2.1 *Olive stone applications and source of bioactive compounds*

The OS is the woody endocarp of the drupe that contains the seed. With the pitting process that derives from the production of table olives and olive oil obtained from pitted olives, whole stones are obtained, unlike the production of traditional olive oil, which does not use the pitting step, were the stones are inside the pomace crushed. As already mentioned previously, given its high calorific value (18,000 kJ/kg), OS is mainly recovered as fuel/pellets for domestic heating systems [69]. Moreover, due to their high content of elemental carbon (40-45%), OS have been investigated for the production and application of activated carbon as an adsorbent for wastewater treatment [70]. Furthermore, OSs are used as natural metallic bio-absorbents for Pb(II), Ni(II), Cu(II), and Cd(II) allowing the removal of heavy metals from aqueous solutions [71,72]. Additionally, OSs have been researched as a plastic filler in an effort to reduce the harmful environmental consequences of some plastic structures while encouraging clean technology and recycled goods [73]. OS is probably the residue produced in the olive fruit industrial sector with the greatest commercial appeal due to its chemical/physical qualities. Currently, the search for new uses of this by-product is of great interest given that, in addition to the lignin component, it is a source of proteins, fats, sugars and polyols [74,75] and it can therefore be considered a good source of macronutrients. Olive seeds contain a great amount of oil (22-27% of weight) in particular it is rich in linoleic acid, different types of sugars including sucrose, glucose, fructose, arabinose, xylose, mannitol and myoinositol and a several bioactive phytochemicals like tocopherols, squalene, steroidal and non-steroidal triterpenoids [76,77]. A key element of the olive seed's nutritional value is its protein content and, in the seed, the amount of protein is higher than the rest of the olive fruit (17% of dry weight). The most abundant proteins belong to the 11S protein family (storage proteins) and represent approximately 70% of total proteins. From the analysis of the amino acid (AA) composition, olive seed proteins are a rich source of essential amino acids particularly valine, and arginine [77,78]. This high protein content makes it interesting as animal feed but also as a source of possible bioactive peptides.

CHAPTER 2

2. Biological properties, absorption mechanisms and bioavailability of olive polyphenols

2.1 Polyphenols and Phenolic Compounds in Olive Oil

Polyphenols are a heterogeneous group of phytochemicals, characterized by a phenol rings, that are present in various plant-based foods. Depending on the strength of phenolic ring, polyphenols can be categorized in many classes: phenolic acids, flavonoids, phenolic alcohols, and lignans. Polyphenols are secondary metabolites typically produced in response to ultraviolet radiation or aggression by pathogens. A main property of natural phenolics is their exceptional antioxidant power and ability to modulate various oxidative pathways. This antioxidant ability is often cited to be the key property underlying the prevention/reduction of oxidative stress-related chronic disease such as cardiovascular disease (CVD), diabetes, cancer and neurodegenerative diseases [79,80] . The phenolic fraction of olive oil is complex and consists of more than 30 phenolic compounds which are present in free, bound, or esterified forms. The composition is influenced by various factors, such as the cultivation territory, the soil characteristics, the climate, the stage of maturation, the time of harvest and the production process. The total phenolic content (TPC) is between 50 and 1000 mg/kg, but in common olive oil it is between 100 and 300 mg/kg [81]. The phenolic fraction is mostly characterized by phenolic acids (vanillic, coumaric, caffeic, protocatechuic, p-hydroxybenzoic, ferulic acid), phenolic alcohols (hydroxytyrosol and tyrosol), secoiridoids (oleuropein derivatives, p-HPEA-EA, oleacein, and oleocanthal), flavonoids (apigenin, luteolin), and lignans (acetoxypinoresinol, pinoresinol). One of the most important classes is that of the secoiridoids. The aglycones of demethyloleuropein, oleuropein (Ole) and ligstroside (Lig) representing 90% of the phenolic compounds present in EVOO and they are responsible for the sensory and organoleptic attributes of EVOO (flavor, bitterness, pungency) [82,83] . Ole is the most abundant, along with its hydrolytic degradation products, hydroxytyrosol (OH-Tyr) and tyrosol (Tyr). Indeed, OH-Tyr and Tyr increase along the storage process because of the hydrolysis of olive oil secoiridoids [84].

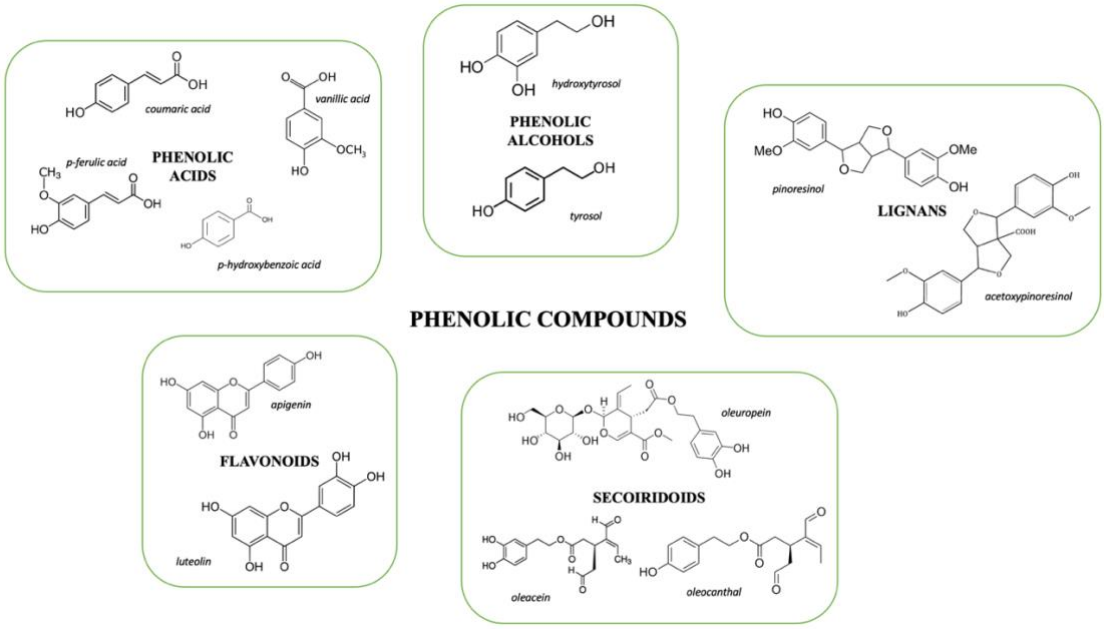

Figure 5. Scheme of the main classes of polyphenols present in olive oil.

2.1.1 Oleuropein

As anticipated, Ole is the main phenolic compound present in olive oil. Ole is not only contained in the oil but is also found in olive leaf extracts, olive fruits and branches. Its range can vary from 113 to 100,000 mg/kg of fresh olive fruit on dry weight basis, and 50–23485 ng/mL of olive leaf extract, depending on the ripening stage, extraction techniques, and storage preservation strategies [85]. Ole belongs to the secoiridoids groups and specifically is an ester of 2-(3,4-dihydroxyphenyl)ethanol (hydroxytyrosol) and has the oleosidic skeleton. In EVOO it is abundant as Oleuropein aglycone (OleA), due to the hydrolysis process by endogenous β-glucosidases during the milling [86]. The quality of the oil is influenced by the presence of Ole and its derivatives, as they increase the shelf-life thanks to their antioxidant and antibacterial properties [87]. Ole can be extracted using conventional and nonconventional strategies. The Soxhlet extraction method and cold solvent extraction are examples of conventional extraction techniques. Nonconventional techniques include ultra-sound-assisted extraction, extraction with supercritical fluid, with pressurized fluid, with membranes, with microfluidic system, acid hydrolysis and liquid-liquid extraction [88]. Several studies have reported the therapeutic and pharmacological properties of Ole, which highlight its importance as a possible biologically active ingredient against many illnesses. Numerous *in vitro* and *in vivo* investigations have been conducted to enhance comprehension of the mechanisms behind the pharmacological characteristics of Ole.

Ole is useful in reducing several metabolic syndromes such as diabetes, hyperlipidemia, neurological diseases, cardio-vascular consequences, obesity, cancer, hypertension, inflammation, and microbial infections. The most known is the antioxidant effect due to the presence of the catechol ring, both in its glycosidic and aglycone form, responsible for the radical scavenging activity through hydrogen donation and stabilization of the ROS via hydrogen bonds [89]. Ole has been shown to inhibit pathways and pro-inflammatory mediators, which lowers inflammation in a variety of experimental models. Its potential for managing inflammatory illnesses, including arthritis, inflammatory bowel disease, and chronic inflammatory ailments, is suggested by its anti-inflammatory action. Actually, Ole has been shown to be anti-inflammatory by increasing the nitric oxide (NO) production in macrophages stimulated with lipopolysaccharide (LPS) within the induction of the inducible form of the enzyme nitric oxide synthase (iNOS) activating the macrophages functional activity [90]. Moreover inhibit the synthesis of pro-inflammatory cytokines, downregulate key marker of inflammation such as cyclooxygenase-2, Matrix Metallopeptidase 9 and Nuclear Factor kappa B [91]. Ole also has a neuroprotective effect, in fact it decreases mortality in brain cells and by enhancing the intracellular calcium influx in mouse hippocampus slices through directed phosphorylation and surface expression of glutamate A1 (GluA1), helps address age-related memory deficits. Furthermore, Ole effectively counteracted the hydrogen peroxide induced stress in human glioblastoma cells and maintained the cell viability [92,93]. Ole has anti-proliferative effects, specifically for its ability to diminishes the *in vitro* proliferation of MCF-7 breast cancer cells [94] and inhibits growth of tumor cell lines derived from advanced-grade human tumors [95]. Additionally, oleuropein has antibacterial effect against a variety of pathogens, such as viruses, fungi, and bacteria. Research have shown that it works well against a variety of infections, including influenza viruses, *Staphylococcus aureus*, *Candida albicans*, and *Escherichia coli* [87,96–98]. The beneficial effects of Ole against CVD have been studied in a variety of experimental applications, including both *in vitro* and *in vivo* research. In fact, Ole is able to reduce blood pressure and lower the serum levels of total cholesterol, LDL-C and triglyceride by lowering the deposit of lipids in the aortic intima. It was demonstrated that administration of Ole produced a cardioprotective effect in rabbits fed a high-cholesterol diet by lowering LDL-c and total cholesterol levels [99]. Furthermore, oleuropein has been shown to increase genes involved in the synthesis, transport, metabolism, and excretion of triglycerides, as well

as activating the liver's LDL-R receptor. In summary, oleuropein appears to be a promising candidate for improving lipid biomarkers and reducing CVD [91,100]. A lack of glucose absorption mediated predominantly by glucose transporter 4 (GLUT4) in muscle defines the classic pathophysiology of type 2 Diabetes Mellitus (DM). Two major routes commonly produce GLUT4 translocation. The first signaling route is that of the insulin receptor/phosphatidylinositol 3-kinase/protein kinase B, which is triggered by insulin. The second signaling pathway is insulin-independent and is triggered by multiple molecules, including 5′ AMP-activated protein kinase (AMPK). By stimulating AMPK/acetyl-CoA carboxylase and MAPKs, but not phosphatidylinositol 3-kinase/protein kinase B, Ole promotes the translocation of GLUT4 from the cytoplasm to the cell membrane, increasing glucose uptake and ameliorating palmitic acid-induced insulin resistance in C2C12 muscle cells [101,102]. Not only does Ole have anti-diabetic properties in cells and diabetic animal models, but it also does so in humans. Numerous markers, including as plasma glucose peak, dipeptidyl peptidase 4 (DPP-4) activity, glucagon-like peptide-1 (GLP-1), insulin secretion, and β-cell reactivity, have been used in clinical investigations to evaluate the effects of oleuropein on blood glucose management. For example, in patients with type 2 DM, a single dosage of oleuropein-enriched chocolate is sufficient to enhance the serum level of GLP-1 and insulin and decrease blood glucose and serum DPP-4 activity two hours after a meal. In an open study of hypertensive patients, many of whom had obesity and/or diabetes, two months oral supplementation of Ole, decreased fasting blood glucose, waist circumference and serum triglycerides [103,104]. Ole appears to be safe, in fact in rats up to 1000 mg/kg no side effects or lethal situations were found. In a parallel, randomized, double-blind and actively controlled clinical research, where 1000 mg per person of olive leaf extract was applied to evaluate hypotensive effects, no abnormalities were observed in hematological, hepatic, renal and in electrolyte balance [105,106].

2.1.2 Oleocanthal and Oleacein

Oleocanthal (2-(4-Hydroxyphenyl)ethyl (3S,4E)-4-formyl-3-(2-oxoethyl)hex-4-enoate, Oleo) and Oleacein (2-(3,4-dihydroxyphenyl)ethyl (Z)-4-formyl-3-(2-oxoethyl)hex-4-enoate, Olea) are secoiridoids identified in olive oil for the first time in the 90s. Oleo is the molecule responsible for the bitter taste present in olive oils with a high content of polyphenols. In addition to this characteristic, it has both anti-inflammatory and

antioxidant activities. Beauchamp *et al.* [107] have shown that Oleo has ibuprofen-like activity inhibiting COX1 and COX2 enzymes in a dose-dependent manner. Oleo inhibits the expression of pro-inflammatory genes such as MIP-1α and IL-6 in murine macrophages (J774) [108] and inhibits inflammatory mediators such as iNOS and MMP-13 upon stimulation with LPS [109]. In collagen-induced arthritis murine model, the diet rich in Oleo prevented bone, joint and cartilage rheumatic affections induced by collagen, diminish pro-inflammatory cytokines levels, COX-2 and iNOS protein expressions [110]. Several *in vitro* and *in vivo* studies have demonstrated a strong antitumor effect of Oleo which has been shown to induce apoptosis in several cancer cell lines and to slow down the development of metastases [111]. Olive oil rich in Oleo has shown several benefits against the metabolic syndrome, including the reduction in insulin resistance, the improvement of the endothelial function and the hepatic steatosis [112–114]. Olea acts as a radical scavenger and has anti-inflammatory properties since significantly reduce the release of pro-inflammatory cytokines and diminish the synthesis of proinflammatory mediators [115,116]. Furthermore, Olea protects against H_2O_2-mediated toxicity, activates cytoprotective and healthy-aging promoting mechanisms [117]. Olea protect from the development of the metabolic syndrome given that inhibits lipid accumulation, lowers protein levels of peroxisome proliferator-activated receptor gamma (PPARγ) and fatty acid synthase (FAS), ameliorated insulin sensitivity, mitigate abdominal fat accumulation and weight gain in mice, [118,119]. Moreover Olea prevent carotid atherosclerotic plaque induced by acute inflammation [120].

2.1.3 Hydroxytyrosol and Tyrosol

Hydroxytyrosol (3,4-dihydroxyphenylethanol, OH-Tyr) is generated by enzymatic cleavage of Ole, during olives maturations, and its amount is severely associated with the oxidative stability of olive oil. It is soluble in lipids but is also moderately soluble in water. It can be found as a simple phenol, or as acetate or secoiridoid derivatives [121]. OH-Tyr beneficial properties for human health are related to the presence of the o-dihydroxyphenyl moiety and therefore the ability of the molecule to scavenge free radicals and reactive oxygen/nitrogen species as well as to activate endogenous antioxidant systems in the body [91,122]. But this molecule does not only have antioxidant activity. OH-Tyr impedes the expression of inflammatory cytokines after LPS stimulation, suppress the iNOS and cyclooxygenase/prostaglandin E2 pathways in

human monocytic cells and in mouse model [123,124]. Numerous studies have shown that OH-Tyr protects LDL from oxidation [125,126] and for this reason in 2011 the European Food Safety Authority (EFSA), which provides scientific declarations on current and emerging risks linked with the food chain, published a health claim (published in Regulation N° 432/2012) related to polyphenols in olive oil and their possible protection of blood lipids against oxidative stress. The panel established: "Olive oil polyphenols contribute to the protection of blood lipids from oxidative stress. The claim may be used only for olive oil, containing at least 5 mg of hydroxytyrosol and its derivatives (e.g. oleuropein complex and tyrosol) per 20 g of olive oil. In order to bear the claim information shall be given to the consumer that the beneficial effect is obtained with a daily intake of 20 g of olive oil." [127,128]. In addition to protecting LDL from oxidation, OH-Tyr intake modulates the expression of genes involved in the development of atherosclerosis and inhibits the de novo fatty acids and cholesterol synthesis [91,129]. OH-Tyr exhibit antidiabetic properties whereas it decreases blood glucose levels [130], modulate transcription factors involved in the development of Type 2 DM, such as Nrf1 (Nuclear respiratory factor 1) and Tfam (Transcription factor A, mitochondrial) [122], lower the thiobarbituric acid reactive substances level and lactate dehydrogenase activity in diabetic rats pancreas [131]. Antiproliferative and proapoptotic effect of the OH-Tyr via activation of caspase signaling was shown in colon cancer Caco-2, in lymphocyte HT-29 and in prostate cancer C4-2 cells. OH-Tyr inhibits the PI3K/Akt/mTOR pathway in MCF-7 breast cancer cells, down-regulates epidermal growth factor receptor (EGFR) expression [91,132,133]. Finally, OH-Tyr shows neuroprotective effects by the modulation of monoamine oxidase (MAO) inhibitor in patients with Parkinson's disease [134]. Tyrosol (2-(4-hydroxyphenyl)-ethanol, Tyr) has a similar structure to that of OH-Tyr, but is more stable and resistant to autoxidation [135]. Tyr also has antioxidant and anti-inflammatory activities. In detail, Tyr defends against the oxidative damage caused by oxidized LDL in Caco-2 cells [136], it diminish oxidative alterations of HDL and improves their functionality, especially the capacity to promote cholesterol efflux [137], it repress palmitic acid-induced oxidative stress in hepatocytes [138], act as scavenger of reactive nitrogen species [139], it decrease C-reactive protein and inflammatory markers in streptozotocin-induced diabetic rats [140] and it enhances the expression of liver enzymes involved in Non-Alcoholic Fatty Liver Disease (NAFLD) in high fat diet-fed C57BL/6 mice.

2.2 Metabolism and Bioavailability of Phenolic Compounds

In the Mediterranean diet, the average intake of olive oil is 25-50 mL/day, which corresponds to the consumption of 9 mg of polyphenols [141]. In order for the polyphenols present in olive oil to be able to exercise their biological function, they must reach the sites of action and interact with their molecular targets. The absorption of the polyphenols contained in olive oil in humans has been measured indirectly by assessing the elevation of plasma's antioxidant capacity. However, their bioactivity is influenced by their absorption and metabolism which are complex processes not fully understood. These steps are affected by multiple elements such as physio-chemical characteristics, basic structural properties, polarity, degree of polymerization or glycosylation, and solubility. In details, the structure of polyphenols significantly affects intestinal absorption. The structural parameters that are most frequently mentioned include esterification, glycosylation, and molecular weight [142]. Once polyphenols have reached the stomach, the ingested polyphenols are partially modified before reaching the small intestine. Secoiridoids are sensitive to the gastric environment where they are exposed to a time-dependent hydrolysis, resulting in a significant increase in their derivates, i.e., free OH-Tyr and Tyr. When the ingested secoiridoids are glycosylated, they are not subjected to gastric hydrolysis and enter the small intestine unaltered. In order to be absorbed, Ole is deglycosylated in Ole Aglycone (OleA) which is then further hydrolyzed in OH-Tyr; Lig is deglycosylated in ligstroside aglycone (LigA) and then hydrolyzed, as Oleo, in Tyr. OH-Tyr and Tyr are dose-dependently absorbed (40-95%) and metabolized, with an increase of their bioavailability when administered as an olive oil solution compared to an aqueous solution [143]. OH-Tyr and Tyr are the best absorbed phenols in the intestine tract, mainly through passive bidirectional transport, because of their polar structure, occurring through the membrane of human enterocytes, and they reach a peak concentration in human plasma 1h following ingestion and after 2h in urine, which underlines that the small intestine is the major site of absorption for these compounds. Due to its larger molecular weight and hydrophobic form, Ole is less absorbed by enterocytes in its free form. As a result, Ole may enter the large intestine after further metabolic and microbial degradation [144–146]. Indeed, polyphenols undergo both phase I and II of metabolism. Polyphenolic aglycones are metabolized through sulfation, glucuronidation, or methylation within the actions of phase-II enzymes (which are

involved in the detoxification process), producing glucuronidated, sulfated and methylated conjugates [147]; they are also modified by the action of gut microbiota. The major enzymes involved in the intestinal hydrolysis are the lactase phlorizin hydrolase (LPH), found on the brush-border of the small intestine epithelial cells, and the cytosolic β-glucosidase present within the epithelial cells, where the glucosides are transported through the active sodium-dependent glucose transporter (SGLT-1) [148,149]. All phenolic molecules that are not absorbed in the small intestine pass through the colon where they can be fermented by gut microbiota. Colon bacteria promote the degradation of certain unabsorbed phenolic compounds, providing a wide range of metabolites, which may be adsorbed or excreted. Afterwards, the metabolites are transported into the hepatic vein and in the systemic circulation or effluxed back into the lumen of small intestine [150]. The sulfated and glucuronidated forms are the prevalent metabolites found in human plasma and urine, but also, they concentrate in the intestinal epithelium [79,144,151]. More the 10 metabolites have been identified in animals and human studies and absorbed OH-Tyr and Tyr are extensively distributed throughout the organism and have been found in skeletal muscle, kidneys, liver, lungs, brain and heart [152]. The kidneys are primarily responsible for excreting polyphenols through urine. Investigations conducted in humans and animal models have contributed to the characterization of the many mechanisms involved in the excretion. Compounds that are unable to be absorbed by the intestinal wall typically exit the body through the feces, either in their natural ingested state or after undergoing chemical changes in the digestive system [153]. Also, the excretion of OH-Tyr and Try varies depending upon the matrix in which the phenols were resuspended. In comparison to the water-based method, the oral administration of oil-based dosing generally produced a higher rate of compound elimination in urine. Ole was found in much lower levels in urine after oral administration. Many biological (e.g., gender, genotype, age, interaction with food) and technical (e.g., route of administration, extraction processes, and analytical) factors influence the bioavailability of these compounds, leading to an additive or synergistic effect that makes it challenging to draw firm conclusions on the subject.

CHAPTER 3

3. *Production, bioactivity, and bioavailability of by-products peptides*

3.1 The sources of Bioactive Peptides

Proteins are one of the major components of human diet and they are formed by the association of amino acids, linked together through peptidic bonds. These macromolecules can be precursors of bioactive peptides (BPs), defined as specific short protein fragments with positive effects on human health. BPs released from the hydrolysis of food proteins represent a current topic in the scientific community. BPs can be generated by any organism, but the choice of host must be carefully considered. The selection between different protein fractions/processes of a matrix, can make a protein source suitable for hydrolysis and BPs release. In the literature, many peptides obtained from foods of both animal origin (i.e. milk, eggs) and plant origin (i.e. soy, lupine), marine organisms (i.e. marine proteins, such as collagen and fish muscle protein) and microbial sources (i.e. strains of bacteria and yeast, fungi) have been characterized [154]. Initially the research focused on animal given their high protein content, the great composition of essential amino acids and high yield. In fact, dairy products and milk have been widely valorized by classifying them as potential sources of BPs [155,156]. However, the cost of production and purification and, not least, the sustainability in the research of BPs should be considered. There was therefore an interest in finding protein sources that were both economical and abundant. The food industry has proven to be an excellent source as large amounts of protein-rich waste and by-products are generated. Especially, the processing of fruit and vegetables is characterized by the generation of most of this waste material, which is partly used for animal feed or biofuels. The recovery of these residues allows the creation of new application opportunities to produce substances with high added value. In plants, the main sources of protein are seeds, cereals, and legumes. Soybean meal or cake is produced in large quantities (~122 million tons/year) and contains valuable amounts of protein (~45%), making it the most widely used vegetable protein source [157,158]. Another protein rich by-product is that of cereals (11-17%), such as wheat, oats and

rice, given their immense production quantities [159]. Finally, pomace and stones, obtained from fruit and vegetable by-products after the production of fruit juices and oils, have the greatest protein content (2-25%) [160].

3.2 Bioactive Peptides production

In literature, the most used strategies for the production of BPs are enzymatic hydrolysis and fermentation [161]. For enzymatic hydrolysis, commercial enzymes derived from plants, animals or microorganisms are used. Table 2 shows a list of main available commercial enzymes used to obtain BPs from food and food industry by-products. Temperature, time, pH, substrate concentration, and enzyme activity are the main elements in enzymatic hydrolysis that must be regulated to reduce outcome variability. Longer hydrolysis times help the process somewhat, although the rate of hydrolysis is not constant and often falls over time for a variety of reasons, including inhibition or denaturation of the enzyme [162].

Enzymes	Origin	Activity
Trypsin	*Bovine pancreas*	Endopeptidase, acts on peptide bonds involving the amino acids lysine and arginine
Chymotrypsin A **Chymotrypsin C**	*Bovine pancreas*	Cleaves peptide bonds on the carboxyl side of aromatic amino acids (phenylalanine, tyrosine, and tryptophan)
Pepsin	*Porcine gastric mucosa*	Active at acidic pH, hydrolyzing peptide bonds in the stomach
Bromelain	*Ananas comosus stem*	Cysteine-type peptidase
Papain **Collupulin**	*Carica papaya*	Cysteine-type peptidase
Ficain	*Figs latex*	Cysteine-type peptidase
Seabzyme L 200	*Carica papaya*	Endoprotease
Alcalase 2.4 L	*Bacillus licheniformis*	Subtilisin, alkaline serin endopeptidase, extracellular neutral metalloprotease, aminopeptidase
Neutrase:	*Bacillus subtilis* *B. amyloliquefaciens*	Neutral protease, metalloprotease
Flavourzyme	*Aspergillus oryzae*	3 endopeptidases, 2 aminopeptidases, 2 dipeptidylpeptidases, 1 α-amylase
Protamex	*Bacillus licheniformis* *Bacillus amyloliquefaciens*	Subtilisin, serin endopeptidase, metalloendopeptidase, neutral protease
Thermolysin	*Bacillus thermoproteolyticus*	metalloproteinase used at elevated temperatures
Protex 6L	*Bacillus licheniformis*	Alkaline proteases

Corolase 7089	*Bacillus subtilis*	Neutral endopeptidase
Esperase	*Bacillus lentus*	Subtilisin, alkaline serin endopeptidase

Table 2. Commercial enzyme employed for protein hydrolysis with origin and specific characteristics.

In detail, after the selection of compatible proteins, the hydrolysis step occurs using single or combined, specific or non-specific enzymes, to release numerous peptide fragments into the hydrolysate. Even though the source of the protein does not completely define the characteristics of the protein itself, some of its features can influence the performance of the enzyme chosen for protein hydrolysis [163]. Therefore, based on the chosen proteins and enzyme, different peptides will be generated, for example by using endopeptidases, peptides of longer lengths will be obtained compared to the use of exopeptidases. Amino exopeptidases are linked with the release of products with one, two, or three amino acid residues from the N-terminus, while carboxy-exopeptidases are capable of liberate free amino acids or dipeptides from the C-terminus. Endopeptidases are not limited to terminal peptide linkages and find a broad range of options for cleaving sites and may also be more selective. The most common enzymes use for research purposes are Alcalase, Protamex and Flavourzyme [164,165]. Several studies have also investigated the release of BPs from food-derived proteins mimicking gastrointestinal (GI) activity applying digestive enzymes such as pepsin, trypsin and chymotrypsin. This approach allows to study if the peptides are able to reach the bloodstream and target organs in active way, evaluating their absorption and bioavailability [166]. The enzymatic approach has proven to be the most widely used as it does not require the use of potentially toxic organic solvents, the enzymes are easily inactivated, and the process uses mild conditions. However, this approach often has low yields, a limited number of enzymes can be used, and it is not cost effective. Alternatively, the proteins could be fermented with specific microorganisms to improve peptide release by microbial proteases [167,168]. The fermentation compared to the conventional enzymatic hydrolysis is cheaper, avoids the cost of extraction and purification of enzymes, and the action of proteolytic bacterial and fungal strains allow to obtain BPs from both animal and plant proteins [169]. In both cases, the hydrolysates are then fractionized and purified based on their structural features. Membrane ultrafiltration and size exclusion chromatography are often used to concentrate peptides of defined molecular weight ranges, in particular to obtain fractions containing low

molecular weight peptides that can withstand further proteolytic digestion *in vivo* and obtain hydrolysates highly active [170–172]. The next step requires the identification of peptides by mass spectrometry analysis [173], while bioinformatics analysis could play an important role to simulate protein hydrolysis, to predict the theoretical bioactive profile of some peptides or to perform molecular docking [174].

3.3 Biological activities and health effects of bioactive peptides derived from by-products

The awareness regarding BPs is rapidly growing, given that they can have a significant impact on human health. The structural properties, amino acid composition, sequence and hydrophobicity are the main characteristics responsible for the biological activity of BPs. The peptides that have been shown to be most active are composed of 2-20 amino acids and have a molecular weight of less than 3 kDa. These peptides, thanks to their small size, have a greater chance of resisting hydrolysis by GI enzymes, so as to enter the bloodstream and reach the target organs [150,175]. To be considered bioactive, peptides must confer a measurable biological effect at a physiological level. At the moment, more than 4700 different biologically active peptide sequences have been reported in BIOPEP-UWM™ database, a well-known tool used in BP research [176]. The bioactivity of a peptide can be exerted at various levels, given that peptides can work on several targets implicated in various metabolic pathways. When inhibiting an enzyme, peptides can interact at the active site and/or outside its catalytic site, preventing the enzyme from interacting with the natural substrate [177]. The bioactivities of BPs from by-products are numerous and include antithrombotic, antihypertensive, immunomodulatory, antilipemic, osteoprotective, antioxidant, antimicrobial, ileus-contracting, anticariogenic, and growth-promoting properties as depicted in Figure 6.

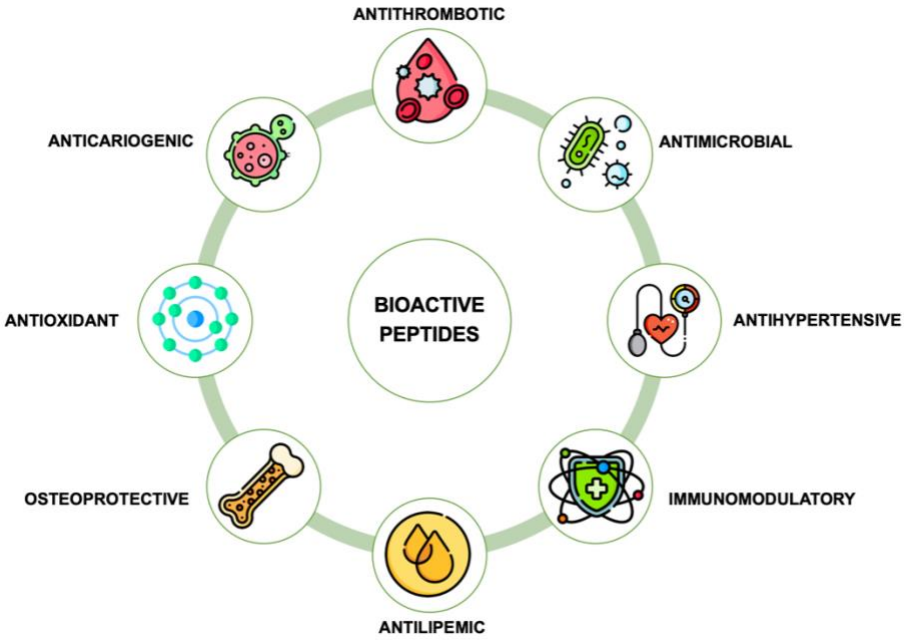

Figure 6. Schematic representation of bioactivities of bioactive peptides.

Peptides can also be multifunctional and show more than one bioactivity. The anticoagulant and/or antithrombotic action of biopeptides can be attributed to their interaction with thrombin (or coagulation factors), thus inhibiting their proteolytic activity on fibrinogen, or it could be due to their binding to fibrin monomers already formed and therefore preventing polymerization. Indeed, the antithrombotic activity of these peptides is often attributed to their ability to interfere with the blood clotting cascade or platelet aggregation. Some sources of antithrombotic bioactive peptides from by-products include collagen peptides derived from fish scales or skin [178,179] ; krill processing by-products [180]; soybean meal [181]; wheat and rice bran [182,183]. Antihypertensive peptides inhibit the angiotensin-converting enzyme (ACE), an enzyme that plays a key role in blood pressure regulation and stimulate vasodilation by modulating the endothelial nitric oxide synthase (NOS) pathway [184]. Lee and Hur [185] showed that the presence of proline, isoleucine or leucine at the N-terminus of the peptide increased the ACE-inhibitory activity of the peptides. Numerous studies reported that some food proteins are sources of ACE- inhibitory peptides. Several ACE-inhibitory peptides have been isolated from enzymatic hydrolysis of various by-products protein sources such as salmon processing discards [186] or trout [187]; milk [188–190] and dairy by-products such as bovine whey proteins [191] or casein-derived peptides from cheese production by-products [192], soybean pulp [193], egg white by-products [194], asparagus by-products [195]. Immunomodulatory peptides act directly

on certain cells of the immune system; however, to date, the mechanisms behind these interactions are still unclear. Immunomodulatory peptides can influence various aspects of the immune system, including the activation of immune cells, regulation of cytokine production, and enhancement of overall immune function. Immunomodulatory peptides can modulate anti-inflammatory responses by interacting with opioid receptors present on the surface of immune cells [196], modulating the secretion of interleukins and factors involved in immune cascades, such as the nuclear factor κB (NF-κB) pathway, or decreasing the production of cytokines [197]. Recently, several investigations have highlighted the immunomodulatory activity of protein hydrolysates obtained from food by-products, e.g. hemp by-products [197,198], seafood and fish processing by-products [199–201]; brewery and distillery residues [202,203]; by-product of dairy processing [204]. Hypocholesterolemic peptides can influence cholesterol metabolism through various mechanisms and several studies have been carried out in this regard, both *in vitro* and in animal models [205]. Hypocholesterolemic peptides may inhibit the activity of 3-hydroxy-3-methylglutaryl-coenzyme A (HMG-CoA) reductase, an enzyme involved in cholesterol synthesis. By reducing the activity of this enzyme, the production of cholesterol in the liver is decreased. Hypocholesterolemic peptides can increase the expression and activity of hepatic low-density lipoprotein (LDL) receptors, promoting the uptake of circulating LDL cholesterol by the liver. Some peptides can interfere with cholesterol absorption by inhibiting specific transporters, reducing the absorption of cholesterol from the diet. Finally, hypocholesterolemic peptides can influence the expression of genes involved in lipid metabolism and cholesterol synthesis [206,207]. In the literature we find numerous hypocholesterolemic peptides derived from fruit and vegetable processing by-products [207–211], from fish [212,213] and cereals by-products [214]. Antidiabetic peptides have been studied for their potential in managing diabetes by exerting various effects on glucose metabolism and insulin function. Some peptides may exhibit insulin-mimetic properties, meaning they can bind to insulin receptors and activate intracellular signaling pathways similar to insulin. These peptides have proven the ability to inhibit key enzymes involved in the digestion as α-amylase and α-glucosidase, which are responsible for breaking down complex carbohydrates into simple sugars, reducing glucose absorption and postprandial hyperglycemia [215]. Moreover, the DPP-4 inhibitory peptides act by inhibiting the enzymatic activity of DPP-4, preventing the degradation of incretins such as GLP-1 and GIP, important for glycemic regulation [216,217]. Also as regards anti-

diabetic peptides have been identified in plants [218–220] and animals by-products [177,221,222].

3.4 Absorption and Bioavailability of Bioactive Peptides

A crucial aspect in research on BPs is to verify their bioavailability since the biological functionality of a peptide depends on this. In fact, the primary limitation of BPs, such as drugs or nutraceuticals, is their poor bioavailability, short half-life due to hydrolysis in the GI and via hepatic and renal clearance; a decreased ability to cross physiological barriers due to their hydrophilic features and frequently poor selectivity for specific receptors, supporting interactions with other sites that could provoke secondary effects [223]. More in detail, once ingested the peptide can interact with the food matrix, which could negatively or positively influence its absorption, modifying its stability and bioavailability [224]. Once in the stomach they can undergo chemical hydrolysis due to the acidic environment and interaction with gastric enzymes. They subsequently undergo the action of pancreatic enzymes, microbiota proteases and a significant change in pH [225]. Finally, further digested peptides and those that are found to be resistant can be absorbed at the intestinal level. BPs are potentially transported through the gastrointestinal epithelium following one or more pathways: PepT1-mediated permeation, paracellular transport via tight junctions, transcytosis, and passive transcellular diffusion [226]. PepT1 is a high-capacity and low-affinity carrier which mostly binds with dipeptides and tripeptides with neutral charge and high hydrophobicity. Paracellular transport allows the transport of hydrophilic oligopeptides with negative charge. Transcytosis is an energy-dependent transcellular transport pathway, which favors the transport of peptide with long chains and high hydrophobicity. Transcytosis allow the transport of peptide by vesicles interaction with the apical lipid bilayer of intestinal epithelium. Finally, the passive transcellular diffusion allows the passive uptake of hydrophobic peptides and their basolateral secretion [227]. Preferential pathways were observed also depending on the concentration. For example, when peptides are at low concentration, the pathway through uptake transport by PepT1 is the main contributor to the total transport rate, whereas passive transport is favored when high concentrations of peptides are available in the uptake environment [228]. Peptide transport pathways are shown in Figure 7.

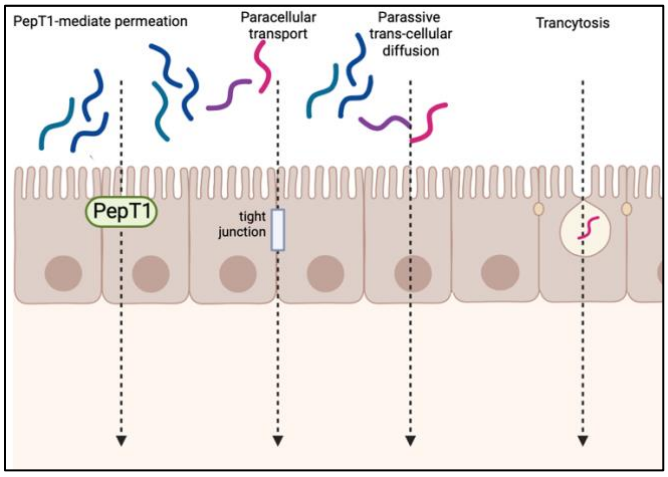

Figure 7. Potential mechanisms for the transport of bioactive peptides across intestinal epithelial cell monolayers.

The most relevant data on the absorption and digestion of peptides/hydrolysates are provided using animal models. Common animals models are dogs, chickens, and pigs, but the most frequently used for protein/peptide absorption assessment is the rat, since it better reflects the human mucosa with respect to paracellular space and metabolism [229]. Animal models generally involve animal death or surgical approaches in which cannulas are inserted into digestive organs to access the contents of the gastrointestinal tract. This approach is high cost, time consuming, and has significant ethical repercussions. Therefore, *in vitro* studies using simulated gastrointestinal digestion and absorption systems are needed to investigate the stability and bioaccessibility of peptides and overcome these limitations. Varieties of cell monolayer models that mimic *in vivo* intestinal epithelium in humans have been developed and are commonly applied. Caco-2 cells are derived from human colonic adenocarcinoma, but once cultured on semipermeable inserts, they differentiate both structurally and functionally into cells resembling mature enterocytes, with a characteristic apical brush border with microvilli, tight junctions, digestive proteases, and active receptors and several transport systems of different molecules [230]. Indeed, despite their colonic origin, Caco-2 cells display most of the morphological and functional features of small intestinal absorptive cells. When Caco-2 cells differentiate on a semi-permeable membrane it's possible to collect the apical and the basolateral compartments samples to assess the trans-epithelial transport of peptides. However, it's known that the permeability of hydrophilic compounds is low in the Caco-2 monolayers due to the relatively tighter junction in comparison with human or animal small intestine [231] and small molecules easily diffuse due to their molecular characteristics [232,233]. Thus, the absorption of BPs

obtained from by-products across Caco-2 monolayers has been demonstrated for peptide derived from fish by-products [234–237], meat by-products [238–240], cereals and plants by-products [241–246].

CHAPTER 4

MANUSCRIPT 1

EXTRA VIRGIN OLIVE OIL PHENOLIC EXTRACT ON HUMAN HEPATIC HEPG2 AND INTESTINAL CACO-2 CELLS: ASSESSMENT OF THE ANTIOXIDANT ACTIVITY AND INTESTINAL TRANS-EPITHELIAL TRANSPORT

Martina Bartolomei [1],† , Carlotta Bollati [1],† , Maria Bellumori [2] , Lorenzo Cecchi [2] , Ivan Cruz-Chamorro [1,3] , Guillermo Santos-Sánchez [1,3] , Giulia Ranaldi [4], Simonetta Ferruzza [4] , Yula Sambuy [4] , Anna Arnoldi [1] , Nadia Mulinacci [2] and Carmen Lammi [1],*

[1] Department of Pharmaceutical Sciences, University of Milan, 20133 Milan, Italy; martina.bartolomei@unimi.it (M.B.); carlotta.bollati@unimi.it (C.B.); icruz-ibis@us.es (I.C.-C.); gsantos-ibis@us.es (G.S.-S.); anna.arnoldi@unimi.it (A.A.)

[2] Department of Neuroscience, Psychology, Drug and Child Health, Pharmaceutical and Nutraceutical Section, University of Florence, 50019 Florence, Italy; maria.bellumori@unifi.it (M.B.); lo.cecchi@unifi.it (L.C.); nadia.mulinacci@unifi.it (N.M.)

[3] Departamento de Bioquímica Médica y Biología Molecular e Inmunología, Universidad de Sevilla, 41009 Seville, Spain

[4] CREA, Food and Nutrition Research Centre, 00178 Rome, Italy; giulia.ranaldi@crea.gov.it (G.R.); simonetta.ferruzza@crea.gov.it (S.F.); yula.sambuy@crea.gov.it (Y.S.)

*Correspondence: carmen.lammi@unimi.it; Tel.: +39-02-50319372

† Authors equally contributed to the work.

4. Abstract

In the framework of research aimed at promoting the nutraceutical properties of the phenolic extract (BUO) obtained from an extra virgin olive oil of the Frantoio cultivar cultivated in Tuscany (Italy), with a high total phenols content, this study provides a comprehensive characterization of its antioxidant properties, both *in vitro* by Trolox equivalent antioxidant capacity, oxygen radical absorbance capacity, ferric reducing antioxidant power, and 2,2-diphenyl-1-picrylhydrazyl assays, and at the cellular level in human hepatic HepG2 and human intestinal Caco-2 cells. Notably, in both cell systems, after H_2O_2 induced oxidative stress, the BUO extract reduced reactive oxygen species, lipid peroxidation, and NO overproduction via modulation of inducible nitric oxide synthase protein levels. In parallel, the intestinal transport of the different phenolic components of the BUO phytocomplex was assayed on differentiated Caco-2 cells, a well-established model of mature enterocytes. The novelty of our study lies in having investigated the antioxidant effects of a complex pool of phenolic compounds in an extra virgin olive oil (EVOO) extract, using either *in vitro* assays or liver and intestinal cell models, rather than the effects of single phenols, such as hydroxytyrosol or oleuropein. Finally, the selective trans-epithelial transport of some oleuropein derivatives was observed for the first time in differentiated Caco-2 cells.

4.1 Introduction

Oxidative stress, which refers to the shift in the oxidants/antioxidants balance in favor of the formers, contributes to many pathological conditions (Dhalla *et al.*, 2000). Aerobic organisms have integrated antioxidant systems, which include enzymatic and nonenzymatic antioxidants, which are usually effective in blocking the harmful effects of reactive oxygen species (ROS). However, in pathological conditions, the antioxidant systems can be destroyed, and the consequent increase of intracellular ROS levels contributes to the development and progression of many chronic and non-communicable diseases. The use of food-derived antioxidants may represent a strategy to cope with the progression of diseases related to oxidative stress (Lorenzo *et al.*, 2018). In fact, experimental, clinical, and epidemiologic studies have shown that the consumption of specific food phenols is positively linked with health-promoting effects (Cory *et al.*, 2018).

The consumption of extra virgin olive oil (EVOO) has been largely associated with numerous health benefits (Gaforio *et al.*, 2018). It has been frequently reported that olive oil has anti- inflammatory, neuroprotective, and immunomodulatory activities (Santangelo, *et al.*, 2018) and can reduce the risk of coronary heart disease by modulating the high-density lipoprotein (HDL) cholesterol levels (Berrougui *et al.*, 2015). The literature indicates that these beneficial effects are due, at least in part, to the presence of some hydrophilic components such as phenols, which are well-recognized for their remarkable antioxidant activity (Visioli *et al.*, 1995). Among these phytochemicals, hydroxytyrosol (OH-Tyr), tyrosol (Tyr), and oleuropein (Ole) have the greatest antioxidant activity and capacity of reducing oxidative stress (Serreli *et al.*, 2020). In particular, EVOO decreases ROS and malon- dialdehyde (MDA) production (Incani *et al.*, 2016) and NO release (Abdallah *et al.*, 2018) and reduces the expression and production of the inducible nitric oxide synthase (iNOS) and cyclooxygenase 2 (COX-2) (Sanchez-Fidalgo *et al.*, 2012). The European Food Safety Authority (EFSA) has published a positive opinion on the health claim that "Olive oil polyphenols contribute to the protection of blood lipids from oxidative stress", determining that 5 mg of OH-Tyr and its derivatives (e.g., Ole and Tyr) in olive oil should be consumed daily for a sufficient avoidance of oxidative damage (NDA, 2021). In this context, the present investigation was conducted on a phenolic extract (BUO) obtained from an EVOO of the Frantoio cultivar cultivated in Tuscany (Italy), with a high content of total phenols. The phenol characterization, reported in a preceding paper, has been performed applying the official method of the International Olive Council (IOC, 2009) for quantifying total phenols content, the 1H-NMR analysis for evaluating the relative abundance of aldehyde derivatives of secoiridoids, and a validated hydrolytic method to evaluate the total content of OH-Tyr and Tyr, as the sum of free and bound forms (Bellumori *et al*, 2019). These analyses have indicated that the concentration of OH-Tyr and Tyr were 208.0 ± 15.6 and 156.0 ± 3.9 μg/g of dried extract, respectively, and that the Ole derivatives were greatly prevalent (444.9 μg/g) (Lammi et al., 2020). The same study has also shown that the BUO extract modulates cholesterol metabolism in human hepatic HepG2 cells, through direct inhibition of the activity of 3-hydroxy-3-methylglutaryl-coenzyme A reductase (HMGCoAR) and consequent activation of the low-density lipoprotein receptor (LDLR) pathway (Lammi *et al.*, 2020). To express their activities, food phytochemicals need to be bioavailable. This means that, after ingestion, they have to be absorbed by enterocytes to reach the target organs and display

their biological activity. Despite their established physiological importance, the literature clearly underlines some limitations and a gap of knowledge on food phenols absorption and metabolism, especially when they are within a phytocomplex. Indeed, when they are consumed within the diet, phenols may undergo numerous structural modifications and their properties may be affected by the interactions with other constituents of the food ma- trix. The interactions with the digestive enzymes can alter their availability, and domestic processing appears to have important effects on the total phenol content and activity (El Gharras, 2009). Interestingly, recent data indicate that a combination of phytochemicals, rather than any single phenolic compound, is responsible for the observed health benefits (Lammi *et al.*, 2020, 2020b, Pandey *et al.*, 2009).

To promote the bioactivity of the BUO phytocomplex, the first objective of the present study was a detailed investigation of its potential antioxidant activity *in vitro* and on hepatic and intestinal cells, due to the physiological interplay existing between these organs. To achieve this goal, the antioxidant activity was evaluated *in vitro* and at the cellular level, by measuring its capacity to reduce the level of intracellular ROS, lipid peroxidation, and NO levels in human hepatic HepG2 and human intestinal Caco-2 cells, where the oxidative stress was induced by H_2O_2. The second objective of the study was an assessment of the intestinal transport of the different phenolic components of the BUO phytocomplex that was performed using differentiated Caco-2 cells as a model of mature enterocytes.

4.2 Materials and Methods

4.2.1 Materials and Cell Cultures

All chemicals and reagents were commercially available, and more details are reported in the Supplementary Materials.

4.2.2 Cell Culture

HepG2 cells and Caco-2 cells were cultured in DMEM high glucose with stable L-glutamine, supplemented with 10% FBS, 100 U/mL penicillin, 100 µg/mL streptomycin (complete growth medium) with incubation at 37 °C under 5% CO_2 atmosphere. Caco-2 cells were routinely sub-cultured at 50% density (Natoli *et al.*, 2012). HepG2 cells were used for no more than 20 passages after thawing, since the

increase in passage number may change the cell morphology and characteristics and impair assay results.

4.2.3 Production of the EVOO Extract

An EVOO sample produced by Società Agricola Buonamici SrL (Fiesole, Florence, Italy) in the 2017 olive oil campaign from monocultivar olives of the typical Tuscan cultivar Frantoio was used for the study (BUO oil). The BUO extract was obtained following the procedures previously described (Lammi *et al.*, 2020). See Supplementary Materials for detailed information and conditions.

4.2.4 3-(4,5-Dimethylthiazol-2-yl)-2,5-Diphenyltetrazolium Bromide (MTT) Assay

A total of 3×10^4 HepG2 cells/well and 5×10^4 Caco-2 cells/well were seeded in 96-well plates and treated with 25.0, 50.0, 100.0, and 200.0 μg/mL of BUO extract, or vehicle (H_2O) in complete growth media for 48 h at 37 ◦C under 5% CO_2 atmosphere. Experiments were performed by a standard method with slight modifications (Lammi *et al.*, 2020b) and more details are provided in Supplementary Materials.

4.2.5 2,2-Diphenyl-1-Picrylhydrazyl (DPPH) Assay

The DPPH assay to determine the antioxidant activity *in vitro* and *in situ* was performed by a standard method with some slight modifications (Lammi *et al.*, 2020b). More details are reported in Supplementary Materials. Briefly, for the *in situ* experiments, 3×10^4 HepG2 and Caco-2 cells/well were seeded in a 96-well plate, overnight in growth medium and the following day they were treated with the BUO extract at a concentration of 25 μg/mL for 24 h at 37 ◦C under 5% CO_2 atmosphere. More details are provided in Supplementary Materials where the calibration curve using Trolox has been obtained (Figure S1).

4.2.6 TEAC Assay

The TEAC assay is based on the reduction of the 2,2-azino-bis-(3-ethylbenzothiazoline-6-sulfonic acid (ABTS) radical induced by antioxidants. The ABTS radical cation (ABTS•+ was prepared by mixing a 7 mM ABTS solution (Sigma-Aldrich, Milan, Italy) with 2.45 mM potassium persulfate (1:1) and stored for 16 h at room temperature and in dark. To prepare the ABTS reagent, the ABTS•+ was diluted in 5 mM phosphate

buffer (pH 7.4) to obtain a stable absorbance of 0.700 (±0.02) at 730 nm. For the assay, 10 μL of BUO extract (at the final concentrations of 0.5, 1.0, 5.0, and 10.0 μg/mL) were added to 140 μL of diluted the $ABTS^{\bullet+}$. The microplate was incubated for 30 min at 30 °C and the absorbance was read at 730 nm using a SynergyTM HT-multimode microplate reader (Biotek Instruments, Winooski, VT, USA). The TEAC values were calculated using a Trolox (Sigma-Aldrich, Milan, Italy) calibration curve (60–320 μM) (Figure S1).

4.2.7 FRAP Assay

The FRAP assay evaluates the ability of a sample to reduce ferric ion (Fe^{3+}) into ferrous ion (Fe^{2+}). Thus, 10 μL of the sample (BUO extract and the lysed cells sample diluted 1:5 in distilled water) was mixed with 140 μL of FRAP reagent. The FRAP reagent was prepared by mixing 1.3 mL of a 10 mM TPTZ (Sigma-Aldrich, Milan, Italy) solution in 40 mM HCl, 1.3 mL of 20 mM $FeCl_3 \times 6H_2O$ and 13 mL of 0.3 M acetate buffer (pH 3.6). The microplate was incubated for 30 min at 37 °C and the absorbance was read at 595 nm. The results were calculated by a Trolox (Sigma-Aldrich, Milan, Italy) standard curve obtained using different concentrations (3–400 μM) (Figure S1). Absorbances were recorded on a SynergyTM HT-multimode microplate reader. Briefly, as regards the FRAP assay at the cellular level, HepG2 and Caco-2 cells (1.5×10^5/well) were seeded on a 24-well plate. The next day, cells were treated with the BUO at 10, and 25 μg/mL for 24 h at 37 °C under a 5% CO_2 atmosphere. After incubation, cells were treated with H_2O_2 (1.0 mM) or vehicle (H_2O) for 60 min, then lysed using 40 μL urea 8 M Subsequently, these were diluted 1:5 in distilled water and the FRAP assay was performed as above described.

4.2.8 ORAC Assay

The ORAC assay is based on the scavenging of peroxyl radicals generated by the azo 2,2′-azobis(2-methylpropionamidine) dihydrochloride (AAPH, Sigma-Aldrich, Mi- lan, Italy). Briefly, 25 μL of BUO extract (with a final concentration of 0.5, 1.0, 5.0, and 10.0 μg/mL) was added to 50 μL sodium fluorescein (2.934 mg/L) (Sigma-Aldrich, MO, USA) and incubated for 15 min at 37 °C. Then, 25 μL of AAPH (60.84 mM) were added and the decay of fluorescein was measured at its maximum emission of 528/20 nm every 5 min for 120 min using a SynergyTM HT-multimode microplate reader (Biotek Instruments, Winooski, VT, USA). The area under the curve (AUC) was

calculated for each sample subtracting the AUC of the blank. The results were calculated using a Trolox calibration curve (2–50 μM) (Figure S1).

4.2.9 Fluorometric Intracellular ROS Assay

The ROS assay was performed by a standard method with some slight modifications (Lammi *et al.*, 2019) and more detailed information are reported in Supplementary Material. Briefly, HepG2 (3×10^4) and Caco-2 (5×10^4) cells were incubated with 5 μL of BUO (1, 10, and 25 μg/mL) for 1 h in the dark. To induce ROS formation, H_2O_2 (0.5 mM) for 30 min at 37 °C in the dark was used. Fluorescence signals (ex./em. 490/525 nm) were recorded using a Synergy H1 microplate reader (Biotek Instruments, Winooski, VT, USA).

4.2.10 Lipid Peroxidation (MDA) Assay

The MDA assay was performed by a standard method with some slight modifications (Lammi *et al.*, 2019). See Supplementary Material for detailed information. Briefly, HepG2 and Caco-2 (2.5×10^5 cells/well) cells were treated with BUO extract (1, 10, and 25 μg/mL) for 24 h. The day after, cells were incubated with H_2O_2 (1 mM) or vehicle (H_2O) for 30 min, then collected and homogenized in 150 μL ice-cold MDA lysis buffer. The MDA-TBA adduct was analyzed by measuring the absorbance at 532 nm using the Synergy H1 fluorescent plate reader (Biotek Instruments, Winooski, VT, USA). To normalize the data, total proteins for each sample were quantified by the Bradford method.

4.2.11 Nitric Oxide Level Evaluation on HepG2 and Caco-2 Cells, Respectively

HepG2 and Caco-2 cells (1.5×10^5/well) were seeded on a 24-well plate. The next day, cells were treated with the EVOO extract at different concentrations (1, 10, and 25 μg/mL) for 24 h at 37 ◦C under a 5% CO_2 atmosphere. After incubation, cells were treated with H_2O_2 (1.0 mM) or vehicle (H_2O) for 60 min, then the cell culture media were collected and centrifuged at 13,000× g for 15 min to remove insoluble material. NO determination was carried out following the conditions reported in the Supplementary Material.

4.2.12 iNOS Protein Level Evaluation by Western Blot Analysis

A total of 1.5×10^5 HepG2 and Caco-2 cells/well were seeded on 24-well plates and incubated at 37 °C under a 5% CO_2 atmosphere. The following day, cells were treated with 1, 10, and 25 μg/mL of the BUO extract in a complete growth medium for 24 h. Western Blot experiments were performed using primary antibodies anti-iNOS and anti- β-actin following conditions previously reported (Zanoni *et al.*, 2017). See Supplementary Material for further details.

4.2.13 Caco-2 Cell Culture and Differentiation

For differentiation, Caco-2 cells were seeded on polycarbonate filters, 12 mm diameter, 0.4 μm pore diameter (Transwell, Corning Inc., Lowell, MA, USA) at a density of 3.5×10^5 cells/cm^2 in complete medium supplemented with 10% FBS in both apical (AP) and basolateral (BL) compartments for 2d to allow the formation of a confluent cell mono- layer. Starting from day three after seeding, cells were transferred to an FBS-free medium in both compartments, supplemented with ITS [final concentration 10 mg/L insulin (I), 5.5 mg/L transferrin (T), 6.7 μg/L sodium selenite (S); GIBCO-Invitrogen, San Giuliano Milanese, Italy] only in the BL compartment, and allowed to differentiate for 21 days with regular medium changes three times weekly (Lammi *et al.*, 2020c).

4.2.14 Cell Monolayers Integrity Evaluation

The transepithelial electrical resistance (TEER) of differentiated Caco-2 cells was measured at 37 °C using the voltmeter apparatus Millicell (Millipore Co., Burlington, MA, USA), immediately before and at the end of the absorption experiments. In addition, at the end of the absorption experiments, cells were incubated from the AP side with 1 mM phenol-red in PBS with $CaCl_2$ and $MgCl_2$ for 1 h at 37 °C, to monitor the paracellular permeability of the cell monolayer. The BL solutions were then collected and NaOH (70 μL, 0.1 N) was added before reading the absorbance at 560 nm in a microplate reader (Synergy H1, Biotek, Winooski, VT, USA). The phenol-red passage was quantified using a standard phenol-red curve. Only filters showing TEER values and phenol red passages similar to untreated control cells were taken into consideration for peptide transport analysis.

4.2.15 Trans-Epithelial Transport of BUO Extract

Prior to experiments, the cell monolayer integrity and differentiation were checked by TEER measurement as described above. Cells were then washed twice, and peptide absorption assayed. Absorption experiments were performed in transport buffer solution (137 mM NaCl, 5.36 mM KCl, 1.26 mM $CaCl_2$, and 1.1 mM $MgCl_2$, 5.5 mM glucose) according to previously described conditions (Aiello *et al.*, 2018). The BUO extract absorption and the metabolism were assayed by loading the upper compartment with BUO extract (at the concentration of 100 and 200 μg/mL) in the AP transport solution (500 μL) and the lower compartment with the BL transport solution (700 μL). Transport experiments were con- ducted for 2 h. See Supplementary Materials for detailed information and conditions.

4.2.16 HPLC-DAD-MS Analysis for Evaluating the Trans-Epithelial Transport of BUO Extract

The dried cellular extracts were dissolved in 150 μL of EtOH:H_2O 2:1 v/v and, after centrifugation at 16,900× g for 5 min, the supernatant was recovered and used for the analyses. The instrument was an HP 1260 MSD mass spectrometer with an API/electrospray interface (Agilent Technologies, Santa Clara, CA, USA). The column was a Poroshell 120, EC-C18 (150 mm × 3.0 mm id, 2.7 μm; Agilent, Santa Clara, CA, USA) with a precolumn of the same phase. The mobile phase was acetonitrile (A) and H_2O at pH 3.2 by HCOOH (B). The following multistep linear gradient was applied: from 5% to 40% A in 40 min, to 88% A in 5 min, and then to 98% A in 10 min, with a final plateau of 3 min (total time 58 min); flow rate was 0.4 mL/min. For the MS detector, the conditions were: negative ion mode, gas temperature 350 ◦C, nitrogen flow rate 10.5 L/min, nebulizer pressure 35 psi (241 KPa), capillary voltage 3500 V, and fragmentation energy between 80 and 150 V.

4.2.17 Statistical Analysis

Statistical analyses were carried out by One-way, and Two-way ANOVA followed by Tukey's post-hoc analysis, respectively (Graph-pad Prism 8). Values were expressed as means ± SD; p-values < 0.05 were considered to be significant.

4.3 Results and Discussion

4.3.1 Antioxidant Activity of the BUO Extract

The *in vitro* antioxidant capacity of the BUO extract was tested at 0.5, 1, 2.5, and 5 μg/mL using the TAEC, FRAP, and ORAC assays, whereas the DPPH assay was tested in the range of 10–100 μg/mL. The phenolic composition of BUO, according to a previous study (Martinez-Gonzalez *et al.*, 2014), is shown in Table S1. The BUO extract scavenged the ABTS radical by 214.9 ± 10.1%, 325 ± 41.1%, 728.2 ± 44.2%, and 1201.4 ± 25.6% at 0.5, 1, 2.5, and 5 μg/mL, respectively ($p < 0.001$, Figure 1A). In addition, in the ORAC test, this extract was able to scavenge the peroxyl radicals generated by 2,2'-azobis(2-methylpropionamidine) dihydrochloride up to 1059 ± 23%, 3638 ± 579%, 7782 ± 1070%, and 9837 ± 1175% versus the control sample at 0.5, 1, 2.5, and 5 μg/mL, respectively ($p < 0.0001$, Figure 1B). Figure 1C shows that the BUO extract increased the FRAP by 246.7 ± 12.8%, 493.2 ± 23.4%, 1250 ± 64.8%, and 2583 ± 73.7% at 0.5, 1, 2.5, and 5 μg/mL, respectively ($p < 0.0001$). Finally, as shown by Figure 1D, the same extract scavenged the DPPH radical by 10.7 ± 0.3%, 23.4 ± 2.3%, 47.6 ± 2.7, and 69.3 ± 1.4% at 10, 25, 50, and 100 μg/mL, respectively. In all the above assays, the response was dependent on the dose. All these results support the efficient antioxidant power of the BUO extract, which has a high content of Ole derivatives and a prevalence of HO-Tyr derivatives (445 μg/g) on Tyr derivatives (333 μg/g), which actively contribute to the *in vitro* scavenging activity. In a previous paper, the antioxidant activity of the phenolic EVOO extract, prepared with the same procedure from an Apulian EVOO from the cultivar Coratina, showed similar antioxidant activity, although this phytocomplex contained a prevalence of Tyr derivatives (Lammi *et al.*, 2020). In parallel, the radical scavenging activity of the BUO extract was also evaluated at the cellular level in HepG2 cells and Caco-2 cells by using DPPH. Before conducting these experiments, however, it was necessary to perform MTT experiments to exclude any potential cytotoxic effect. As shown in Figure S2, after 48 h of incubation of Caco-2 cells at the highest concentration (200 μg/mL), the BUO extract slightly reduced cell viability by 7.5 ± 0.9%. This result is in line with a previous investigation showing that it significantly impairs the viability of HepG2 cells at 200 μg/mL, but not at lower concentrations (Martinez-Gonzalez *et al.*, 2014). The DPPH assay was performed directly on HepG2 and Caco-2 cell lysates, after treatment with the BUO extract at the fixed concentration of 25 μg/mL, which is roughly 10 times lower than the first cytotoxic dose on HepG2 cells. The BUO extract reduced the DPPH radical by 35.5 ± 8.3% and 22.8 ± 9.0% on HepG2 and Caco-2 cells, respectively (Figure S3).

4.3.2 The BUO Extract Decreases the H_2O_2-Induced Oxidative Stress in Hepatic and Intestinal Cells

These preliminary results prompted us to carry out a deeper investigation on the antioxidant effect of the BUO extract at the cellular level, measuring its protective effect after induction of oxidative stress using H_2O_2 by the FRAP assay. As shown in Figure 2, treatment with 25 μg/mL of the BUO extract reverted the H_2O_2-induced oxidative stress in both HepG2 (Figure 2A) and Caco-2 (Figure 2B) cells. Furthermore, the experiments in HepG2 cells showed that 10 μg/mL of the BUO extract were sufficient to reverse the effects induced by hydrogen peroxide. More in detail, H_2O_2 (1 mM) decreased the antioxidant capacity measured by FRAP up to 81.0 ± 21.0% and 71.6 ± 27.8%, respectively, in HepG2 and Caco-2 cells. The pre-treatment of HepG2 cells with the BUO extract restored the FRAP up to 120.7 ± 31.7% and 141.6 ± 35.3% at 10 and 25 μg/mL, respectively, while the pre- treatment of Caco-2 cells increased FRAP up to 99.1 ± 33% and 124.6 ± 30%, respectively, at the same two concentrations (Figure 2A,B).

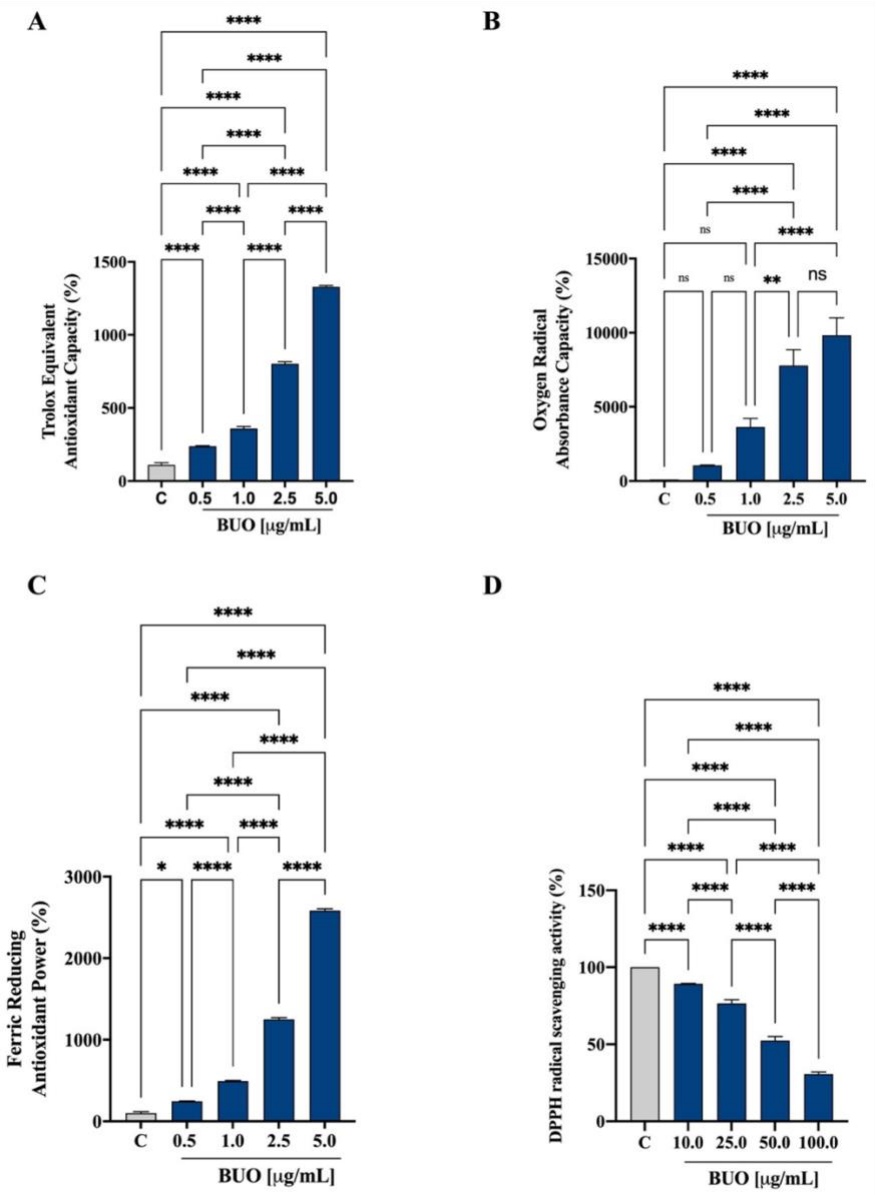

Figure 1. *In vitro* antioxidant power evaluation of the phenolic extract (BUO) extract by 2,2-azino-bis-(3-ethylbenzothia-6-sulfonic acid (ABTS) (**A**), Oxygen Radical Absorbance Capacity (ORAC) (**B**), ferric reducing antioxidant power (FRAP) (**C**), and 2,2-diphenyl-1-picrylhydrazyl (DPPH) (**D**) assays. The data points represent the averages ± SD of four independent experiments performed in duplicate. All data sets were analyzed by One-way ANOVA followed by Tukey's post-hoc test. ns: not significant and C: control sample (H_2O). (*) $p < 0.5$; (**) $p < 0.01$; (****) $p < 0.0001$.

All these results support the efficient antioxidant power of the BUO extract, which has a high content of Ole derivatives and a prevalence of HO-Tyr derivatives (445 µg/g) on Tyr derivatives (333 µg/g), which actively contribute to the *in vitro* scavenging activity. In a previous paper, the antioxidant activity of the phenolic EVOO extract, prepared with the same procedure from an Apulian EVOO from the cultivar Coratina, showed similar antioxidant activity, although this phytocomplex contained a prevalence of Tyr derivatives (Lammi *et al.*, 2020). In parallel, the radical scavenging activity of the BUO

extract was also evaluated at the cellular level in HepG2 cells and Caco-2 cells by using DPPH. Before conducting these experiments, however, it was necessary to perform MTT experiments to exclude any potential cytotoxic effect. As shown in Figure S2, after 48 h of incubation of Caco-2 cells at the highest concentration (200 µg/mL), the BUO extract slightly reduced cell viability by 7.5 ± 0.9%. This result is in line with a previous investigation showing that it significantly impairs the viability of HepG2 cells at 200 µg/mL, but not at lower concentrations (Martinez-Gonzaleze *et al.*, 2014). The DPPH assay was performed directly on HepG2 and Caco-2 cell lysates, after treatment with the BUO extract at the fixed concentration of 25 µg/mL, which is roughly 10 times lower than the first cytotoxic dose on HepG2 cells. The BUO extract reduced the DPPH radical by 35.5 ± 8.3% and 22.8 ± 9.0% on HepG2 and Caco-2 cells, respectively (Figure S3).

4.3.3 The BUO Extract Decreases the H_2O_2-Induced Oxidative Stress in Hepatic and Intestinal Cells

These preliminary results prompted us to carry out a deeper investigation on the antioxidant effect of the BUO extract at the cellular level, measuring its protective effect after induction of oxidative stress using H_2O_2 by the FRAP assay. As shown in Figure 2, treatment with 25 µg/mL of the BUO extract reverted the H_2O_2-induced oxidative stress in both HepG2 (Figure 2A) and Caco-2 (Figure 2B) cells. Furthermore, the experiments in HepG2 cells showed that 10 µg/mL of the BUO extract were sufficient to reverse the effects induced by hydrogen peroxide. More in detail, H_2O_2 (1 mM) decreased the antioxidant capacity measured by FRAP up to 81.0 ± 21.0% and 71.6 ± 27.8%, respectively, in HepG2 and Caco-2 cells. The pre-treatment of HepG2 cells with the BUO extract restored the FRAP up to 120.7 ± 31.7% and 141.6 ± 35.3% at 10 and 25 µg/mL, respectively, while the pre-treatment of Caco-2 cells increased FRAP up to 99.1 ± 33% and 124.6 ± 30%, respectively, at the same two concentrations (Figure 2A,B).

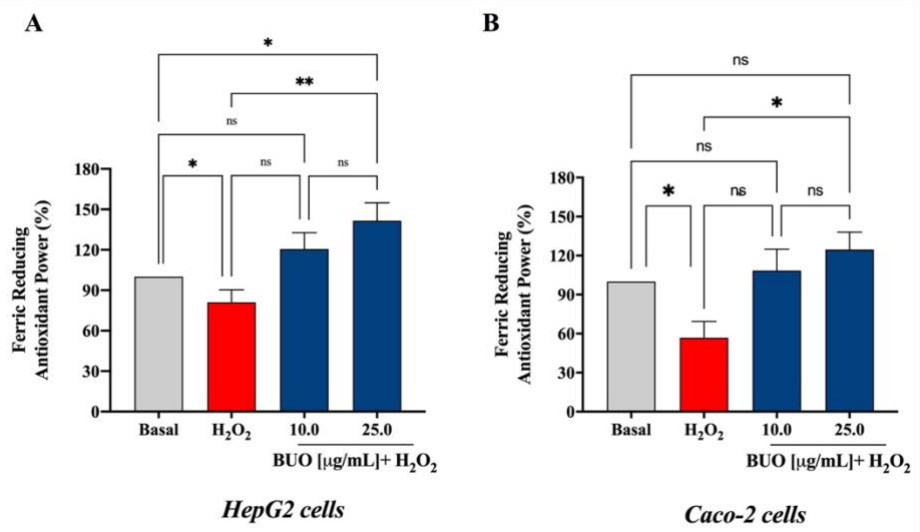

Figure 2. Antioxidant capacity of the BUO extract assayed at the cellular level, by ferric reducing antioxidant power (FRAP) assay. On (**A**) HepG2 and (**B**) Caco-2 cells, the BUO extract reverted the oxidative stress induced by 1 mM H_2O_2. Data represent the mean ± SD. of three independent experiments performed in duplicate. All data sets were analyzed by One-way ANOVA followed by Tukey's post-hoc test. ns: not significant; (*) $p < 0.5$; (**) $p < 0.01$. Basal: untreated cells.

4.3.4 The BUO Extract Decreases the H_2O_2-Induced ROS in Hepatic and Intestinal Cells

The exposure of HepG2 and Caco-2 cells to H_2O_2 alone produced a dramatic increment of the intracellular ROS levels by 223.8 ± 4.3% and 186.2 ± 3.3%, respectively, versus the control cells (basal value = 100%, $p < 0.5$ in HepG2 cells and $p < 0.001$ in Caco-2 cells), whereas these increments were attenuated by the pre-treatment with the BUO extract in both cell lines (Figure 3A,B). In HepG2 cells, the BUO extract reduced the H_2O_2-induced intracellular ROS by 104.6 ± 7.6%, 82.9 ± 7.6%, and 51.4 ± 0.9%, respectively, at 1.0, 10, and 25 µg/mL ($p < 0.0001$) (Figure 3A), whereas in Caco-2 cells by 101.5 ± 4.9, 78.0 ± 5.1, and 57.6 ± 6.3 at 1, 10, and 25 µg/mL ($p < 0.0001$), respectively (Figure 3B). These findings suggest that after oxidative stress induced by H_2O_2, HepG2 cells are more susceptible than Caco-2 cells ($p < 0.0001$) to the ROS level production and that the pre-treatment with the BUO extract significantly protects both cell lines against the induced oxidative stress. Interestingly, despite the presence of any inducing stimulus, at the highest concentrations (10 and 25 µg/mL), the ROS levels are significantly reduced below the basal values in both HepG2 ($p < 0.5$) and Caco-2 cells ($p < 0.01$). It is important to emphasize that, at 10 and 25 µg/mL, the BUO extract was much more effective in decreasing the H_2O_2-induced ROS levels in HepG2 cells (82.9

± 7.6%, and 51.4 ± 0.9%, respectively) than the extract from the *Coratina* cultivar (198.8 ± 12.5% and 130.3 ± 11.3%, respectively) (Lammi *et al.*, 2020). This difference may possibly be explained by their different phenolic profiles, since the BUO extract contains much more Ole derivatives (444.9 µg/g, measured as total OH-Tyr after hydrolysis), whereas the *Coratina* extract much more ligstroside derivatives (308.6 µg/g, measured as total Tyr after hydrolysis) (Lammi *et al.*, 2020). In fact, OH-Tyr is a very efficient inhibitor of the ROS generation induced by tert-butylhydroperoxide (t-BOOH) in HepG2 cells (Goya *et al.*, 2007).

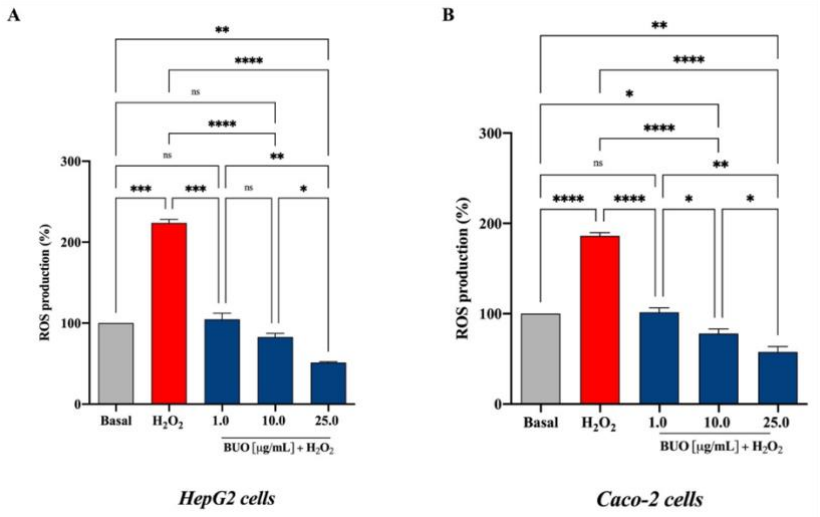

Figure 3. Evaluation of the effects of the BUO extracts on H_2O_2-induced reactive oxygen species (ROS) production levels in human hepatic HepG2 (**A**) and intestinal Caco-2 (**B**) cells. The data points represent the averages ± SD of six independent experiments in duplicate. Basal vs. H2O2 samples were analyzed by t-student test, whereas All data sets were analyzed by One-way ANOVA followed by Tukey's post-hoc test. ns: not significant; (*) $p < 0.5$; (**) $p < 0.01$; (***) $p < 0.001$; (****) $p < 0.0001$. Basal: untreated cells.

4.3.5 The BUO Extract Decreases H_2O_2-Induced Lipid Peroxidation in HepG2 and Caco-2 Cells

The attack of oxygen free radicals on cellular lipids results in the formation of aldehydic lipid hydroperoxide decomposition products, such as MDA, which is traditionally considered a reliable marker of lipid peroxidation. Therefore, to link the BUO capacity of reducing the ROS production with its effect on the stability and integrity of hepatic and intestinal cells, lipid peroxidation was evaluated by intracellular levels of MDA after induction of oxidative stress using H_2O_2. The exposure of HepG2 and Caco-2 cells to H_2O_2 alone produced an increment of intracellular MDA levels by 125.1 ± 7.1% and 132.1 ± 8.5%, respectively, versus control cells (basal value = 100%, $p < 0.0001$ in

HepG2 cells and $p < 0.0001$ in Caco-2 cells). This was attenuated by a pre-treatment with the BUO extract in both cell lines (Figure 4A,B). In fact, the BUO extract decreased the MDA levels below the basal ones in both cell models. In particular, in HepG2 cells ($p < 0.001$) the BUO extract diminished the H_2O_2-induced intracellular MDA by 55.9 ± 4.4%, 53.3 ± 8.9%, and 48.6 ± 7.3%, respectively, at 1, 10, and 25 µg/mL (Figure 4A), and in Caco-2 cells ($p < 0.0001$) by 75.8 ± 10.3, 70.1 ± 8.1, and 62.7 ± 9.6, respectively, at 1, 10, and 25 µg/mL (Figure 4B). After treatment with 1 mM H_2O_2, Caco-2 cells appeared to be slightly more sensitive to the MDA production than HepG2 cells, as shown by the increased MDA levels in HepG2 versus Caco-2 cells ($p < 0.01$). OH-Tyr and Tyr may be the most relevant phenolic compounds responsible for the modulation of intracellular lipid peroxidation levels. Indeed, clear evidence suggests that OH-Tyr protects the integrity of the HepG2 cellular membrane leading to a reduction of MDA levels after t-BOOH induced oxidative stress (Goya *et al.*, 2007). Similarly, Tyr reduces lipid peroxidation in HepG2 cells exposed to acute ethanol treatment (Stiuso *et al.*, 2016). Other evidence confirms that Tyr has a protective effect on membrane integrity also in other cellular systems. On the contrary, the Ole-mediated protective effect against oxidative stress is not associated with a reduction of MDA generation (Katsoulieris *et al.*, 2016). Interestingly, the BUO extract does not contain any intact Ole but only its non-glycosylated derivatives, which presumably show a greater ability to interact with membrane lipids.

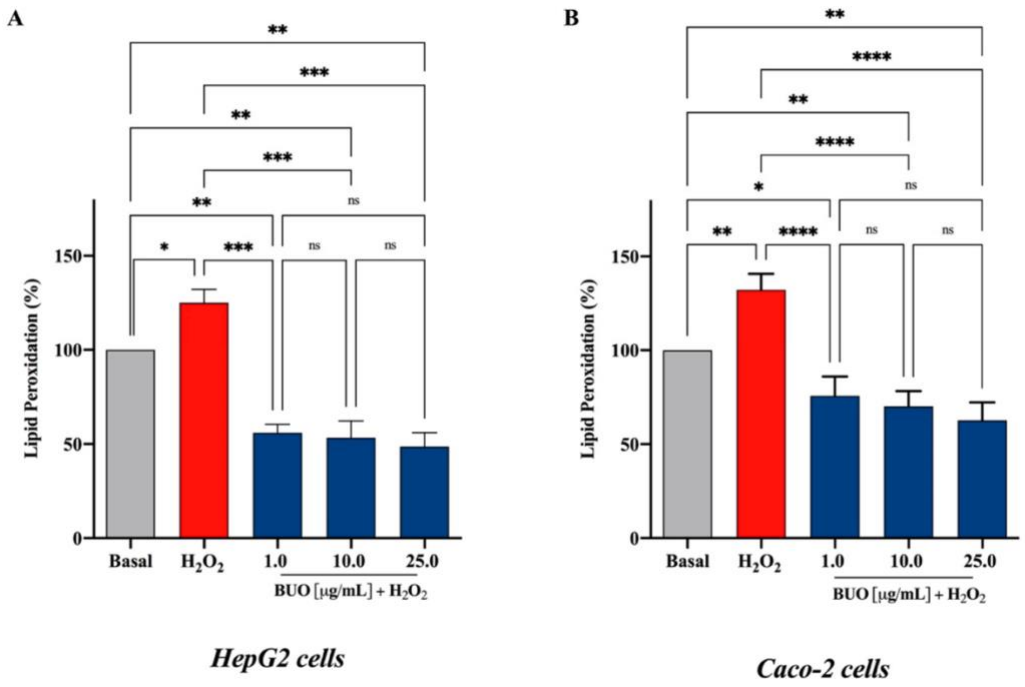

Figure 4. Evaluation of the effects of the BUO extract on H_2O_2-induced lipid peroxidation levels in human hepatic HepG2 cells (**A**) and intestinal Caco-2 cells (**B**) as assessed by intracellular MDA levels. The data points represent the averages ± SD of six independent experiments in duplicate. All data sets were analyzed by One-way ANOVA followed by Tukey's post-hoc test. ns: not significant; (*) $p < 0.5$, (**) $p < 0.01$, (***) $p < 0.001$, (****) $p < 0.0001$. Basal: untreated cells.

4.3.6 The BUO Extract Modulates the H_2O_2-Induced NO Level Production via the iNOS Protein Modulation in HepG2 and Caco-2 Cells

ROS can act either as signaling molecules or as mediators of inflammation (Mittal *et al.*, 2014). Superoxide can rapidly combine with NO to form reactive nitrogen species (RNS), such as peroxynitrite, with a reaction rate that is faster than the dismutation of superoxide by superoxide dismutase (Beckman *et al.*, 1996). In addition, RNS leads to nitrosative stress, which parallels the pro-inflammatory activity of ROS (Sunil *et al.*, 2012). Emerging evidence has clearly underlined the intricate relation between oxidative stress and inflammation (Mittal *et al.*, 2014). Based on these considerations, the effects of the BUO extract on NO production were evaluated on both human hepatic HepG2 and intestinal Caco-2 cells, after oxidative stress induction. H_2O_2 (1 mM) treatment induced oxidative stress which led to an increase of intracellular NO levels up to 153.5 ± 18% and 152.4 ± 11.6%, respectively, in HepG2 and Caco-2 (Figure 5). Pre-treatment with the BUO extract reduced the H_2O_2-induced NO overproduction, reducing the values closer or even lower than the basal levels ($p < 0.0001$). Notably, the BUO extract reduced NO up to 92 ± 14.4%, 63.3 ± 8.1%, and 54.3 ± 10.2%,

respectively, at 1, 10, and 25 µg/mL in HepG2 cells ($p < 0.0001$, Figure 5A), whereas, up to 85.7 ± 18%, 57.7 ± 12.8%, and 20.4 ± 12.6%, respectively, at 1.0, 10.0, and 25.0 µg/mL in Caco-2 cells ($p < 0.0001$, Figure 5B). iNOS, is an enzyme expressed in different cell types (Soskić *et al.*, 2011) that is usually induced during inflammatory events (Habib *et al.*, 2011). The generation of NO by iNOS is associated with the alteration of NO homeostasis, which is linked to many pathophysiological conditions. In this study, the effect of the BUO extract on iNOS protein levels after oxidative stress induction was assessed by western blot experiments, in which the iNOS protein band at 130 kDa was detected and quantified (Figure 5C,F). After H_2O_2 treatment (1 mM), the iNOS protein increased up to 127 ± 14.8% ($p < 0.5$) and 148 ± 6.7% ($p < 0.0001$) in HepG2 and Caco-2 cells, respectively. In agreement with the modulation of NO production, the pre-treatment of both cell models with the BUO extract reduced the H_2O_2-induced iNOS protein, bringing their levels close to basal conditions. In particular, the BUO extract reduced iNOS levels up to 111.5 ± 16.5%, 109.8 ± 10%, and 78.6 ± 12.6% at 1, 10, and 25 µg/mL, respectively, in HepG2 cells ($p < 0.01$, Figure 5C,E), whereas in Caco-2 cells, they were reduced up to 118.3 ± 9%, 109.9 ± 0.2%, 101.4 ± 1.3% at 1, 10, and 25 µg/mL, respectively, ($p < 0.001$, Figure 5D,F). Many studies underline the importance of EVOO phenols in limiting the NO production, but most of them are focused on the characterization of the effects of single phenols rather than of the total EVOO phytocomplex. In fact, it has been demonstrated that mostly OH-Tyr (Bigagli *et al.*, 2017, Maiuri *et al.*, 2005, Takeda *et al.*, 2014) can inhibit the NO overproduction induced by lipopolysaccharides (LPS) in monocytes and macrophages. In addition, glucuronide and sulfate metabolites of OH-Tyr and Tyr, together with their free forms, counteract the LPS-induced release of NO, acting as inhibitors of iNOS expression (Serreli *et al.*, 2019) Only scarce evidence exists regarding the ability of complex EVOO extracts to impair NO overproduction. In agreement with our results, EVOO phenolic extracts from the *Bosana* cultivar (South of Sardinia) have been reported to limit oxysterols-mediated NO and cytokines overproduction, by modulating iNOS expression in Caco-2 cells (Serra *et al.*, 2018). These pieces of evidence together with our results highlight the need to direct more efforts to the characterization of the bioactivity of the whole EVOO phytocomplex for a fruitful valorization of this food, which is more complex than the sum of each single bioactive component (Jacobs *et al.*, 2007).

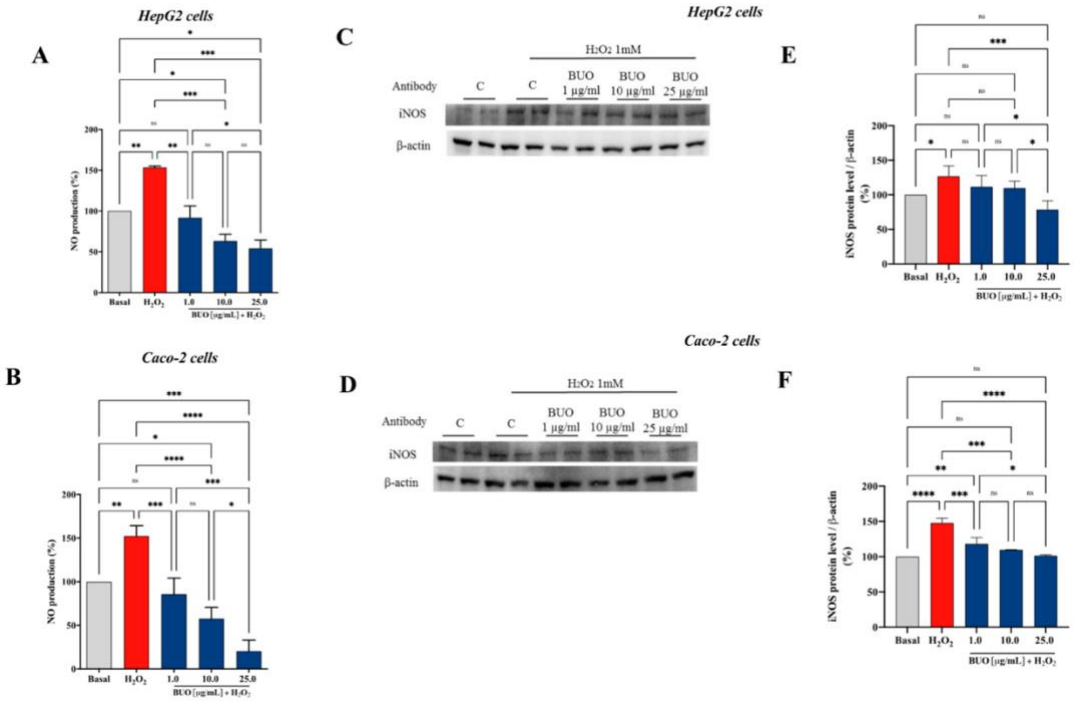

Figure 5. Effect of the BUO extract on the H_2O_2 (1 mM)-induced NO levels (A,B) and inducible nitric oxide synthase (iNOS) protein levels (C–F) in human hepatic HepG2 cells (A,C,E) and intestinal Caco-2 cells (B,D,F). The data points represent the averages ± SD of six independent experiments in duplicate. All data sets were analyzed by One-way ANOVA followed by Tukey's post-hoc test. ns: not significant; (*) $p < 0.5$, (**) $p < 0.01$, (***) $p < 0.001$, (****) $p < 0.0001$. Basal: untreated cells.

4.3.7 Evaluation of the Steady-State Trans-Epithelial Transport of the BUO Extract Using Caco-2 Cells

The intestinal transport of polyphenols is potentially influenced by several affecting factors, such as the food matrix, biotransformation, and conjugation occurring during absorption (D'Archivio *et al.*, 2010, Soler *et al.*, 2010). Up to now, many studies have investigated the absorption of single EVOO phenols, demonstrating that both single OH-Tyr and Tyr are well transported but also metabolized by the intestinal cells (Bailey *et al.*, 2016). On the contrary, little is known about the absorption of the total EVOO phytocomplex and how its complex composition may modulate the transport of single components. To fill this gap, the trans-epithelial transport of the BUO phytocomplex was investigated using differentiated Caco-2 cells. The steady-state study was designed to treat Caco-2 cells with the BUO extract at 100 and 200 µg/mL for 2 h. In all tested conditions, the treatment did not affect the monolayer integrity as monitored by TEER values and phenol red passage (data not shown). After 2 h of incubation, the AP and BL samples were collected from each filter, desalted, dried, and re-dissolved in a

suitable solution to allow their analysis by HPLC-DAD-MS. The phenols recovered in the AP gave some information on the stability of the BUO extract components after incubation with the brush border of intestinal cells (Figure 6, Figure 7 and Figure 8). Instead, the phenols recovered in the BL side provided information on their transport by differentiated Caco-2 cells (Figure 9 and Figure 10).

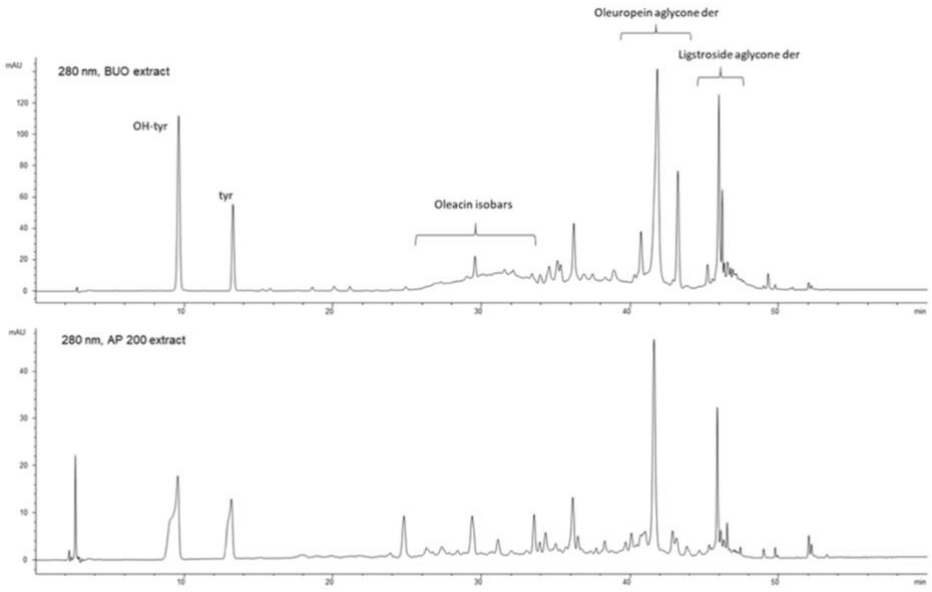

Figure 6. Chromatographic profiles at 280 nm showing OH-Tyr, Tyr, and the main secoiridoidic compounds in BUO and AP200 (AP side of the cells treated at 200 µg/mL) samples after 2 h incubation in the AP compartment.

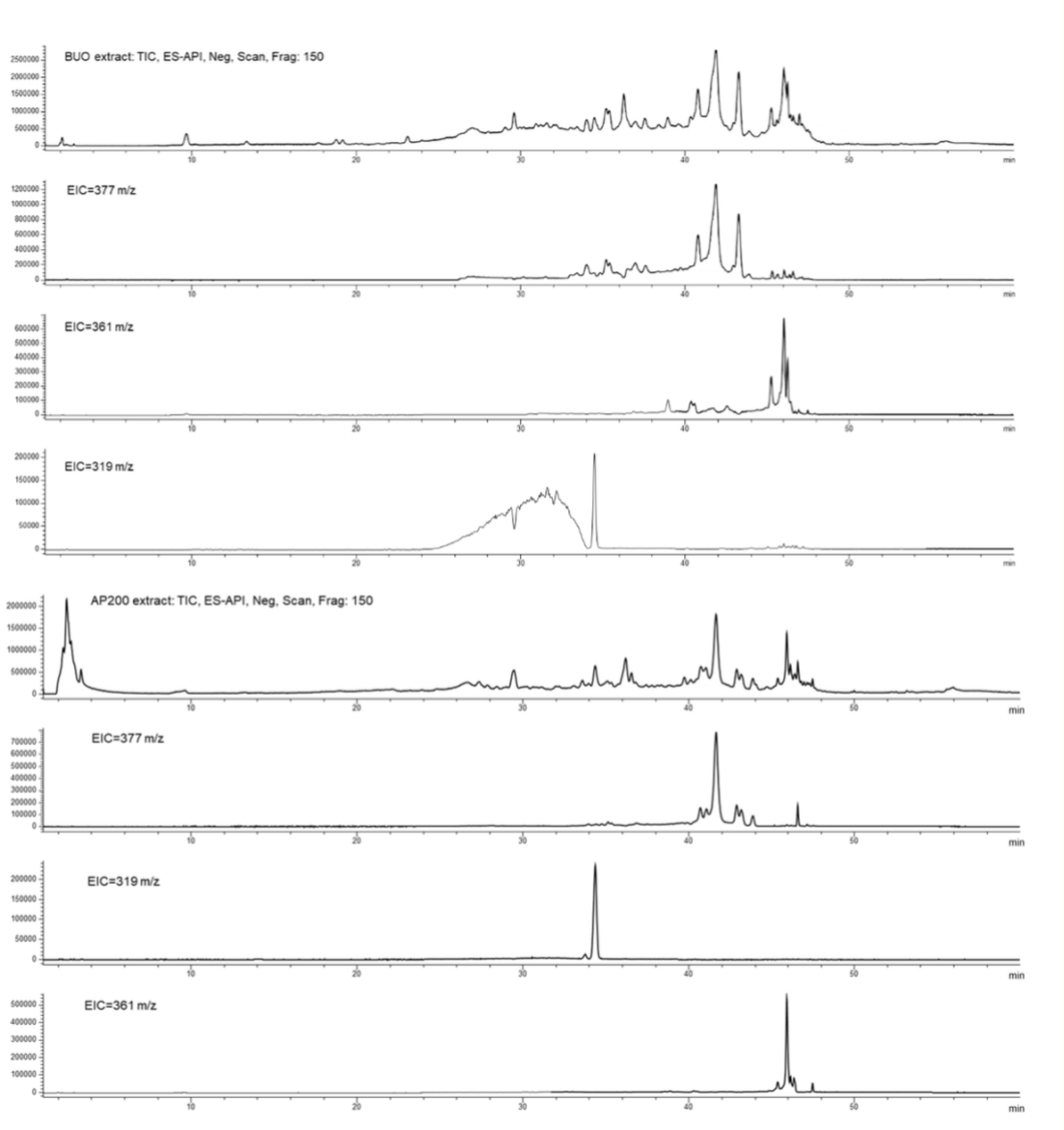

Figure 7. Total ion current (TIC) and extract ion current (IC) profiles of the BUO extract (top) and AP200 sample after incubation (bottom); in both the samples isobars of oleuropein aglycone at 377 m/z, isobars of oleacin at 319 m/z, and isobars of ligstroside aglycones at 361 m/z.

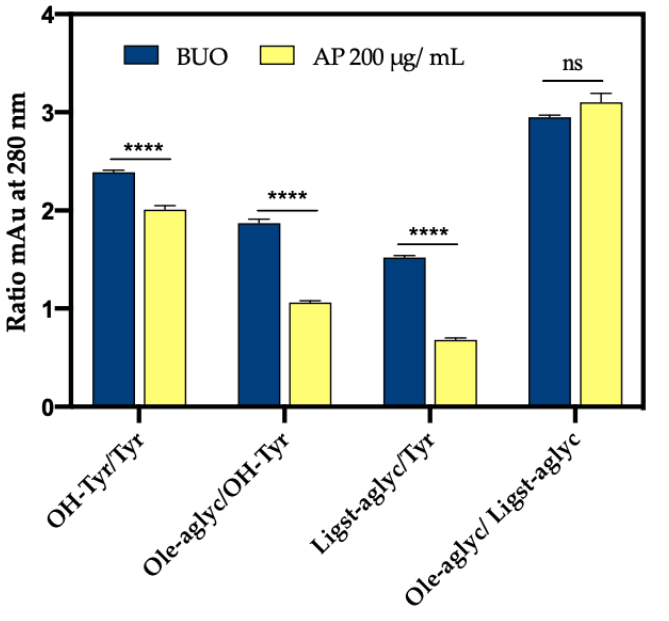

Figure 8. Specific ratios involving OH-Tyr, Tyr, Ole-aglyc, (rt 41.6 min) and ligstroside aglycone (Ligst-aglyc, rt 45.8 min), evaluated as area values at 280 nm for BUO extract and AP sample (AP 200 µg/mL) after 2 h incubation with 200 µg/mL BUO. (****, $p < 0.0001$). ns: not significant. Bars were analyzed by Two-Way ANOVA followed by Tukey's test.

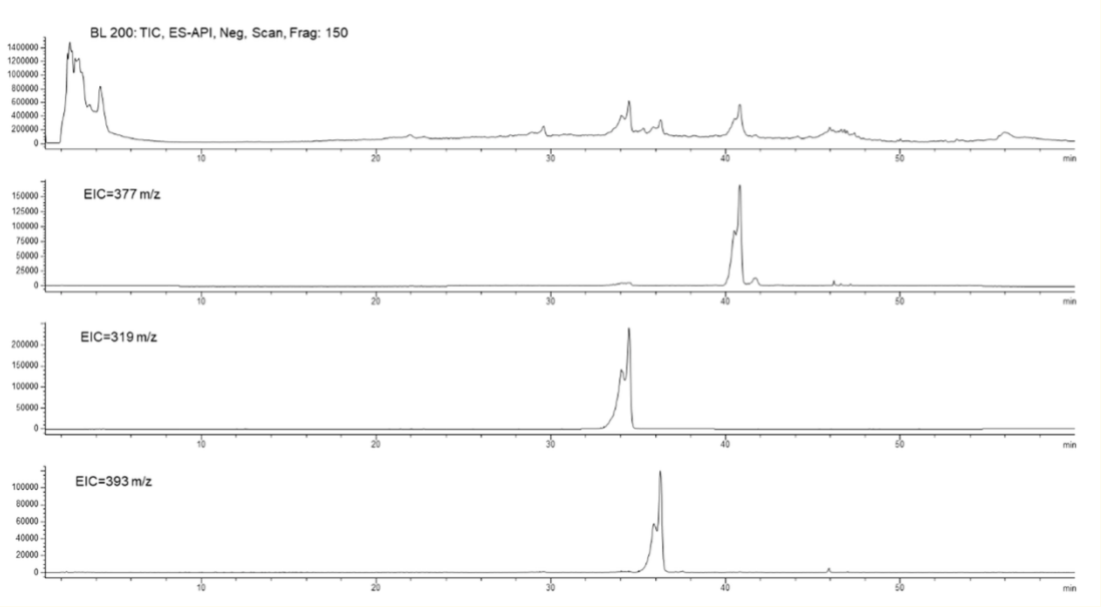

Figure 9. Chromatographic profiles of the BL sample after incubation for 2 h of 200 µg/mL BUO extract in the AP side of Caco-2 cells with, from top to bottom: TIC, EIC at 377 m/z, EIC at 319 m/z, and EIC at 393 m/z.

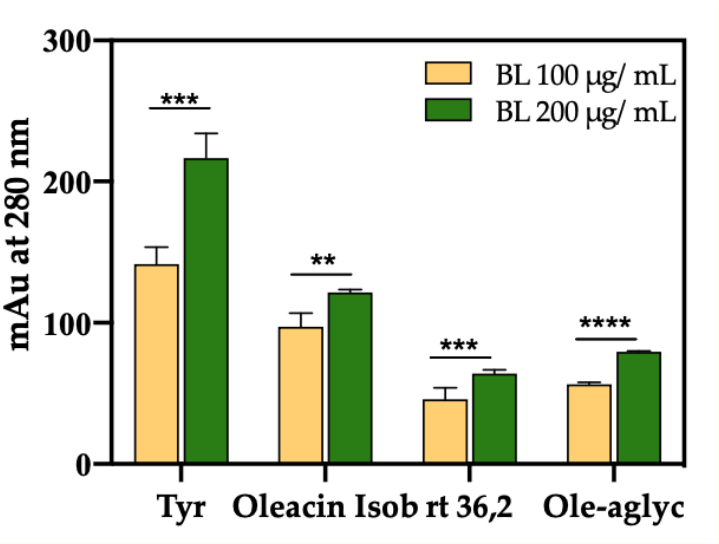

Figure 10. Main phenols in the BL samples were evaluated after incubation with the BUO extract at 100 and 200 µg/mL for 2 h, respectively. The data are the mean of triplicate experiments; the Ole aglycone isobar had rt 41.6 min, its oxidated derivative rt 36.2 and oleacin isobar rt 34.4 min (**, $p < 0.01$; ***, $p < 0.001$; ****, $p < 0.0001$). Bars were analyzed by Two-Way ANOVA followed by Tukey's test.

4.3.7.1 BUO Metabolism in AP Compartment

The chromatographic profiles of the AP solution of the untreated samples did not show any peak in the retention time range corresponding to the elution of the EVOO phenols (Supplementary Figure S4). Overall, the treated AP samples showed a profile very similar to that of the BUO extract (Figure 6), which has a phenolic composition summarized in Table S1. The small variation in peak shape of the most polar phenols (OH-Tyr and Tyr) was determined by the higher injected volume for the AP samples (10 µL), compared to the BUO extract (2 µL). With respect to BUO profile, changes involving the pool of secoiridoid derivatives [retention time (rt) range 28–34 min, rt 43 min, and rt 46 min], and the formation of some new minor compounds at 24.7 min, 26.2 min, and 27.3 min were observed in AP samples. It was hypothesized that these latter metabolites derive from the transformation of some phenols of the extract (Supplementary Figure S5). In particular, the metabolites at 26.2 and 27.3 min present a similar UV-Vis spectrum with a maximum absorption approximately at 360 nm and a shape different from those observed in the BUO extract. The metabolite at 24.8 min shows a UV-Vis spectrum more similar to the secoiridoid derivatives of oleuropein with a relative maximum at 280 nm, and a molecular ion $[M-H]^-$ at 195 *m/z*. The available spectral data did not allow their identification so far. The UV-Vis spectra and the screening by mass spectrometry of the BUO extract confirmed the presence of several

isobars of Ole aglycone and ligstroside aglycone, while the presence of oleocanthal (mw 304 Dalton) was not confirmed applying the EI at 303 *m/z*. After 2 h incubation, only one isobaric form of Ole aglycone (rt 41.6 min) and one of ligstroside aglycone (rt 45.8 min) were detected in the AP sample suggesting changes in the equilibrium among these species after interaction with the mature intestinal CaCo-2 cells. In relation to the isobaric forms of oleacin, another relevant difference between the BUO extract and the AP sample was observed: the EI profile of the BUO extract showed at 319 *m/z* a very wide unresolved peak which was not detected in the AP sample containing only one isobar of oleacin at 34.4 min. Conversely, the OH-Tyr and Tyr proportions, evaluated as the ratio of the areas at 280 nm, showed values of about 2.0 in the AP samples and about 2.3 in the BUO extract. This suggests a significant 13.1% reduction of the OH-Tyr/Tyr in the AP samples vs. the BUO extract. This difference may be explained considering that the interaction of both OH-Tyr and Tyr with intestinal cells may modulate their presence and stability. The comparison of other ratios of some main phenols detected in the BUO extract and AP sample (200 µg/mL) can help to summarize similarities and differences between these samples. Notably, a reduction of Ole-aglyc/OH-Tyr and Ligst-aglyc/Tyr ratios by 43.3% and 55.3%, respectively, in the AP samples (200 µg/mL) was observed in respect to the BUO extract. The lower values for Ole-aglyc/OH-Tyr and Ligst-aglyc/Tyr ratios in the AP samples may suggest that the little phenols OH-Tyr and Tyr are more transformed and absorbed than their precursors by Caco-2 cells. Further confirmation of this hypothesis is furnished by the same value obtained for Ole-aglyc/Ligst-aglyc in the BUO extract and the AP samples.

4.3.7.2 BUO Phenols Transport to the BL Compartment

The chromatographic profiles of the BL samples after 2 h incubation of the BUO extract in the AP compartment were simpler than those of the AP samples. This suggests a selective transport of only some of the BUO phenols by Caco-2 cells into the BL compartment. Only Tyr, one isobaric form of the oleacin, and one of the Ole-aglyc were found, while OH-Tyr and the isobars of the aglycone ligstroside were not detectable (Figure 9). The identification of the isobar of oleacin was further confirmed by the presence in its mass spectrum of the ion corresponding to the dimer specie (639 *m/z*) together with the [M-H]−molecular ion at 319 *m/z*. Notably, the metabolite at 36.2 min, according to the UV-Vis and MS spectra (Supplementary, Figure S6) was identified as

an oxidation product of the Ole aglycone (mw 394 Dalton). This compound, detected in the BUO and AP sample, reached the BL compartment showing a concentration comparable to that of Ole aglycone. Similarly, a recent study, investigating EVOO phenol extract absorption across Caco-2/TC7, has described five caffeic acid derivatives recovered from the BL side of the cells, which were not detected in the AP compartment (D'Antuono *et al.*, 2016). This evidence contributes to confirming the active contribution of the intestinal epithelium in the modification of the phenolic profile of the EVOO phytocomplex. In a previous paper, Manna and co-workers (Manna *et al.*, 2000) showed that in Caco-2 cells OH-Tyr transport occurs via a passive bidirectional diffusion mechanism and that 3-hydroxy-4-methoxyphenyl ethanol is the main metabolite (approx 10% of the initial amount of OH-Tyr). Furthermore, the authors observed that the OH-Tyr absorption was not modified after incubation in the presence of structurally related phenols. Recently, D'Antuono *et al.*, performed a study aimed at characterizing the absorption of a phenolic extract obtained from Apulian naturally debittered table olives of the Bella di Cerignola cultivar (Italy), in which the debittering leads to the hydrolysis of Ole, the compound responsible for the characteristic bitter taste. Their results showed that OH-Tyr and Tyr, followed by verbascoside and luteolin, were among the best absorbed phenolic compounds by Caco-2 cells/TC7. In our study, however, the transepithelial transport of OH-Tyr was not observed. Although after 2 h of incubation the AP samples showed a higher amount of OH-Tyr compared to Tyr and almost the same OH-Tyr/Tyr ratio than in BUO extract, only Tyr appeared to be transported to the BL compartment. As for the Ole derivatives, only two selected isobaric forms of Ole aglycone and oleacin were found in the BL compartment, suggesting a selective release of the cells and/or an involvement of the other secoiridoid compounds in intracellular metabolic transformations into undetectable metabolites under the applied conditions. Differences in the major phenolic compounds shown to be transported by Caco-2 cells may derive from the use in our study of a whole phenolic extract instead of the single OH-Tyr (Manna *et al.*, 2000) or to the different initial product, i.e., the EVOO versus debittered table olives (D'Antuono *et al.*, 2016).

4.4 Conclusions

Using a multidisciplinary strategy, our study supports the bioactivity of an EVOO phenolic extract through the comprehensive characterization of its antioxidant power both *in vitro* and at the cellular level. Hence, this is the first study aimed at evaluating the behavior of a real complex pool of phenolic compounds of an EVOO, rather than of single molecules, such as OH-Tyr or Ole, on differentiated human intestinal Caco-2 cells. The protective effect against the oxidative stress induced by H_2O_2 was demonstrated in two different cellular models, i.e., Caco-2 and HepG2 cells. In addition, our results showed for the first time a selective transepithelial transport of some Ole derivatives by differentiated Caco-2 cells. Further investigations into the effects of extracts obtained from different monocultivar EVOOs would be highly desirable to understand the mechanisms underlying the interaction between the different phenols and the intestinal cells.

4.5 Supporting information

Materials and cell cultures: All chemicals and reagents were of analytical grade. DPPH, ROS and lipid peroxidation (MDA) assays were from Sigma-Aldrich (St. Louis, MO, USA). The HepG2 cell line was bought from ATCC (HB-8065, ATCC from LGC Standards, Milan, Italy), whereas Caco-2 cells were obtained from INSERM (Paris, France) and were cultured following the conditions previously described (Lammi *et al.*, 2015). The iNOS primary antibody came from Cell Signaling Technology (Danvers, MA, USA).

Cell culture: HepG2 cell line and Caco-2 cells were cultured in DMEM high glucose with stable L- glutamine, supplemented with 10% FBS, 100 U/mL penicillin, 100 µg/mL streptomycin (complete growth medium) with incubation at 37 °C under 5% (HepG2) or 10% (Caco-2) CO_2 atmosphere. Caco-2 cells were routinely sub-cultured at 50% density. HepG2 cells were used for no more than 20 passages after thawing, because the increase in number of passages may change the cell morphology and characteristics and impair assay results.

Production of the EVOO extract: An EVOO sample produced by Società Agricola Buonamici SrL (Fiesole, Florence, Italy) in the 2017 olive oil campaign from monocultivar olives of the typical Tuscan cultivar Frantoio was used for the study (BUO oil). The BUO extract was obtained following the procedures previously

described (Lammi *et al.*, 2020). Briefly, the extraction of total phenols and their chromatographic analyses were carried out respectively with MeOH:H_2O 80:20 v/v, and using a column SphereClone ODS (2) column, 250×4.6 mm (5μm) (Phenomenex, CA, USA), respectively, applying the analytical conditions reported by the IOC method [IOC/T.20/Doc No. 29]. An acidic hydrolysis was applied to the obtained extract for determining total OH-tyrosol (OH-Tyr) and total tyrosol (Tyr); the hydrolyzed extracts were not used for the biological tests, but only for analytical purposes. A RP18-Gemini column, 150×3 mm (5 μm) (Phenomenex, CA, USA) was used for the analysis of this latter extract. The Tyr content was evaluated at 280 nm using the calibration curve of Tyr standard (purity grade 98%), while the OH-Tyr content was expressed using the same calibration curve and applying a corrective factor (mg OH-Tyr = mg Tyr × 0.65).

4 3-(4,5-dimethylthiazol-2-yl)-2,5-diphenyltetrazolium bromide (MTT) assay: A total of 3×10^4 HepG2 cells/well and 5×10^4 Caco-2 cells/well were seeded in 96- well plates and treated with 25, 50, 100 and 200 μg/mL of BUO EVOO extract, or vehicle (H_2O) in complete growth media for 48 h at 37°C under 5% CO_2 atmosphere. Subsequently, the treatment solvent was aspirated and 100 μL/well of filtered 3-(4,5-dimethylthiazol-2-yl)-2,5-diphenyltetrazolium bromide (MTT) solution was added. After 2 h of incubation at 37 °C under 5% CO_2 atmosphere, 0.5 mg/mL solution was aspirated and 100 μL/well of the lysis buffer (8 mM HCl + 0.5% NP-40 in DMSO) added. After 5 min of slow shaking, the absorbance at 575 nm was read on a Synergy H1 fluorescence plate reader (Biotek, Bad Friedrichshall, Germany).

2,2-. Diphenyl-1-picrylhydrazyl (DPPH) assay: The DPPH assay to determine the antioxidant activity *in vitro* and *in situ* was performed by a standard method with some slight modifications. For the *in situ* experiment, 3×10^4 HepG2 and Caco-2 cells/well were seeded in a 96-well plate, overnight in growth medium and the following day they were treated with the BUO extract at a concentration of 25 μg/mL for 24 h at 37 °C under 5% CO_2 atmosphere. The day after, cells were collected and homogenized in 100 μL/well ice-cold lysis buffer and samples were centrifuged at 13,000 g for 10 min at 4 °C. The supernatants were recovered and transferred into a new ice-cold tube. The DPPH solution (12.5 μM in methanol, 45 μL) was added to 15 μL of lysate or BUO EVOO extract at different concentrations (10 – 50 μg/mL) in a 96-well half area plate.

The reaction for scavenging DPPH radicals was performed in the dark at room temperature and the absorbance was measured at 520 nm after 30 min incubation.

Trolox equivalent antioxidant capacity (TEAC) assay: TEAC assay is based in the reduction of ABTS (2,2-azino-bis-(3-ethylbenzothiazoline- 6-sulfonic acid) radical induced by antioxidants. The ABTS radical cation (ABTS+·) was prepared by mixing a 7mM ABTS solution (Sigma) with 2.45 mM potassium persulfate (1:1) and stored for 16 h at room temperature and in dark. To prepare the ABTS reagent, the ABTS+· was diluted in 5 mM phosphate buffer (pH 7.4) to obtain a stable absorbance of 0.700 (±0.02) at 730 nm. For the assay, 10 µL of BUO extract (at final concentration of 0.5, 1, 5 and 10 µg/mL) were added to 140 µL of diluted the ABTS+·. The microplate was incubated for 30 min at 30 °C and the absorbance was read at 730 nm using a SynergyTM HT-multimode microplate reader. The TEAC values were calculated using a Trolox (Sigma) calibration curve (60 - 320 µM).

Ferric reducing antioxidant power (FRAP) assay: FRAP assay evaluated the ability of the sample to reduce ferric ion (Fe^{3+}) into ferrous ion (Fe^{2+}). Thus, 10 µL of the sample (the lysed cells sample was diluted 1:5 in distilled water) was mixed with 140 µL of FRAP reagent. The FRAP reagent was prepared mixing 1.3 mL of a 10 mM TPTZ (Sigma) solution in 40 mM HCl, 1.3 mL of 20 mM $FeCl_3x6H_20$ and 13 mL of 0.3 M acetate buffer (pH 3.6). The microplate was incubated for 30 min at 37°C and the absorbance was read at 595 nm. The results were calculated by a Trolox (Sigma) standard curve obtained using different concentrations (3-400 µM). Absorbances were recorded on a SynergyTM HT-multimode microplate reader.

Oxygen radical absorbance capacity (ORAC) assay: ORAC assay is based on the scavenging of peroxyl radicals generating by the azo 2,2′-azobis(2-methylpropionamidine) dihydrochloride (AAPH, Sigma). Briefly, 25 µL of BUO extract (with a final concentration of 0.5, 1, 5 and 10 µg/mL) was added to 50 µL sodium fluorescein (2.934 mg/L) (Sigma) and incubated for 15 min at 37 °C. Then, 25 µL of AAPH (60.84 mM) were added and the decay of fluorescein was measured at its maximum emission of 528/20 nm every 5 min for 120 minutes using a SynergyTM HT-multimode microplate reader. The area under the curve (AUC) was calculated for each sample subtracting the AUC of the blank. The results were calculated using a Trolox calibration curve (2-38 µM).

Fluorometric intracellular ROS assay: For cells preparation, 3×10^4 HepG2 cells/well and 5×10^4 Caco-2 cells/well were seeded on a 96-well plate overnight in growth medium. The day after, the medium was removed, 50 µL/well of Master Reaction Mix were added and the cells were incubated at 5% CO_2 and 37 °C for 1 h in the dark. Then, cells were treated with 5 µL of BUO extract to reach the final concentrations of 1, 10, and 25 µg/mL and incubated at 37 °C for 1 h in the dark. To induce ROS formation, cells were treated with H_2O_2 at a final concentration of 0.5 mM for 30 min a 37 °C in the dark and fluorescence signals (ex./em. 490/525 nm) were recorded using a Synergy H1 microplate reader.

Lipid peroxidation (MDA) assay: HepG2 and Caco-2 cells (2.5×10^5 cells/well) were seeded in a 24 well plate and, the following day, they were treated with the BUO extract at 1, 10, and 25 µg/mL for 24 h at 37 °C under 5% CO_2 atmosphere. The day after, cells were incubated with 1 mM H_2O_2 or vehicle (H_2O) for 30 min, then collected and homogenized in 150 µL ice-cold MDA lysis buffer containing 3 µL of BHT (100×). Samples were centrifuged at 13,000 g for 10 min, then they were filtered through a 0.2 µm filter to remove insoluble materials. To form the MDA-TBA adduct, 300 µL of the TBA solution were added into each vial containing 100 µL samples and incubated at 95 °C for 60 min, then cooled to RT for 10 min in an ice bath. For the analysis, each reaction mixture (100 µL) was pipetted into a 96 well plate and the absorbance was measured at 532 nm using the Synergy H1 fluorescent plate reader. To normalize the data, total proteins for each sample were quantified by the Bradford method.

Nitric oxide level evaluation on HepG2 and Caco-2 cells, respectively: HepG2 and Caco-2 cells (1.5×10^5/well) were seeded on a 24-well plate. The next day, cells were treated with the EVOO extract at different concentrations (1, 10, and 25µg/mL) for 24 h at 37 °C under 5% CO_2 atmosphere. After incubation, cells were treated with H_2O_2 1 mM or vehicle (H_2O) for 60 min, then the cell culture media were collected and centrifuged at 13,000 g for 15 min to remove insoluble material. For the experiments, the supernatants were transferred in a 96-well plate and the buffer solution was added to each well in a ratio 1:2 to bring samples to final volumes of 50 µL and 40 µL for background and samples detection, respectively. Then, 5 µL of nitrate reductase solution and 5 µL of the enzyme co-factors solution were added to the samples and the plate was incubated at 25 °C for 2 h. Afterward, 25 µL of Griess Reagent A were added

to each well and, after 5 min, 25 µL of Griess Reagent B were added for 10 min. For the detection step, the absorbance at 540 nm was measured using a Synergy H1 microplate reader.

iNOS protein level evaluation by western blot analysis: A total of 1.5×10^5 HepG2 and Caco-2 cells/well were seeded on 24-well plates and incubated at 37 °C under 5% CO_2 atmosphere. The following day, cells were treated with 1, 10, and 25 µg/mL of the BUO extract in complete growth medium for 24 h. The day after, cells were incubated with 1 mM H_2O_2 or vehicle (H_2O) for 60 min and, after each treatment, cells were scraped in 40 µL ice-cold lysis buffer (RIPA buffer + inhibitor cocktail + 1:100 PMSF + 1:100 Na-orthovanadate + 1:1000 β-mercaptoethanol) and transferred in ice-cold microcentrifuge tubes. After centrifugation at 13,300 g for 15 min at 4 °C, the supernatants were recovered and transferred into new ice-cold tubes. Total proteins were quantified by the Bradford's method and 50 µg of total proteins loaded on a pre-cast 7.5% sodium dodecyl sulfate-polyacrylamide (SDS-PAGE) gel at 130 V for 45 min. Subsequently, the gel was pre-equilibrated in H_2O for 5 min at room temperature (RT) and transferred to a nitrocellulose membrane (Mini nitrocellulose Transfer Packs,) using a Trans-Blot Turbo at 1.3 A, 25 V for 7 min. Target proteins, on milk or BSA blocked membrane, were detected by primary antibodies anti-iNOS and anti-β-actin. Secondary antibodies conjugated with HRP and a chemiluminescent reagent were used to visualize target proteins and their signal was quantified using the Image Lab Software (Biorad, Hercules, CA). The internal control β-actin was used to normalize loading variations.

Caco-2 cell culture and differentiation: For differentiation, Caco-2 cells were seeded on polycarbonate filters, 12 mm diameter, 0.4 µm pore diameter (Transwell, Corning Inc., Lowell, MA, US) at a 3.5×10^5 cells/cm^2 density in complete medium supplemented with 10% FBS in both apical (AP) and basolateral (BL) compartments for 2 days in order to allow the formation of a confluent cell monolayer. Starting from day 3 after seeding, cells were transferred to a FBS-free medium in both compartments, supplemented with ITS [final concentration 10 mg/L insulin (I), 5.5 mg/L transferrin (T), 6.7 µg/L sodium selenite (S); GIBCO-Invitrogen, San Giuliano Milanese, Italy] only in the BL compartment, and allowed to differentiate for 18-21 days with regular medium changes three times weekly

Cell monolayers integrity evaluation: The transepithelial electrical resistance (TEER) of differentiated Caco-2 cells was measured at 37 °C using the voltmeter apparatus Millicell (Millipore Co., USA,), immediately before and at the end of the absorption experiments. In addition, at the end of the absorption experiments, cells were incubated from the AP side with 1 mM phenol- red in PBS with 1 mM $CaCl_2$ and 1mM $MgCl_2$ for 1 h at 37 °C, to monitor the paracellular permeability of the cell monolayer. The BL solutions were then collected and NaOH (70 µL, 0.1 N) was added before reading the absorbance at 560 nm by a microplate reader Synergy H1 from Biotek (Winooski, VT, USA). The phenol-red passage was quantified using a standard phenol-red curve. Only filters showing TEER values and phenol red passages similar to untreated control cells were considered for peptide transport analysis.

Trans-epithelial transport of BUO extract: Prior to experiments, the cell monolayer integrity and differentiation were checked by TEER measurement as described in detail above. Cells were then washed twice, and peptide absorption assayed. Absorption experiments were performed in transport buffer solution (137 mM NaCl, 5.36 mM KCl, 1.26 mM $CaCl_2$, and 1.1 mM $MgCl_2$, 5.5 mM glucose). In order to reproduce the pH conditions existing *in vivo* in the small intestinal mucosa, the AP solutions were maintained at pH 6.0 (buffered with 10 mM morpholinoethane sulfonic acid), and the BL solutions were maintained at pH 7.4 (buffered with 10 mM N-2-hydroxyethylpiperazine-N-4-butanesulfonic acid). Prior to absorption experiments, cells were washed twice with 500 µL PBS with 1mM $CaCl_2$ and 1mM $MgCl_2$ The BUO extract absorption was assayed by loading the AP compartment with BUO extract (100 and 200 µg/mL) in the AP transport solution (500 µL) and the BL compartment with the BL transport solution (700 µL). The plates were incubated at 37 °C and the BL solutions were collected 120 min. All BL solutions together with the AP solutions collected at the end of the transport experiment were stored at -80 °C prior to analysis. Three independent absorption experiments were performed, each in duplicate.

HPLC-DAD-MS analysis for evaluating the trans-epithelial transport of BUO extract: The dried cellular extracts were dissolved in 150 µL of the mixture EtOH:H_2O 2:1 v/v and, after centrifugation at 16,900 xg for 5 min, the supernatant was recovered and used for the analyses. The instrument was a HP 1260 MSD mass spectrometer with an API/electrospray interface (Agilent Technologies). The column was a Poroshell 120,

EC- C18 (150 mm × 3.0 mm id, 2.7 μM Agilent, USA) with a precolumn of the same phase. The mobile phase was acetonitrile (A) and H_2O at pH 3.2 by HCOOH (B). The following multistep linear gradient was applied: from 5% to 40% A in 40 min, to 88% A in 5 min, and then to 98% A in 10 min, with a final plateau of 3 min (total time 58 min); flow rate was 0.4 mL·min−1. For the MS detector the conditions were: negative ion mode, gas temperature 350 °C, nitrogen flow rate 10.5 L/min, nebulizer pressure 35 psi (241 KPa), capillary voltage 3500 V and fragmentation energy between 80 and 150 V.

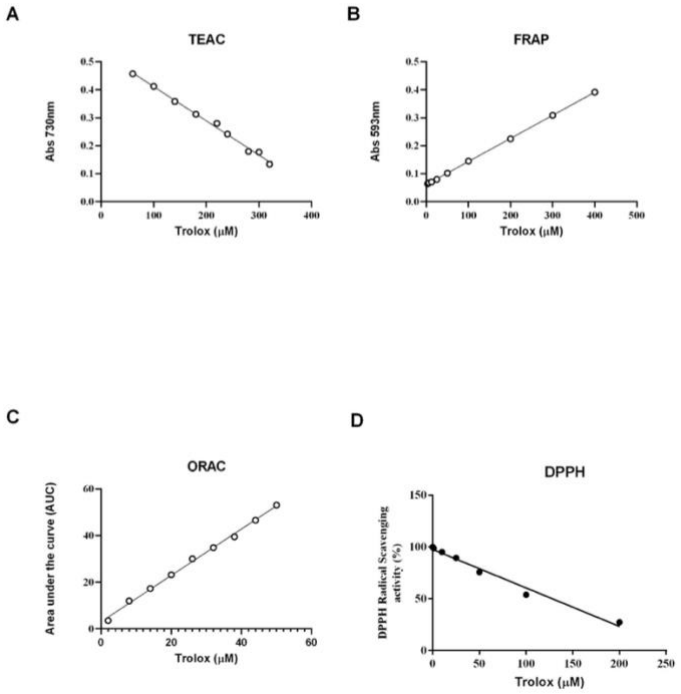

Figure S1: Trolox's calibration curves obtained using TAEC (A), FRAP (B), ORAC (C), and DPPH (D) assays.

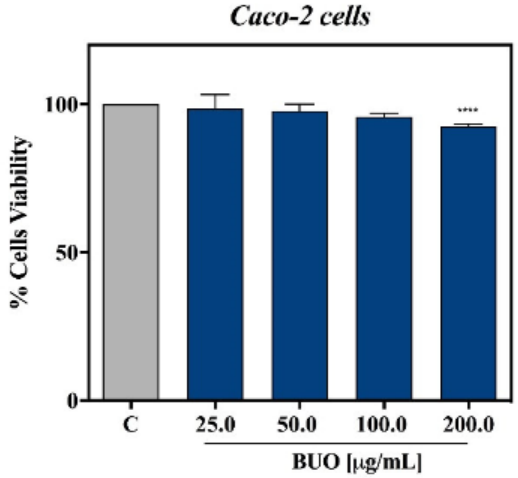

Figure S2. Caco-2 cell vitality after treatment with BUO phenol extracts by MTT assay. The BUO extract did not affect the Caco-2 vitality after 48 h of incubation up to 100 μg/mL, whereas at 200 μg/mL the cell viability was reduced by 7.5% (****) $p < 0.0001$. Data represent the mean ± SD of three independent experiments performed in triplicate. C: untreated Caco-2 cells.

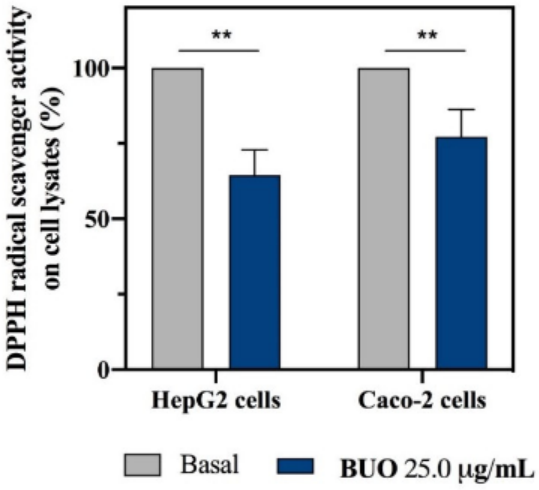

Figure S3. Cellular evaluation of the DPPH radical scavenger activity of BUO extract on HepG2 and Caco-2 cells lysates. The data points represent the averages ± SD of four independent experiments in duplicate. (**) $p < 0.01$.

Figure S4. Chromatographic profiles at 280 nm and TIC of the two controls: Apical (AP) and basolateral (BL)samples

	BUO (before hydrolysis)	
	EVOO (µg/g)	**dry extract (µg/mg)**
Free hydroxytyrosol	9.3 ± 0.9	4.0 ± 0.1
Free tyrosol	5.1 ± 0.1	2.0 ± 0.1
Total Phenols	617.9 ± 34.1	289.3 ± 15.6
	BUO (after hydrolysis)	
	EVOO (µg/g)	**dry extract (µg/mg)**
Total hydroxytyrosol	444.9 ± 33.4	208.0 ± 15.6
Total tyrosol	332.9 ± 7.9	156.0 ± 3.9
Tyr+OH-tyr	777.8 ± 41.3	364.1 ± 19.5

Table S1 . Phenolic content in BUO (EVOO and dried extract) before and after acid hydrolysis expressed on EVOO (in µg/g) and on dry extract (in µg/mg) basis. Data are expressed as mean ± SD of three replicates. (According to Lammi, *et al.* . Extra Virgin Olive Oil Phenol Extracts Exert Hypocholesterolemic Effects through the Modulation of the LDLR Pathway: In Vitro and Cellular Mechanism of Action Elucidation. Nutrients: 2020; Vol. 12 (6), p 1723)

(A)

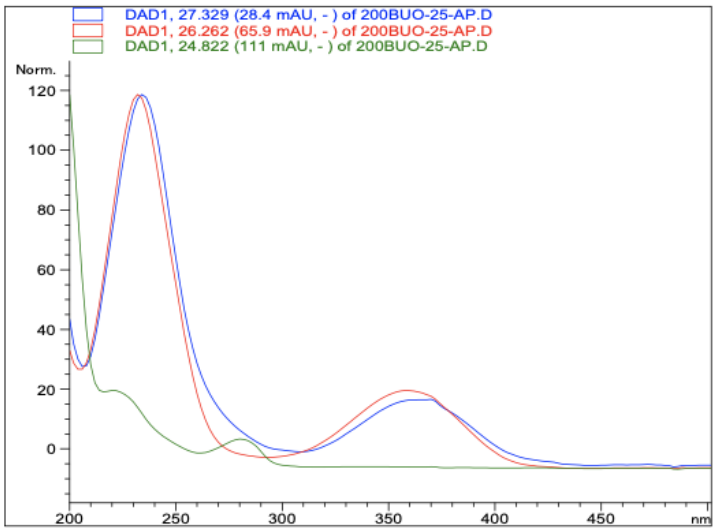

(B)

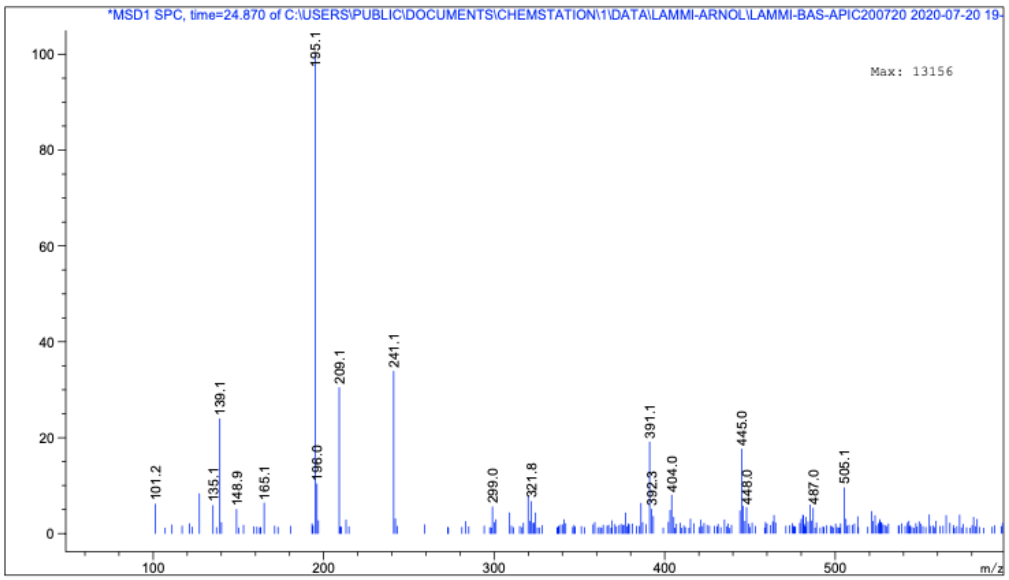

Figure S5. UV-Vis spectra of some minor unidentified compounds found in the AP sample after incubation of two hours with BUO extract: rt 24.7, 26.2 and 27.3 min (**A**); the mass spectrum of the compound eluted at 24.8 min in negative ionization mode (the only detectable within the three new metabolites) (**B**).

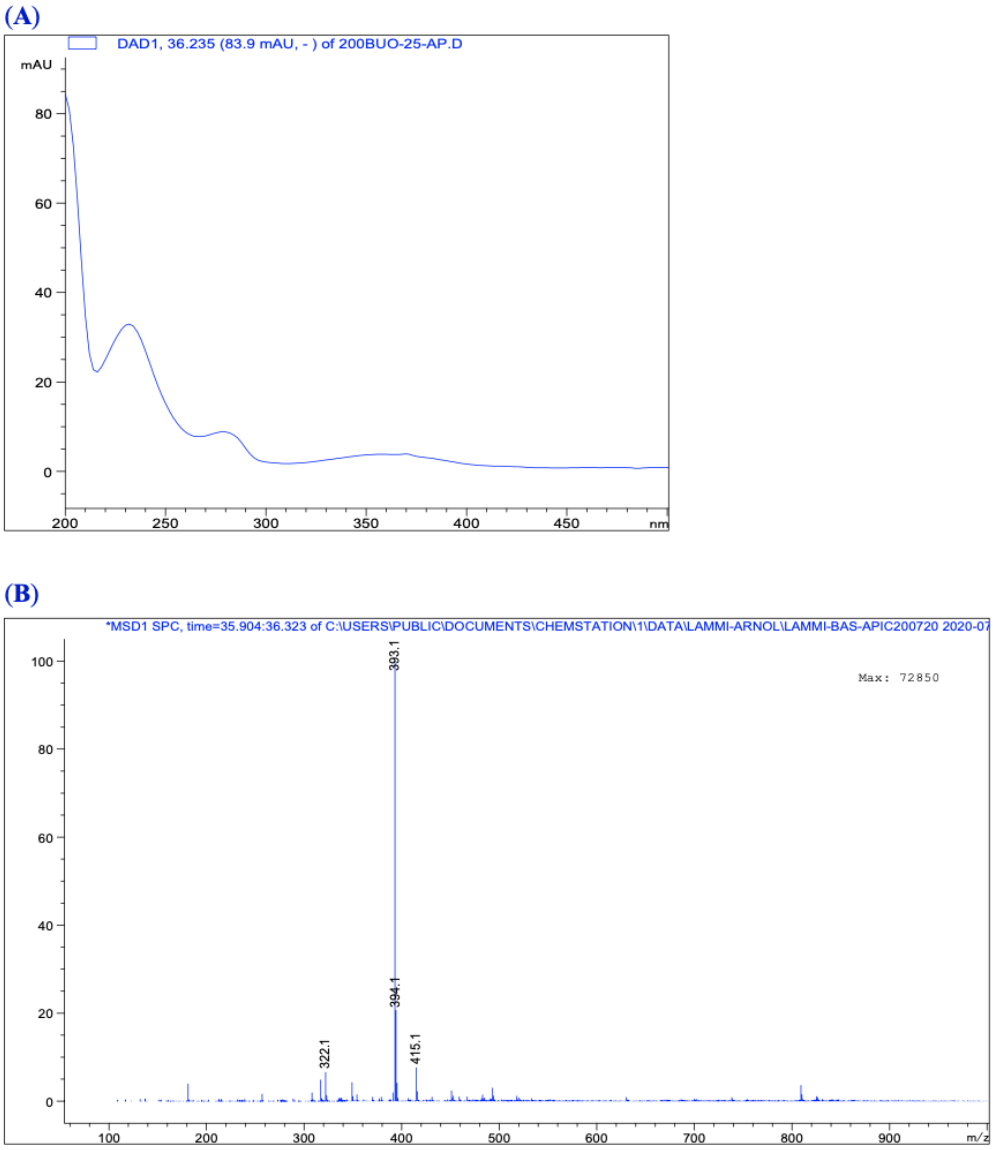

Figure S6. UV-Vis spectrum (**A**) and mass spectrum in negative mode (**B**) of the compound at 36.2 min detected in BUO sample, in Apical (AP) and Basal (BL) samples was tentatively identified as an oxidized derivative of oleuropein aglycone (mw 394 Dalton).

4.6 References

Abdallah M., Marzocco S., Adesso S., Zarrouk M., Guerfel M. Olive oil polyphenols extracts inhibit inflammatory markers in J774A.1 murine macrophages and scavenge free radicals. Acta Histochem. 2018;120:1–10. doi: 10.1016/j.acthis.2017.10.005.

Aiello G., Ferruzza S., Ranaldi G., Sambuy Y., Arnoldi A., Vistoli G., Lammi C. Behavior of three hypocholesterolemic peptides from soy protein in an intestinal model based on differentiated Caco-2 cell. J. Funct. Foods. 2018;45:363–370. doi: 10.1016/j.jff.2018.04.023.

Beckman J.S. Oxidative damage and tyrosine nitration from peroxynitrite. Chem. Res. Toxicol. 1996;9:836–844. doi: 10.1021/tx9501445.

Bellumori M., Cecchi L., Innocenti M., Clodoveo M.L., Corbo F., Mulinacci N. The EFSA Health claim on olive oil polyphenols: Acid hydrolysis validation and total hydroxytyrosol and tyrosol determination in Italian virgin olive oils. Molecules. 2019;24:2179. doi: 10.3390/molecules24112179.

Berrougui H., Ikhlef S., Khalil A. Extra virgin olive oil polyphenols promote cholesterol efflux and improve HDL functionality. Evid. Based Complement Alternat. Med. 2015;2015:208062. doi: 10.1155/2015/208062.

Bigagli E., Cinci L., Paccosi S., Parenti A., D'Ambrosio M., Luceri C. Nutritionally relevant concentrations of resveratrol and hydroxytyrosol mitigate oxidative burst of human granulocytes and monocytes and the production of pro-inflammatory mediators in LPS-stimulated RAW 264.7 macrophages. Int. Immunopharmacol. 2017;43:147–155. doi: 10.1016/j.intimp.2016.12.012.

Cory H., Passarelli S., Szeto J., Tamez M., Mattei J. The role of polyphenols in human health and food systems: A mini-review. Front. Nutr. 2018;5:87. doi: 10.3389/fnut.2018.00087.

D'Antuono I., Garbetta A., Ciasca B., Linsalata V., Minervini F., Lattanzio V.M., Logrieco A.F., Cardinali A. Biophenols from table olive cv bella di cerignola: Chemical characterization, bioaccessibility, and intestinal absorption. J. Agric. Food Chem. 2016;64:5671–5678. doi: 10.1021/acs.jafc.6b01642.

D'Archivio M., Filesi C., Varì R., Scazzocchio B., Masella R. Bioavailability of the polyphenols: Status and controversies. Int. J. Mol. Sci. 2010;11:1321–1342. doi: 10.3390/ijms11041321.

Dhalla N.S., Temsah R.M., Netticadan T. Role of oxidative stress in cardiovascular diseases. J. Hypertens. 2000;18:655–673. doi: 10.1097/00004872-200018060-00002.

El Gharras H. Polyphenols: Food sources, properties and applications—A review. Inter. J. Food Sci. Technol. 2009;44:2512–2518. doi: 10.1111/j.1365-2621.2009.02077.x.

Gaforio J.J., Visioli F., Alarcón-de-la-Lastra C., Castañer O., Delgado-Rodríguez M., Fitó M., Hernández A.F., Huertas J.R., Martínez-González M.A., Menendez J.A., et al. Virgin olive oil and health: Summary of the III international conference on virgin olive oil and health consensus report, JAEN (Spain) 2018. Nutrients. 2019;11:2039. doi: 10.3390/nu11092039.

Goya L., Mateos R., Bravo L. Effect of the olive oil phenol hydroxytyrosol on human hepatoma HepG2 cells—Protection against oxidative stress induced by tert- butylhydroperoxide. Eur. J. Nutr. 2007;46:70–78. doi: 10.1007/s00394-006-0633-8.

Habib S., Ali A. Biochemistry of nitric oxide. Indian J. Clin. Biochem. 2011;26:3–17. doi: 10.1007/s12291-011-0108-4

Incani A., Serra G., Atzeri A., Melis M.P., Serreli G., Bandino G., Sedda P., Campus M., Tuberoso C.I.G., Deiana M. Extra virgin olive oil phenolic extracts counteract the pro-oxidant effect of dietary oxidized lipids in human intestinal cells. Food Chem. Toxicol. 2016;90:171–180. doi: 10.1016/j.fct.2016.02.015.

Jacobs D., Tapsell L. Food, not nutrients, is the fundamental unit in nutrition. Nutr. Rrev. 2007;65:439–450. doi: 10.1111/j.1753-4887.2007.tb00269.x.

Katsoulieris E.N. The olive leaf extract oleuropein exerts protective effects against oxidant-induced cell death, concurrently displaying pro-oxidant activity in human hepatocarcinoma cells. Redox Rep. 2016;21:90–97. doi: 10.1179/1351000215Y.0000000039.

Lammi C., Aiello G., Dallafiora L., Bollati C., Boschin G., Ranaldi G., Ferruzza S., Sambuy Y., Galaverna G., Arnoldi A. Assessment of the multifunctional behavior of lupin peptide P7 and its metabolite using an integrated strategy. J. Agric. Food Chem. 2020c;68:13179–13188. doi: 10.1021/acs.jafc.0c00130.

Lammi C., Bellumori M., Cecchi L., Bartolomei M., Bollati C., Clodoveo M.L., Corbo F., Arnoldi A., Nadia M. Extra virgin olive oil phenol extracts exert hypocholesterolemic effects through the modulation of the LDLR pathway: *In vitro* and cellular mechanism of action elucidation. Nutrients. 2020;12:1723. doi: 10.3390/nu12061723.

Lammi C., Bollati C., Arnoldi A. Antioxidant activity of soybean peptides on human hepatic HepG2 cells. J. Food Bioact. 2019;7:43–47.

Lammi C., Mulinacci N., Cecchi L., Bellumori M., Bollati C., Bartolomei M., Franchini C., Clodoveo M.L., Corbo F., Arnoldi A. Virgin olive oil extracts reduce oxidative stress and modulate cholesterol metabolism: Comparison between oils obtained with traditional and innovative processes. Antioxidants. 2020b;9:17. doi: 10.3390/antiox9090798.

Lorenzo J.M., Munekata P.E.S., Gómez B., Barba F.J., Toldrá F. Bioactive peptides as natural antioxidants in food products–A review. Trends Food Sci. Tech. 2018;79:136–147. doi:

Maiuri M.C., De Stefano D., di Meglio P., Irace C., Savarese M., Sacchi R., Cinelli M.P., Carnuccio R. Hydroxytyrosol, a phenolic compound from virgin olive oil, prevents macrophage activation. Naunyn Schmiedebergs Arch. Pharmacol. 2005;371:457–465. doi: 10.1007/s00210-005-1078-y.

Manna C., Galletti P., Maisto G., Cucciolla V., D'Angelo S., Zappia V. Transport mechanism and metabolism of olive oil hydroxytyrosol in Caco-2 cells. FEBS Lett. 2000;470:341–344. doi: 10.1016/S0014-5793(00)01350-8.

Mittal M., Siddiqui M.R., Tran K., Reddy S.P., Malik A.B. Reactive oxygen species in inflammation and tissue injury. Antioxid. Redox Signal. 2014;20:1126–1167. doi: 10.1089/ars.2012.5149.

Natoli M., Leoni B.D., D'Agnano I., Zucco F., Felsani A. Good Caco-2 cell culture practices. Toxicol *In Vitro*. 2012;26:1243–1246. doi: 10.1016/j.tiv.2012.03.009.

NDA (Scientific Panel on Dietetic Products N.a.A.O.o.t.S.p.o.D.P) Nutrition and Allergies on a Request from the Commission Related to the Polyphenols in Olive and. [(accessed on 8 January 2021)];Protection of LDL Particle from the Oxidative Damage. Available online: https://efsa.onlinelibrary.wiley.com/doi/pdf/10.2903/j.efsa.2011.2033

Official Method of Analysis. Determination of Biophenols in Olive Oil by HPLC. International Olive Council; Madrid, Spain: 2009. IOC/T.20/Doc No. 29

Pandey K.B., Rizvi S.I. Plant polyphenols as dietary antioxidants in human health and disease. Oxid Med. Cell Longev. 2009;2:270–278. doi: 10.4161/oxim.2.5.9498.

Sanchez-Fidalgo S., de Ibarguen L.S., Cardeno A., de la Lastra C.A. Influence of extra virgin olive oil diet enriched with hydroxytyrosol in a chronic DSS colitis model. Eur. J. Nutr. 2012;51:497–506. doi: 10.1007/s00394-011-0235-y.

Santangelo C., Vari R., Scazzocchio B., De Sanctis P., Giovannini C., D'Archivio M., Masella R. Anti-inflammatory activity of extra virgin olive oil polyphenols: Which role in the prevention and treatment of immune-mediated inflammatory diseases? Endocr. Metab. Immune. Disord. Drug Targets. 2018;18:36–50. doi: 10.2174/1871530317666171114114321.

Serra G., Incani A., Serreli G., Porru L., Melis M.P., Tuberoso C.I.G., Rossin D., Biasi F., Deiana M. Olive oil polyphenols reduce oxysterols -induced redox imbalance and pro-inflammatory response in intestinal cells. Redox Biol. 2018;17:348–354. doi: 10.1016/j.redox.2018.05.006.

Serreli G., Deiana M. Extra virgin olive oil polyphenols: Modulation of cellular pathways related to oxidant species and inflammation in aging. Cells. 2020;9:478. doi: 10.3390/cells9020478.

Serreli G., Melis M.P., Corona G., Deiana M. Modulation of LPS-induced nitric oxide production in intestinal cells by hydroxytyrosol and tyrosol metabolites: Insight into the mechanism of action. Food Chem. Toxicol. 2019;125:520–527. doi: 10.1016/j.fct.2019.01.039.

Soler A., Romero M.P., Macia A., Saha S., Furniss C.S.M., Kroon P.A., Motilva M.J. Digestion stability and evaluation of the metabolism and transport of olive oil phenols in the human small-intestinal epithelial Caco-2/TC7 cell line. Food Chem. 2010;119:703–714. doi: 10.1016/j.foodchem.2009.07.017.

Soskić S.S., Dobutović B.D., Sudar E.M., Obradović M.M., Nikolić D.M., Djordjevic J.D., Radak D.J., Mikhailidis D.P., Isenović E.R. Regulation of Inducible Nitric Oxide Synthase (iNOS) and its potential role in insulin resistance, diabetes and heart failure. Open Cardiovasc. Med. J. 2011;5:153–163. doi: 10.2174/1874192401105010153.

Stiuso P., Bagarolo M.L., Ilisso C.P., Vanacore D., Martino E., Caraglia M., Porcelli M., Cacciapuoti G. Protective effect of tyrosol and S-Adenosylmethionine against ethanol-induced oxidative stress of Hepg2 cells involves sirtuin 1, P53 and Erk1/2 Signaling. Int. J. Mol. Sci. 2016;17:622. doi: 10.3390/ijms17050622.

Sunil V.R., Shen J., Patel-Vayas K., Gow A.J., Laskin J.D., Laskin D.L. Role of reactive nitrogen species generated via inducible nitric oxide synthase in vesicant-induced lung injury, inflammation and altered lung functioning. Toxicol. Appl. Pharmacol. 2012;261:22–30. doi: 10.1016/j.taap.2012.03.004.

Takeda Y., Bui V.N., Iwasaki K., Kobayashi T., Ogawa H., Imai K. Influence of olive-derived hydroxytyrosol on the toll-like receptor 4-dependent inflammatory response of mouse peritoneal macrophages. Biochem. Biophys. Res. Commun. 2014;446:1225–1230. doi: 10.1016/j.bbrc.2014.03.094.

Visioli F., Vinceri F.F., Galli C. 'Waste waters' from olive oil production are rich in natural antioxidants. Experientia. 1995;51:32–34.

Zanoni C., Aiello G., Arnoldi A., Lammi C. Investigations on the hypocholesterolaemic activity of LILPKHSDAD and LTFPGSAED, two peptides from lupin β-conglutin: Focus on LDLR and PCSK9 pathways. J. Funct. Foods. 2017;32:1–8. doi: 10.1016/j.jff.2017.02.009.

MANUSCRIPT 2

PHENOLIC EXTRACTS FROM EXTRA VIRGIN OLIVE OILS INHIBIT DIPEPTIDYL PEPTIDASE IV ACTIVITY: *IN VITRO*, CELLULAR, AND IN SILICO MOLECULAR MODELING INVESTIGATIONS

Carmen Lammi,[1,*] Martina Bartolomei,[1] Carlotta Bollati,[1] Lorenzo Cecchi,[2] Maria Bellumori,[2] Emanuela Sabato,[1] Vistoli Giulio,[1] Nadia Mulinacci,[2] and Anna Arnoldi[1]

[1] Department of Pharmaceutical Sciences, University of Milan, 20133 Milan, Italy; martina.bartolomei@unimi.it (M.B.); carlotta.bollati@unimi.it (C.B.); emanuela.sabato@studenti.unimi.it (E.S.); giulio.vistoli@unimi.it (V.G.); anna.arnoldi@unimi.it (A.A.)

[2] Department of Neuroscience, Psychology, Drug and Child Health, Pharmaceutical and Nutraceutical Section, University of Florence, 50019 Florence, Italy; lo.cecchi@unifi.it (L.C.); maria.bellumori@unifi.it (M.B.); nadia.mulinacci@unifi.it (N.M.)

*Correspondence: carmen.lammi@unimi.it; Tel.: +39-02-50319372

5. Abstract

Two extra virgin olive oil (EVOO) phenolic extracts (BUO and OMN) modulate DPP-IV activity. The *in vitro* DPP-IV activity assay was performed at the concentrations of 1, 10, 100, 500, and 1000 μg/mL, showing a dose-dependent inhibition by 6.8 ± 1.9, 17.4 ± 6.1, 37.9 ± 2.4, 57.8 ± 2.9, and 81 ± 1.4% for BUO and by 5.4 ± 1.7, 8.9 ± 0.4, 28.4 ± 7.2, 52 ± 1.3, and 77.5 ± 3.5% for OMN. Moreover, both BUO and OMN reduced the DPP-IV activity expressed by Caco-2 cells by 2.9 ± 0.7, 44.4 ± 0.7, 61.2 ± 1.8, and 85 ± 4.2% and by 3 ± 1.9, 35 ± 9.4, 60 ± 7.2, and 82 ± 2.8%, respectively, at the same doses. The concentration of the most abundant and representative secoiridoids within both extracts was analyzed by nuclear magnetic resonance (^{1}H-NMR). Oleuropein, oleacein, oleocanthal, hydroxytyrosol, and tyrosol, tested alone, reduced the DPP-IV activity, with IC_{50} of 472.3 ± 21.7, 187 ± 11.4, 354.5 ± 12.7, 741.6 ± 35.7, and 1112 ± 55.6 μM, respectively. Finally, *in silico* molecular docking simulations permitted the study of the binding mode of these compounds.

5.1 Introduction

Dipeptidyl-peptidase-IV (DPP-IV), a serine exopeptidase expressed on the surface of most cell types, is able to cleave Xaa-proline or Xaa-alanine dipeptides from the N-terminus of polypeptides. Among all DPP-IV substrates, the most widely investigated are glucagon-like peptide 1 (GLP-1) and glucose-dependent insulinotropic polypeptide (GIP), two incretins playing essential roles in controlling post-prandial glycemia (Kreymann *et al.*, 1997, Dupre *et al.*, 1973). In more detail, incretins such as GLP-1 and GIP are secreted by the distal small intestine in response to its stimulation and bind receptors in the endocrine pancreas, thus eliciting insulin secretion and lowering post-prandial blood glucose (Rhee *et al.*, 2014, Smilowitz *et al.*, 2014, Doupis *et al.*, 2008). Notably, both hormones are rapidly inactivated by DPP-IV, whose activation is increased by oxidative stress (Ishibashi *et al.*, 2016). Hence, its inhibition is an established glucose-lowering therapy in type 2 diabetes (Carr *et al.*, 2016, Bailey *et al.*, 2016). Post-prandial glucose has been associated with a higher incidence of cardiovascular events in patients with (Cavalot *et al.*, 2011) and without (Lin *et al.*, 2009) diabetes. Indeed, reducing post-prandial glycemia and the lipid profile could have

a positive impact on the progression of atherosclerosis (Tushuizen *et al.*, 2005). Observational and interventional studies consistently demonstrated a potentially beneficial effect of EVOO consumption on the atherosclerotic process and diabetes (Violi *et al.*, 2015, Salas-Salvado *et al.*, 2014, Babio *et al.*, 2014). However, the underlying mechanism is still unknown, and a substantial gap of information exists regarding the mechanism of action through which EVOO modulates glycemia. Recently, it was demonstrated that the supplementation of a meal with 10 g EVOO had positive effects on postprandial glycemic profile, due to an increase in incretins concomitantly with a decrease in DPP-IV protein levels and therefore in activity in a group of healthy subjects that consumed a meal supplemented with 10 g of corn oil (Violi *et al.*, 2015). Other evidence indicates that oleuropein has similar effects on incretins (GLP-1 and GIP) and the glycemic profile of healthy subjects, suggesting that oleuropein may be the major phenolic component within EVOO responsible for incretin upregulation through the control of DPP-IV protein-level modulation (Carnevale *et al.*, 2018). Based on these considerations, the assessment of the mechanism of action through which EVOO extracts may directly modulate the DPP-IV activity was carried out using *in vitro* and cellular fluorescent assays. The present investigation was conducted on two phenolic extracts previously obtained from two different cultivars (Lammi *et al.*, 2020): one from the EVOO of the cultivar Frantoio cultivated in Tuscany (Italy), named BUO, and the other from the cultivar Coratina cultivated in Apulia (Italy), named OMN. Both extracts result in cholesterol-lowering activity (Lammi *et al.*, 2020) in human hepatic HepG2 cells and antioxidant activity (Lammi *et al.*, 2020b) in intestinal Caco-2 and HepG2 cells. Phenol characterization, as reported in a preceding paper, was performed by applying the official method (International Olive Council, 2009) for quantifying the total phenol content, and a validated hydrolytic method was used to evaluate the total content of hydroxytyrosol and tyrosol as the sum of free and bound forms (Bellumori *et al.*, 2019b). The analysis of BUO and OMN extracts highlighted that the total phenolic contents of the two extracts are significantly different (Lammi *et al.*, 2020). Hence, in order to foster and better highlight the advantageous of EVOO phytocomplex against diabetes, the health-promoting effects of the BUO and OMN extracts were investigated by evaluating their potential hypoglycemic effect through the modulation of DPP-IV activities. In more detail, the first objective of the study was the measurement of the concentration of the secoiridoids oleuropein, oleacein, oleocanthal, and ligstroside aglycone in the two EVOO extracts BUO and OMN by

proton nuclear magnetic resonance (1H-NMR) analysis. The second objective was the assessment of the DPP-IV inhibitory activity of the two extracts and of the pure standards of oleuropein, oleacein, oleocanthal, hydroxytyrosol, and tyrosol, which are the most abundant and representative compounds within the extracts, by a biochemical assay. Finally, for a further reinforcement of the study, the third objective was an investigation of the possible binding of these compounds to DPIV by in silico molecular docking simulations.

5.2 Materials and Methods

5.2.1 Chemicals

All reagents are commercially available. More details are reported in the Supplementary Material.

5.2.2 Preparation of the BUO and OMN Samples and Quantification of the Main Secoiridoids

The EVOO extracts were prepared as previously reported (Lammi *et al.*, 2020): the extracts were prepared starting from 5 mL of oil, obtaining a dry weight of 10 mg and 5.7 mg for BUO and OMN, respectively. Their total phenolic content and total hydroxytyrosol and tyrosol were determined applying to validated methods (Lammi *et al.*, 2020). To evaluate the concentration of oleacein, oleuropein, oleocanthal, and ligstroside aglycone, the ^{1}H NMR spectra of BUO and OMN samples were registered by a 400 MHz instrument Advance 400 (Bruker, Bremen, Germany). The extracts were dissolved in 1 mL of $CDCl_3$, and 1 µL of the solution of the internal standard (maleic acid 30 mg/mL in CH_3CN) was added. According to our previous studies (Khatib *et al.*, 2016), to reference guidelines for quantitation by NMR (Schönberger *et al.*, 2014), and to Karkoula *et al.*, 2012, the evaluation of oleacein, oleocanthal, oleuropein aglycone, and ligstroside aglycone in their monoaldehyde forms was done applying the following formula:

$$C(\%) = I_{CHO}/I_{mal} \times N_{mal}/N_{CHO} \times MW_X/MW_{mal} \times W_{mal}/W_{sample} \times P_{mal} \quad (1)$$

$C(\%)$, concentration of each of the four secoiridoid aldehydes.
I_{mal}, integral of 2 protons of the ISTD, maleic acid.
I_{CHO}, integral area of the proton signal of the aldehyde of each secoiridoid.
N_{CHO}, the number of the aldehyde proton of each secoiridoid.
N_{mal}, the number of the protons of maleic acid.
MW_X, the molecular weight of each secoiridoid (oleacein 320 g/moL, oleuropein aglycone 378 g/moL, oleocanthal 304 g/moL, and ligstroside aglycone 362 g/moL).
MW_{mal}, the mw of ISTD maleic acid, 116.1 g/moL.
W_{mal}, weight in mg of maleic acid.
W_{sample}, dry weight in mg of BUO or OMN.
P_{mal}, purity grade of maleic acid.

5.2.3 In Vitro DPP-IV Activity Assay

The DPP-IV enzyme was provided by Cayman Chemicals (Ann Arbor, MI, USA), while the DPP-IV substrate (Gly-Pro-amido-4-methylcoumarin hydrobromide (Gly-Pro-AMC)) was from AnaSpec Inc. (Freemont, CA, USA). The experiments were carried out in triplicate in a half-volume 96-well solid plate (white) following conditions previously optimized (Lammi *et al.*, 2016). More details are available in the Supplementary Material.

5.2.4 Cell Culture

Caco-2 cells, obtained from INSERM (Paris, France), were routinely sub-cultured following a previously optimized protocol (Aiello *et al.*, 2018). More details are available in the Supplementary Material.

5.2.5 In Situ DPP-IV Activity Assay

In total, 5×10^4 Caco-2 cells/well were seeded in black 96-well plates with clear bottom. The second day after seeding, the spent medium was discarded and cells were treated with 100 µL/well of BUO and OMN extracts at concentrations of 10, 100, 500, or 1000 µg/mL or vehicle (C) in growth medium for 24 h at 37 °C. Experiments were carried out following previously optimized conditions (Lammi *et al.*, 2019). More details are available in the Supplementary Material.

5.2.6 Computational Methods

The structures of the 6 simulated phenolic compounds were built using 2 different strategies. Hydroxytyrosol, tyrosol, oleacein, and oleocanthal were downloaded from PubChem, while Ole and La were first downloaded from PubChem in their glucoside form and then manually modified to their aglycone form using the Molecular Editor functions of the VEGA suite of programs. The obtained structures were then minimized by using AMMP as implemented in the VEGA environment (Pedretti *et al.*, 2021). Among the resolved DPP-IV structures, this study involved the complex between the enzyme and the inhibitor 75 M, PDB ID: 5T4F, chosen due to its very high resolution (1.90 Å). After deleting water molecules ions and crystallographic additives, the selected dimer was completed by adding the hydrogen atoms to amino acid residues and ionizing the protein considering physiologic pH at 7.4. The H^{++} server was chosen to predict the protonation state of ionizable protein groups. The protein was then refined by 2 minimization procedures using NAMD (Phillips *et al.*, 2005). The first procedure was carried out with all the protein atoms fixed except for hydrogens; the second was performed with the backbone atoms under constraints to preserve the resolved folding. The prepared protein structure underwent the following docking simulations. Docking simulations were carried out using PLANTS (Protein-Ligand ANT System) (Korb *et al.*, 2009), which generates reliable ligand poses using the ant colonization algorithm (ACO). In detail, the search was focused on a 10 Å radius sphere around the bound ligand 75 M, thus including the entire binding cavity. For all the simulated ligands, PLANTS was used with default settings and without geometric constraints, speed 1 was used, and 100 poses were generated and scored by using the ChemPLP function. The obtained poses were evaluated considering both the docking scores and the involved residues.

5.2.7 Statistical Analysis

All the data sets were checked for normal distribution by the D'Agostino and Pearson test. Since they are all normally disturbed with p-values < 0.05, we proceeded with statistical analyses by one-way ANOVA followed by Tukey's post-hoc tests and using Graphpad Prism 9 (San Diego, CA, USA). Values were reported as means ± standard deviation (S.D.); p-values < 0.05 were considered to be significant.

5.3 Results

5.3.1 BUO and OMN Extracts Inhibit the In Vitro and Cellular DPP-IV Activity

To evaluate the DPP-IV inhibitory activity of both BUO and OMN, *in vitro* experiments were performed by using the purified human recombinant DPP-IV enzyme and H-Gly-Pro-AMC as a substrate. The reaction was monitored by measuring the fluorescence signals at 465 nm after excitation at 350 nm, deriving from the release of a free AMC group after the cleavage of H-Gly-Pro-AMC catalyzed by DPP-IV. Figure 1A,B indicates that both extracts significantly reduced the DPP-IV activity *in vitro*: BUO reduced the DPP-IV activity by 6.8 ± 1.9, 17.4 ± 6.1, 37.9 ± 2.4, 57.8 ± 2.9, and 81 ± 1.4%, respectively (Figure 1A), at 1, 10, 100, 500, and 1000 µg/mL, whereas OMN reduced activity by 5.4 ± 1.7, 8.9 ± 0.4, 28.4 ± 7.2, 52 ± 1.3, and 77.5 ± 3.5%, respectively, at the same concentrations (Figure 1B).

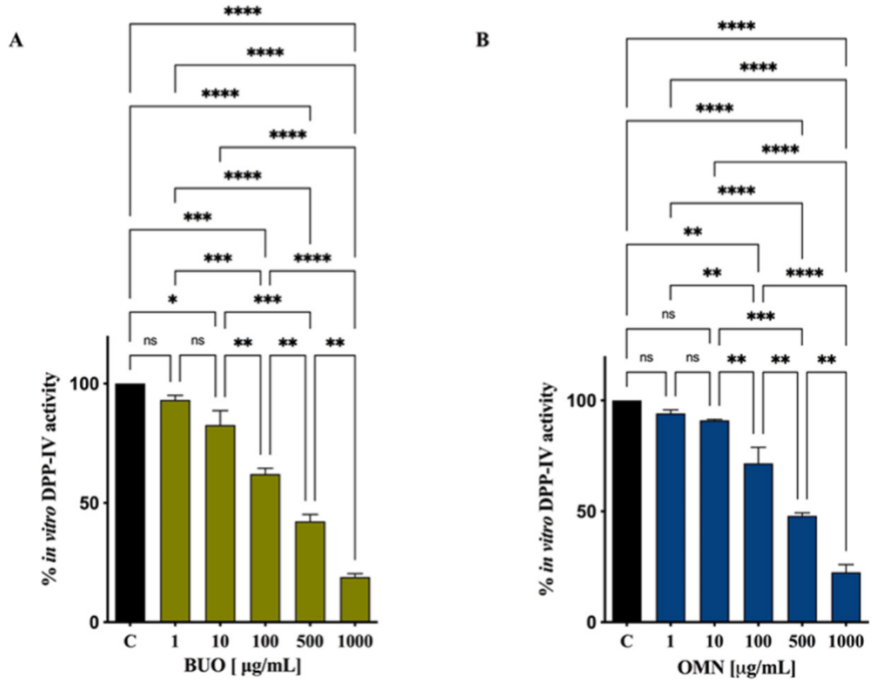

Figure 1. Effect of BUO (**A**) and OMN (**B**) on the *in vitro* DPP-IV activity. The data points represent the averages ± SD of 4 independent experiments performed in triplicate. All data sets were analyzed by one-way ANOVA followed by Tukey's post-hoc test. ns: not significant; C: control sample (H_2O). (*) $p < 0.5$; (**) $p < 0.01$; (***) $p < 0.001$; (****) $p < 0.0001$.

Then, the DPP-IV inhibitory activity was assessed in cellular experiments using Caco-2 cells, which are an improved tool for the screening of DPP-IV inhibitors, since they

are a reliable model of intestinal epithelial cells and express high levels of DPP-IV (Lammi *et al.*, 2018). Since at *in vitro* level the concentration of 1 µg/mL was only slightly effective with regard to DPP-IV activity reduction, we decided to test only the concentrations of 10, 1000, 500, and 1000 µg/mL at cellular level. By monitoring the same fluorescent reaction, clear DPP-IV inhibitory effects were observed on Caco-2 cells also, as shown by Figure 2A,B. Notably, BUO reduced the cellular DPP-IV activity by 2.9 ± 0.7, 44.4 ± 0.7, 61.2 ± 1.8, and 85 ± 4.2% at 10, 100, 500, and 1000 µg/mL, respectively (Figure 2A), and OMN reduced the activity 3 ± 1.9, 35 ± 9.4, 60 ± 7.2, and 82 ± 2.8% at 10, 100, 500, and 1000 µg/mL, respectively (Figure 2B).

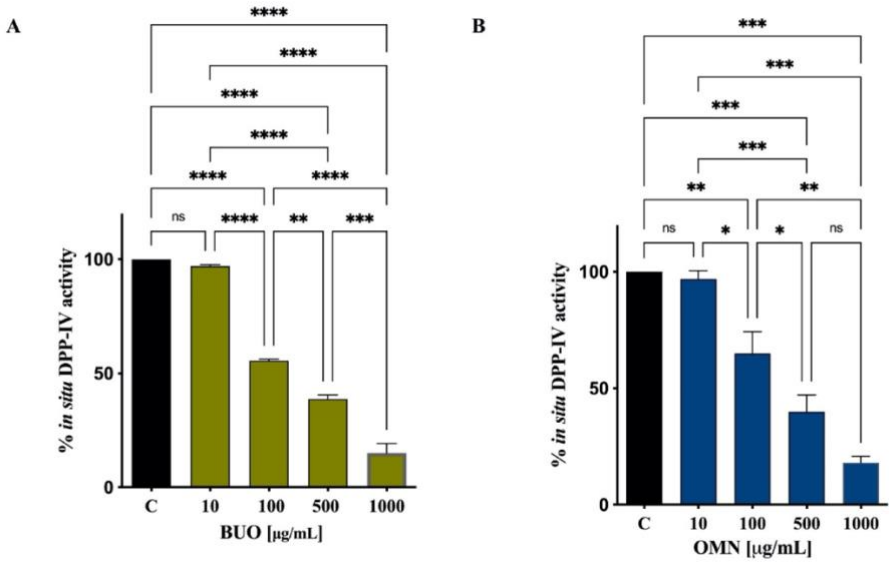

Figure 2. Effect of BUO (**A**) and OMN (**B**) on the cellular DPP-IV activity. The data points represent the averages ± SD of 4 independent experiments performed in triplicate. All data sets were analyzed by one-way ANOVA followed by Tukey's post-hoc test. ns: not significant; C: control sample (H_2O). (*) $p < 0.5$; (**) $p < 0.01$; (***) $p < 0.001$; (****) $p < 0.0001$.

5.3.2 Analysis of Secoiridoids in BUO and OMN Extracts

To investigate on the concentration of some specific secoiridoids in BUO and OMN, ^{1}H-NMR was used to quantitate four typical molecules that characterize the fresh EVOOs: oleacein, oleuropein, oleocanthal, and ligstroside aglycone. Using the manuscript of Karkoula *et al.*, 2012, the signals of the aldehydic protons of these secoiridoids were identified and their integral used for determining their percent concentration in the sample. This was possible by adding maleic acid as internal standard, that has a singlet at 6.29 ppm, in a range of the spectrum without interfering

signals of the sample. The results shown in Table 1 were obtained applying the formula described in Section 2.2. As for the ^{1}H-NMR, only the use of $CDCl_3$ guaranteed an adequate resolution to allow the quantitative evaluation of the selected secoiridoids. Furthermore, to avoid a perturbation of the chemical shifts of the target signals after the addition of the ISTD, it was necessary to add a very low volume of the maleic acid solution dissolved in CH_3CN.

µg/mg Dry Extracts						
	^{1}H-NMR				HPLC-DAD After Hydrolysis	
	Olc	Ol	Lig	Ole	Tot HT	Tot Tyr
BUO	88.4	77.1	86.2	156.2	208.0	156.0
OMN	69.7	135.2	466.8	297.5	151.0	275.1

Table 1: Concentration of the 2 secoiridoids derived by oleuropein (Olc and Ole) and those derived by ligstroside (Ol and Lig); the data are compared with the amount determined by HPLC-DAD after acidic hydrolysis (Lammi *et al.*, 2020), and express the total content of the oleuropein derivatives and ligstroside derivatives as total hydroxytyrosol (HT) and total tyrosol (Tyr), respectively.

5.3.3 Assessment of the In Vitro Inhibition of DPP-IV Activity by Main EVOO Phenols

Based on the EVOO phenol extract composition, it was decided to investigate the effect of the main secoiridoids on the *in vitro* DPP-IV activity. Therefore, oleuropein, oleacein, oleocanthal, hydroxytyrosol, and tyrosol were tested in the range of concentrations 1–1000 µM. Results clearly suggested that all the compounds inhibited the enzyme activity with a dose–response trend and IC_{50} values equal to 472.3 ± 21.7, 187 ± 11.4, 354.5 ± 12.7, 741.6 ± 35.7, and 1112 ± 55.6 µM for oleuropein, oleocanthal, oleacein, hydroxytyrosol, and tyrosol, respectively (Figure 3).

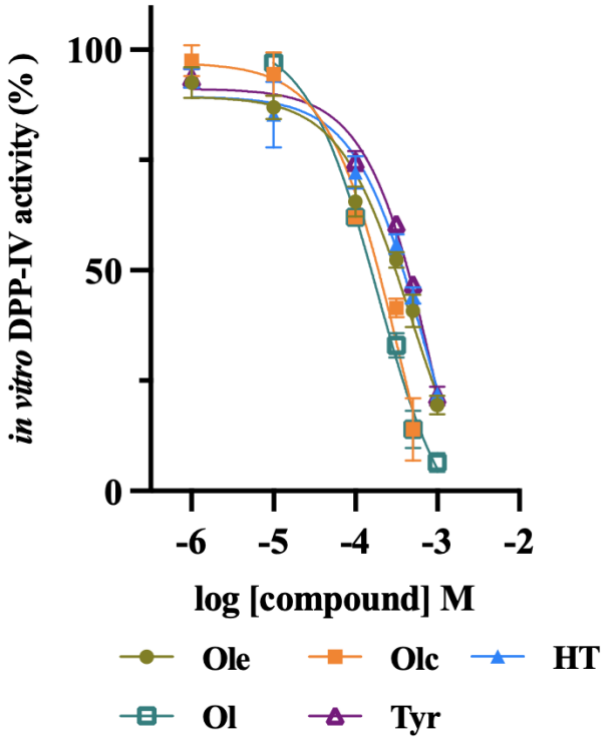

Figure 3: Dose—response effect of oleuropein (Ole), oleocanthal (Ol), oleacein (Olc), and hydroxytyrosol (HT), and tyrosol (Tyr) on the *in vitro* DPP-IV activity. The data points represent the averages ± SD of 3 independent experiments performed in triplicate.

5.3.4 Molecular Docking Investigation

To better investigate the mechanism of action that lies beneath the DPP-IV inhibitory activity of BUO and OMN, a molecular docking investigation of their main phenolic components was carried out. As this study was performed a posteriori, the objective was not to obtain a prediction but instead a rationalization of the observed inhibition activity by analyzing the binding mode of the interaction with DPP-IV. Ligstroside aglycone was not tested *in vitro*, since it is not commercially available. However, due to its similarity with oleuropein aglycone, one may assume that this phytochemical also shares the DPP-IV inhibitory activity of the other secoiridoids. Figure 4 shows the putative complexes that DPP-IV stabilizes with oleuropein aglycone or ligstroside aglycone, which appear fully superimposable. In detail, the aromatic rings of both molecules establish π-π stacking interactions with Trp629, while Ser630 is involved in H-bonds with both the carbonyl group of oleuropein aglycone/ligstroside aglycone and the hydroxy function of the dihydropyran ring. This hydroxy group is also involved in an H-bond with His740.

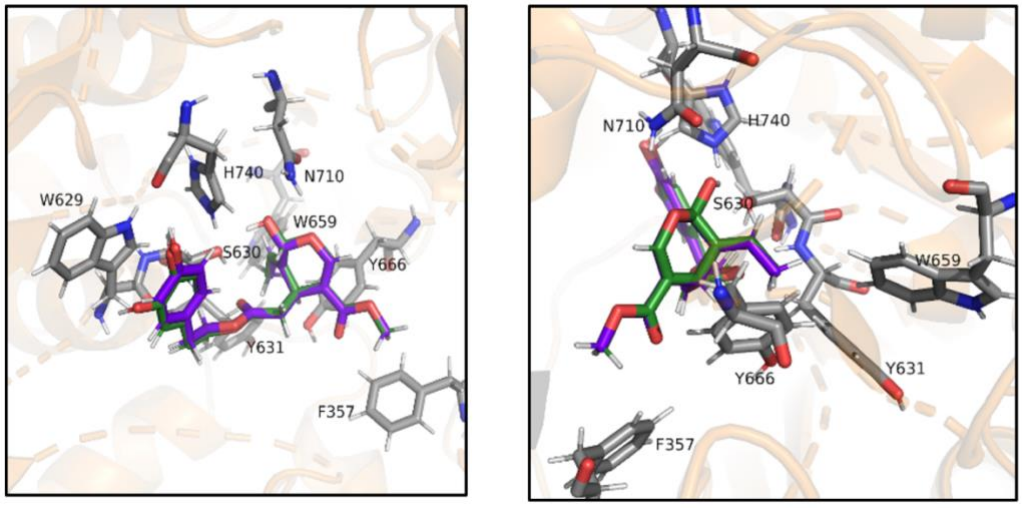

Figure 4: Putative complex between DPP-IV and oleuropein aglycone or ligstroside aglycone. Oleuropein aglycone (dark green) and ligstroside aglycone (purple) in complex with DPP-4, seen from the front (top) and the back (bottom). Key residues S630 and H740 of the catalytic triad appear to be evidently involved in the binding of both ligands.

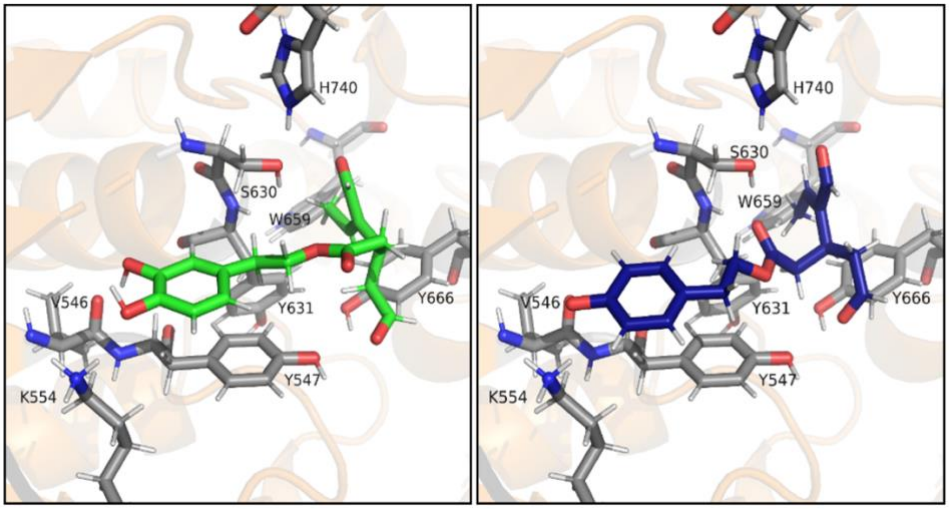

Figure 5: Putative complex between DPP-IV and oleacein or oleocanthal. Oleacin (blue) and oleocanthal (light green) in complex with DPP-4. Key residues S630 and H740 of the catalytic triad appear to be evidently involved in the binding of both ligands.

Moreover, the ethylidene moiety of the dihydropyran is placed within a hydrophobic pocket lined by residues Tyr631, Trp659, and Tyr666 with which it stabilizes ***p-p*** stacking interactions. The heterocyclic oxygen atom establishes an H-bond with Asn710 and the carboxymethyl group further stabilizes the binding through apolar interactions with Phe357. Figure 5 shows the binding of oleacein and oleocanthal to DPP-4. The two poses are less superimposed than before, as a consequence of the higher

flexibility of these dialdehydes compared to the parent secoiridoids. The catechol and phenol rings partially overlap and are responsible for the π-π stacking interactions with Tyr547. Moreover, the phenolic functions establish H-bonds with the carbonyl group of Val546 and with Lys554. Ser630 is involved in an H-bond either with the aldehydic carbonyl oxygen atom of oleacein or with the ester carbonyl oxygen atom of oleocanthal. In both ligands, the ethylidene group is located within the hydrophobic pocket formed by Tyr631, Trp659, and Tyr666 and contributes to the binding as described above. For both oleacein and oleocanthal an aldehyde carbonyl oxygen atom is involved in an H-bond with Tyr547. Moreover, since oleocanthal interacts with Ser630 with the ester carbonyl, the remaining aldehyde establishes an H-bond with His740. Figure 6 displays the binding modes of hydroxytyrosol and tyrosol. Indeed, due to their smaller size, two putative binding modes appear worth mentioning. In Figure 6A both hydroxytyrosol and tyrosol bind within the S2 subsite, and their alcoholic hydroxy group establishes an H-bond with Glu205. The binding of both ligands is further stabilized by the π-cation interaction between the aromatic rings and Arg125, while the catechol hydroxy groups and the phenolic hydroxyl establish H-bonds with Asp739. Figure 6B shows the other possible binding mode in which hydroxytyrosol displays the same binding mode previously described for oleacein and oleocanthal. In detail, the catechol ring establishes π-π stacking Tyr547 and the catechol hydroxy groups are engaged in H-bonds with Val546 and Lys554. The alcoholic hydroxy group of hydroxytyrosol interacts with Ser630. On the other hand, the pose for Tyr involves other residues seen before for larger ligands. The phenol ring establishes π-π stacking interactions with the Tyr666 while the phenolic hydroxyl is involved in an H-bond with Tyr547. At the same time, the alcoholic hydroxyl of Tyr is engaged in an H-bond with Ser630. Figure 6C provides an overall view of the two binding modes of hydroxytyrosol and tyrosol within the binding site of DPP-IV.

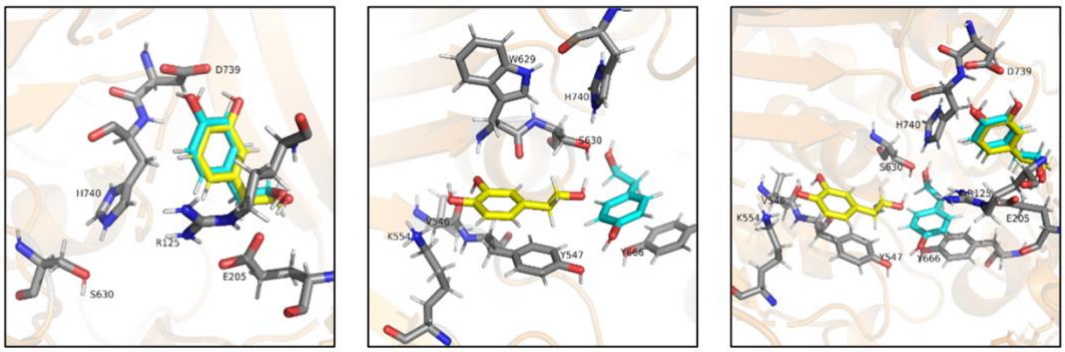

Figure 6: Putative complexes between DPP-IV and hydroxytyrosol or tyrosol. Hydroxytyrosol (yellow) and tyrosol (cyan) in complex with DPP-4. Binding mode A in subsite S2 (A) and binding mode B (B), involving key residue S630 of the catalytic triad. Overall view of both binding modes (C) for an easy comparison.

5.4 Discussion

Recently, the effect of EVOO and oleuropein on the post-prandial glycemic profile was investigated in randomized studies performed on healthy and pre-diabetic subjects. These studies revealed reduced activity and plasma levels of the enzyme DDP-IV and an improvement of the GLP-1 and GIP hormones, responsible for the release of insulin after food ingestion. With DPP-IV being upregulated in the presence of oxidative stress, the observed diminished activity and plasma levels after the consumption of EVOO or oleuropein have been rightly attributed to their antioxidant effect (Violi *et al.*, 2015, Salas-Salvado *et al.*, 2014). These findings prompted us to investigate whether a direct inhibition of the enzyme concomitantly occurred. Notably, our results indicate that both BUO and OMN directly modulate the *in vitro* and cellular DPP-IV activity with a dose–response behavior. In detail, the *in vitro* DPP-IV activity assay was performed at the concentrations of 1, 10, 100, 500, and 1000 μg/mL, showing a statistically significant and dose-dependent inhibition by 6.8 ± 1.9, 17.4 ± 6.1, 37.9 ± 2.4, 57.8 ± 2.9, and 81 ± 1.4% for BUO and by 5.4 ± 1.7, 8.9 ± 0.4, 28.4 ± 7.2, 52 ± 1.3, and 77.5 ± 3.5% for OMN, respectively (Figure 1A,B). Generally, in the area of food bioactive compounds able to inhibit DPP-IV activity, the investigations are carried out exclusively using biochemical tools based on the purified enzyme (Nongonierma *et al.*, 2014, 2015, Oliveira *et al.*, 2018). This traditional approach represents a great limitation for a more realistic characterization of the hydrolysates with DPP-IV inhibitory activity. In light of these observations, a specific feature of our work was the employment of an intestinal cell-based assay for measuring the enzymatic activity, which represents a

complementary and cost-effective strategy for a more efficient discovery of food-derived DPP-IV inhibitors (Lammi *et al.*, 2018,2019). The enterocyte luminal surface expresses a great quantity of DPP-IV and for this reason, human intestinal Caco-2 cells represent a reliable tool for characterizing food derived DPP-IV inhibitors. Therefore, with the concentration of 1 µg/mL being only slightly effective *in vitro*, both BUO and OMN in the range of concentrations between 10 and 1000 µg/mL were assessed at cellular levels. Findings suggested that BUO and OMN caused a reduction in DPP-IV activity by 2.9 ± 0.7, 44.4 ± 0.7, 61.2 ± 1.8, and 85 ± 4.2% and by 3 ± 1.9, 35 ± 9.4, 60 ± 7.2, and 82 ± 2.8% at 10, 100, 500, and 1000 µg/mL, respectively (Figure 2A,B), corroborating the *in vitro* results. In fact, comparing the *in vitro* (Figure 1) and cellular (Figure 2) data, the activity of both extracts is very similar, suggesting that both phytocomplexes may be stable to the metabolic activity of Caco-2 cells. Moreover, although these extracts were characterized by slightly different total phenolic contents, with OMN being richer, and by a different quantitative composition in the secoiridoid profile, with BUO being richer than OMN in hydroxytyrosol derivatives such as oleocanthal and oleacein (Lammi *et al.*, 2020), in *in vitro* and cellular experiments no statistically significant differences were observed between the EVOO phenolic extracts. In addition, our findings are in line with previous work that demonstrated that a grape seed procyanidin extract (GSPE) can directly inhibit DPP4 activity (Gonzalez-Abuin *et al.*, 2012). In particular, GSPE inhibits *in vitro* DPP-IV activity by 54.67 ± 0.7 at 100 µg/mL. It seems therefore possible to affirm that *in vitro* the behavior of BUO and OMN extracts is similar to that of GSPE, whereas the EVOO phenolic extracts are more active than GSPE on human intestinal Caco-2 cells. In fact, while GSPE reduces the activity of the cellular enzyme by only 7.45 ± 1.5% at 100 µg/mL, BUO and OMN are 6- and 5-fold more active at the same concentrations on the same cellular model (Gonzalez-Abuin *et al.*, 2012). This different behavior may be explained by the different metabolic stabilities of the phytocomplexes in the presence of intestinal cells or by different affinities to the DPP-IV enzyme expressed on the Caco-2 cell membranes. In fact, GSPE is more active on the plasmatic and salivary DPP-IV than on the isoform, which is expressed on the membrane of Caco-2 cells (Gonzalez-Abuin *et al.*, 2012). To better describe the chemical characteristics of the two samples, the concentration of specific secoiridoids typically abundant in fresh EVOOs was evaluated by quantitative 1H-NMR. The use of HPLC-DAD to evaluate the effects of the acid hydrolysis on the extracts provides an interesting indirect estimation of the total

secoiridoid forms produced by the transformation of the precursors, namely oleuropein and ligstroside (Table 1). The values obtained by 1H-NMR did not consider all the secoiridoid forms in the samples but were useful to confirm that BUO was richer in oleuropein derivatives (oleacein and oleuropein aglycone), in agreement with the results of the HPLC-DAD analyses. From the 1H-NMR spectra, it was possible to highlight a high concentration of the ligstroside aglycone, which is more than five times higher in OMN than in BUO. In parallel, the effects of oleuropein, oleocanthal, oleacein, hydroxytyrosol, and tyrosol, the main secoridoids within both extracts, on the *in vitro* DPP-IV activity were analyzed. Results indicate that all the compounds inhibited the enzyme activity with a dose-response trend, with IC_{50} values equal to 472.3 ± 21.7, 187 ± 11.4, 354.5 ± 12.7, 741.6 ± 35.7, and 1112 ± 55.6 μM, respectively (Figure 3). Although all the compounds are active in the high micromolar range, oleocanthal is the most active, while hydroxytyrosol and tyrosol are less active. However, so far only a few phenolic compounds have been shown to inhibit DPP-IV activity. Notably, it has been demonstrated that some flavonoids show an interesting ability to modulate the glucose homeostasis through the inhibition of DPP-IV activity. Indeed, luteolin, apigenin, quercetin, curcumin, kaempferol, and resveratrol reduce *in vitro* enzyme activity, with IC_{50} values ranging from 0.6 ± 0.4 nM (resveratrol) to 10.36 ± 0.09 μM (eriocitrin) (Fan *et al.*, 2013). In addition, it was demonstrated that curcumin is more active than resveratrol (Huang *et al.*, 2019), whereas rutin, narirutin, naringin, hesperidin, limonin, neohesperidin, genistin, catechin, epicatechin, chlorogenic acid, and protocatechuic acid are totally inactive against DPP-IV activity. The binding pose of resveratrol and curcumin in the DPP-IV active site, obtained by molecular docking, showed that they interact closely with key residues of sites S1, S2, and S3 within the active pocket of the enzyme (Fan *et al.*, 2013, Huang *et al.*, 2019) and that they act as competitive DPP-IV inhibitors, while luteolin and apigenin bound to DPP-IV in a noncompetitive manner. Hence, in order to better explain these results and understand the mechanism of action of these extracts, an in silico molecular docking investigation was performed. Indeed, Figure 4 and Figure 5 show the binding of the bigger ligands oleuropein aglycone, ligstroside aglycone, oleacein, and oleocanthal that interact with the amino acidic residues present in the binding pocket and are cited in the literature as part of subsites S1, S1′, and S2′ (Nabeno *et al.*, 2013) or Site 1 and 2 (Pantaleão *et al.*, 2018), especially Ser630 and His740 of the catalytic triad, thus preventing the endogenous peptide from collocating in the binding pocket and being cleaved by the

protease. Being smaller molecules, hydroxytyrosol and tyrosol possess two different possible binding modes (Figure 6A,B). Binding mode A (Figure 6A) is interesting because the ligands interact, among others, with residue Glu205 of the S2 subsite, which is usually filled with the protonated N-terminus (called residue P2) of the endogenous peptide and represents the anchoring site of the peptide substrate. According to this docking pose, the presence of either hydroxytyrosol or tyrosol in this subsite impedes the binding and cleavage of the peptide even if the catalytic triad is not involved. Binding mode B (Figure 6B), on the other hand, is in line with the binding mode of the bigger ligands and involves the residues of the catalytic triad, preventing the substrate from binding and being cleaved. The possible existence of two different binding modes by hydroxytyrosol and tyrosol with the enzyme could explain the higher value of IC_{50} for these compounds, suggesting that binding mode A may be less efficient in blocking DPP-IV activity than binding mode B, which is the same for all the other compounds tested. Apart from the fact that literature is very scarce with regard to phenolic DPP-IV inhibitors, an important aspect of these docking simulations lies in the fact that the putative binding of these molecules is built on hydrogen bonds and van der Waals interactions. Such an interaction pattern is very different from the binding mode of marketed DPP-IV inhibitors, which is characterized by a protonated amino group which stabilizes ion pairs with Glu205 and Glu206, mimicking what occurs for the endogenous peptide. This is well-mirrored by the IC_{50} values, which are in the high micromolar range, and thus very far from those of synthetic inhibitors that all share IC_{50} values in the low nanomolar range. However, these results emphasize that a weak but non-negligible inhibition can be induced even without eliciting those ionic interactions which are considered mandatory for the DPP-IV inhibition.

5.5 Conclusions

Thanks to a combination of biochemical, cellular, and computational techniques, this study for the first time provides relevant and innovative insights regarding the direct inhibition of DPP-IV by phenolic EVOO extracts. In addition, for the first time, we have demonstrated the inhibitory effects of the main secoridoids (oleuropein, oleocanthal, oleacein, hydroxytyrosol, and tyrosol) against DPP-IV activity. Possibly, the presence of less abundant biophenols within each extract, i.e., apigenin and luteolin,

may synergistically contribute to the biological effect. Overall, these results allow us to explain the molecular mechanism of action through which EVOO contributes to post-prandial glycemia modulation.

5.6 Supporting information

Chemicals*:* Tris-HCl, ethylendiaminetetraacetic acid (EDTA) and NaCl were from Sigma-Aldrich (St. Louis, MO, USA) The DPP-IV assay kit was from (Cayman Chemicals (Michigan, USA), while Gly-Pro-amido-4-methylcoumarin hydrobromide (Gly-Pro-AMC) was from AnaSpec (Freemont, CA, USA). Dulbecco's modified Eagle medium (DMEM), fetal bovine serum (FBS), L- glutamine, phosphate buffered saline (PBS), penicillin/streptomycin, 24 and 96- well plates were from Euroclone (Milan, Italy), polycarbonate filters, 12 mm in diameter, 0.4 mm in pore diameter, were from Transwell Corning Inc. (Lowell, MA, USA). Tyrosol (≥98%), hydroxytyrosol (≥98%), and oleocanthal (≥95%) were from Merck Life Science S.r.l. (Milano, Italy); oleuropein (≥98%) was from Extrasynthese (Genay, France), whereas oleacin was from Phytolab (Vestenbergsgreuth, Germany).

In Vitro* DPP-IV Activity Assay:* The DPP-IV enzyme was provided by Cayman Chemicals (Michigan, USA), while the DPP-IV substrate (H-Gly-Pro-AMC) was from AnaSpec Inc. (Freemont, CA, USA). The experiments were carried out in triplicate in a half volume 96-well solid plate (white). Each reaction (50 μL) was prepared adding the reagents in a microcentrifuge tube in the following order: 1 X assay buffer (30 μL) [20 mM Tris-HCl, pH 8.0, containing 100 mM NaCl and 1 mM EDTA], BUO and OMN EVOO extracts at final concentrations of 1, 10, 100, 500 and 1000 μg/mL or vehicle (C) or standard oleuropein, hydroxytyrosol, tyrosol, oleacein and oleocanthal (1-1000 μM) (10 μL), and finally the DPP-IV enzyme (10 μL). Subsequently, the samples were mixed and 50 μL of each reaction was transferred in each plate well. Each reaction was started by adding 50 μL of substrate solution to each well and incubated at 37° for 30 minutes. Fluorescence signals deriving from the release of free AMC were measured using a Synergy H1 fluorescence plate reader from BioTek (excitation/emission wavelength 350/465 nm respectively).

Cell Culture*:* Caco-2 cells, obtained from INSERM (Paris, France), were routinely sub- cultured at 50% density and maintained at 37°C in a 90% air/10% CO_2 atmosphere in DMEM containing 25 mM of glucose, 3.7 g/L of NaHCO3, 4 mM of stable L-glutamine, 1% non-essential amino acids, 100 U/L of penicillin and 100 μg/L of streptomycin (complete medium), supplemented with 10% heat- inactivated fetal bovine serum (FBS; Hyclone Laboratories, Logan, UT, USA).

In Situ **DPP-IV Activity Assay***:* A total of 5 x 10^4 Caco-2 cells/well were seeded in black 96-well plates with clear bottom. The second day after seeding, the spent medium was discarded and cells were treated with 100 μL/well of BUO and OMN extracts at the concentration of 10, 100, 500, 1000 μg/mL or vehicle (C) in growth medium for 24 h at 37°C. Afterwards, treatments were removed and Caco-2 cells were washed once with 100 μL of phosphate buffered saline (PBS) without Ca^{2+} and Mg^{2+}, before the addition to each well of 100 μL of Gly-Pro-AMC substrate at the concentration of 50.0 μM in PBS without Ca^{2+} and Mg^{2+}. Fluorescence signals deriving from the release of free AMC were measured using a Synergy H1 fluorescence microplate reader from BioTek (excitation/emission wavelength 350/465 nm respectively) every 1 min for up to 10 minutes.

5.7 References

Aiello G., Ferruzza S., Ranaldi G., Sambuy Y., Arnoldi A., Vistoli G., Lammi C. Behavior of three hypocholesterolemic peptides from soy protein in an intestinal model based on differentiated Caco-2 cell. J. Funct. Foods. 2018;45:363–370. doi: 10.1016/j.jff.2018.04.023.

Babio N., Toledo E., Estruch R., Ros E., Martinez-Gonzalez M.A., Castaner O., Bullo M., Corella D., Aros F., Gomez-Gracia E., et al. Mediterranean diets and metabolic syndrome status in the PREDIMED randomized trial. Can. Med. Assoc. J. 2014;186:E649–E657. doi: 10.1503/cmaj.140764.

Bailey C.J., Tahrani A.A., Barnett A.H. Future glucose-lowering drugs for type 2 diabetes. Lancet Diabetes Endocrinol. 2016;4:350–359. doi: 10.1016/S2213-8587(15)00462-3.

Bellumori M., Cecchi L., Innocenti M., Clodoveo M.L., Corbo F., Mulinacci N. The EFSA Health Claim on Olive Oil Polyphenols: Acid Hydrolysis Validation and Total Hydroxytyrosol and Tyrosol Determination in Italian Virgin Olive Oils. Molecules. 2019;24:2179. doi: 10.3390/molecules24112179.

Carnevale R., Silvestri R., Loffredo L., Novo M., Cammisotto V., Castellani V., Bartimoccia S., Nocella C., Violi F. Oleuropein, a component of extra virgin olive oil, lowers postprandial glycaemia in healthy subjects. Br. J. Clin. Pharmacol. 2018;84:1566–1574. doi: 10.1111/bcp.13589.

Carr R.D. Drug development from the bench to the pharmacy: With special reference to dipeptidyl peptidase-4 inhibitor development. Diabet. Med. 2016;33:718–722. doi: 10.1111/dme.13066.

Cavalot F., Pagliarino A., Valle M., Di Martino L., Bonomo K., Massucco P., Anfossi G., Trovati M. Postprandial blood glucose predicts cardiovascular events and all-cause mortality in type 2 diabetes in a 14-year follow-up: Lessons from the San Luigi Gonzaga Diabetes Study. Diabetes Care. 2011;34:2237–2243. doi: 10.2337/dc10-2414.

Doupis J., Veves A. DPP4 inhibitors: A new approach in diabetes treatment. Adv. Ther. 2008;25:627–643. doi: 10.1007/s12325-008-0076-1.

Dupre J., Ross S.A., Watson D., Brown J.C. Stimulation of insulin secretion by gastric inhibitory polypeptide in man. J. Clin. Endocrinol. Metab. 1973;37:826–828. doi: 10.1210/jcem-37-5-826.

Fan J.F., Johnson M.H., Lila M.A., Yousef G., de Mejia E.G. Berry and Citrus Phenolic Compounds Inhibit Dipeptidyl Peptidase IV: Implications in Diabetes Management. Evid. Based Complement. Altern. Med. 2013;2013:479505. doi: 10.1155/2013/479505.

Gonzalez-Abuin N., Martinez-Micaelo N., Blay M., Pujadas G., Garcia-Vallve S., Pinent M., Ardevol A. Grape Seed-Derived Procyanidins Decrease Dipeptidyl-peptidase 4 Activity and Expression. J. Agric. Food Chem. 2012;60:9055–9061. doi: 10.1021/jf3010349.

Huang P.K., Lin S.R., Chang C.H., Tsai M.J., Lee D.N., Weng C.F. Natural phenolic compounds potentiate hypoglycemia via inhibition of Dipeptidyl peptidase IV. Sci. Rep. 2019;9:15585. doi: 10.1038/s41598-019-52088-7.

International Olive Council . Official Method of Analysis. Determination of Biophenols in Olive Oil by HPLC. International Olive Council; Madrid, Spain: 2009. IOC/T.20/Doc No. 29.

Ishibashi Y., Matsui T., Maeda S., Higashimoto Y., Yamagishi S. Advanced glycation end products evoke endothelial cell damage by stimulating soluble dipeptidyl peptidase-4 production and its interaction with mannose 6-phosphate/insulin-like growth factor II receptor. Cardiovasc. Diabetol. 2013;12:125. doi: 10.1186/1475-2840-12-125.

Karkoula E., Skantzari A., Melliou E., Magiatis P. Direct measurement of oleocanthal and oleacein levels in olive oil by quantitative (1)H NMR. Establishment of a new index for the characterization of extra virgin olive oils. J. Agric. Food Chem. 2012;60:11696–11703. doi: 10.1021/jf3032765.

Khatib M., Pieraccini G., Innocenti M., Melani F., Mulinacci N. An insight on the alkaloid content of Capparis spinosa L. root by HPLC-DAD-MS, MS/MS and (1)H qNMR. J. Pharm. Biomed. Anal. 2016;123:53–62. doi: 10.1016/j.jpba.2016.01.063.

Korb O., Stützle T., Exner T.E. Empirical scoring functions for advanced protein-ligand docking with PLANTS. J. Chem. Inf. Model. 2009;49:84–96. doi: 10.1021/ci800298z.

Kreymann B., Williams G., Ghatei M.A., Bloom S.R. Glucagon-like peptide-1 7-36: A physiological incretin in man. Lancet. 1987;2:1300–1304. doi: 10.1016/S0140-6736(87)91194-9.

Lammi C., Bellumori M., Cecchi L., Bartolomei M., Bollati C., Clodoveo M.L., Corbo F., Arnoldi A., Nadia M. Extra Virgin Olive Oil Phenol Extracts Exert Hypocholesterolemic Effects through the Modulation of the LDLR Pathway: In Vitro and Cellular Mechanism of Action Elucidation. Nutrients. 2020;12:1723. doi: 10.3390/nu12061723.

Lammi C., Bollati C., Ferruzza S., Ranaldi G., Sambuy Y., Arnoldi A. Soybean- and Lupin-Derived Peptides Inhibit DPP-IV Activity on In Situ Human Intestinal Caco-2 Cells and Ex Vivo Human Serum. Nutrients. 2018;10:1082. doi: 10.3390/nu10081082.

Lammi C., Bollati C., Gelain F., Arnoldi A., Pugliese R. Enhancement of the stability and anti-DPPIV activity of hempseed hydrolysates through self-assembling peptide-based hydrogels. Front. Chem. 2019;6:670. doi: 10.3389/fchem.2018.00670.

Lammi C., Mulinacci N., Cecchi L., Bellumori M., Bollati C., Bartolomei M., Franchini C., Clodoveo M.L., Corbo F., Arnoldi A. Virgin Olive Oil Extracts Reduce Oxidative Stress and Modulate Cholesterol Metabolism: Comparison between Oils Obtained with Traditional and Innovative Processes. Antioxidants. 2020b;9:17. doi: 10.3390/antiox9090798.

Lammi C., Zanoni C., Arnoldi A., Vistoli G. Peptides derived from soy and lupin protein as Dipeptidyl-Peptidase IV inhibitors: In vitro biochemical screening and in silico molecular modeling study. J. Agric. Food Chem. 2016;64:9601–9606. doi: 10.1021/acs.jafc.6b04041.

Lin H.J., Lee B.C., Ho Y.L., Lin Y.H., Chen C.Y., Hsu H.C., Lin M.S., Chien K.L., Chen M.F. Postprandial glucose improves the risk prediction of cardiovascular death beyond the metabolic syndrome in the nondiabetic population. Diabetes Care. 2009;32:1721–1726. doi: 10.2337/dc08-2337.

Martinez-Gonzalez M.A., Garcia-Arellano A., Toledo E., Bes-Rastrollo M., Bullo M., Corella D., Fito M., Ros E., Lamuela-Raventos R.M., Rekondo J., et al. Obesity Indexes and Total Mortality among Elderly Subjects at High Cardiovascular Risk: The PREDIMED Study. PLoS ONE. 2014;9:e103246. doi: 10.1371/journal.pone.0103246.

Nabeno M., Akahoshi F., Kishida H., Miyaguchi I., Tanaka Y., Ishii S., Kadowaki T. A comparative study of the binding modes of recently launched dipeptidyl peptidase IV inhibitors in the active site. Biochem. Biophys. Res. Commun. 2013;434:191–196. doi: 10.1016/j.bbrc.2013.03.010.

Nongonierma A.B., FitzGerald R.J. An in silico model to predict the potential of dietary proteins as sources of dipeptidyl peptidase IV (DPP-IV) inhibitory peptides. Food Chem. 2014;165:489–498. doi: 10.1016/j.foodchem.2014.05.090.

Nongonierma A.B., Fitzgerald R.J. Investigation of the Potential of Hemp, Pea, Rice and Soy Protein Hydrolysates as a Source of Dipeptidyl Peptidase IV (DPP-IV) Inhibitory Peptides. Food Dig. Res. Curr. Opin. 2015;6:19–29. doi: 10.1007/s13228-015-0039-2.

Oliveira V.B., Araujo R.L.B., Eidenberger T., Brandao M.G.L. Chemical composition and inhibitory activities on dipeptidyl peptidase IV and pancreatic lipase of two underutilized species from the Brazilian Savannah: Oxalis cordata A.St.-Hil. and Xylopia aromatica (Lam.) Mart. Food Res. Int. 2018;105:989–995. doi: 10.1016/j.foodres.2017.11.079.

Pantaleão S.Q., Philot E.A., de Resende-Lara P.T., Lima A.N., Perahia D., Miteva M.A., Scott A.L., Honorio K.M. Structural Dynamics of DPP-4 and Its Influence on the Projection of Bioactive Ligands. Molecules. 2018;23:490. doi: 10.3390/molecules23020490.

Pedretti A., Mazzolari A., Gervasoni S., Fumagalli L., Vistoli G. The VEGA suite of programs: An versatile platform for cheminformatics and drug design projects. Bioinformatics. 2021;37:1174–1175. doi: 10.1093/bioinformatics/btaa774.

Phillips J.C., Braun R., Wang W., Gumbart J., Tajkhorshid E., Villa E., Chipot C., Skeel R.D., Kalé L., Schulten K. Scalable molecular dynamics with NAMD. J. Comput. Chem. 2005;26:1781–1802. doi: 10.1002/jcc.20289.

Rhee N.A., Østoft S.H., Holst J.J., Deacon C.F., Vilsbøll T., Knop F.K. The impact of dipeptidyl peptidase 4 inhibition on incretin effect, glucose tolerance, and gastrointestinal-mediated glucose disposal in healthy subjects. Eur. J. Endocrinol. 2014;171:353–362. doi: 10.1530/EJE-14-0314.

Salas-Salvado J., Bullo M., Estruch R., Ros E., Covas M.I., Ibarrola-Jurado N., Corella D., Aros F., Gomez-Gracia E., Ruiz-Gutierrez V., et al. Prevention of Diabetes with Mediterranean Diets A Subgroup Analysis of a Randomized Trial. Ann. Intern. Med. 2014;160:1–10. doi: 10.7326/M13-1725.

Schönberger T., Monakhova Y.B., Lachenmeier D.W., Kuballa T. Guide to NMR method development and validation—Part 1: Identification and quantification. EUROLAB Tech. Rep. 2014;2014:1–20.

Smilowitz N.R., Donnino R., Schwartzbard A. Glucagon-like peptide-1 receptor agonists for diabetes mellitus: A role in cardiovascular disease. Circulation. 2014;129:2305–2312. doi: 10.1161/CIRCULATIONAHA.113.006985.

Tushuizen M.E., Diamant M., Heine R.J. Postprandial dysmetabolism and cardiovascular disease in type 2 diabetes. Postgrad. Med. J. 2005;81:1–6. doi: 10.1136/pgmj.2004.020511.

Violi F., Loffredo L., Pignatelli P., Angelico F., Bartimoccia S., Nocella C., Cangemi R., Petruccioli A., Monticolo R., Pastori D., et al. Extra virgin olive oil use is associated with improved post-prandial blood glucose and LDL cholesterol in healthy subjects. Nutr. Diabetes. 2015;5:e172. doi: 10.1038/nutd.2015.23.

CHAPTER 5

MANUSCRIPT 3

ASSESSMENT OF THE CHOLESTEROL-LOWERING EFFECT OF MOMAST®: BIOCHEMICAL AND CELLULAR STUDIES

Martina Bartolomei,† Carlotta Bollati,† Jianqiang Li, Anna Arnoldi, and Carmen Lammi*

Department of Pharmaceutical Sciences, University of Milan, Via Mangiagalli 25, 20133 Milan, Italy

* Author to whom correspondence should be addressed

† These authors contributed equally to this work.

6. Abstract

MOMAST® is a patented phenolic complex derived from the olive oil vegetation water, a by-product of the olive oil supply chain, in which hydroxytyrosol (OH-Tyr) and tyrosol (Tyr) and verbascoside are the main compounds. This study was aimed at investigating its hypocholesterolemic effect by assessing the ability to modulate the low-density lipoprotein (LDL) receptor (LDLR)/sterol regulatory element-binding protein 2 (SREBP-2), and proprotein convertase subtilisin/kexin type 9 (PCSK9) pathways. MOMAST® inhibits the *in vitro* activity of 3-hydroxy-3-methylglutaryl coenzyme A reductase (HMGCoAR) with a dose-response trend. After the treatment of HepG2 cells, MOMAST® increases the SREBP-2, LDLR, and HMGCoAR protein levels leading, from a functional point of view to an improved ability of hepatic cells to up-take LDL from the extracellular environment with a final cholesterol-lowering effect. Furthermore, MOMAST®decreased the PCSK9 protein levels and its secretion in the extracellular environment, presumably via the reduction of the hepatic nuclear factor 1-α (HNF1-α). The experiments were performed in parallel, using pravastatin as a reference compound. Results demonstrated that MOMAST® may be exploited as a new ingredient for the development of functional foods and/or nutraceuticals for cardiovascular disease prevention.

6.1 Introduction

The production of extra virgin olive oil (EVOO) has a significant economic value for the Mediterranean countries. In particular, Spain, Italy, and Greece are responsible for 63% of international olive annual production (Banias *et al.*, 2017). However, the production process has a noteworthy environmental impact, since it involves the consumption of large amounts of resources and generates emissions and water and soil pollution. More in detail, olive oil production generates huge amounts of waste, i.e., wood, branches, leaves, and by-products, such as olive pomace, olive mill wastewater, olive stones, with a relevant impact at environmental level. These residues are not only undesirable in terms of sustainability and environmental impact, but also create high management and disposal costs (Mallamaci *et al.*, 2021). Nevertheless, the olive oil production by-products are rich in high-value molecules such as phenolic compounds, particularly abundant in olive oil vegetation water (OVW) (Banias *et al.*, 2017, Pandey

et al., 2009). Nowadays, there is an increasing interest in natural polyphenols given their well-known health-promoting effects, i.e., antioxidant, anti-inflammatory, anti-diabetic, anti-mutagenic, neuro-protective, and cardio-protective (Visioli *et al.*, 2011, Covas *et al.*, 2006). Moreover, in the area of cardiovascular diseases prevention, it has been widely demonstrated that the consumption of an EVOO rich in phenolic compounds reduces low-density lipoprotein (LDL) cholesterol (LDL-C) and triglyceride, decreases oxidative stress and lipid oxidation, and enhances the high-density lipoprotein (HDL) cholesterol (HDL-C) (Covas *et al.*, 2006, Rees *et al.*, 2019). In this context, recent evidence contributes to defining the molecular mechanism at the basis of the hypocholesterolemic effect exerted by the EVOO phenolic compounds (Romani et al., 2019). Notably, a phenolic phytocomplex extracted from the EVOO of the Cultivar Coratina (OMN) increases the low-density lipoprotein (LDL) receptor (LDLR) protein levels as a result of the activation of the sterol regulatory element-binding proteins (SREBP-2) transcription factor, allowing human hepatic HepG2 cells to uptake LDL particles from the extracellular environment with a final cholesterol-lowering effect (Lammi *et al.*, 2020). MOMAST® is a patented natural phenolic complex, rich in tyrosol (Tyr) and hydroxytyrosol (OH-Tyr), which is obtained from the OVW by-products of *Coratina* cultivar using exclusively physical and mechanical methods, without the use of solvents and other chemical processes. This sustainable product, currently on the market, is directly used in its original form or has the potential to become the main ingredient in the formulations of nutraceutical, pharmaceutical, and cosmetic products. Indeed, MOMAST® has shown antioxidant and anti-inflammatory properties in rat isolated tissues after LPS stimuli (Recinella *et al.*,2019). In light of this evidence, the present study was aimed at fostering the pleotropic health-promoting activity of this sustainable product investigating the hypocholesterolemic properties of MOMAST® through the use of *in vitro* and cellular techniques. In particular, dedicated experiments were performed in order to verify its direct ability to modulate *in vitro* the 3-hydroxy-3-methylglutaryl coenzyme A reductase (HMGCoAR) activity. In parallel, human hepatic HepG2 cells were treated with MOMAST® (50 µg/mL) and western blotting experiments were carried out for assessing its effect on the modulation of the intracellular cholesterol metabolism. All the experiments were performed using pravastatin as reference compound.

6.2 Materials and Methods

6.2.1 Chemicals

The Dulbecco's modified Eagle's medium (DMEM), L-glutamine, foetal bovine serum (FBS), phosphate buffered saline (PBS), penicillin/streptomycin, chemiluminescent reagent, and 24 or 96-well plates were purchased from Euroclone (Milan, Italy). MTT [3-(4,5-dimethylthiazol-2-yl)-2,5-diphenyltetrazolium bromide], Janus Green bovine serum albumin (BSA), RIPA buffer, the antibody against β-actin, Pravastatin and HMGCoAR assay kit were bought from Sigma-Aldrich (St. Louis, MO, USA). The antibody against HMGCoAR was bought from Abcam (Cambridge, UK). Phenylmethanesulfonyl fluoride (PMSF), Na-orthovanadate inhibitors, and the antibodies against rabbit Ig-horseradish peroxidase (HRP), mouse Ig-HRP, and SREBP-2 were purchased from Santa Cruz Biotechnology Inc. (Santa Cruz, CA, USA). The antibodies against the LDLR were bought from Pierce (Rockford, IL, USA). The inhibitor cocktail Complete Midi from Roche (Basel, Swiss). Mini protean TGX pre-cast gel 7.5% and Mini nitrocellulose Transfer Packs were purchased from BioRad (Hercules, CA, USA). LDL-DyLight™ 549 from Cayman Chemical (Michigan, USA).

6.2.2 MOMAST® Description

Bioenutra S.R.L. (Italy) supplies the patented MOMAST® sample as liquid 50 mL units (production lot: B20-01/PL, 100 mg/mL) directly from the production process. Table 1 shows the main characteristics of this MOMAST® sample, whereas the technical data sheets, provided by the company, are available as Supplementary Materials.

Name	Type	Phenols Composition (%)	Appearance
MOMAST®	PLUS 30	OH-Tyr = 4.35 Tyr = 0.95 Verbascoside = 0.46 Total polyphenols = 6.47	Red liquid

OH-Tyr: hydroxytyrosol; Tyr: tyrosol.

Table 1. MOMAST® sample features and phenols composition. OH-Tyr: hydroxytyrosol; Tyr: tyrosol.

6.2.3 Cell Culture Conditions

Research HepG2 cell line was bought from ATCC (HB-8065, ATCC from LGC Standards, Milan, Italy) and was cultured in DMEM high glucose with stable l-glutamine, supplemented with 10% FBS, 100 U/mL penicillin, 100 µg/mL

streptomycin (complete growth medium) with incubation at 37 °C under 5% CO_2 atmosphere.

6.2.4 MTT assay

A total of 3 x 10^4 HepG2 cells/well were seeded in 96-well plates and treated with 10.0 – 500.0 µg/mL of MOMAST®, or vehicle (H_2O) in complete growth media for 48 h at 37 °C under 5% CO_2 atmosphere. Subsequently, the treatment solvent was aspirated and 100 µL/well of 3-(4,5-dimethylthiazol-2-yl)-2,5-diphenyltetrazolium bromide (MTT) filtered solution added. After 2h of incubation at 37 °C under 5% CO_2 atmosphere, 0.5 mg/mL solution was aspirated and 100 µL/well of the lysis buffer (8 mM HCl + 0.5% NP-40 in DMSO) added. After 10 min of slow shaking, the absorbance at 575 nm was read on the Synergy H1 fluorescence plate reader (Biotek, Bad Friedrichshall, Germany).

6.2.5 HMGCoAR activity assay

The assay buffer, NADPH, substrate solution, and HMGCoAR were provided in the HMGCoAR Assay Kit (Sigma). The experiments were carried out following the manufacturer's instructions at 37 °C. In particular, each reaction (200 µL) was prepared, adding the reagents in the following order: 1 x assay buffer, Pravastatin 1.0 µM or MOMAST® (10.0 – 500.0 µg/ mL) or vehicle (C), the NADPH (4 µL), the substrate solution (12 µL), and finally the HMGCoAR (catalytic domain) (2 µL). Subsequently, the samples were mixed and the absorbance at 340 nm read by a microplate reader Synergy H1 from Biotek at time 0 and 15 min. The HMGCoAR-dependent oxidation of NADPH and the inhibition properties of MOMAST® were measured by absorbance reduction, which is directly proportional to enzyme activity.

6.2.6 Western blot analysis

A total of 1.5 × 10^5 HepG2 cells/well (24-well plate) were treated with 50.0 µg/mL of MOMAST® or Pravastatin 1.0 µM for 24 h. After each treatment, cells were scraped in 30 µL ice-cold lysis buffer [RIPA buffer + inhibitor cocktail + 1:100 PMSF + 1:100 Na-orthovanadate] and transferred in an ice-cold microcentrifuge tube. After centrifugation at 13300 g for 15 min at 4 °C, the supernatant was recovered and

transferred into a new ice-cold tube. Total proteins were quantified by Bradford method and 50 µg of total proteins loaded on a pre-cast 7.5% Sodium Dodecyl Sulphate-Polyacrylamide (SDS-PAGE) gel at 130 V for 45 min. Subsequently, the gel was pre-equilibrated with 0.04% SDS in H_2O for 15 min at room temperature (RT) and transferred to a nitrocellulose membrane (Mini nitrocellulose Transfer Packs,) using a trans-Blot Turbo at 1.3 A, 25 V for 7 min. Target proteins, on milk or BSA blocked membrane, were detected by primary antibodies as follows: anti-SREBP2, anti-LDLR, anti-HMGCoAR and anti-β-actin. Secondary antibodies conjugated with HRP and a chemiluminescent reagent were used to visualize target proteins and their signal was quantified using the Image Lab Software (Bio-Rad). The internal control β-actin was used to normalize loading variations.

6.2.7 In-Cell Western (ICW) assay

A total of 3 x 10^4 HepG2 cells/well were seeded in 96-well plate and, the following day, they were treated with 50.0 µg/mL MOMAST(®) or Pravastatin 1.0 µM in complete growth medium for 24 h. Subsequently, they were fixed in 4% paraformaldehyde for 20 min at Room Temperature (RT). Cells were washed 5 times with 100 µL of PBS/well (each wash was for 5 min at RT) and the endogenous peroxides activity quenched adding 3% H_2O_2 for 20 min at RT. Non-specific sites were blocked with 100 µL/well of 5% Bovine Serum Albumin (BSA, Sigma) in PBS for 1.5h at RT. LDLR primary antibody solution (Abcam) (1:3000 in 5% BSA in PBS, 25 µL/well) was incubated O/N at + 4 °C. Subsequently, the primary antibody solution was discarded and each sample was washed 5 times with 100 µL/well of PBS (each wash was for 5 min at RT). Goat anti-rabbit Ig-HRP secondary antibody solution (Santa Cruz) (1:6000 in 5% BSA in PBS, 50 µL/well), was added and incubated 1h at RT. The secondary antibody solution was washed 5 times with 100 µL/well of PBS (each wash for 5 min at RT). Fresh prepared TMB Substrate (Pierce, 100 µL/well) was added and the plate was incubated at RT until desired color is developed. The reaction was stopped with 2 M H_2SO_4 and then the absorbance at 450 nm was measured using a microplate reader Synergy H1 from Biotek. Cells were stained by adding 1 × Janus green stain, incubating for 5 min at RT. The dye was removed and the sample washed 5 times with water. Afterward 0.1 mL 0.5 M HCl per well were added and incubated for 10 min. After 10 s shaking, the OD at 595 nm was measured using the Synergy H1 fluorescent plate reader from Biotek.

6.2.8 Assay for evaluation of fluorescent LDL uptake by HepG2 cells

A total of 3×10^4 HepG2 cells/well were seeded in 96-well plates and kept in complete growth medium for 2 days before treatment. On the third day, cells were treated with 50.0 µg/mL of MOMAST(®) and Pravastatin 1.0 µM or vehicle (H_2O) for 24 h. At the end of the treatment period, the culture medium was replaced with 50.0 µL/well LDL-DyLight™ 550 working solution. The cells were additionally incubated for 2 h at 37 °C and then the culture medium was aspirated and replaced with PBS (100 µL/well). The degree of LDL uptake was measured using the Synergy H1 fluorescent plate reader from Biotek (excitation and emission wavelengths 540 and 570 nm, respectively).

6.2.9 Quantification of secreted PCSK9 in cell culture experiments by ELISA

The supernatants, collected from HepG2 cells previously treated with 50.0 µg/mL of MOMAST(®), were centrifuged at 600 g for 10 min at 4 °C. They were recovered and diluted with the ratio 1:10 with DMEM in a new ice-cold tube. The experiments were carried out at 37 °C following the manufacturer's instructions. Briefly, this assay employs the quantitative sandwich enzyme immunoassay techniques. In facts, a monoclonal antibody specific for human PCSK9 has been pre-coated onto a microplate. Before starting the assay, Human PCSK9 Standards (20, 10, 5, 2,5, 1,25 and 0.625 ng/mL) were prepared from the stock solution PCSK9 Standard (40 ng/mL) with serial dilutions (for building the standard curve) and meanwhile 100 µl the Assay Diluent RD1-9 (provided into the kit) was added to each well. Afterward, standards and samples (50 µL) were pipetted into the wells and the ELISA plate was allowed to incubate for 2h at RT. Subsequently, wells were washed 4 times with Wash Buffer, and 200 µl of Human PCSK9 Conjugate (HRP-labeled anti-PCSK9) was added to each well for a 2h incubation at RT. Following aspiration, wells were washed 4 times with Wash Buffer. After the last wash, 200 µl of Substrate Solution were added to the wells and allowed to incubate for 30 min at RT. The reaction was stopped with 50 µl of Stop Solution (2 N sulfuric acid) and the absorbance at 450 nm was measured using Synergy H1 (Biotek).

6.2.10 Statistically analysis

All the data set were checked for normal distribution by D'Agostino & Pearson test. Since they are all normally disturbed with p-values < 0.05, we proceeded with statistical

analyses by One-way ANOVA followed by Tukey's post-hoc tests and using Graphpad Prism 9. Values were reported as means ± S.D.; p-values < 0.05 were considered to be significant.

6.3 Results

6.3.1 Effect of MOMAST® on the HMGCOAR Activity

The HMGCoAR, a key enzyme in the intracellular cholesterol biosynthesis, is the target of statins, the main drugs employed for the hypercholesterolemia management and control (Istvan *et al.*, 2001, Brown *et al.*, 1997). Based on this consideration, for assessing the MOMAST® capacity to modulate the HMGCoAR activity, a biochemical investigation was carried out. Findings suggest that MOMAST® inhibits the enzyme activity with dose response trend (Figure 1), since it drops the enzyme activity by 10 ± 5.2%, 34.5 ± 3.2%, 48.5 ± 0.5%, 80.2 ± 1.9%, and 90 ± 0.3%, at 10.0, 50.0, 75.0, 100.0, and 500.0 µg/mL, respectively.

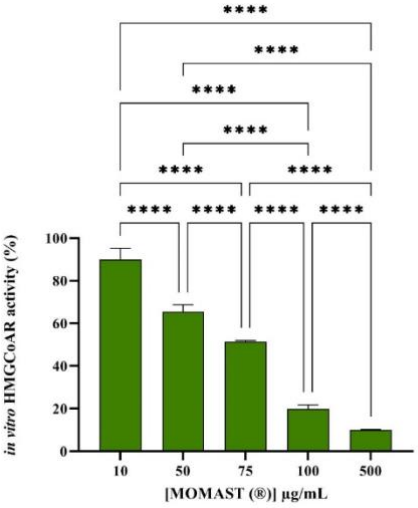

Figure 1. Bars indicate the effects of MOMAST(®) (10.0, 50.0, 75.0, 100.0 and 500.0 µg/mL) on the HMGCoAR activity. The decrease in absorbance at 340 nm, which represents the oxidation of NADPH by the catalytic subunit of HMGCoAR in the presence of the substrate HMG-CoA, was measured spectrophotometrically. The data points represent the averages ± SD of three experiments in triplicate. (****) $p < 0.0001$ *vs* control (C).

6.3.2 Effect of MOMAST® on the HepG2 Cell Vitality

MTT experiments were conducted for sorting out those concentrations of MOMAST® that may potentially determine cytotoxic effects on HepG2 cells. Notably, no cytotoxic effect was observed up to 50.0 µg/mL, after 48 h treatment, whereas at 100.0 µg/mL a 47.2 ± 3.4% cell mortality was observed (Figure 2). Hence, the following experiments performed at the cellular level were carried out at concentrations equal to 50.0 µg/mL.

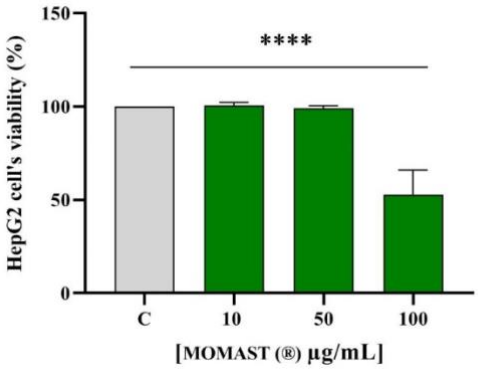

Figure 2. Bar graphs indicating the results of MTT cell viability assay of HepG2 cells after MOMAST(®) 10.0 – 100.0 µg/mL treatment for 48 h. The data points represent the averages ± SD of three experiments in triplicate. (****) $p < 0.0001$ *vs* control (C).

6.3.3 Effect of MOMAST® on the LDLR Pathway Modulation

To evaluate the modulating effects on cholesterol metabolism, western blotting experiments were carried out on cell lysates of HepG2 cells treated with MOMAST® (50.0 µg/mL) and with pravastatin (1 µM) as a reference control. Figure 3 indicates that MOMAST® increased the level of the SREBP-2 transcription factor protein by 142.8% ± 12.8% ($\boldsymbol{p} < 0.0001$, Figure 3A) and this increase led to an improvement of total LDLR and HMGCoAR proteins up to 155.9 ± 18.2% ($\boldsymbol{p} < 0.0001$, Figure 3B) and 137.4 ± 13.5% ($\boldsymbol{p} < 0.0001$, Figure 3C), respectively.

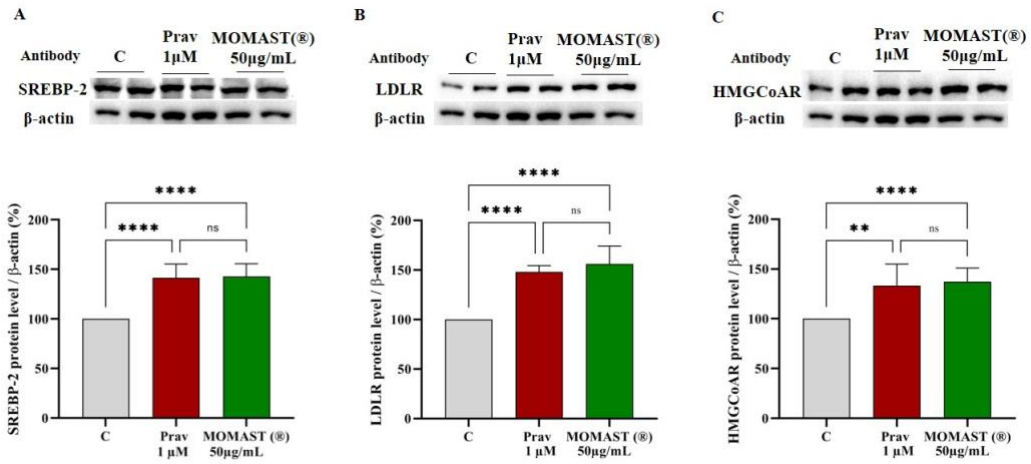

Figure 3. HepG2 cells (1.5 x 10^5) were treated with MOMAST$^{(®)}$ (50.0 µg/mL) and Pravastatin 1.0 µM for 24 h respectively. The SREBP2, LDLR, HMGCoAR and β-actin immunoblotting signals were detected using specific anti-SREBP2, anti-LDLR, anti-HMGCoAR, and anti-β-actin primary antibodies respectively. The SREBP2 (Panel A), the LDLR (Panel B) and the HMGCoAR (Panel C) signals were quantified by ImageJ Software and normalized with β-actin signals. Bars represent the averages of duplicate samples ± SD, ns: not significant, (**) $p < 0.01$, (****) $p < 0.0001$ *vs* control (C).

In the same set of experiments, pravastatin (1 µM), improved the SREBP-2 protein level by 156 ± 4.6% ($p < 0.0001$, Figure 3A), the LDLR by 152 ± 19.7% ($p < 0.0001$, Figure 3B), and the HMGCoAR protein by 133.4 ± 12.4% ($p < 0.01$, Figure 3C). From a statistical point of view, no significant difference was observed between MOMAST® and pravastatin.

6.3.4 Functional Effect of MOMAST® on the Ability of HepG2 Cells to Uptake LDL from the Extracellular Environment

The ability of MOMAST® to modulate the protein level of LDLR on the HepG2 cell surface was assessed by using an ICW assay, i.e., a quantitative colorimetric cell-based assay that allows the detection of target proteins in fixed cultured cells (Lammi *et al.*, 2015). An improvement of the LDLR levels specifically localized on the cellular membrane of hepatocytes, up to 157.5 ± 16.2% ($p < 0.0001$) was observed (Figure 4A). In the same set of experiments, at 1 µM, the positive control pravastatin increased the LDLR by 127.3 ± 14.3% ($p < 0.0001$. Figure 4A). The increase of membrane LDLR protein levels led to an improved functional ability of HepG2 cells to absorb the extracellular LDL by 279.6 ± 40.1% after the treatment with MOMAST® at the same concentration of 50 µg/mL ($p < 0.001$, Figure 4B). In the same conditions, pravastatin

(1 µM) improves the ability of hepatic cells to uptake LDL by 226.9 ± 11.1% from the extracellular space ($p < 0.01$, Figure 4B).

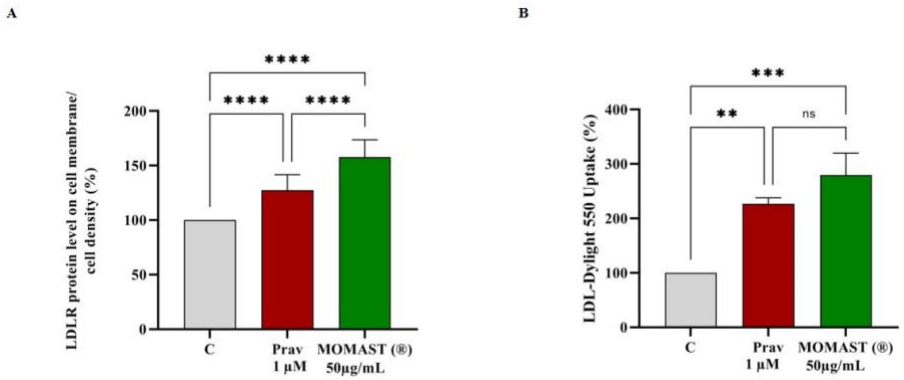

Figure 4. HepG2 cells (3 x 10^4) were treated with MOMAST(®) (50.0 µg/mL) and Pravastatin 1.0 µM for 24 h. The percentage of LDLR protein up-regulation was measured by ICW (Panel A). The data points represent the averages ± SD of three experiments in duplicate. (****) $p < 0.0001$ *vs* control (C). (Panel B) The specific fluorescent LDL-uptake signals were analyzed by Synergy H1 (Biotek). The data points represent the averages ± SD of three experiments in triplicate. ns: not significative, (**) $p < 0.01$, and (***) $p < 0.001$ *vs* control (C).

6.3.5 Effect of MOMAST® on the Modulation of PCSK9 Pathway

To evaluate the effect of MOMAST® on the modulation of PCSK9 and its transcription factor HNF1-α, HepG2 cells were treated at 50.0 µg/mL and, in parallel, with pravastatin (1 µM) as a positive control. Figure 5 indicates that MOMAST® caused a reduction of intracellular PCSK9 protein levels of 16.7 ± 3.8% towards untreated cells ($p < 0.001$ Figure 5A), this finding agrees with the ability of MOMAST® to reduce the HNF1-α transcription factor levels by 16.9 ± 2.5% compared to untreated cells ($p < 0.0001$ Figure 5B). Pravastatin (1 µM), on the other hand, increases the levels of this target up to 120.1 ± 6.2% ($p < 0.001$ Figure 5A) and this agrees with the increase of the HNF1-α transcription factor up to 116.7 ± 3, 4 ($p < 0.0001$, Figure 5B).

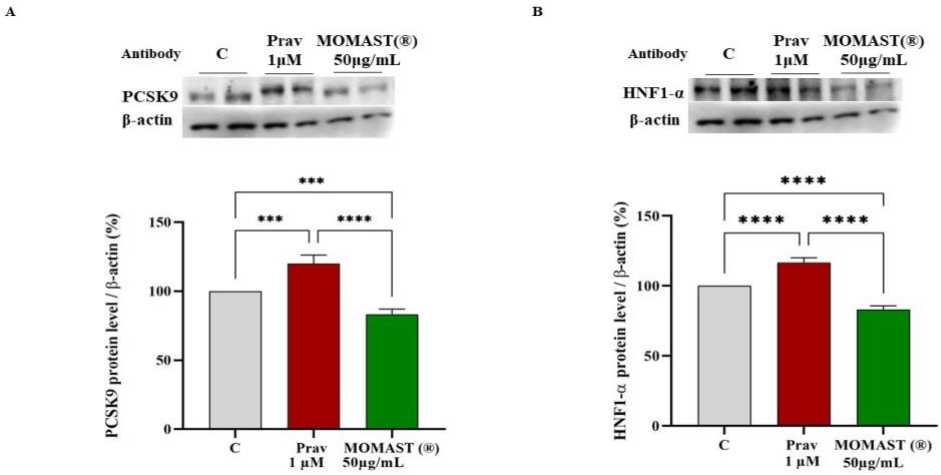

Figure 5. HepG2 cells (1.5 x 10^5) were treated with MOMAST$^{(®)}$ (50.0 µg/mL) and Pravastatin 1.0 µM for 24 h respectively. The PCSK9, HNF1-α and β-actin immunoblotting signals were detected using specific anti-PCSK9, anti-HNF1-α, and anti-β-actin primary antibodies respectively. The PCSK9 (Panel A) and the HNF1-α (Panel B) signals were quantified by ImageJ Software and normalized with β-actin signals. Bars represent the averages of duplicate samples ± SD (***) $p < 0.001$ and (****) $p < 0.0001$ *vs* control (C).

Based on the results, the effect of MOMAST® on the modulation of mature PCSK9 secretion by HepG2 cells was evaluated by ELISA assay. In agreement with molecular results, MOMAST® reduces the secretion of the mature PCSK9 by 28.7 ± 4.1%, ($p < 0.0001$, Figure 6), while pravastatin increases PCSK9 secretion up to 119.6 ± 1.2% ($p < 0.001$, Figure 6).

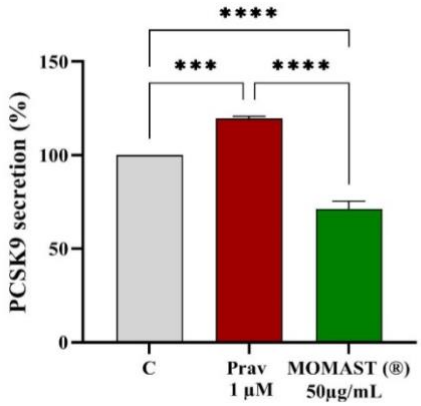

Figure 6. HepG2 cells (1.5 × 10^5) were treated with MOMAST$^{(®)}$ (50.0 µg/mL) for 24 h. After each treatment, the medium was collected and the secreted PCSK9 measured by ELISA. This assay employs the quantitative sandwich enzyme immunoassay techniques. A calibration curve was built using a recombinant human PCSK9. The absorbance of each reaction was measured at 450 nm using the Synergy H1 fluorescent plate reader from Biotek. Data points represent averages ± SD of three independent experiments in duplicate. (***) $p < 0.001$ and (****) $p < 0.0001$ *vs* control (C).

6.4 Discussion

The beneficial effects of OMW extracts have been demonstrated both in cellular and *in vivo* studies, in particular in the field of cancer prevention, cellular aging in neurodegenerative diseases, and in the prevention of coronary diseases (Donner *et al.*, 2021). Notably, clear evidence suggests that the OH-Tyr purified from OMW and OMW extract exert hypocholesterolemic effects in rats fed with a cholesterol-rich diet (Fki *et al.*, 2007). Indeed, the administration of a low-dose (2.5 mg/kg of body weight) of OH-tyr and a high-dose (10 mg/kg of body weight) of OMW extract significantly lowered the serum levels of total cholesterol (TC) and low-density lipoprotein cholesterol (LDL-C) while increasing the serum levels of high-density lipoprotein cholesterol (HDL-C) (Fki *et al.*, 2007). In this context, MOMAST® is a patented phenolic extract of OMW from Coratina *cultivar* rich in OH-Tyr, Tyr, and verbascoside. Our study provides a deeper mechanistic investigation demonstrating how MOMAST® modulates cholesterol metabolism. The results clearly suggest that this product significantly reduces the HMGCoAR activity in a dose-dependent manner. Hence, this effect prompted us to investigate in a detailed way the cellular modulation of the LDLR pathway, upon HMGCoAR inhibition. The cellular study was carried out on HepG2 cells because the hepatocyte is the major cell involved in the clearance of plasma LDL cholesterol expressing the most numbers of active LDLR on its surface (Horton *et al.*, 2007). In addition, since HepG2 expresses differentiated hepatic functions, these cells are worldwide recognized as a good model for assessing the hypocholesterolemic effects of bioactive compounds from different sources (Shin *et al.*, 2016, Ho *et al.*, 2005, Lammi *et al.*, 2016, 2016b, Donato *et al.*, 2015). Preliminary MTT experiments were carried out to exclude any potential cytotoxic effect of MOMAST® showing that it is safe for HepG2 cells up to 50 µg/mL. Based on these results, hepatic cells were treated with 50 µg/mL of MOMAST®. Similarly, to pravastatin (1 µM, the positive control), by inhibiting the HMGCoAR activity, MOMAST® modulated the intracellular cholesterol pathway, leading to an increase of the LDLR and HMGCoAR protein levels through the modulation of SREBP-2 (Figure 3 and Figure 4). By using ICW assay, it was demonstrated that MOMAST® increases the LDLRs which are localized on the surface of HepG2 cells leading from a functional point of view to an increased ability of hepatic cells to absorb LDL from the extracellular environment with a final hypocholesterolemic effect (Figure 4).

The molecular behavior of MOMAST® is similar to pravastatin (Figure 3 and Figure 4), however, a different effect was observed on the PCSK9 pathway. PCSK9 is a secreted protein, which binds the LDLR expressed on the surface of the hepatocytes (Horton *et al.*, 2007) and the PCSK9-LDLR binding activates the receptor catabolism leading to the hepatic LDLR degradation. Indeed, a promising strategy for the development of a new hypocholesterolemic drug consists of the PCSK9 inhibition and/or modulation (Seidah *et al.*, 2007). Interestingly since both PCSK9 and LDLR contain functional sterol regulatory elements (SREs) in their promoters, both these proteins are co-regulated by SREBP-2 (Dubuc *et al.*, 2004, Maxwell *et al.*, 2005). However, since the HNF1-α binding site is unique to the PCSK9 promoter and is not present in the LDLR promoter, the modulation of the PCSK9 transcription through HNF1-α does not affect the LDLR pathway. Thus, the co-regulation of PCSK9 from LDLR and other SREBP target genes is disconnected by the HNF1-α binding site (Maxwell *et al.*, 2005, Dong *et al.*,2015). In this context, it is important to highlight that statins increase the PCSK9 expression, which dampens an effective LDL clearing by promoting LDLR degradation (Chaudhary *et al.*, 2017), thereby counteracting the therapeutic effects of these drugs Dubuc *et al.*, 2004). In light with these considerations, our results confirm that pravastatin increases the mature PCSK9 protein levels through the augmentation of HNF1-α, on the contrary, MOMAST® significantly reduces HNF1-α leading to a decrease of PCSK9 levels. In agreement with these results, it was observed that only MOMAST®, and not pravastatin, is able to reduce the secretion of PCSK9 in the extracellular environments. In fact, MOMAST® decreased its secretion by 28.7 ± 4.1%, whereas pravastatin increased it by 19.6 ± 1.2%. This result contributes to explain the better ability of MOMAST® to raise the level of LDLR population localized on the surface of HepG2 cells than pravastatin. In fact, as shown in Figure 5A, MOMAST® is significantly more effective than pravastatin in the LDLR increment. Therefore, taking together all these results, it clearly appears that MOMAST® is able to mediate a complementary cholesterol-lowering effect, overcoming the intrinsic limits of the mechanism of action of statin. Recently, we have demonstrated that OMN displays a hypocholesterolemic effect with a molecular mechanism that is similar to MOMAST® (Lammi *et al.*, 2020). OMN contains OH-Tyr (16.7%) and Tyr (30.8%) and other secoiridoidic compounds, i.e., oleuropein and ligstroside and their derivatives. Through the comparison of their effects on the modulation of the key target involved in the cholesterol metabolism pathway, it appears clear that both samples modulate the

LDLR pathway via the activation of SREBP-2 transcription factors, showing similar behavior, however, only MOMAST® is able to modulate the PCSK9 pathway, displaying the complementary cholesterol-lowering mechanism of action. Doubtlessly, this difference may be explained considering the different compositions of these phytocomplexes, even though from a functional point of view, their biological effects are comparable. Thus, our results support the functional role of both OH-Tyr and Tyr within a phytocomplex for exerting the hypocholesterolemic effect.

6.5 Conclusions

Since the exploitation of by-products is becoming more and more important in recent years, MOMAST® represents a useful and sustainable alternative to solve the OVW problems, through the valorization of OVW derived phenolic extract. Notably, this study provides clear evidence regarding the cholesterol-lowering effect of MOMAST® which can be used as an ingredient for the development of new dietary supplements and or functional food for the prevention of cardiovascular disease. In light of these preliminary *in vitro* results and with the aim at fostering practical exploitation of this ingredient, further *in vivo* study will be realized.

6.6 Patents

Patent n. 102021000019226 of the 20 July 2021 entitled “Processo produttivo di complessi polifenolici da acque di vegetazione olearie con processo fermentativo e relativi complessi polifenolici prodotti” - inventors: Arnoldi A., Clodoveo M. L., Corbo F.F.R., Franchini C., Lammi C., Lentini, G. Lorenzo, V., Massari C.D, Milani G., Moretti P., Pisano I.

6.7 Supporting information

Technical data and analysis sheets of MOMAST® provided by Bioenutra S.r.l.

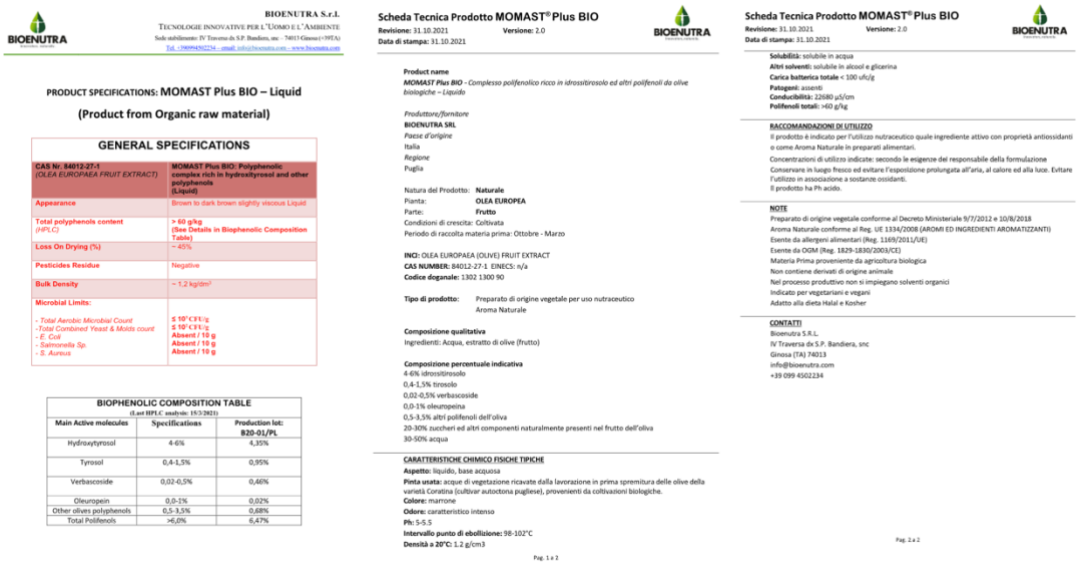

BIOENUTRA S.r.l.
TECNOLOGIE INNOVATIVE PER L'UOMO E L'AMBIENTE
Sede stabilimento: IV Traversa da S.P. Bandiera, snc - 74013 Ginosa (<39TA)
Tel. +3909945022234 - email: info@bioenutra.com - www.bioenutra.com

PRODUCT SPECIFICATIONS: MOMAST Plus BIO – Liquid
(Product from Organic raw material)

GENERAL SPECIFICATIONS

CAS Nr. 84012-27-1 (OLEA EUROPAEA FRUIT EXTRACT)	MOMAST Plus BIO: Polyphenolic complex rich in hydroxityrosol and other polyphenols (Liquid)
Appearance	Brown to dark brown slightly viscous Liquid
Total polyphenols content (HPLC)	> 60 g/kg (See Details in Biophenolic Composition Table)
Loss On Drying (%)	~ 45%
Pesticides Residue	Negative
Bulk Density	~ 1,2 kg/dm³
Microbial Limits:	
- Total Aerobic Microbial Count	≤ 10⁴ CFU/g
-Total Combined Yeast & Molds count	≤ 10³ CFU/g
- E. Coli	Absent / 10 g
- Salmonella Sp.	Absent / 10 g
- S. Aureus	Absent / 10 g

BIOPHENOLIC COMPOSITION TABLE
(Lest HPLC analysis: 15/3/2021)

Main Active molecules	Specifications	Production lot: B20-01/PL
Hydroxytyrosol	4-6%	4,35%
Tyrosol	0,4-1,5%	0,95%
Verbascoside	0,02-0,5%	0,46%
Oleuropein	0,0-1%	0,02%
Other olives polyphenols	0,5-3,5%	0,68%
Total Polifenoli	>6,0%	6,47%

Scheda Tecnica Prodotto MOMAST® Plus BIO
Revisione: 31.10.2021 Versione: 2.0
Data di stampa: 31.10.2021

Product name
MOMAST Plus BIO - Complesso polifenolico ricco in idrossitirosolo ed altri polifenoli da olive biologiche – Liquido

Produttore/fornitore
BIOENUTRA SRL
Paese d'origine
Italia
Regione
Puglia

Natura del Prodotto: Naturale
Pianta: OLEA EUROPEA
Parte: Frutto
Condizioni di crescita: Coltivata
Periodo di raccolta materia prima: Ottobre - Marzo

INCI: OLEA EUROPAEA (OLIVE) FRUIT EXTRACT
CAS NUMBER: 84012-27-1 EINECS: n/a
Codice doganale: 1302 1300 90

Tipo di prodotto: Preparato di origine vegetale per uso nutraceutico
Aroma Naturale

Composizione qualitativa
Ingredienti: Acqua, estratto di olive (frutto)

Composizione percentuale indicativa
4-6% idrossitirosolo
0,4-1,5% tirosolo
0,02-0,5% verbascoside
0,0-1% oleuropeina
0,5-3,5% altri polifenoli dell'oliva
20-30% zuccheri ed altri componenti naturalmente presenti nel frutto dell'oliva
30-50% acqua

CARATTERISTICHE CHIMICO FISICHE TIPICHE
Aspetto: liquido, base acquosa
Pinta usata: acque di vegetazione ricavate dalla lavorazione in prima spremitura delle olive della varietà Coratina (cultivar autoctona pugliese), provenienti da coltivazioni biologiche.
Colore: marrone
Odore: caratteristico intenso
Ph: 5-5,5
Intervallo punto di ebollizione: 98-102°C
Densità a 20°C: 1,2 g/cm3

Pag. 1 a 2

Scheda Tecnica Prodotto MOMAST® Plus BIO
Revisione: 31.10.2021 Versione: 2.0
Data di stampa: 31.10.2021

Solubilità: solubile in acqua
Altri solventi: solubile in alcool e glicerina
Carica batterica totale < 100 ufc/g
Patogeni: assenti
Conducibilità: 22680 µS/cm
Polifenoli totali: >60 g/kg

RACCOMANDAZIONI DI UTILIZZO
Il prodotto è indicato per l'utilizzo nutraceutico quale ingrediente attivo con proprietà antiossidanti o come Aroma Naturale in preparati alimentari.
Concentrazioni di utilizzo indicate: secondo le esigenze del responsabile della formulazione
Conservare in luogo fresco ed evitare l'esposizione prolungata all'aria, al calore ed alla luce. Evitare l'utilizzo in associazione a sostanze ossidanti.
Il prodotto ha Ph acido.

NOTE
Preparato di origine vegetale conforme al Decreto Ministeriale 9/7/2012 e 10/8/2018
Aroma Naturale conforme al Reg. UE 1334/2008 (AROMI ED INGREDIENTI AROMATIZZANTI)
Esente da allergeni alimentari (Reg. 1169/2011/UE)
Esente da OGM (Reg. 1829-1830/2003/CE)
Materia Prima proveniente da agricoltura biologica
Non contiene derivati di origine animale
Nel processo produttivo non si impiegano solventi organici
Indicato per vegetariani e vegani
Adatto alla dieta Halal e Kosher

CONTATTI
Bioenutra S.R.L.
IV Traversa da S.P. Bandiera, snc
Ginosa (TA) 74013
info@bioenutra.com
+39 099 4502234

Pag. 2 a 2

AB	*Lot. N*	*Product*
BACTIN	07M4799V	A5441
HMGCoAR	GR211866-24	Ab174830
LDLR	VB2951773A	PA5-22976
PCSK9	41752	GTX129859
HNF1α	41080	GTX 113850
SREBP2	K1913	Sc-13552

Table S1. Product and lot number details of antibodies used.

Data File C:\Chem32\1\Data\2021-03-15\Momast PLUS L B20-01 2021-03-15 14-55-15.D
Sample Name: Momast PLUS L B20-01

```
    ======================================================================
    Acq. Operator   : SYSTEM
    Sample Operator : SYSTEM
    Acq. Instrument : HPLC 1220                    Location :   1
    Injection Date  : 3/15/2021 3:11:13 PM
                                                 Inj Volume : Manually
    Acq. Method     : C:\CHEM32\1\METHODS\Q-SHORT-2019.M
    Last changed    : 3/15/2021 1:18:01 PM by SYSTEM
                      (modified after loading)
    Analysis Method : C:\CHEM32\1\METHODS\Q-SHORT-2019.M
    Last changed    : 3/15/2021 3:48:29 PM by SYSTEM
                      (modified after loading)
    Sample Info     : Momast PLUS L B20-01
                      Campione: 0.025mg+ 0.6 mg S.I.+ 1.3Meoh


    Sample-related custom fields:

    Name                          |Value
    ------------------------------|-------------------------------------
    Additional Info : Peak(s) manually integrated
    ======================================================================
```

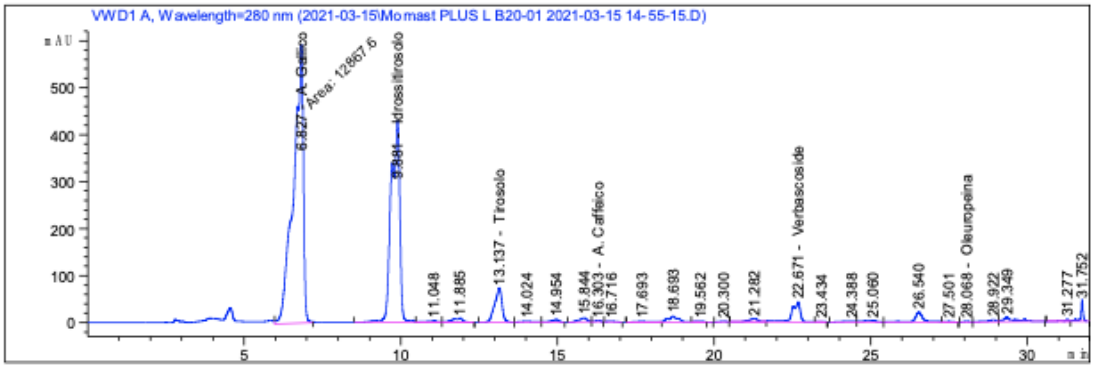


```
    ======================================================================
                          Internal Standard Report
    ======================================================================

    Sorted By             :      Signal
    Calib. Data Modified  :      3/15/2021 3:47:21 PM
    Multiplier            :      1.0000
    Dilution              :     80.0000
    Use Multiplier & Dilution Factor with ISTDs
    Sample ISTD Information:
    ISTD  ISTD Amount   Name
      #     [mg/kg]
    ----|------------|------------------------
      1    300.00000   A. Gallico
```

Data File C:\Chem32\1\Data\2021-03-15\Momast PLUS L B20-01 2021-03-15 14-55-15.D
Sample Name: Momast PLUS L B20-01

```
    ======================================================================
    Acq. Operator   : SYSTEM
    Sample Operator : SYSTEM
    Acq. Instrument : HPLC 1220                      Location :   1
    Injection Date  : 3/15/2021 3:11:13 PM
                                                   Inj Volume : Manually
    Acq. Method     : C:\CHEM32\1\METHODS\Q-SHORT-2019.M
    Last changed    : 3/15/2021 1:18:01 PM by SYSTEM
                      (modified after loading)
    Analysis Method : C:\CHEM32\1\METHODS\Q-SHORT-2019.M
    Last changed    : 3/15/2021 3:48:29 PM by SYSTEM
                      (modified after loading)
    Sample Info     : Momast PLUS L B20-01
                      Campione: 0.025mg+ 0.6 mg S.I.+ 1.3Meoh


    Sample-related custom fields:

    Name                          |Value
    ------------------------------|-------------------------------------
    Additional Info : Peak(s) manually integrated
    ======================================================================


    Signal 1: VWD1 A, Wavelength=280 nm

    RetTime  Type  ISTD    Area     Amt/Area    Amount   Grp   Name
     [min]         used  [mAU*s]     ratio     [mg/kg]
    -------|------|----|----------|----------|----------|--|------------------
      6.827 MM   I    1 1.28676e4     1.00000 2.40000e4     A. Gallico
      9.881 BV R       1 8114.22949    2.87595 4.35253e4     Idrossitirosolo
     13.137 BB         1 1163.19373    4.38726 9518.29981    Tirosolo
     16.303 VB         1   33.20021    0.00000    0.00000    A. Caffeico
     22.671 VV R       1  808.54376    3.07737 4640.84889    Verbascoside
     28.068 BB         1   16.12370    7.28050  218.94723    Oleuropeina

    Totals without ISTD(s) :                  5.79034e4

    Uncalibrated Peaks    :      using compound Idrossitirosolo

    RetTime  Type  ISTD    Area     Amt/Area    Amount   Grp   Name
     [min]         used  [mAU*s]     ratio     [mg/kg]
    -------|------|----|----------|----------|----------|--|------------------
     11.048 VV E          61.35201 9.07951e-2   10.38974    ?
     11.885 VB E         184.95044    1.96623  678.27248    ?
     14.024 BV            49.11551    0.00000    0.00000    ?
     14.954 VB            89.37666 9.70752e-1  161.82520    ?
     15.844 BV           143.59846    1.69815  454.82086    ?
     16.716 BB            22.58212    0.00000    0.00000    ?
     17.693 BV E          53.56312    0.00000    0.00000    ?
     18.693 VV R         286.33420    2.29585 1226.11487    ?
     19.562 VB E          25.67476    0.00000    0.00000    ?
     20.300 BB            16.83798    0.00000    0.00000    ?
     21.282 BV E         143.47691    1.69714  454.16404    ?
     23.434 VB E           8.00803    0.00000    0.00000    ?
     24.388 BV            48.25426    0.00000    0.00000    ?
     25.060 VB            85.04366 8.72600e-1  138.41118    ?
     26.540 BV R         369.71191    2.43146 1676.65890    ?
```

Data File C:\Chem32\1\Data\2021-03-15\Momast PLUS L B20-01 2021-03-15 14-55-15.D
Sample Name: Momast PLUS L B20-01

```
    ======================================================================
    Acq. Operator   : SYSTEM
    Sample Operator : SYSTEM
    Acq. Instrument : HPLC 1220                       Location :   1
    Injection Date  : 3/15/2021 3:11:13 PM
                                                    Inj Volume : Manually
    Acq. Method     : C:\CHEM32\1\METHODS\Q-SHORT-2019.M
    Last changed    : 3/15/2021 1:18:01 PM by SYSTEM
                      (modified after loading)
    Analysis Method : C:\CHEM32\1\METHODS\Q-SHORT-2019.M
    Last changed    : 3/15/2021 3:48:29 PM by SYSTEM
                      (modified after loading)
    Sample Info     : Momast PLUS L B20-01
                      Campione: 0.025mg+ 0.6 mg S.l.+ 1.3Meoh


    Sample-related custom fields:

    Name                          |Value
    ------------------------------|-------------------------------------
    Additional Info : Peak(s) manually integrated
    ======================================================================

     RetTime  Type  ISTD    Area     Amt/Area    Amount   Grp   Name
      [min]         used  [mAU*s]     ratio     [mg/kg]
     -------|------|----|----------|----------|----------|--|-----------------
      27.501 VB E          14.99064    0.00000    0.00000    ?
      28.922 BV           90.28904 9.90218e-1  166.75536    ?
      29.349 VB          251.28638    2.21199 1036.72870    ?
      31.277 BV E          37.76133    0.00000    0.00000    ?
      31.752 VBAR         221.97673    2.12151  878.34961    ?

     Uncalib. totals :                          6882.49096


     10 Warnings or Errors :

     Warning : Negative results set to zero (cal. curve intercept)
     Warning : Negative results set to zero (cal. curve intercept), (A. Caffeico)
     Warning : Negative results set to zero (cal. curve intercept)
     Warning : Negative results set to zero (cal. curve intercept)
     Warning : Negative results set to zero (cal. curve intercept)
     Warning : Negative results set to zero (cal. curve intercept)
     Warning : Negative results set to zero (cal. curve intercept)
     Warning : Negative results set to zero (cal. curve intercept)
     Warning : Negative results set to zero (cal. curve intercept)
     Warning : Negative results set to zero (cal. curve intercept)

     ======================================================================
                              *** End of Report ***
```

6.8 References

Banias G., Achillas C., Vlachokostas C., Moussiopoulos N., Stefanou M. Environmental impacts in the life cycle of olive oil: A literature review. J. Sci. Food Agric. 2017;97:1686–1697. doi: 10.1002/jsfa.8143.

Brown S.B., Goldstein J.L. The SREBP Pathway: Regulation of Cholesterol Metabolism by Proteolysis of a Membrane-Bound Transcription Factor. Cell. 1997;89:331–340. doi: 10.1016/S0092-8674(00)80213-5.

Chaudhary R., Garg J., Shah N., Sumner A. PCSK9 inhibitors: A new era of lipid lowering therapy. World J. Cardiol. 2017;9:76–91. doi: 10.4330/wjc.v9.i2.76.

Covas M.J.A.I.M., Nyyssönen K., Poulsen H.E., Kaikkonen J., Zunft H.J.F., Kiesewetter H., Gaddi A., de la Torre R., Mursu J., Baumler H. The effect of polyphenols in olive oil on heart disease risk factors: A randomized trial. Ann. Int. Med. 2006;145:333–341. doi: 10.7326/0003-4819-145-5-200609050-00006.

Donato M.T., Tolosa L., Gómez-Lechón M.J. Culture and Functional Characterization of Human Hepatoma HepG2 Cells. In: Vinken M., Rogiers V., editors. Protocols in In Vitro Hepatocyte Research. Springer; New York, NY, USA: 2015. pp. 77–93.

Dong B., Li H., Singh A.B., Cao A., Liu J. Inhibition of PCSK9 transcription by berberine involves down-regulation of hepatic HNF1α protein expression through the ubiquitin-proteasome degradation pathway. J. Biol. Chem. 2015;290:4047–4058. doi: 10.1074/jbc.M114.597229.

Donner M., Radić I. Innovative Circular Business Models in the Olive Oil Sector for Sustainable Mediterranean Agrifood Systems. Sustainability. 2021;13:2588. doi: 10.3390/su13052588.

Dubuc G., Chamberland A., Wassef H., Davignon J., Seidah N.G., Bernier L. Prat A: Statins Upregulate PCSK9, the Gene Encoding the Proprotein Convertase Neural Apoptosis-Regulated Convertase-1 Implicated in Familial Hypercholesterolemia. Arterioscler. Thromb. Vasc. Biol. 2004;24:1454–1459. doi: 10.1161/01.ATV.0000134621.14315.43.

Fki I., Sahnoun Z., Sayadi S. Hypocholesterolemic Effects of Phenolic Extracts and Purified Hydroxytyrosol Recovered from Olive Mill Wastewater in Rats Fed a Cholesterol-Rich Diet. J. Agric. Food Chem. 2007;55:624–631. doi: 10.1021/jf0623586.

Ho S.S., Pal S. Margarine phytosterols decrease the secretion of atherogenic lipoproteins from HepG2 liver and Caco2 intestinal cells. Atherosclerosis. 2005;182:29–36. doi: 10.1016/j.atherosclerosis.2005.01.031.

Horton J.D., Cohen J.C., Hobbs H.H. Molecular biology of PCSK9: Its role in LDL metabolism. Trends Biochem. Sci. 2007;32:71–77. doi: 10.1016/j.tibs.2006.12.008.

Istvan E.S., Deisenhofer J. Structural Mechanism for Statin Inhibition of HMG-CoA Reductase. Science. 2001;292:1160–1164. doi: 10.1126/science.1059344.

Lammi C., Bellumori M., Cecchi L., Bartolomei M., Bollati C., Clodoveo M.L., Corbo F., Arnoldi A., Mulinacci N. Extra Virgin Olive Oil Phenol Extracts Exert Hypocholesterolemic Effects

through the Modulation of the LDLR Pathway: In Vitro and Cellular Mechanism of Action Elucidation. Nutrients. 2020;12:1723. doi: 10.3390/nu12061723.

Lammi C., Mulinacci N., Cecchi L., Bellumori M., Bollati C., Bartolomei M., Franchini C., Clodoveo M.L., Corbo F., Arnoldi A. Virgin Olive Oil Extracts Reduce Oxidative Stress and Modulate Cholesterol Metabolism: Comparison between Oils Obtained with Traditional and Innovative Processes. Antioxidants. 2020;9:798. doi: 10.3390/antiox9090798.

Lammi C., Zanoni C., Arnoldi A. A simple and high-throughput in-cell Western assay using HepG2 cell line for inves-tigating the potential hypocholesterolemic effects of food components and nutraceutics. Food Chem. 2015;169:59–64. doi: 10.1016/j.foodchem.2014.07.133.

Lammi C., Zanoni C., Calabresi L., Arnoldi A. Lupin protein exerts cholesterol-lowering effects targeting PCSK9: From clinical evidences to elucidation of the in vitro molecular mechanism using HepG2 cells. J. Funct. Foods. 2016;23:230–240. doi: 10.1016/j.jff.2016.02.042.

Lammi C., Zanoni C., Ferruzza S., Ranaldi G., Sambuy Y., Arnoldi A. Hypocholesterolaemic Activity of Lupin Peptides: Investigation on the Crosstalk between Human Enterocytes and Hepatocytes Using a Co-Culture System Including Caco-2 and HepG2 Cells. Nutrients. 2016;8:437. doi: 10.3390/nu8070437.

Mallamaci R., Budriesi R., Clodoveo M.L., Biotti G., Micucci M., Ragusa A., Curci F., Muraglia M., Corbo F., Franchini C. Olive Tree in Circular Economy as a Source of Secondary Metabolites Active for Human and Animal Health Beyond Oxidative Stress and Inflammation. Molecules. 2021;26:1072. doi: 10.3390/molecules26041072.

Maxwell K.N., Fisher E.A., Breslow J.L. Overexpression of PCSK9 accelerates the degradation of the LDLR in a post-endoplasmic reticulum compartment. Proc. Natl. Acad. Sci. USA. 2005;102:2069. doi: 10.1073/pnas.0409736102.

Pandey K., Rizvi S. Plant polyphenols as dietary antioxidants in human health and disease. Oxid. Med. Cell. Longev. 2009;2:270–278. doi: 10.4161/oxim.2.5.9498.

Recinella L., Chiavaroli A., Orlando G., Menghini L., Ferrante C., Di Cesare Mannelli L., Ghelardini C., Brunetti L., Leone S. Protective Effects Induced by Two Polyphenolic Liquid Complexes from Olive (Olea europaea, mainly Cultivar Coratina) Pressing Juice in Rat Isolated Tissues Challenged with LPS. Molecules. 2019;24:3002. doi: 10.3390/molecules24163002.

Rees K., Takeda A., Martin N., Ellis L., Wijesekara D., Vepa A., Das A., Hartley L., Stranges S. Mediterranean-style diet for the primary and secondary prevention of cardiovascular disease. Cochrane Database Syst. Rev. 2019;3:CD009825. doi: 10.1002/14651858.CD009825.pub3.

Romani A., Ieri F., Urciuoli S., Noce A., Marrone G., Nediani C., Bernini R. Health Effects of Phenolic Compounds Found in Extra-Virgin Olive Oil, by-Products, and Leaf of Olea europaea L. Nutrients. 2019;11:1776. doi: 10.3390/nu11081776.

Seidah N.G. Prat A: The proprotein convertases are potential targets in the treatment of dyslipidemia. J. Mol. Med. 2007;85:685–696. doi: 10.1007/s00109-007-0172-7.

Shin E.J., Park J.H., Sung M.J., Chung M.-Y., Hwang J.-T. Citrus junos Tanaka peel ameliorates hepatic lipid accumulation in HepG2 cells and in mice fed a high-cholesterol diet. BMC Complement. Altern. Med. 2016;16:499. doi: 10.1186/s12906-016-1460-y.

Visioli F., Lastra C.A.D.L., Andres-Lacueva C., Aviram M., Calhau C., Cassano A., D'Archivio M., Faria A., Favé G., Fogliano V., et al. Polyphenols and Human Health: A Prospectus. Crit. Rev. Food Sci. Nutri. 2011;51:524–546. doi: 10.1080/10408391003698677.

MANUSCRIPT 4

MOMAST® REDUCES THE PLASMATIC LIPID PROFILE AND OXIDATIVE STRESS AND REGULATES CHOLESTEROL METABOLISM IN A HYPERCHOLESTEROLEMIC MOUSE MODEL: THE PROOF OF CONCEPT OF A SUSTAINABLE AND INNOVATIVE ANTIOXIDANT AND HYPOCHOLESTEROLEMIC INGREDIENT

Ivan Cruz-Chamorro [1,2,†], Guillermo Santos-Sánchez [1,2,†], Eduardo Ponce-España [1,2], Carlotta Bollati [3], Lorenza d'Adduzio [3], Martina Bartolomei [3], Jianqiang Li [3], Antonio Carrillo-Vico [1,2], Carmen Lammi [3*]

[1] Instituto de Biomedicina de Sevilla (IBiS), Hospital Universitario Virgen del Rocío, Consejo Superior de Investigaciones Científicas (CSIC), Universidad de Sevilla, 41013 Seville, Spain

[2] Departamento de Bioquímica Médica y Biología Molecular e Inmunología, Facultad de Medicina, Universidad de Sevilla, 41009 Seville, Spain

[3] Department of Pharmaceutical Sciences, University of Milan, 20133 Milan, Italy

[*] Author to whom correspondence should be addressed.

[†] These authors contributed equally to this work.

7. Abstract

MOMAST® is a patented natural phenolic complex, rich in tyrosol (9.0 g/kg, Tyr), hydroxityrosol (43,5 g/kg, OH-Tyr), and verbascoside (5.0 g/Kg), which is obtained from the OVW by-product of the *Coratina* cultivar with potent direct antioxidant activity (measured by DPPH and FRAP assays, respectively). Indeed, MOMAST® represents an innovative sustainable bioactive ingredient which has been obtained with ethical and empowering behavior by applying the principles of a circular economy. In the framework of research aimed at fostering its health-promoting activity, in this study it was clearly demonstrated that MOMAST® treatment reduced the oxidative stress and levels of total cholesterol (TC) and low-density lipoprotein (LDL) cholesterol, and increased the HDL levels, without changes in the triglyceride (TG) levels in Western diet (WD)-fed mice. The modulation of the plasmatic lipid profile is similar to red yeast rice (RYR) containing Monacolin K (3%). In addition, at the molecular level in liver homogenates, similarly to RYR, MOMAST® exerts cholesterol-lowering activity through the activation of LDL receptor, whereas, unlike RYR, MOMAST® reduces proprotein convertase subtilisin/kexin type 9 (PCSK9) protein levels via hepatic nuclear factor 1 (HNF1)-α activation. Hence, this study provides the *proof of concept* regarding the hypocholesterolemic activity of MOMAST, which could be successfully exploited as an active ingredient for the development of innovative and sustainable dietary supplements and functional foods.

7.1 Introduction

During the olive oil extraction process, only a small percentage of polyphenols of the total present in the olives is transferred to the oil, while an important percentage is retained in the olive oil vegetation water (OVW) (Obied *et al.*, 2007, Mulinacci *et al.*, 2001). The quantity of phenols is very variable in relation to the type of olives, their state of ripeness, storage, and the degradation that they had to undergo between harvesting and processing (De Luca *et al.*, 2022). In this context, MOMAST® is a patented natural phenolic complex, rich in tyrosol (9.0 g/kg, Tyr) hydroxityrosol (43.5 g/kg, OH-Tyr), and verbascoside (5.0 g/kg), which is obtained from the OVW by-product of the *Coratina* cultivar using exclusively physical and mechanical methods, without the use of solvents and other chemical processes (Bartolomei *et al*., 2022). The high content of both Tyr and OH-Tyr is clearly due to the hydrophilic nature of these

phenolic compounds which tend to accumulate in the OVW. In light of these observations, MOMAST® represents an innovative sustainable bioactive ingredient which has been obtained through ethical and empowering behavior by applying the principles of a circular economy which are perfectly in line with the sustainable development goals (SDG) of the 2030 Agenda and the Farm to Fork Strategy (McBean, 2021). The literature widely reports the antioxidant properties of polyphenols both at the cellular and *in vivo* levels (Kaminski *et al*., 2023, Aires *et al*., 2019). In agreement, given that its composition is rich in Tyr and OH-Tyr, MOMAST® exerts both antioxidant and anti-inflammatory activities in isolated rat tissues after LPS stimulus (Recinella *et al*., 2019). Interestingly, MOMAST® displays a hypocholesterolemic property through a mechanism of action which is not only correlated to the antioxidant or anti-inflammatory effect, but to its direct ability to modulate the activity of 3-hydroxy-3-methylglutaryl Coenzyme A reductase (HMGCoAR), the enzyme targeted by statins or by Monacolin K, which is present in red yeast rice (RYR) (Bartolomei *et al.*, 2022). In more detail, MOMAST® reduced the in vitro enzyme activities with a dose–response trend and an IC_{50} equal to 75 µg/mL. Through the HMGCoAR inhibition, MOMAST® activated the intracellular cholesterol pathway with a dual mechanism of action, leading to an increase in low-density lipoprotein (LDL) receptor (LDLR) and HMGCoAR protein levels via sterol regulatory element binding protein (SREBP)-2 activation. In this context, dedicated experiments confirmed that MOMAST® specifically increases the LDLRs localized on the surface of human hepatic HepG2 cells. In addition, unlike statin, MOMAST® significantly reduced the hepatic nuclear factor 1 (HNF1)-α, leading to a decrease in mature proprotein convertase subtilisin/kexin type 9 (PCSK9) levels and to a functional reduction in its secretion in extracellular environments (Bartolomei *et al.*, 2022). In agreement with evidence from the literature (Lammi *et al*., 2021, Lammi *et al*., 2020), the reduction in PCSK9 production and secretion along with the selective improvement of LDLRs localized on the surface of hepatocytes led, from a functional point of view, to an increased ability of hepatic cells to absorb LDL from the extracellular environment with a final *in vitro* hypocholesterolemic effect (Bartolomei *et al.*, 2022).

In light of the evidence obtained at the *in vitro* level (Bartolomei *et al*., 2022, Recinella *et al*., 2019), the present study aimed at obtaining the *proof of concept* of the antioxidant and hypocholesterolemic activities of MOMAST® by performing a dedicated *in vivo* study. Notably, the direct antioxidant activity of MOMAST® was determined by

performing DPPH and FRAP assays, respectively. Furthermore, an *in vivo* study on C57BL/6 mice fed a Western diet (WD) was carried out to evaluate the antioxidant activity of MOMAST® at the plasmatic level and its effect on the plasmatic lipid profile (measuring total cholesterol (TC), LDL and high-density lipoprotein (HDL), and triglyceride (TG) parameters) and the liver cholesterol metabolism pathway.

7.2 Materials and Methods

7.2.1 Chemicals

All chemicals and reagents were commercially available, and more details are reported in the Supplementary Materials.

MOMAST® Description

Bioenutra S.R.L. (Ginosa (TA) Italy) supplied the patented MOMAST® sample directly from the production process. MOMAST® sample is a phenolic complex, rich in tyrosol (9.0 g/kg, Tyr), hydroxityrosol (43.5 g/kg, OH-Tyr), and verbascoside (5.0 g/Kg). Its chromatogram is available as a Supplementary Material (Figure S1).

7.2.2 In Vitro MOMAST® Antioxidant Activity

7.2.2.1 2,2-Diphenyl-1-picrylhydrazyl (DPPH) Assay

To estimate the radical scavenging capacity of MOMAST®, the DPPH assay was carried out. More details are reported in the Supplementary Material.

7.2.2.2 Ferric Reducing Antioxidant Power (FRAP) Assay

A volume of 15 μL of a sample containing MOMAST® was combined with 140 μL of FRAP solution, which consisted of 0.83 mM TPTZ, 1.66 mM $FeCl_3 \times 6H_2O$, and 0.25 M acetate buffer (pH 3.6). More experimental details are provided in Supplementary Material.

7.2.3 Study Design

Twenty-six C57BL/6 4-week-old mice were housed at the Animal Facility of the Instituto de Biomedicina de Sevilla (IBiS) under standard conditions and were fed with a WD (45% energy from fat, TestDiet, St. Louis, MO, USA, $n = 21$) or with a standard diet (SD, rodent maintenance diet, ENVIGO, IN, USA, $n = 5$). When mice were 6

weeks old, they were separated into three groups and intragastrically treated with (1) saline (control group, C, *n* = 7), (2) red yeast rice (3% Monacolin K, RYR, ADVA s.r.l., Milan, Italy, *n* = 7), or (3) MOMAST® (Bioenutra s.r.l., Ginosa (TA) Italy, *n* = 7) at 20 mg/kg for eight weeks (Figure 1). Further details are available in the Supplementary Material.

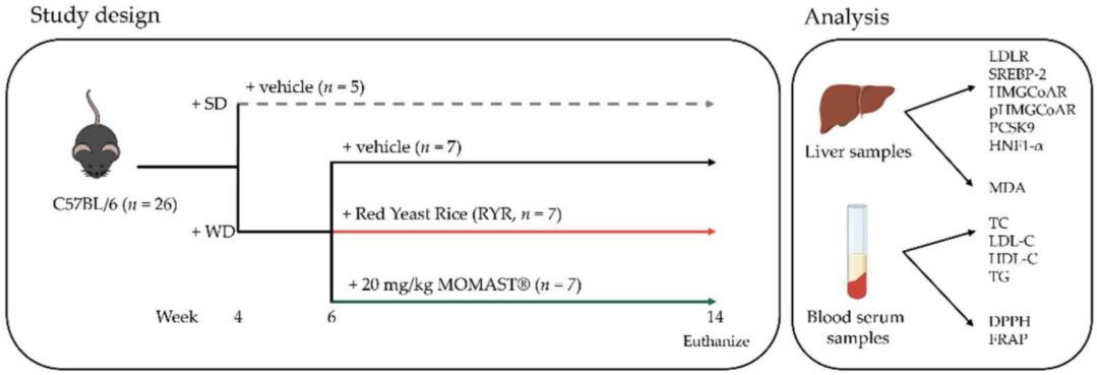

Figure 1. Schematic representation of the study design, and of lipidic and antioxidant parameters analysis. SD, standard diet; WD, Western diet.

7.2.4 Biochemical Parameters

All biochemical parameters were quantified in the serum samples using the COBAS E601 modular analyzer (Roche Diagnostic, Basel, Switzerland). Castelli risk indexes (CRI) I and II were calculated as TC/HDL and LDL/HDL, respectively.

7.2.5 In Vivo Antioxidant Activity of MOMAST®

7.2.5.1 DPPH and FRAP Assays

Serum antioxidant capacity was evaluated using DPPH and FRAP assays and both tests were carried out according to the manufacturer's instructions. See Supplementary Material for further details.

7.2.5.2 Determination of Hepatic Malondialdehyde (MDA) Levels

Liver samples were processed following the manufacturer's instructions. Experimental details are reported in the Supplementary Material.

7.2.6 Western Blot Analysis

Tissues were homogenized in a lysis buffer and the protein concentration was determined by Bradford's method. Western Blot experiments were performed using primary antibodies against SREBP-2, HMGCoAR, LDLR, phospho HMGCoAR

(Ser872), PCSK9, HNF1-α, and β-actin following conditions previously reported. See Supplementary Material for further details.

7.2.7 Statistical Analysis

All the data sets were checked for normal distribution by D'Agostino and Pearson test. Since they are all normally distributed with *p*-values < 0.05, statistical analysis was carried out by one-way ANOVA followed by Tukey's post hoc analysis (GraphPad Software 9, San Diego, CA, USA). Values were expressed as means ± standard deviation; *p*-values ≤ 0.05 were considered to be significant.

7.3 Results

7.3.1 MOMAST® Has In Vitro DPPH Radical Scavenging and Ferric Reducing Capacities

As Figure 2A shows, MOMAST® reduced the DPPH radical by 13.33 ± 2.858% and 72.57 ± 0.61% at. 0.1 and 0.5 mg/mL, respectively. Regarding the effect of MOMAST® on the capacity to reduce Fe^{3+} to Fe^{2+}, it is able to improve the FRAP levels tested at 0.1 mg/mL (0.175 mmol equiv. Trolox/L) and 0.5 mg/mL (0.728 mmol equiv. Trolox/L), versus the control (H_2O) (Figure 2B).

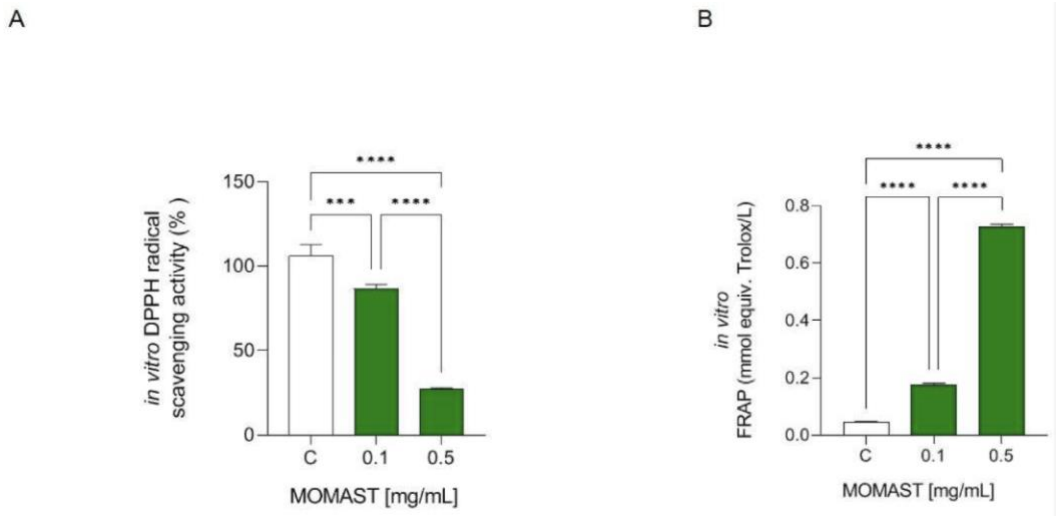

Figure 2. *In vitro* DPPH radical scavenging (**A**) and ferric reducing capacities (**B**) of MOMAST®. Data are represented as mean ± standard deviation. ***, $p \leq 0.001$; ****, $p \leq 0.0001$; C: control; ns: no statistical differences.

7.3.2 Effect of MOMAST® on Body Weight

As shown in Figure 3A, WD-fed mice showed a higher increase in body weight throughout the experiment in comparison to the SD-fed mice. This effect was palliated by the treatment with MOMAST® and RYR, whose body weight increase was significantly lower than the WD group. This fact was reflected in the body weight gain (Figure 3B), which was significantly lower in the groups treated with MOMAST® (11.25 ± 1.93 g, $p = 0.036$) and RYR (9.5 ± 1.83 g, $p = 0.011$) than in the WD group (16.57 ± 2.66 g). Regarding the daily food intake (Figure 2C), WD-fed mice showed a lower food ingestion (2.83 ± 0.38 g/mouse/day) in comparison to the SD-fed mice (3.25 ± 0.21 g/mouse/day) ($p = 0.023$). However, no significant differences were found between the WD group, and the groups treated with MOMAST® (2.69 ± 0.38 g/mouse/day, $p = 0.55$) and RYR (2.80 ± 0.25 g/mouse/day, $p = 0.99$).

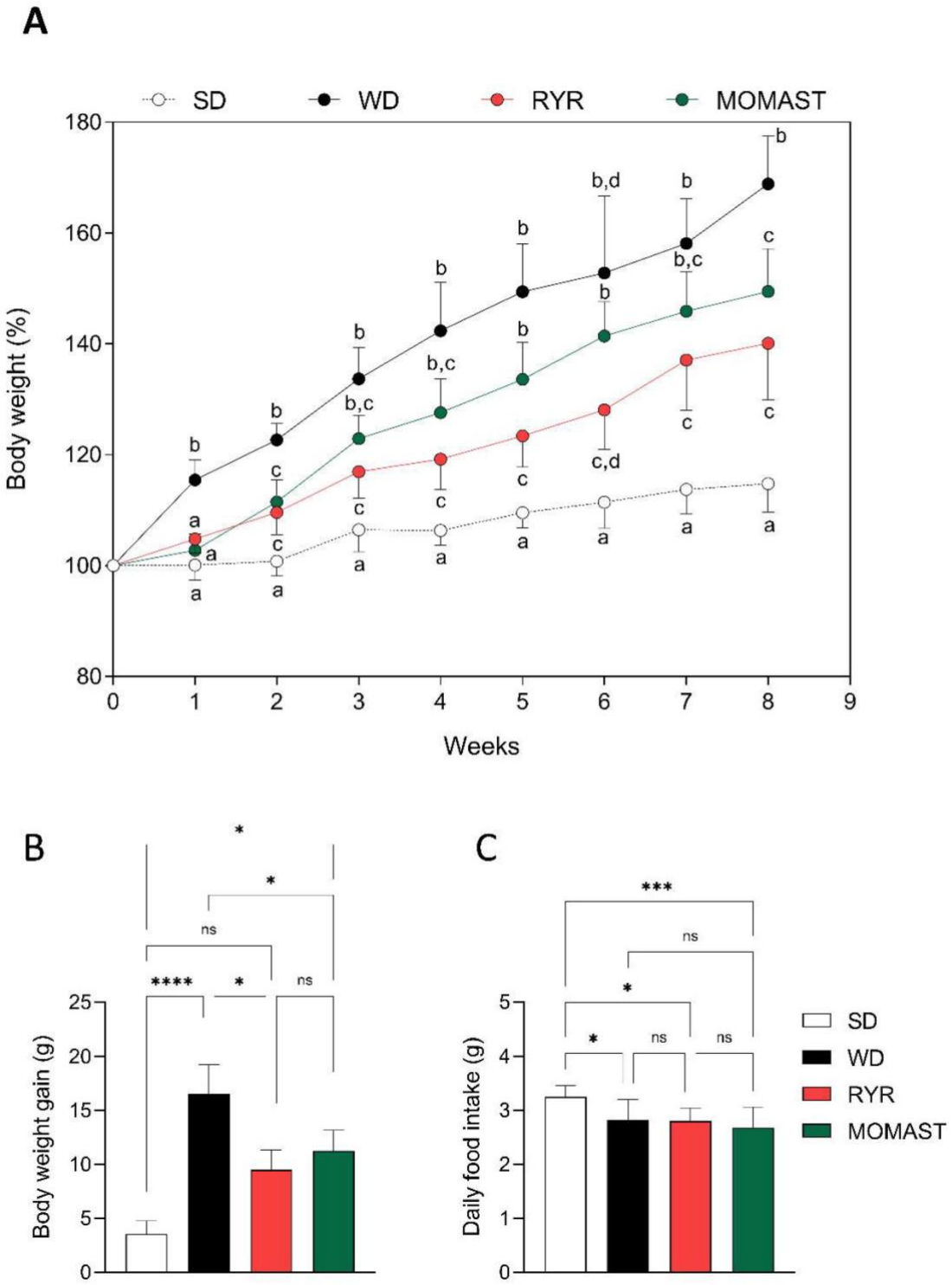

Figure 3. Effects of the MOMAST® on body weight. Body weight monitored over time on each group (**A**), body weight gain (**B**), daily food intake (**C**). Data are represented as mean ± standard deviation. Different letters represent a statistical difference ($p \leq 0.05$). *, $p \leq 0.05$; ***, $p \leq 0.001$; ****, $p \leq 0.0001$; ns, no statistical differences.

7.3.3 MOMAST® Exerts Antioxidant Effects at Serum and Hepatic Levels

Regarding the antioxidant effect on serum, as indicated Figure 4A, MOMAST®-fed mice showed an ability to decrease the DPPH radical by 3.51 ± 2.11% compared with

WD-fed mice, which showed an increase in DPPH radical of 4.60 ± 4.80% at the serum level. As indicated in Figure 4B, MOMAST®-treated mice showed an increase in the FRAP levels (0.17 mmol equiv. Trolox/L) compared to the WD-fed mice (0.14 mmol equiv. Trolox/L, $p = 0.039$). There were no significant differences between the SD and WD groups ($p = 0.43$), nor between the WD and RYR groups ($p = 0.99$).

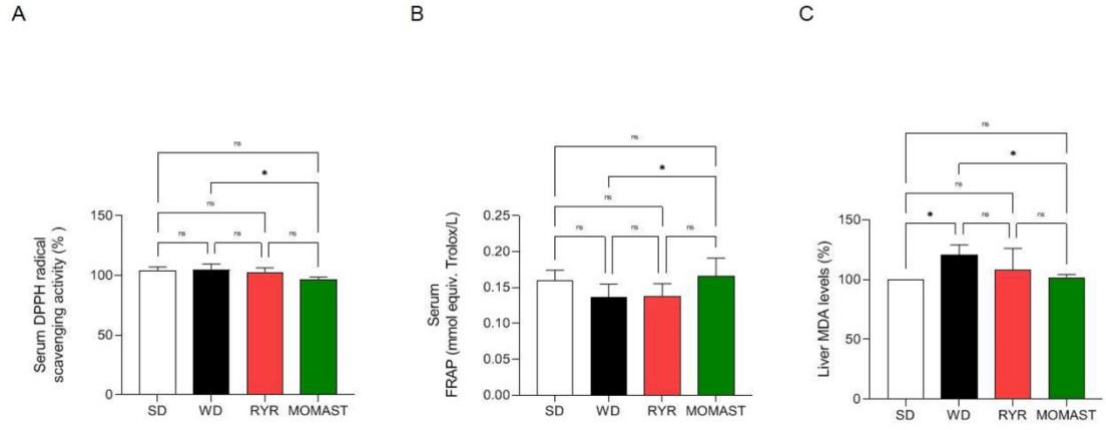

Figure 4. (**A**) DPPH radical scavenging and (**B**) ferric reducing capacities of MOMAST® in serum. (**C**) Modulation of lipid peroxidation in liver. Data are represented as mean ± standard deviation. *, $p \leq 0.05$; ns: no statistical differences.

Moreover, the capacity of MOMAST® to regulate the lipid peroxidation in mice livers was assessed by the MDA evaluation (Figure 4C). As illustrated in Figure 4C, WD-fed mice showed an increase in MDA levels in comparison to the SD-fed mice. In fact, MDA levels were augmented by 121.0 ± 8.12 % in WD-fed mice, whereas the treatment with MOMAST® resulted in a reduction in MDA levels to 101.2 ± 3.33%, restoring the SD lipid peroxidation baseline levels. On the contrary, no significant decrease was observed in the RYR group, in which the MDA levels were increased by 108.1 ± 18.04 vs. the SD group.

7.3.4 MOMAST® Improves the Plasmatic Lipidic Profile

To investigate the *in vivo* lipid-lowering effect of MOMAST®, the plasma lipid profile and the main cardiovascular risk indexes were analyzed. As shown in Figure 5, WD ingestion increased the TC (153.60 ± 19.65 mg/dL, $p < 0.0001$), LDL (0.94 ± 0.15 mmol/L, $p < 0.0001$), and HDL (2.66 ± 0.22 mmol/L, $p = 0.004$) values, in comparison to the SD-fed mice (TC: 81.32 ± 3.86 mg/dL; LDL: 0.25 ± 0.03 mmol/L; HDL: 2.10 ± 0.26 mmol/L). The treatment with MOMAST® for 8 weeks palliates these effects. Specifically, the treatment reduced by 12.5% (134.40 ± 12.86 mg/dL, $p= 0.017$) and 24.47% (0.71 ± 0.13 mmol/L, $p = 0.002$) the levels of TC and LDL, respectively. In

addition, MOMAST® treatment increased the levels of HDL by 16.16% (3.09 ± 0.29 mmol/L, $p = 0.004$). Interestingly, the values in the MOMAST®-treated mice were similar to those treated with RYR. More in detail, RYR treatment showed lower TC (108.30 ± 4.96 mg/dL, $p < 0.0001$) and LDL (0.54 ± 0.07 mmol/L, $p < 0.0001$) levels, in comparison to the WD group, without differences in HDL values ($p = 0.92$). No significant differences between groups were found in TG levels ($p > 0.05$).

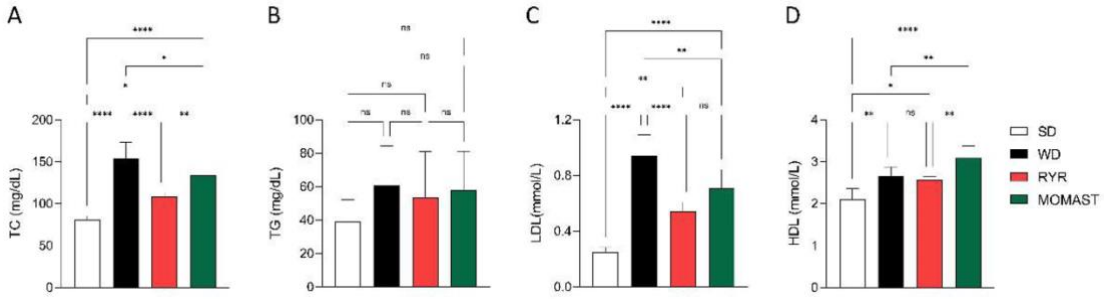

Figure 5. Effects of the MOMAST® on plasma lipidic profile. Plasma concentration of total cholesterol (**A**), triglycerides (**B**), low-density lipoprotein (**C**), and high-density lipoprotein (**D**). Data are represented as mean ± standard deviation. *, $p \leq 0.05$; **, $p \leq 0.01$; ****, $p \leq 0.0001$; ns, no statistical differences.

When the cardiovascular risk indexes were calculated, as shown in Figure 6, mice fed with the WD showed increased CRI I and II levels by 43.53% (58.56 ± 6.63, $p < 0.0001$) and 191.67% (0.35 ± 0.036, $p < 0.0001$) compared to the SD-fed mice (CRI I: 40.80 ± 0.81, CRI II: 0.12 ± 0.022). The MOMAST® treatment counteracted this increase, reducing both CRI I by 25.94% (43.37 ± 3.83, $p < 0.0001$) and CRI II by 34.29% (0.23 ± 0.039, $p < 0.0001$), reaching similar values to the RYR-treated mice (CRI I: 42.21 ± 0.97, CRI II: 0.21 ± 0.031).

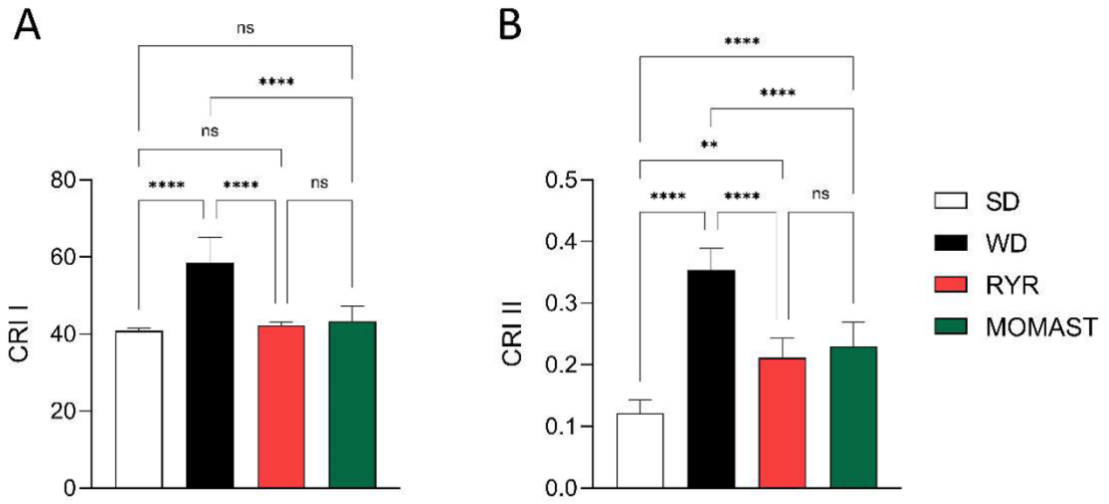

Figure 6. Assessment of the effects of MOMAST® on cardiovascular disease risk indexes. Evaluation of cardiovascular disease risk through Castelli risk index (CRI) I (TC/HDL) (**A**) and II (LDL/HDL) (**B**). Data are represented as mean ± standard deviation. **, $p \leq 0.01$; ****, $p \leq 0.0001$; ns, no statistical differences.

7.3.5 MOMAST® Activates the SREBP-2/LDLR Pathway and Modulates the Active HMGCoAR Enzyme

SREBP-2 and LDLR proteins were quantified in the liver of the mice of the four experimental groups to investigate the effects of MOMAST® on the LDLR pathway. Figure 5 shows that WD ingestion significantly reduced the LDLR protein level (Figure 7A) and the SREBP2 transcription factor (Figure 7B) by 24.78 ± 10.01% ($p < 0.05$) and 24.7 ± 9.95% ($p < 0.05$), respectively. The treatment with both RYR and MOMAST® augmented LDLR by 34.7 ± 13.7% ($p < 0.01$) and 32.4 ± 13.39% ($p < 0.01$), respectively (Figure 7A), and in parallel, the SREBP-2 levels were increased, restoring the SD group values. In detail, the RYR and MOMAST® diets lead to a decrease in SREBP-2 levels by 8.98 ± 6.08% and 1.13 ± 5.45%, respectively, versus the SD group Figure 5A.

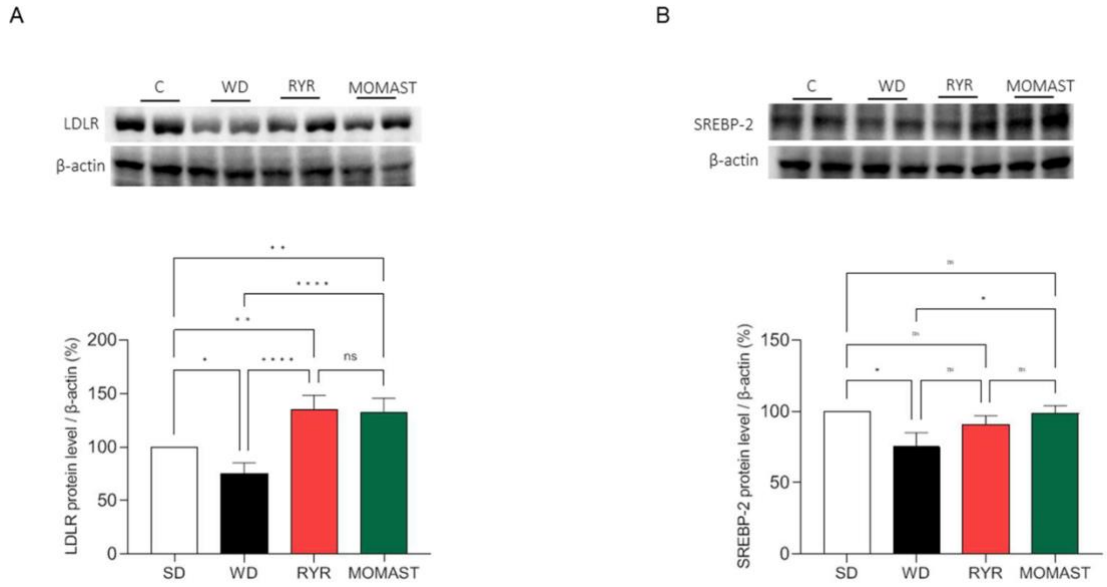

Figure 7. Modulation of the LDLR pathway by MOMAST®. MOMAST® increases the LDLR (**A**) and SREBP-2 transcription factor (**B**) modulated by the Western diet. Data are represented as mean ± standard deviation. *, $p \leq 0.05$); **, $p \leq 0.01$; ****, $p \leq 0.0001$; ns, no statistical difference.

The effects of MOMAST® on the HMGCoAR protein levels were also evaluated by Western blotting. As shown in Figure 6, mice fed with the WD showed a decrease in HMGCoAR protein levels by 30.4 ± 11,91% compared to the SD-fed mice (Figure 8A). On the other hand, RYR treatment augmented HMGCoAR protein levels by 23.2 ± 25.78%, and MOMAST® treatment by 3.8± 12.06% (Figure 8A). In parallel, in WD-fed mice, the SREBP-2 modulation led to a decline in the total phosphorylated and inactive p-HMGCoAR protein by 38.33 ± 7.79% ($p < 0.0001$, Figure 6 B), while the

RYR diets restored the p-HMGCoAR protein levels by up to 2.2 ± 4.23% and the MOMAST® diet reduced these target levels by 17.84 ± 7.91%, versus the SD diet (p < 0.01; Figure 6B).

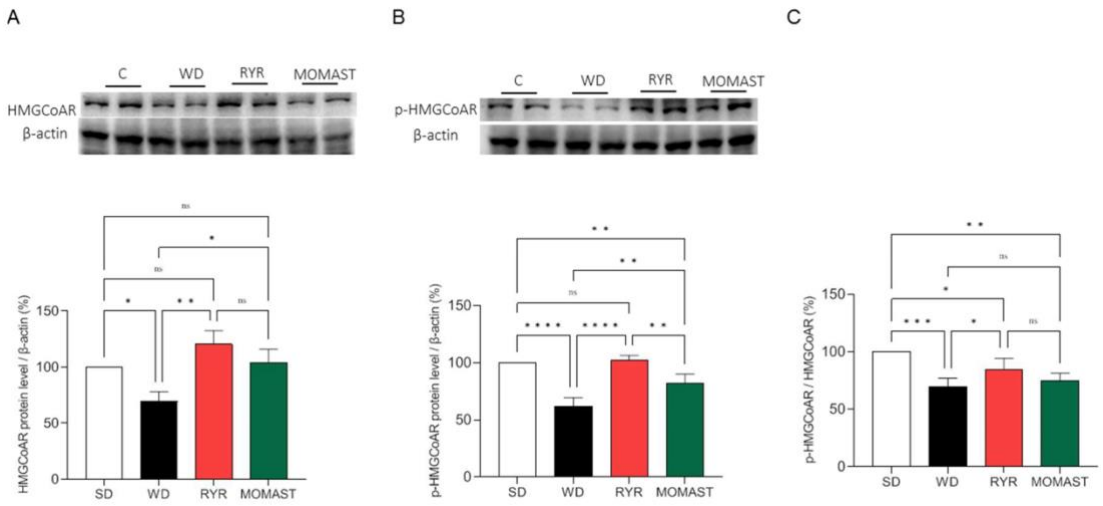

Figure 8. Effects of the MOMAST® on HMGCoAR and p-HMGCoAR protein levels. Representative Western blot analyses of the HMGCoAR (**A**) and p-HMGCoAR (**B**) protein levels. The ratio of the inactive phosphorylated and active non-phosphorylated forms of HMGCoAR (**C**). Data are represented as mean ± standard deviation. *, $p \leq 0.05$; **, $p \leq 0.01$); ***, $p \leq 0.001$; ****, $p \leq 0.0001$; ns, no statistical differences.

Furthermore, the p-HMGCoAR/HMGCoAR ratio was calculated. As shown in **Figure 8**C, the ratio was reduced by 30.47 ± 7.56 % (p < 0.001) in the WD-fed mice compared to the SD-fed mice. The treatment with both RYR and MOMAST® reduced the p-HMGCoAR/HMGCoAR ratio by 15.35 ± 9.63 % (p < 0.05) and 25.17 ± 6.49 % (p < 0.01), respectively, compared to the SD group.

7.3.6 MOMAST® Treatment Reduces the PCSK9 Protein Levels Increased by WD Ingestion

As indicated in Figure 7, the effects of MOMAST® on the modulation of PCSK9 and its transcription factor HNF1-α were evaluated. Our results demonstrate that the ingestion of the WD leads to a significant augmentation of PCSK9 protein by 117.40 ± 41.59% (p < 0.01), whereas in RYR-fed mice the levels of this target increase up to 119.10 ± 9.72% (p < 0.01, Figure 9A). On the other hand, the mice treated with MOMAST® showed a reduction in PCSK9 protein levels by up to 19.10 ± 10.72%, restoring the SD levels (Figure 9A).

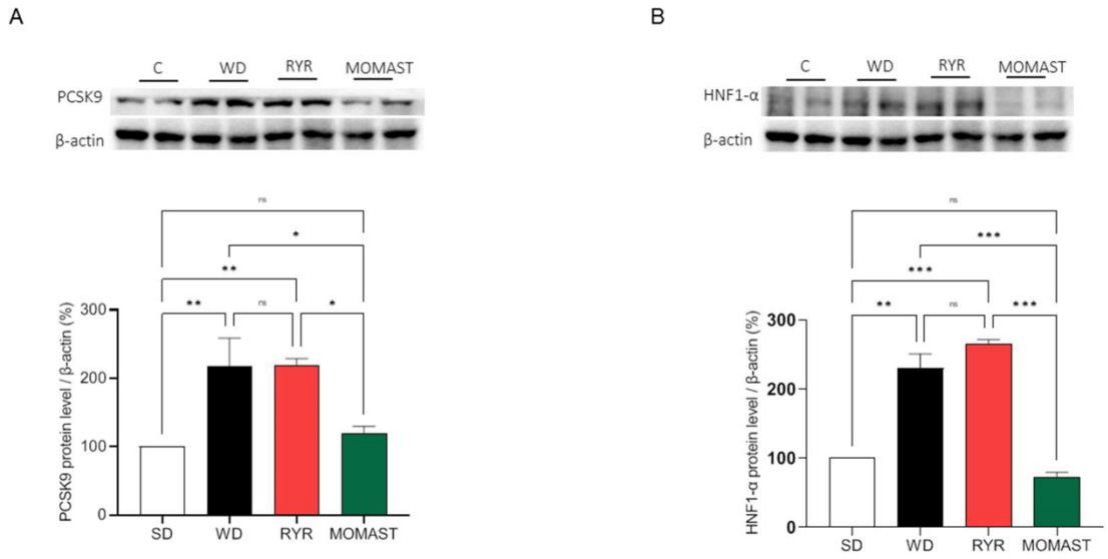

Figure 9. Effects of the MOMAST® on PCSK9 and HNF1-α protein levels. The MOMAST® counteracts the increase in PCSK9 (A) and its transcription factor HNF1-α (B) caused by the ingestion of WD. Data are represented as mean ± standard deviation. *, $p \leq 0.05$; **, $p \leq 0.01$; ***, $p \leq 0.001$.

This finding agrees with the HNF1-α transcription factor level modulations. Indeed, only MOMAST® showed the capability to reduce the HNF1-α transcription factor levels. In detail, WD increased the HNF1-α protein levels by 130.0 ± 20.88% ($p < 0.01$), while RYR augmented the HNF1-α levels by 165.5 ± 5.87% ($p < 0.001$), and MOMAST® diminished its levels by 27.68 ± 7.25%, compared with the SD group (Figure 9B).

7.4 Discussion

MOMAST® is an innovative sustainable and bioactive ingredient rich in OH-Tyr and Tyr (Figure S1) which displays a potent direct antioxidant activity (Figure 2). The results indicated that MOMAST® successfully scavenged the DPPH radicals and improved the FRAP capacity at 0.1 and 0.5 mg/mL, respectively. This innovative ingredient showed the positive ability to modulate the cholesterol metabolism in human hepatic HepG2 cells with a mechanism of action which is not only linked to its antioxidant and anti-inflammatory behavior (Bartolomei *et al.*, 2022). In order to obtain the *proof of concept* regarding its *in vivo* antioxidant and hypocholesterolemic effect, a suitable study was realized using mice in which the hypercholesterolemic condition was induced by feeding with the WD and then treating with MOMAST® (20 mg/kg) and RYR (3% Monacolin) for eight weeks. The results observed in this study are independent of the daily food intake, which remained unchanged between the WD-fed groups. Firstly, the body weight results showed that MOMAST® is capable of palliating

the increase in body weight caused by WD ingestion (Figure 3). This is of great interest due to overweight and obesity having been pointed out as one of the pivotal risk factors in the development of the principal non-transmissible chronic diseases (Pugliese et al., 2022, De Lorenzo et al., 2019, Al-Jawaldeh et al., 2022, Pi-Sunyer et al., 2009).

The findings clearly indicated that MOMAST® improves the WD-induced oxidative stress measured in mice serum and liver (Figure 4). In more detail, it was observed that unlike in the RYR-fed mice, MOMAST® showed an ability to decrease the DPPH radical compared with WD-fed mice, which showed an increase in DPPH radicals at the serum level. The *in vivo* antioxidant effect was also confirmed by performing a FRAP assay for mice serum. Indeed, MOMAST®-treated mice showed an increase in the FRAP levels (0.17 mmol equiv. Trolox/L) compared to the WD-fed ones (0.14 mmol equiv. Trolox/L, $p = 0.039$); also, in this case, RYR was not able to modulate the FRAP capacity in mice (Figure 4B). Furthermore, MOMAST® showed an ability to reduce the hepatic WD-induced MDA, restoring the SD lipid peroxidation baseline levels, whereas RYR was confirmed to not modulate the lipid peroxidation in mice livers. In addition, an increase in plasmatic lipid concentration was observed in the WD-fed mice compared to the SD-fed ones and a significant decrease in plasmatic lipid marker concentration in WD + MOMAST®-treated mice compared to the WD-fed mice, restoring the normal values observed in SD-fed mice, was successfully achieved. In particular, it was observed that MOMAST® treatment reduces the WD-induced levels of TC and LDL and increases the HDL levels, without changing the TG levels (Figure 5A–D). The behavior of MOMAST® in the modulation of the plasmatic lipid profile is similar to WD + RYR®-treated mice; however, unlike it, in the WD + MOMAST®-treated mice a significantly augmentation of HDL was observed, suggesting a potentially better anti-atherogenic effect of MOMAST® (Nagao *et al.*, 2018). The Castelli risk index-I (TC/HDL ratio), also known as the cardiac risk ratio, reflects the formation of coronary plaques with a diagnostic value as good as the determination of total cholesterol (Cai *et al.*, 2017, Olamoyegun *et al.*, 2016). On the other hand, the Castelli risk index-II (LDL/HDL ratio) has been shown to be an excellent predictor of cardiovascular risk (Millàn *et al*., 2009). Interestingly, MOMAST®, similarly to RYR, reduces both CRI-I and II compared to WD-fed mice, restoring the normal condition observed in the SD-fed mice, suggesting that MOMAST®ameliorated the cardiovascular risk factors (Figure 6A,B). Using this hypercholesterolemic animal model, similarly to RYR behavior, we did not observe effects of MOMAST® on

triglyceride modulation (Figure 5B). Basis on these results and to link the plasmatic lipid parameter modulation with the effects of MOMAST® on the hepatic cholesterol metabolism pathway, Western blotting experiments were performed using liver homogenates. Our findings show that WD-fed mice presented reduced protein levels of LDLR, HMGCoAR, and SREBP-2 than SD-fed mice, and that the WD + MOMAST®-fed mice restored their protein levels of all the targets towards the normal condition observed in the SD-fed mice (Figure 7 and Figure 8A). HMGCoAR activity can be modulated by a reversible phosphorylation-dephosphorylation, with the phosphorylated form of the enzyme being inactive (70%) and the dephosphorylated form active (30%). Thus, when HMGCoAR is phosphorylated, the synthesis of de novo cholesterol is reduced (Zammit *et al.*, 1987, Parker *et al.*, 1986). Interestingly, in this study, it was observed that in the WD-fed mice the phosphorylated form of HMGCoAR was significantly reduced and that both RYR and MOMAST® consumption increased the phosphorylated form of the enzyme towards the normal level observed in SD-fed mice (Figure 8B,C). Overall, in agreement with the literature, the capability of MOMAST® to modulate the LDLR-SREBP-2 pathway is similar to RYR treatment (Zou *et al.*, 2022, Cicero *et al.*, 2019). However, in line with a previous mechanistic study performed on HepG2 cells (Bartolomei *et al*., 2022), it was confirmed that, unlike RYR, only MOMAST® positively modulates the PCSK9 pathway via HNF1-α activation (Figure 7A,B). Notably, since the HNF1-α binding site is unique to the PCSK9 promoter and is not present in the LDLR promoter, the modulation of the PCSK9 transcription through HNF1-α does not affect the LDLR pathway. Thus, the co-regulation of PCSK9 by LDLR and other SREBP target genes is disconnected by the HNF1-α binding site (Maxwell *et al.*, 2005). In this context, it is important to highlight that a significant increase in HNF1-α and PCSK9 protein levels, respectively, were observed in WD-fed mice, which are clearly reduced by MOMAST® toward the normal levels observed in SD-fed mice. On the contrary, the findings suggest that RYR is completely ineffective in the modulation of PCSK9 protein levels, being unable to reduce the increase in HNF1-α levels (Figure 9A,B).

7.5 Conclusions

In light of these results, MOMAST® can be considered an innovative and sustainable antioxidant and hypocholesterolemic ingredient which is able to act with a mechanism of action which is different from RYR; therefore, it can be used alone or in combination

with RYR (as strategy for reducing its amount of use) for the potential development of a new generation of dietary supplements or functional foods for the prevention of cardiovascular disease. In addition, further clinical studies can be performed to corroborate the ability of MOMAST® to modulate cholesterol metabolism and oxidative stress in humans.

7.6 Patents

Patent n. 102021000019226 of the 20 July 2021 entitled "*Processo produttivo di complessi polifenolici da acque di vegetazione olearie con processo fermentativo e relativi complessi polifenolici prodotti*"—inventors: Arnoldi A., Clodoveo M.L., Corbo F.F.R., Franchini C., Lammi C., Lentini, G. Lorenzo, V., Massari C.D, Milani G., Moretti P., and Pisano I.

7.7 Institutional Review Board Statement

The experiments were performed under the Spanish legislation and the EU Directive 2010/63/EU for animal experiments and were approved by the Virgen Macarena and Virgen del Rocío University Hospitals Ethics Committee (reference CEEA-US2023-18).

7.8 Supporting information

Chemicals

Bovine serum albumin (BSA), β-mercaptoethanol, RIPA buffer, the antibody against phospho-HMGCoAR (Ser872) and the antibody against β- actin were bought from Sigma Aldrich (St. Louis, MO, USA). The antibody against HMGCoAR was bought from Abcam (Cambridge, UK). Lipid Peroxidation (MDA) Assay Kit (MAK085), phenylmethanesulfonyl fluoride (PMSF), Na-orthovanadate and the antibodies against rabbit Ig-horseradish peroxidase (HRP), mouse Ig-HRP, and SREBP-2 were purchased from Santa Cruz Biotechnology Inc. (Santa Cruz, CA, USA). The antibodies against the LDLR was bought from Pierce (Rockford, IL, USA). The antibodies against HNF1-α and PCSK9 were bought from GeneTex (Irvine, CA, USA). The inhibitor cocktail Complete Midi from Roche (Basel, Swiss). The chemiluminescent reagent was purchased from Euroclone (Milan, Italy). Mini protean TGX pre-cast gel 7.5% and Mini nitrocellulose Transfer Packs were purchased from BioRad (Hercules,CA, USA).

MOMAST® Description: Bioenutra S.R.L. (Italy) supplies the patented MOMAST® sample directly from the production process. MOMAST® sample is a phenolic complex, rich in tyrosol (4.2 g/kg, Tyr) and hydroxityrosol (12,4 g/kg, OH-Tyr). Its chromatogram is available as Supplementary Materials (Figure 1S).

In vitro MOMAST® antioxidant activity 2.2.1 2,2-diphenyl-1-picrylhydrazyl (DPPH) assay

To estimate the radical scavenging capacity of MOMAST®, the DPPH assay was carried out. Briefly, 45µL of DPPH solution (0.0125mM in methanol) was added to 15µL MOMAST® at 1-600 mg/mL. The scavenging reaction was performed in the dark for 30 min of incubation. After this time, the absorption was measured at 520 nm using a CLARIOstar Plus microplate reader (BMG Labtech, Ortenberg, Germany).

Ferric Reducing Antioxidant Power (FRAP) Assay

A volume of 15µL of a sample containing MOMAST® was combined with 140 µL of FRAP solution, which consisted of 0.83 mM TPTZ, 1.66 mM $FeCl_3 \times 6H_2O$, and 0.25 M acetate buffer(pH 3.6). The final concentrations of MOMAST® were 0.1 and 0.5 mg/mL. Following an incubation period of 30 minutes at 37 °C, the absorbance at 595 nm was measured usinga SynergyTMHT-multimode microplate reader (BiotekInstruments, Winooski,VT, USA). The measured values were extrapolated using a Trolox (Sigma-Aldrich) standard curve.

Study design

26 C57BL/6 4-weeks-old mouse were housed at the Animal Facility of the Instituto de Biomedicina de Sevilla (IBiS) under standard conditions and were fed with WD (45% energy from fat, TestDiet, St. Louis, MO, USA, n = 21) or with standard diet (SD, Rodent maintenance diet, ENVIGO, IN, USA, n = 5). When mice were 6-weeks-old, they were separated in three group and intragastrically treated with: **1**) saline (control group, C, n = 7), **2**) red yeast rice (3% Monacolin K, RYR, ADVA s.r.l., Italy, n = 7), or **3**) MOMAST® (Bioenutra s.r.l., Italy, n = 7) at 20 mg/kg for eight weeks. The individual body weight and the daily food intake were weekly recorded. At the final of the experiment, an intraperitoneal injection of sodium thiopental (B. Braun Medica SA, Barcelona, Spain) was used to sacrifice the 12 h fasted-mice. By cardiac puncture the

blood was collected in the MiniCollect tubes (Greiner Bio-One, Kremsmünster, Austria), which was centrifuged at 3,000 g for 10 minutes at 4 °C to obtain the serum that was immediately frozen and stored at −20 °C until use. Also, the liver was extracted, weighed, and finally rapidly frozen and stored at −80 °C until use. All procedures were approved by the Ethical Committee (reference number 16/03/2023/004).

Biochemical parameters

All biochemical parameters were quantified in the serum samples using the COBAS E601 modular analyzer (Roche Diagnostic, Bassel, Switzerland). Castelli risk index (CRI) I and II were calculated as TC/HDL and LDL/HDL, respectively.

***In vivo* antioxidant activity of MOMAST® 2.5.1 DPPH and FRAP assays**

Serum antioxidant capacity was evaluated using DPPH and FRAP assays. Briefly, for the FRAP assay,15 µL of serum was combined with 140 µL of FRAP solution, while for DPPH assay,15µL of serum was added to 45µL of DPPH solution. Both assays test were carried out according to the manufacture's instruction.

Determination of liver malondialdehyde (MDA) levels

Each liver sample (10 mg) was homogenized in 300 µ L ice-cold MDA lysis buffer containing 3 µ L of BHT (100×) and was centrifuged at 13,000× g for 10 min. To form the MDA- thiobarbituric acid (TBA) adduct, 600 µL of the TBA solution were added into each vial containing 200 µ L of samples and incubated at 95 ◦C for 60 min, then cooled to RT for 10 min in an ice bath. For analysis, 100 µ L of each reaction mixture were pipetted into a 96 well plate and the absorbance was measured at 532 nm using the Synergy H1 fluorescence plate reader (Biotek, Bad Friedrichshall, Germany).

Western-blot analysis

Tissues were homogenized in a lysis buffer (RIPA buffer +protease inhibitor cocktail + 1:100 PMSF + 1:100 Na-orthovanadate + 1:1000 β- mercaptoethanol). Protein concentration was determined by the Bradford's method and 50 µg of total proteins were run into a precast 7.5% sodium dodecyl sulfate-polyacrylamide gel (SDS-PAGE) at 130 V for 45 min and then transferred to a nitrocellulose membrane (Mini nitrocellulose Transfer Packs, BioRad, Hercules, CA, USA) using a Trans-Blot Turbo (BioRad) at 1.3 A, 25 V for 7 min, and stained with Ponceau red solution (Sigma-Aldrich). To

investigate proteins of different sizes on the same membrane, the membrane was cut into horizontal stripes. The milk or BSA blocked membrane were overnight incubated at 4 °C with primary antibodies against SREBP2, HMGCoAR, LDLR, phospho HMGCoAR (Ser872), PCSK9, HNF1-α, and β- actin. After washing, the blots were incubated with secondary antibodies conjugated with horseradish peroxidase. A chemiluminescent reagent (Euroclone, Milan, Italy) was used to visualize target proteins and the densitometry analysis was performed using the software Image Lab 6.1 (BioRad). The internal control β-actin was used to normalize loading variations.

Statistical analysis

All the data sets were checked for normal distribution by D'Agostino and Pearson test. Since they are all normally distributed with p-values < 0.05, statistical analysis was carried out by One-way ANOVA followed by Tukey's post-hoc analysis (GraphPad Software 9, San Diego, CA, USA). Values were expressed as means ± standard deviation; p-values ≤ 0.05 were considered to be significant.

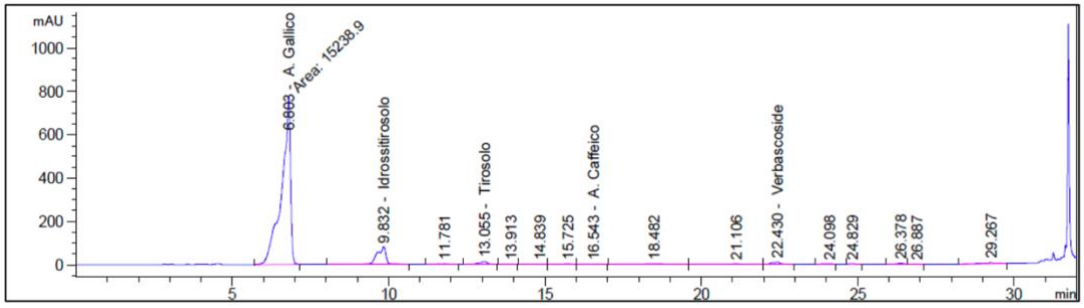

FigureS1: Chromatogram of the MOMAST® phytocomplex.

7.9 References

Aires, V.; Labbé, J.; Deckert, V.; Pais de Barros, J.P.; Boidot, R.; Haumont, M.; Maquart, G.; Le Guern, N.; Masson, D.; Prost-Camus, E.; et al. Healthy Adiposity and Extended Lifespan in Obese Mice Fed a Diet Supplemented with a Polyphenol-Rich Plant Extract. Sci. Rep. 2019, 9, 9134.

Al-Jawaldeh, A.; Abbass, M.M.S. Unhealthy Dietary Habits and Obesity: The Major Risk Factors Beyond Non-Communicable Diseases in the Eastern Mediterranean Region. Front. Nutr. 2022, 9, 817808.

Bartolomei, M.; Bollati, C.; Li, J.; Arnoldi, A.; Lammi, C. Assessment of the Cholesterol-Lowering Effect of MOMAST®: Biochemical and Cellular Studies. Nutrients 2022, 14, 493.

Cai, G.; Shi, G.; Xue, S.; Lu, W. The Atherogenic Index of Plasma Is a Strong and Independent Predictor for Coronary Artery Disease in the Chinese Han Population. Medicine 2017, 96, e8058.

Cicero, A.F.G.; Fogacci, F.; Banach, M. Red Yeast Rice for Hypercholesterolemia. Methodist Debakey Cardiovasc. J. 2019, 15, 192.

De Lorenzo, A.; Gratteri, S.; Gualtieri, P.; Cammarano, A.; Bertucci, P.; Di Renzo, L. Why Primary Obesity Is a Disease? J. Transl. Med. 2019, 17, 169.

De Luca, P.; Sicilia, V.; Candamano, S.; Macario, A. Olive Vegetation Waters (OVWs): Characteristics, Treatments and Environmental Problems. IOP Conf. Ser. Mater. Sci. Eng. 2022, 1251, 012011.

Kaminski, J.; Haumont, M.; Prost-Camus, E.; Durand, P.; Prost, M.; Lizard, G.H.; Latruffe, N. Protection of C2C12 Skeletal Muscle Cells towards Oxidation by a Polyphenol Rich Plant Extract. Redox Exp. Med. 2023, 2023, e230002.

Lammi, C.; Aiello, G.; Bollati, C.; Li, J.; Bartolomei, M.; Ranaldi, G.; Ferruzza, S.; Fassi, E.M.A.; Grazioso, G.; Sambuy, Y.; et al. Trans-epithelial Transport, Metabolism and Biological Activity Assessment of the Multi-target Lupin Peptide Lilpkhsdad (P5) and Its Metabolite Lpkhsdad (P5-met). Nutrients 2021, 13, 863.

Lammi, C.; Bellumori, M.; Cecchi, L.; Bartolomei, M.; Bollati, C.; Clodoveo, M.L.; Corbo, F.; Arnoldi, A.; Mulinacci, N. Extra Virgin Olive Oil Phenol Extracts Exert Hypocholesterolemic Effects through the Modulation of the LDLR Pathway: In Vitro and Cellular Mechanism of Action Elucidation. Nutrients 2020, 12, 1723.

Maxwell, K.N.; Fisher, E.A.; Breslow, J.L. Overexpression of PCSK9 Accelerates the Degradation of the LDLR in a Post-Endoplasmic Reticulum Compartment. Proc. Natl. Acad. Sci. USA 2005, 102, 2069–2074.

McBean, G.A. Integrating Science to Address Food and Health within Global Agenda 2030. npj Sci. Food 2021, 5, 8.

Millán, J.; Pintó, X.; Muñoz, A.; Zúñiga, M.; Rubiés-Prat, J.; Pallardo, L.F.; Masana, L.; Mangas, A.; Hernández-Mijares, A.; González-Santos, P.; et al. Lipoprotein Ratios: Physiological Significance and Clinical Usefulness in Cardiovascular Prevention. Vasc. Health Risk Manag. 2009, 5, 757–765.

Mulinacci, N.; Romani, A.; Galardi, C.; Pinelli, P.; Giaccherini, C.; Vincieri, F.F. Polyphenolic Content in Olive Oil Waste Waters and Related Olive Samples. J. Agric. Food Chem. 2001, 49, 3509–3514.

Nagao, M.; Nakajima, H.; Toh, R.; Hirata, K.I.; Ishida, T. Cardioprotective Effects of High-Density Lipoprotein beyond Its Anti-Atherogenic Action. J. Atheroscler. Thromb. 2018, 25, 985–993.

Obied, H.K.; Karuso, P.; Prenzler, P.D.; Robards, K. Novel Secoiridoids with Antioxidant Activity from Australian Olive Mill Waste. J. Agric. Food Chem. 2007, 55, 2848–2853.

Olamoyegun, M.; Oluyombo, R.; Asaolu, S. Evaluation of Dyslipidemia, Lipid Ratios, and Atherogenic Index as Cardiovascular Risk Factors among Semi-Urban Dwellers in Nigeria. Ann. Afr. Med. 2016, 15, 194.

Parker, R.A.; Miller, S.J.; Gibson, D.M. Phosphorylation State of HMG CoA Reductase Affects Its Catalytic Activity and Degradation. Adv. Enzym. Regul. 1986, 25, 329–343.

Pi-Sunyer, X. The Medical Risks of Obesity. Postgrad. Med. 2009, 121, 21–33.

Pugliese, G.; Liccardi, A.; Graziadio, C.; Barrea, L.; Muscogiuri, G.; Colao, A. Obesity and Infectious Diseases: Pathophysiology and Epidemiology of a Double Pandemic Condition. Int. J. Obes. 2022, 46, 449–465.

Recinella, L.; Chiavaroli, A.; Orlando, G.; Menghini, L.; Ferrante, C.; Di Cesare Mannelli, L.; Ghelardini, C.; Brunetti, L.; Leone, S. Protective Effects Induced by Two Polyphenolic Liquid Complexes from Olive (Olea Europaea, Mainly Cultivar Coratina) Pressing Juice in Rat Isolated Tissues Challenged with LPS. Molecules 2019, 24, 3002.

Zammit, V.A.; Easom, R.A. Regulation of Hepatic HMG-CoA Reductase in Vivo by Reversible Phosphorylation. BBA Mol. Cell Res. 1987, 927, 223–228.

Zou, J.; Yan, C.; Wan, J.B. Red Yeast Rice Ameliorates Non-Alcoholic Fatty Liver Disease through Inhibiting Lipid Synthesis and NF-KB/NLRP3 Inflammasome-Mediated Hepatic Inflammation in Mice. Chin. Med. 2022, 17, 17.

CHAPTER 6

MANUSCRIPT 5

EXPLOITATION OF OLIVE (*Olea Europaea L.*) SEED PROTEINS AS UPGRADED SOURCE OF BIOACTIVE PEPTIDES WITH MULTIFUNCTIONAL PROPERTIES: FOCUS ON ANTIOXIDANT AND DIPEPTIDYL-DIPEPTIDASE– IV INHIBITORY ACTIVITIES, AND GLUCAGON-LIKE PEPTIDE 1 IMPROVED MODULATION.

Martina Bartolomei [1], Anna Laura Capriotti [2], Yuchen Li [3], Carlotta Bollati [1], Jianqiang Li [1], Andrea Cerrato [2], Lorenzo Cecchi [4], Raffaele Pugliese [5], Maria Bellumori [4], Nadia Mulinacci [4], Aldo Laganà [2], Anna Arnoldi [1], Carmen Lammi [1],*

[1] Department of Pharmaceutical Sciences, University of Milan, 20133 Milan, Italy; martina.bartolomei@unimi.it (M.B.); carlotta.bollati@unimi.it (B.C.); jianqiang.li@unimi.it (J.L.); anna.arnoldi@unimi.it (A.A.)

[2] Department of Chemistry, Sapienza University of Rome, Piazzale Aldo Moro 5, 00185 Rome, Italy; annalaura.capriotti@uniroma1.it (A.L.C.), andrea.cerrato@uniroma1.it (A.C.), aldo.lagana@uniroma1.it. (A.L.)

[3] Longping Biotech Co Ltd., 572000 Sanya, China

[4] Department of Neuroscience, Psychology, Drug and Child Health, Pharmaceutical and Nutraceutical Section, University of Florence, 50019 Florence, Italy; maria.bellumori@unifi.it (M.B.); lo.cecchi@unifi.it (L.C.); nadia.mulinacci@unifi.it (N.M.)

[5] NeMO Lab, ASST Grande Ospedale Metropolitano Niguarda, 20162 Milan, Italy; raffale.pugliese@nemolab.it

* Correspondence: carmen.lammi@unimi.it; Tel.: +39-02-50319372

8. Abstract

Agri-food industry wastes and by-products include highly valuable components that can upgraded, providing low-cost bioactives or used as an alternative protein source. In this context, by-products from olive production and olive oil extraction process, i.e., seeds, can be fostered. In particular, this work was aimed at extracting and characterizing proteins for *Olea europaea* L. seeds and at producing two protein hydrolysates using alcalase and papain, respectively. Peptidomic analysis were performed, allowing to determine both medium- and short-sized peptides and to identify their potential biological activities. Moreover, an extensive characterization of the antioxidant properties of *Olea europaea* L. seed hydrolysates was carried out both *in vitro* by 2,2-diphenyl-1-picrylhydrazyl (DPPH), by ferric reducing antioxidant power (FRAP), and by 2,2′-Azino-bis(3-ethylbenzothiazoline-6-sulfonic acid) diammonium salt (ABTS) assays, respectively, and at cellular level by measuring the ability of these hydrolysates to significant reduce the H_2O_2-induced reactive oxygen species (ROS) and lipid peroxidation levels in human intestinal Caco-2 cells. The results of the both hydrolysates showed significant antioxidant properties by reducing the free radical scavenging activities up to 65.0 ± 0.1% for the sample hydrolyzed with alcalase and up to 75.7 ± 0.4% for the papain hydrolysates tested at 5 mg/mL, respectively. Moreover, similar values were obtained by the ABTS assays, whereas the FRAP increased up to 13,025.0 ± 241.5% for the alcalase hydrolysates and up to 12,462.5 ± 311.9% for the papain hydrolysates, both tested at 1 mg/mL. According to the *in vitro* results, both papain and alcalase hydrolysates restore the cellular ROS levels up 130.4 ± 4.24% and 128.5 ± 3.60%, respectively, at 0.1 mg/mL and reduce the lipid peroxidation levels up to 109.2 ± 7.95% and 73.0 ± 7.64%, respectively, at 1.0 mg/mL. In addition, results underlined that the same hydrolysates reduced the activity of dipeptidyl peptidase-IV (DPP-IV) *in vitro* and at cellular levels up to 42.9 ± 6.5% and 38.7 ± 7.2% at 5.0 mg/mL for alcalase and papain hydrolysates, respectively. Interestingly, they stimulate the release and stability of glucagon-like peptide 1 (GLP-1) hormone through an increase of its levels up to 660.7 ± 21.9 pM and 613.4 ± 39.1 pM for alcalase and papain hydrolysates, respectively. Based on these results, olive seed hydrolysates may represent new ingredients with antioxidant and anti-diabetic properties for the development of nutraceuticals and functional foods for the prevention of metabolic syndrome onset.

8.1 Introduction

The use of food-derived bioactive peptides for the development of functional foods and/or nutraceuticals it is becoming an attractive practice, and currently, products containing peptides with health-promoting effects are accessible on the market (Aguilar-Toalá *et al.*, 2017). Over the last ten years, a considerable number of scientific investigations have highlighted the beneficial effects of protein hydrolysates and peptides recovered from a wide range of food by-products, including antimicrobic, antihypertensive, and especially antioxidant and antidiabetic (Cabizza *et al.*, 2021, Eckert *et al.*,2014, Ferri *et al.*, 2017, Jin *et al.*, 2020, Lammi *et al.*, 2018, Lima *et al.*, 2019, Rivero-Pino *et al.*, 2020, Zamora-sillero *et al.*., 2018). By-products are secondary products obtained from primary agro-food production processes and traditionally disposed of in landfills, with consequent air and water pollution and soil contamination. Food waste, by-products, and side-streams from several agricultural and food industries represent an attractive source of potentially functional or bioactive compounds, which can easily find application in the nutraceutical and pharmaceutical fields as an economic source (Socas-Rodrìguez *et al.*., 2021). In this context, the literature reports the presence of several food-origin peptides with antioxidant properties and hypoglycemic activity, such as dipeptidyl peptidase-IV (DPP-IV) inhibitors (Power *et al.*., 2013, Liu *et al.*., 2015, De Campos Zani, *et al.*., 2018). Indeed, these two biological activities are among the most studied; however, the combination of their biological effects could be further investigated. Generally, a high oxidative state is found in individuals with diabetes mellitus (DM), where the main molecular mechanisms involved are related to glucose and lipid metabolism. Rudich and Maddux observed a decrease in glucose uptake, in oxidative stress condition, and in muscle and fat cells and the reduction of the quantity and quality of insulin secreted by pancreatic β-cells (Rudich *et al.*, 1998, Maddux *et al.*, 2001). Additionally, the over-production of reactive oxygen species (ROS) in β-cells lead to cell damage and activation of pathways involved in DM complications, i.e., neuropathy, endothelial dysfunction, nephropathy, and retinopathy (Ceriello *et al.*, 2016, Harding *et al.*, 2019). A novel approach to control diabetes is based on incretin hormone glucagon-like peptide 1 (GLP-1), which normalizes blood glucose levels and reduces postprandial glycemia by stimulating insulin secretion (Dicker, 2011). Since DPP-IV is a serine protease responsible for the rapid degradation of GLP-1 in blood plasma (Barnett, 2006), the use of inhibitors of this enzyme could

prolong the half-life of GLP-1 by increasing its levels. Considering the beneficial effects of bioactive peptides on human health, various antioxidant and/or hypoglycemic peptides were obtained from the recovery of food by-products (Zambrowicz *et al.*, 2015, Saidi *et al.*, 2018, Choksawangkarn *et al.*, 2018) and bioactive molecules, such as lignans, tocopherols, flavonoids, secoiridoids, and especially hydroxytyrosol, and have already been obtained from waste and by-products of olive production (Ibáñez *et al.*, 2000, Wang *et al.*, 2018, Stathopoulos *et al.*, 2014, Vilaplana-Pérez *et al.*, 2014, Bertelli *et al.*, 2020), which generates 16 million tons of green and black table olives and 2.7 million tons of oil, according to FAOSTAT (Food and Agriculture Organization Corporate Statistical Database), and 95% is produced mainly in Spain and Italy. In this scenario, this study focuses on fostering the olive stones or seeds (OS), a lignocellulosic, low-moisture by-product obtained after separation through horizontal centrifugation of the crushed seeds, peels, and pulp. OSs are good source of dietary fiber but also lipids and proteins rich in essential amino acids, especially valine and arginine (Pedroza *et al.*, 2015). Therefore, the first objective of this work was the physicochemical and conformational characterization of the total proteins extracted from three different cultivars of *Olea europaea* L., i.e., *Leccino*, *Moraiolo*, and *Frantoio*, by a combination of different techniques. Hence, total proteins were hydrolyzed using two food-grade enzymes, i.e., alcalase and papain, in the optimal conditions to obtain potential bioactive peptides. The second objective of the work was to evaluate the potential biological effects of the olive stone hydrolysates, specifically the antioxidant effects of the extracted peptides, using *in vitro* and cellular assays. Considering that the modulation of the DPP-IV enzyme can occur in the presence of oxidative stress (Ishibashi *et al.*, 2013), in parallel, the antidiabetic activity was evaluated by investigating the *in vitro* and cellular inhibition of the DPP-IV enzyme. In addition, the modulation of incretin hormones GLP-1 levels was assessed through an innovative assay based on a co-culture system. The aim was to simulate the intestinal barrier in which the GLP-1 hormone is physiologically produced by endocrine cells (L cells of the intestinal mucosa) through the cleavage of proglucagon. Here, murine intestinal secretin tumor cell line (STC-1) was used as a model in order to achieve GLP-1 production.

8.2 Materials and Methods

8.2.1 Chemical and Samples

All chemicals and reagents were commercially available, and more details are reported in the Supplementary Materials.

8.2.2 Protein Extraction from Olive Seed

Olive seed samples were obtained from the fruits of three cultivars, namely *Leccino*, *Frantoio*, and *Moraiolo*, harvested in Tuscany (soc. agr. Buonamici, Fiesole). Each sample was obtained mixing the fruits collected at different ripening degrees from September to November. The pulp was separated from the kernel by a spatula, the nuts were manually broken with a hammer, and the whole seeds were removed. From 100 g of dried olives were obtained the following mean yields: *Leccino* 4.0%, *Frantoio* 3.2%, and *Moraiolo* 3.0%. Olive seeds were grounded with a domestic mill. Olive seed powder was defatted with hexane for 1 h (ratio 1:20 *w*/*v*) under magnetic stirring. After drying, olive seeds were grounded with a domestic mill. Olive seed powder was defatted with hexane for 1 h (ratio 1:20 *w*/*v*) under magnetic stirring. After drying, the defatted powder was subjected to protein extraction. In detail, 1.5 g of defatted powder were mixed with 30 mL of extracting solution containing UREA 6 M, 0.1 M Tris-HCl (pH 8), 0.5 M NaCl, 0.5% SDS, and 0.1% DTT. More details are reported in the Supplementary Materials.

8.2.3 Protein Solubility (PS), Water-Binding Capacity (WBC), and Oil-Binding Capacity (OBC)

PS and OBC were determined according to a method described previously (Malomo *et al.*, 2014) with slight alterations. WBC was assessed as previously described (Aiello *et al.*, 2021). More details are reported in the Supplementary Materials.

8.2.4 Free-Sulfhydryl Group Determination

Ellman's reagent (DTNB) is a compound used for quantifying free-sulfhydryl groups in solution, observing the production of a yellow-colored product when it reacts with sulfhydryl groups. More details are reported in the Supplementary Materials.

8.2.5 Intrinsic Fluorescence Spectroscopy

The intrinsic fluorescence spectrum of each sample was obtained using a fluorescence spectrophotometer (Synergy H1, Biotek, Bad Friedrichshall, Germany). More details are reported in the Supplementary Materials.

8.2.6 Raman Spectroscopy

Raman analysis was conducted using Progeny™ spectrophotometer (Rigaku Corporation, Akishima, Japan) with a 1064 nm laser source and selectable laser output set at 490 mW. The spectral range was 200–2500 cm^{-1} with transmission-type volume phase grating. The spectral resolution was 15–18 cm^{-1}, and the detector is a thermoelectrically cooled indium gallium arsenide (InGaAs). The samples were analyzed with 60 cumulative scans with optimized laser power, aperture size, and duration (7 s) per exposure in order to achieve the best signal-to-noise ratio. All of the obtained spectra were reported using Origin™ 8 software (OriginLab Corporation, Northampton, MA, USA).

8.2.7 Olive Seed Protein Hydrolysis for Releasing Bioactive peptides

The enzymatic hydrolysis of olive seed proteins was performed using alcalase and papain enzymes using optimal hydrolysis conditions (Table 1). All recovered peptides were lyophilized and stored at −80 °C until use. The DH (%) for each hydrolysate was identified by the o-phthaldialdehyde (OPA) method as previously described (Aiello *et al.*, 2017). More details are reported in the Supplementary Materials.

Enzyme	Temperature (°C)	Hydrolysis Time	Enzyme: Substrate Ratio	pH
Alcalase	50	4 h	0.15 UA/g	8.5
Papain	65	8 h	100 UA/g	7

Table 1. Alcalase and papain enzymes hydrolysis conditions: temperature (°C), hydrolysis time, E:S ratio, and pH.

8.2.8 Short Peptide Purification and Analysis by High-Performance Liquid Chromatography–High-Resolution Mass Spectrometry

Before analysis, short-sized peptides were purified from longer peptides and other macromolecules using a solid-phase extraction cartridge packed with 500 mg of carbograph 4 with a procedure that was optimized in a previous study (Piovesana *et al.*, 2019). The purified samples were then subject to HPLC-HRMS analysis using a Vanquish binary pump H (Thermo Fisher Scientific, Milan, Italy) coupled through a

heated electrospray (ESI) source to a hybrid quadrupole–Orbitrap mass spectrometer Q Exactive (Thermo Fisher Scientific, Milan, Italy). More details are reported in the Supplementary Materials.

8.2.9 Profile of Potential Biological Activities and Peptide Ranking

The open-access tool PeptideRanker, a web-based tool used to predict the eventuality of biological activity of peptide sequences, was used to forecast the potential bioactivities of olive seed peptides (Malomo *et al.*, 2014). Using N-to-1 neural network probability, PeptideRanker provides peptide scores in the range of 0–1. The peptides with a score higher than 0.6 were considered as potentially "bioactive". Subsequently, the lists of best-ranked peptides were submitted to the web-available database BIOPEP.

8.2.10 Cell Culture

Caco-2 cells, kindly obtained from INSERM (Paris, France), and STC-1, commercialy available from ATCC (HB-8065, ATCC from LGC Standards, Milan, Italy), were routinely sub-cultured following a previously optimized protocol (Aiello *et al.*, 2018). More details are reported in the Supplementary Materials.

8.2.11 3-(4,5-Dimethylthiazol-2-yl)-2,5-Diphenyltetrazolium Bromide (MTT) Assay

A total of 3×10^4 cells/well were seeded in 96-well plates and treated with different concentrations of hydrolysates and/or vehicle (H_2O) in complete growth medium for 48 h at 37 °C under a 5% CO_2 atmosphere. Experiments were performed by a standard method with slight modifications (Lammi *et al.*, 2014), and more details are provided in Supplementary Materials.

8.2.12 Antioxidant Activity of Olive Seed Hydrolysates

8.12.1 Diphenyl-2-Picrylhydrazyl Radical (DPPH) Assay

The DPPH assay was performed by a standard method with a slight modification. The experimental method is detailed in the Supplementary Materials.

8.12.2 2,2'-Azino-Bis(3-Ethylbenzothiazoline-6-Sulfonic Acid) Diammonium Salt Assay

The Trolox equivalent antioxidant capacity (TEAC) assay is based on the reduction of the 2,2-Azino-bis-(3-ethylbenzothiazoline-6-sulfonic acid) (ABTS) radical induced by antioxidants. The experimental method is detailed in the Supplementary Materials.

8.12.3 FRAP Assay

The FRAP assay evaluates the ability of a sample to reduce ferric ion (Fe^{3+}) into ferrous ion (Fe^{2+}). The experimental method is detailed in the Supplementary Materials.

8.12.4 Fluorometric Intracellular ROS Assay

For cells preparation, 3×10^4 Caco-2 cells/well were seeded on a black 96-well plate overnight in growth medium. The experimental method is detailed in the Supplementary Materials.

8.12.5 Lipid Peroxidation (MDA) Assay

Furthermore, 2.5×10^5 Caco-2 cells/well were seeded in a 24 well plate, and the following day, they were treated the OA and OP hydrolysates for 24 h at 37 °C under 5% CO_2 atmosphere. The experimental method is detailed in the Supplementary Materials.

8.2.13 Antidiabetic Activity of Olive Seed Hydrolysates

8.2.13.1 In Vitro Measurement of the DPP-IV Inhibitory Activity

The experiments were carried out in triplicate in a half-volume 96-well solid plate (white) using conditions previously optimized (Lammi *et al.*, 2016). More details are reported in the Supplementary Materials.

8.2.13.2 Evaluation of the Inhibitory Effect of Olive Seed Hydrolysates on Cellular DPP-IV Activity

A total of 3×10^4 cells/well were seeded in black 96-well plates with a clear bottom. The second day after seeding, the spent medium was discarded, and cells were treated with 1.5 and 5.0 mg/mL of olive seed hydrolysates for 1 h at 37 °C. Experiments were carried out following previously optimized conditions (Lammi *et al.*, 2019). More details are available in the Supplementary Materials.

8.2.13.3 Evaluation of the GLP-1 Stability and Secretion at Cellular Level

STC-1 GLP-1 secretion was measured by an active GLP-1 ELISA kit (catalog no. EGLP-35K; Millipore, Watford, UK) read on a a Synergy H1 fluorescence microplate reader from BioTek, Milan Italy. More details are available in the Supplementary Materials.

8.2.14 Statically Analysis

All measurements were performed in triplicate, and results were expressed as the mean ± standard deviation (s.d.), where *p*-values < 0.05 were considered to be significant. All the data sets were checked for normal distribution by D'Agostino and Pearson test. Since they are all normally disturbed with *p*-values < 0.05, we proceeded with statistical analyses. Statistical analyses were performed by one- and two-way ANOVA followed by Dunnett's and Tukey's post-test (Graphpad Prism 9, GraphPad Software, La Jolla, CA, USA).

8.3 Results

8.3.1 Extraction of Olive Seed Proteins

The *Olea europaea* L. seed proteome is predominantly composed of seed storage proteins (SSPs), which are fundamental molecules for the germination phase and rich in carbon and nitrogen (Ibáñez *et al.*, 2000, Wang *et al.*, 2018). In most of the already available studies, olive seed proteins are extracted by using Tris-HCl buffer in reducing conditions (Suda *et al.*, 2000, Shewry *et al.*, 1995, De Dios Alché *et al.*, 2006). In order to obtain both a good extraction yield and a favorable variety of proteins, in this study, different extraction buffers and methods were tested, and the best one was selected for all the further analysis. In order to optimize the extraction method of olive seed protein, three main buffers were investigated (Table 2).

ID	Extraction Buffer	(mg/mL)
U	UREA 8 M, 1% CHAPS, 0.1% DTT, NH_4HCO_3	9.2
T	0.1 M Tris (pH 7.5), 0.5 M NaCl, 0.5% SDS, 0.1% DTT	1.9
U/T	UREA 6 M, 0.1 M Tris-HCl (pH 8), 0.5 M NaCl, 0.5% SDS, 0.1% DTT	5.3

Table 2. Description of buffers used for protein extraction and yield in mg/mL.

The use of UREA 8 M buffer (U) allowed to obtain an excellent extraction yield of 9.2 mg/mL. Three intense bands were detected in the U lane of the SDS-PAGE at 41 kDa

corresponding to the large precursor of the 11S proteins (Pro2), at 30.5 kDa corresponding to the 11S globulin subunit β-like protein, and at ~18 kDa corresponding to the 11S globulin seed storage protein 2 (Figure 1A) (Liu *et al.*, 2015). Tris-HCl buffer (T) showed the worst performance with a yield of 1.9 mg/mL. As underlined in the SDS-PAGE, the 40 kDa band was missing, and most of the other bands were detected in the 20–18 kDa range, which could be attributed to SSPs from Solea I precursor. Even though U buffer was the best compared to T buffer, it is known that urea can interfere with the activity of different enzymes, such as the proteases, therefore causing a problem during the hydrolysis process (Power *et al.*, 2013). Therefore, the buffer containing both urea at a lower concentration of 6 M and Tris-HCl was selected as the best condition for the extraction process obtaining a yield of 5.3 mg/mL. As can be seen from the SDS-PAGE, in the U/T lane, the most intense bands were obtained in the range from 25 to 30 kDa, which could match the SSPs from the Solea II precursor, and in the range from 20 to 18 kDa (Figure 1A) (De Campos Zani *et al.*, 2018). To further reduce the urea concentration, the extracted proteins were subjected to dialysis against 1 M Tris-HCl (pH 8). Ultrasound pretreatment was also applied for improving extraction yield, but this strategy did not bring any significant advantage, and therefore it was excluded. Indeed, the extraction yield obtained using ultrasound/U buffer was 10.7 mg/mL compared to 9.2 mg/mL obtained using U buffer alone. Comparing the extraction yields obtained using T buffer with and without ultrasound pre-treatment, no significant differences were observed.

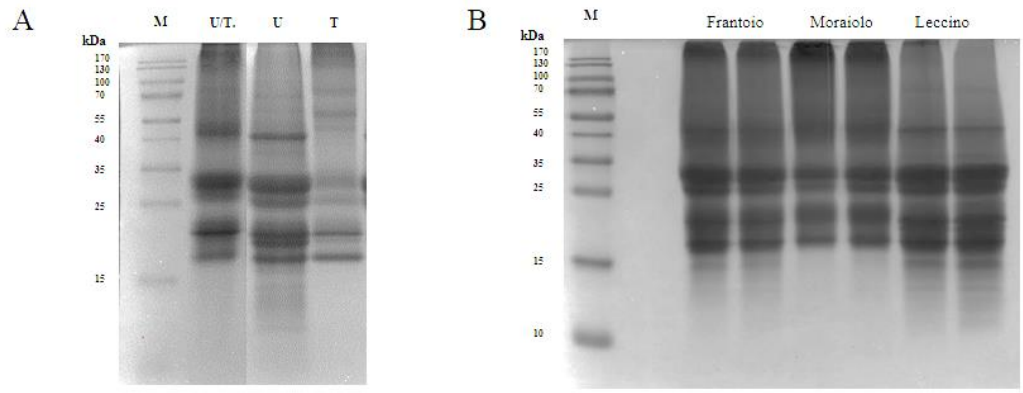

Figure 1. Proteins (50 µg) were loaded in each lane, and protein size markers are indicated in kilodaltons (kDa). (**A**) SDS-PAGE of olive seed proteins extracted with different buffers U/T: UREA 6M, 0.1 M Tris-HCl (pH 8), 0.5 M NaCl, 0.5 % SDS, 0.1 % DTT; U: UREA 8M, 1 % CHAPS, 0.1 % DTT, T: 0.1 M Tris (pH 7.5), 0.5 M NaCl, 0.5 % SDS, 0.1 % DTT. (**B**) SDS-PAGE of different cultivars of olive seed proteins extracted with the final buffer. For each *cultivar* were performed two different extractions.

As we can see in the SDS-PAGE (Figure 1B), where we loaded the proteins that were extracted from the three different cultivars, (*Frantoio*, *Moraiolo,* and *Leccino)* using the U/T buffer, we observed significant bands at 30.5 kDa and at 20–18 kDa. In *Frantoio* and *Moraiolo,* stronger bands at 41 kDa were observed. Below 15 kDa, on the other hand, we observed no bands only in the *Moraiolo* sample.

8.3.2 Structural Properties Characterization: Raman Spectroscopy, Free-Sulfhydryl Group (SH) Content, and Intrinsic Fluorescence (IF)

The secondary structure of *Frantoio, Leccino,* and *Moraiolo* proteins was assessed by Raman spectroscopy (Figure 2A). Raman spectra of all samples revealed similar vibrational peaks. In the amide I region, all samples showed vibrational peak found in β-sheet structures and turns ascribable to the C–O stretching. In the amide II region, a narrow peak is associated with the coupled vibration of the polypeptide backbone, mainly resulting from the coupled C–N stretching and N–H bending. A narrow band at 1000 cm^{-1} is associated with Phe vibration. Moreover, the bands observed at 500 and 750 cm^{-1} are assigned to S–S stretching and Trp vibration, respectively. Further bands at approximately 831 cm^{-1} and 850 cm^{-1} are ascribable to interaction between the ring breathing fundamental and the overtone of the C–C–O deformation in the para-substituted benzene ring of Tyr. Sulfhydryl (SH) groups and disulfide bonds (S-S) have a significant influence on functional properties of proteins, such as foaming and emulsifying abilities (Wu *et al.*, 2021). The evaluation of the content of free-SH groups located on the surface of olive seed protein was used to evaluate if there were differences between the different olive cultivars and to confirm the denatured state of the proteins. Figure 2B shows significant difference in free-SH content between cultivars. In details, the free-SH content was 4.2 ± 0.25% μmol/g, 7.3 ± 0.37% μmol/g, and 5.8 ± 0.37% for *Frantoio, Leccino,* and *Moraiolo* olive seed total protein extract (OTPE), respectively (****, $p < 0.0001$). These findings surely indicate that the protein structure in *Frantoio* presents a reduced exposure of the hydrophobic amino acids containing thiol groups, likely due to the formation of intermolecular disulfide bonds (S-S), whereas the *Leccino* sample shows higher free-thiol group content than the *Moraiolo* and *Frantoio* samples, respectively, indicating that in this sample, hydrophobic amino acids such as cysteine (Cys) and methionine (Met) are exposed on the surface of the protein structure. More information about the 3D protein structure was obtained by applying intrinsic fluorescence spectroscopy, a technique that can be

used to monitor the fluoresce due to the presence of specific amino acids in proteins, i.e., phenylalanine (Phe), tyrosine (Tyr), and tryptophan (Trp). Figure 2C shows two main peaks at 300–310 nm and 360–370 nm, which represent Tyr in a hydrophilic environment, confirming the denatured state of the proteins in agreement with the results obtained from the characterization of the free-thiol groups. All the extracted proteins show comparable IF values.

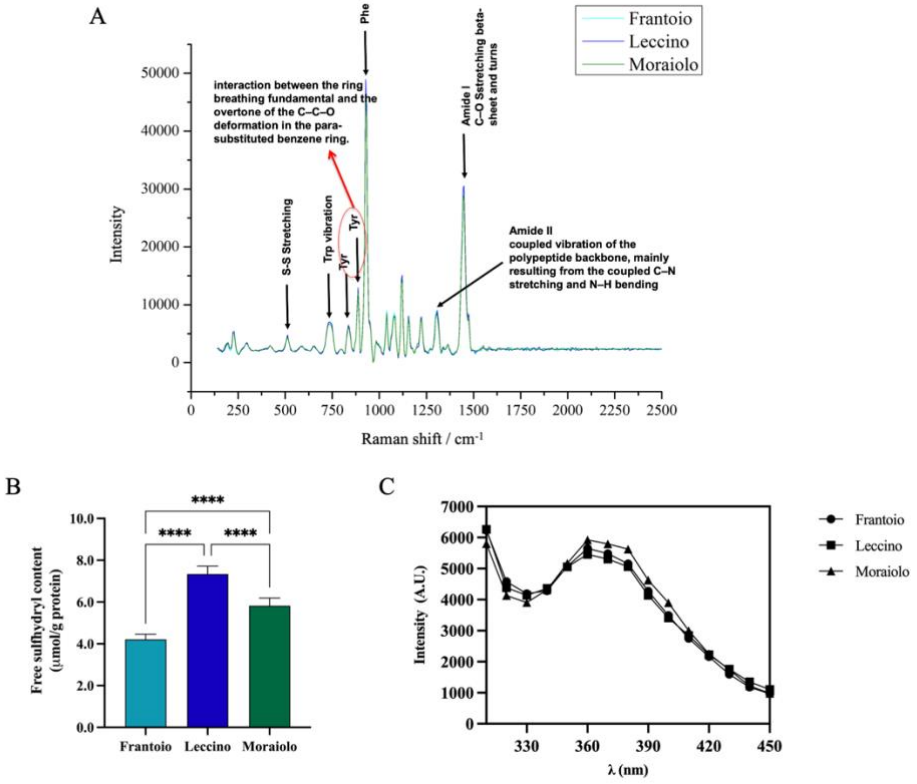

Figure 2. (**A**) Secondary structure analysis by Raman spectroscopy (125–2500 cm^{-1} region). Tertiary structure analysis. (**B**) Free SH group determination. (**C**) Intrinsic fluorescence signal detection. Statistical analysis was performed by one-way ANOVA followed by Tukey's post-hoc test (****) $p<0.0001$. The data are represented as the means ± s.d. of three independent experiments.

8.3.3 Protein Solubility (PS), Water-Binding Capacity (WBC), and Oil-Biding Capacity (OBC) of Extracted Proteins

Solubility is a functional property of food proteins that is commonly measured, and it is influenced by several factors including the pH, which is an essential environmental feature. For all samples, complete insolubility was observed across the pH 2 to 5 range. Protein solubility gradually increased when pH values were raised from 6 to In detail, *Frantoio*, *Leccino*, and *Moraiolo* proteins reached 89.4 ± 1.3%, 95.6 ± 0.4%, and 68.8 ± 0.7% solubility at pH 6 and 62.3% ± 0.4%, 87.9 ± 0.2%, and 68.8 ± 1.0% at pH 12, respectively. Particularly, the highest solubility was achieved at pH 7

for *Frantoio* and *Moraiolo* proteins and at pH 10 for *Leccino* ones. These results are in agreement with protein solubility of proteins isolated from other seeds, showing the best solubility in alkaline pH regions (Wang *et al.*, 2007). Another commonly valued property is the ability of extracted proteins to interact with water, which is dependent on their water-binding property. Many factors can influence WBC, including amino acid composition, protein conformation, surface polarity, and surface hydrophobicity (Haque *et al.*, 2016). In details, *Frantoio* and *Moraiolo* have a similar WBC equal to 2.3 and 2.0 g H_2O/g sample; instead, *Leccino* has a higher WBC of 2.9 g H_2O/g sample, which probably has a higher hydrophilic protein content (**, $p < 0.01$, Figure 3B). OBC corresponds to the amount of oil that a sample can absorb per unit of weight. Hence, *Frantoio* shows a reduced holding capacity compared with *Leccino* and *Moraiolo* (**, $p < 0.01$). In detail, *Leccino* and *Moraiolo* showed the same OBC values equal to 1.6 g oil/g sample and for *Frantoio* 1.4 g oil/g sample (Figure 3C).

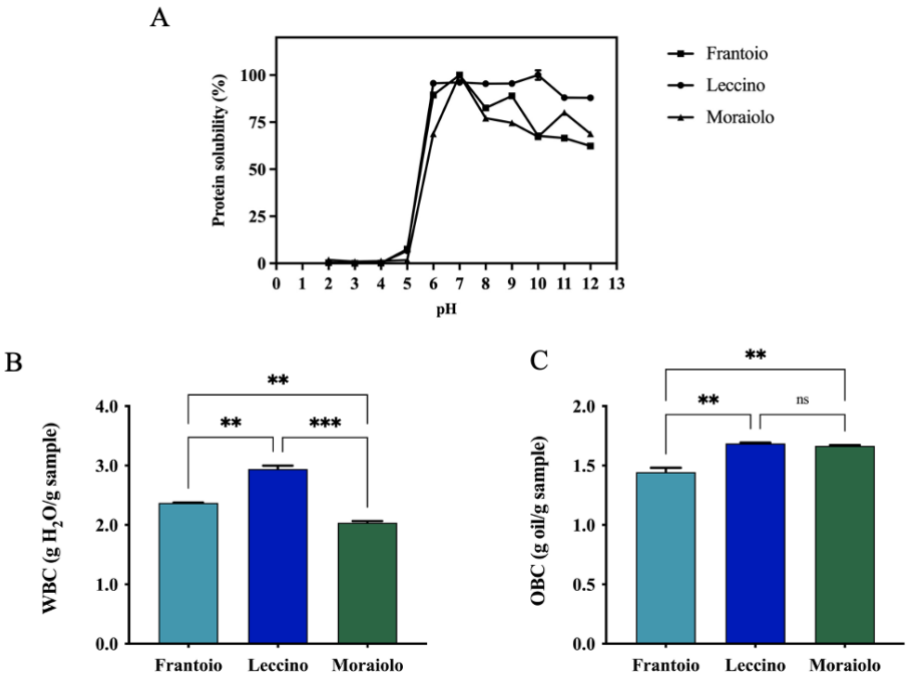

Figure 3. (**A**) Protein solubility. (**B**) Water binding capacity (WBC). (**C**) Oil binding capacity (OBC). Statistical analysis was performed by one-way ANOVA followed by Tukey's post-hoc test. (***) p<0.001, (**) p<0.01, ns: not significant. The data are represented as the means ± s.d. of three independent experiments.

8.3.4 Production of Olive Seed Protein Hydrolysates Using Alcalase and Papain

The use of digestive enzymes is a technique commonly used for the digestion of proteins and the release of peptides by implementing their bio-accessibility. In this study, two food-grade enzymes, namely alcalase and papain, which have different cleavage properties, were used for enzymatic hydrolysis. Alcalase cleaves peptide bonds and involves the Phe, Tyr, Trp, and Lys carboxyl groups, while papain cleaves the peptide bonds of hydrophobic regions, including the amino acids Ala, Val, Leu, Ile, Phe, Trp, and Tyr (Ulloa *et al.*, 2017). The efficiency of the hydrolysis was evaluated comparing the OTPE profiles and the olive seed proteins digested by alcalase and olive seed proteins digested by papain. From the SDS-PAGE (Figure 4A,C), it appears evident that all proteins were completely hydrolyzed during the enzymatic process with both enzymes. For alcalase, we compared for each cultivar an untreated sample (before hydrolysis), a sample at time zero (immediately after the addition of the enzyme), and a sample after 4 h of hydrolysis. In the case of papain, we compared for each cultivar an untreated sample, a sample at 4 h, and a sample at 8 h of hydrolysis, respectively. The DHs using papain was lower than those obtained using alcalase (Table 3). Given the different cleavage properties, both the degree of hydrolysis and the peptides sequences generated are different. However, with the use of papain, the DH is the same for all cultivars, while *Leccino* hydrolyzed with alcalase has a lower DH than *Frantoio* and *Moraiolo*. In fact, we observed stronger signals after 4 h in the SDS-PAGE at the level of 10–15 kDa. As far as papain hydrolysis is concerned, a more intense signal at the level of 10–15 kDa compared to the other samples was observed in the *Moraiolo* sample. Both alcalase (Haque *et al.*, 2016, Ulloa *et al.*, 2017, Kanu *et al.*, 2009) and papain (Haque *et al.*, 2016, Kanu *et al.*, 2009) DH results are in agreement with the result obtained on different matrices.

Cultivar	DH % Alcalase digestion	DH % Papain digestion
Frantoio	26.9 %	12.5 %
Leccino	27.5 %	15.7 %
Moraiolo	15.3 %	14.7 %

Table 3. Description the degree of hydrolysis (DH, %) using Alcalase and Papain enzymes.

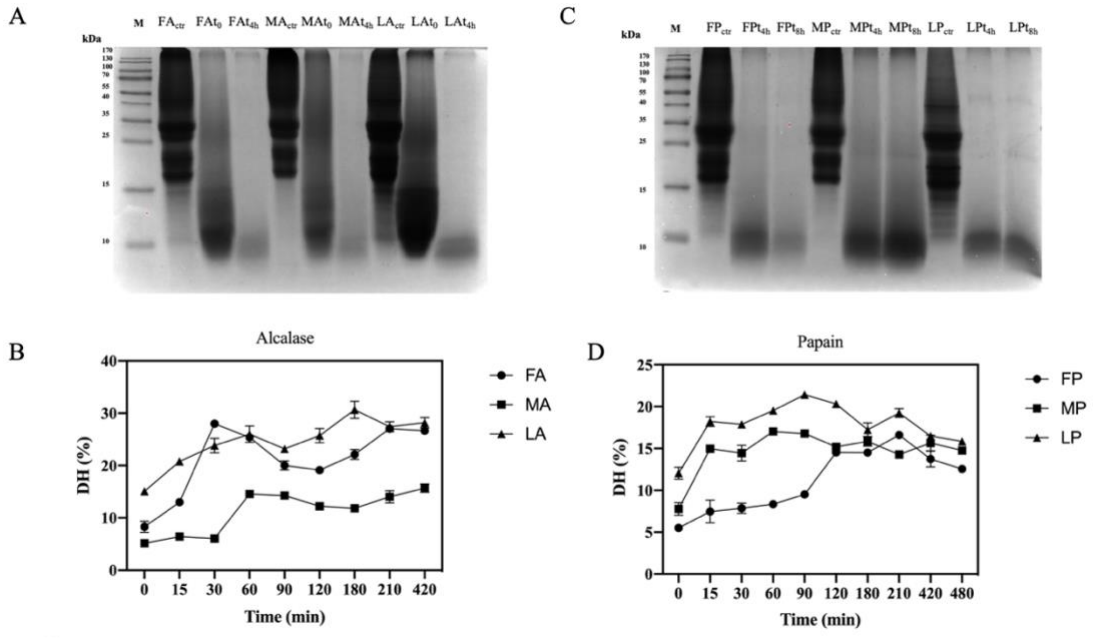

Figure 4. Digestion efficiency of olive seed total protein extract, degree of hydrolysis (DH) trend. (**A**) SDS-PAGE analysis of Alcalase hydrolysates at different hydrolysis time points, FA: *Frantoio* digested by Alcalase, MA: *Moraiolo* digested by Alcalase, LA: *Leccino* digested by Alcalase. (**B**) Alcalase DH at different time points. (**C**) SDS-PAGE analysis of Papain hydrolysates at different hydrolysis time points, FP: *Frantoio* digested by Papain, MP: *Moraiolo* digested by Papain, LP: *Leccino* digested by Papain. (**D**) Papain DH at different time points. The data are represented as the means ± s.d. of three independent experiments, each experiment was performed in triplicate.

8.3.5 Peptidomics Characterization of Olive Seed Hydrolysates: Analysis of Medium- and Short-Sized Peptides

Olive seed hydrolysates were extensively investigated for the comprehensive characterization of both medium- and short-sized peptides. However, given the intrinsic differences between these two classes of peptides (mainly related to the length of the chain), two different strategies were employed. Medium-sized peptides were investigated using the conventional nanoHPLC-HRMS approaches borrowed from bottom-up proteomics. Short peptides, on the other hand, are incompatible with such analytical platform since loss could occur during sample preconcentration, and thus, they cannot be properly identified with the database approaches. Therefore, a dedicated metabolomics-based approach was employed (Cerrato *et al.*, 2020). After peptide validation, 104 and 491 medium- and short-sized peptide were annotated in the olive seed hydrolysates, respectively. Figure 5 shows the percent distribution of the peptides deriving from specific parent proteins. The olive seed hydrolysate contained peptides derived from several proteins, with a small prevalence of protein TIC 214, a protein involved in protein precursor import into chloroplasts (13%) and a phosphopyruvate

hydratase (10%). Other parent proteins include aquaporin PIP26 (8%), polyubiquitin OUB1 (8%), and superoxide dismutase (Cu-Zn) (7%). To broaden the investigation to potential bioactivities, the short peptides were ranked by the tool PeptideRanker (http://bioware.ucd.ie/~compass/biowareweb/Server_pages/peptideranker.php; accessed on 4 May 2022). At the end of this process, only those peptides showing score values higher than 0.6 were considered as potentially bioactive and submitted to BIOPEP search (http://www.uwm.edu.pl/biochemia/index.php/pl/biopep/; accessed on 4 May 2022), an open-access database that allows to hypothesize potential biological activities of peptides based on the presence of some short amino acid sequences (Table 4). The presumed biological activities included the inhibition of DPP-IV and the antioxidant property. Of all the short peptides identified, 77 with potential biological activity were identified. Most of these bioactivities are predominantly provided by short sequences of two or three amino acids included in their structures.

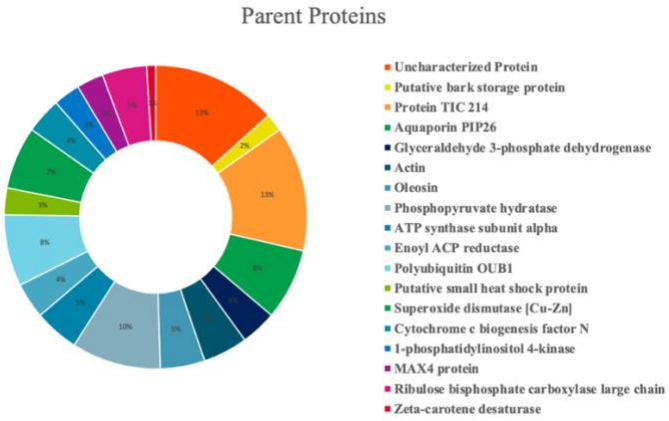

Figure 5. Percent distribution of identified peptides according to their parent proteins.

Score[a]	Sequence	Potential bioactive peptides.[b]	Biological functions [c]
0.998974	FF	FF	DPP IV inhibitor
0.996643	MF	MF	DPP IV inhibitor
0.994712	GF	GF	DPP IV inhibitor,
0.994084	GGFF	GF, GG, FF	DPP IV inhibitor
		GF	DPP III inhibitor
0.993120	FFJ	FF	DPP IV inhibitor
0.991656	WPM	WP, PM	DPP IV inhibitor
0.989681	VY	VY	DPP IV inhibitor, Antioxidant,
0.987345	GGF	GF, GG	DPP IV inhibitor
		GF	DPP III inhibitor
0.985719	FR	FR	DPP IV inhibitor,
0.977983	WJAF	AF	DPP IV inhibitor
0.977525	FGQW	QW	DPP IV inhibitor
0.974885	WY	WY	DPP IV inhibitor, Antioxidant
0.968518	SMF	MF	DPP IV inhibitor

0.962442	FFJA	FF	DPP IV inhibitor
0.954571	FNFJ	NF, FN	DPP IV inhibitor
0.952926	HW	HW	DPP IV inhibitor
0.951176	FN	FN	DPP IV inhibitor
0.948462	FFDR	FF, DR	DPP IV inhibitor
0.947101	WSM	WS	DPP IV inhibitor
0.946135	QF	QF	DPP IV inhibitor
0.941387	AGRF	AG	DPP IV inhibitor
		RF	DPP III inhibitor
0.940972	QGF	GF, QG	DPP IV inhibitor
0.937189	FPAG	PA, FP, AG	DPP IV inhibitor
0.915352	AYF	AY	DPP IV inhibitor
0.913344	DGJF	DG	DPP IV inhibitor, DPP III inhibitor
0.912957	WVAF	AF, VA, WV	DPP IV inhibitor
0.909891	WQ	WQ	DPP IV inhibitor
0.906764	KF	KF	DPP IV inhibitor
0.905338	NGJF	NG	DPP IV inhibitor
0.894996	FJPH	PH	DPP IV inhibitor
0.888582	MPJ	MP	DPP IV inhibitor
0.887708	KGF	GF, KG	DPP IV inhibitor
0.887194	JAF	AF	DPP IV inhibitor
0.881235	AFPA	PA, FP, AF	DPP IV inhibitor
0.879704	AYFG	AY	DPP IV inhibitor, Antioxidant
		YF	DPP IV inhibitor
0.874411	SFY	FR	DPP IV inhibitor
		QR	DPP IV inhibitor
0.873986	WSMH	MH, WS	DPP IV inhibitor
0.867049	SFJ	SF	DPP IV inhibitor
0.867026	FNR	FN NR	DPP IV inhibitor
0.866328	PFGD	FG, GD	DPP IV inhibitor
			DPP III inhibitor
0.865974	GPR	GP	DPP IV inhibitor
0.863356	RFN	FN	DPP IV inhibitor
0.85592	HWJY	HW	DPP IV inhibitor
0.849148	MR	MR	DPP IV inhibitor
0.846587	RPFD	RP	DPP IV inhibitor
		PF	DPP IV inhibitor
0.843478	MY	MY	DPP IV inhibitor, Antioxidant
0.835091	JSF	SF	DPP IV inhibitor
0.833322	AAF	AF, AA	DPP IV inhibitor
0.825853	FQR	FQ	DPP IV inhibitor
0.820516	SAF	AF	DPP IV inhibitor
0.798127	JWQ	WQ	DPP IV inhibitor
0.796676	WJYN	YN	DPP IV inhibitor
0.785013	YMDM	YM	DPP IV inhibitor
0.768611	GJYP	YP	DPP IV inhibitor
0.761687	RFT	TF	DPP IV inhibitor
			DPP III inhibitor
0.759378	JFQ	FQ	DPP IV inhibitor
0.754757	JJSF	SF	DPP IV inhibitor
0.739381	YP	YP	DPP IV inhibitor

0.728473	FYP	YT	DPP IV inhibitor
0.72244	WVEF	VE	DPP IV inhibitor
		WV	DPP IV inhibitor
0.720745	SRSF	SF	DPP IV inhibitor
0.720069	GFE	GF	DPP IV inhibitor, DPP III inhibitor
0.717504	QQF	QF, QQ	DPP IV inhibitor
0.717158	JSAF	AF	DPP IV inhibitor
0.714532	AQFJ	QF	DPP IV inhibitor
0.713582	AAFJ	AF, AA	DPP IV inhibitor
0.693293	MA	MA	DPP IV inhibitor
0.689222	GQGP	GP, QG	DPP IV inhibitor
0.679365	JVF	VF	DPP IV inhibitor
0.659026	KGFA	GF	DPP IV inhibitor
		KG	DPP IV inhibitor
		FA	DPP IV inhibitor
0.65522	SJVF	VF	DPP IV inhibitor
0.642689	GQP	QP	DPP IV inhibitor
0.64074	JPVM	VM	DPP IV inhibitor
		PV	DPP IV inhibitor
0.636164	HFQ	FQ	DPP IV inhibitor
		HF	DPP IV inhibitor
0.623398	MPJQ	MP	DPP IV inhibitor
0.612254	SFJQ	SF	DPP IV inhibitor
0.601894	KFN	KF	DPP IV inhibitor
		FN	DPP IV inhibitor

[a.] According to PeptideRanker database; http://bioware.ucd.ie/~compass/biowareweb/Server_pages/peptideranker.php.
[b-c.] According to BIOPEP-UWM database; https://biochemia.uwm.edu.pl/biopep-uwm/.

Table 4. Potential bioactivities according to PeptideRanker and BIOPEP database search.

8.3.6 Antioxidant Activity of Olive Seed Hydrolysates

8.3.6.1 Direct Radical Scavenging Activity of Olive Seed Hydrolysates by DPPH Assay

The radical scavenging activities of DPPH have regularly been used to evaluate the antioxidant potentials of natural compounds to act as free radical scavengers (Mishra *et al.*, 2012). Figure 6 shows the DPPH radical scavenging activity of olive seed hydrolysates in the range of concentrations 1.0–5.0 mg/mL. FA, LA, and MA scavenged the DPPH radical by 19.5 ± 1.1%, 13.4 ± 4.3%, and 19.5 ± 3.8% at 1.0 mg/mL, respectively; they scavenged the DPPH radical by 39.5 ± 2.1%, 33.2 ± 0.1%, and 39.8 ± 2.4% at 2.5 mg/mL, respectively. For 5 mg/mL, the DPPH radical is reduced by 63.9 ± 0.2%, 58.0 ± 1.4%, and 65.0 ± 0.1% for FA, LA, and MA, respectively. FP,

LP, and MP scavenged the DPPH radical by 20.1 ± 6.5%, 17.4 ± 2.7%, and 20.2 ± 7.1% at 1.0 mg/mL respectively, and they scavenged the DPPH radical by 40.4 ± 2.1%, 35.6 ± 1.2%, and 41.4 ± 3.1% at 2.5 mg/mL, respectively. For 5 mg/mL, the DPPH radical is reduced by 72.5 ± 0.5%, 59.0 ± 0.3%, and 75.7 ± 0.4% for FP, LP, and MP, respectively.

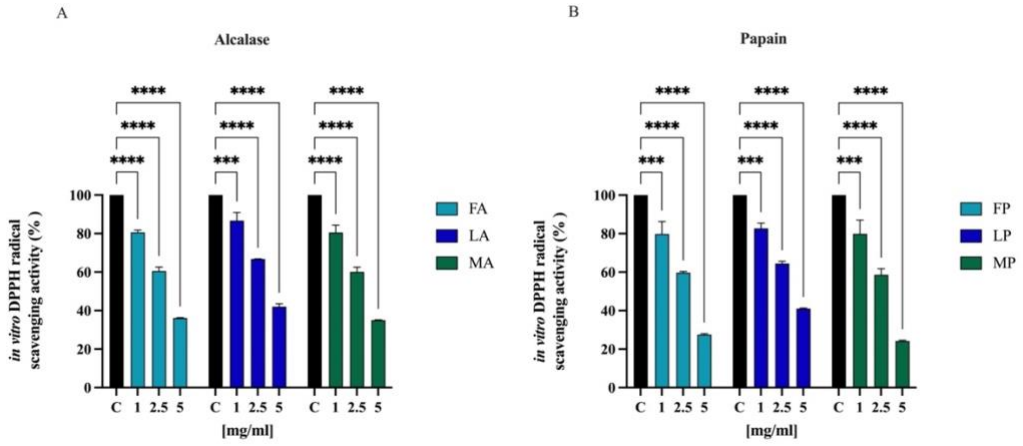

Figure 6. Direct radical scavenging activity of olive seed hydrolysates rom *Frantoio* (F), *Leccino* (L), and *Moraiolo* (M) obtained using Alcalase (A) (**A**) and Papain (P) (**B**) by DPPH assay. Data represent the mean ± s.d. of six independent experiments and each experiment was performed in triplicate. All the data sets have been analyzed by Two-way ANOVA. (****) $p < 0.0001$, (***) $p < 0.001$, (**).

8.3.6.2 Direct Radical Scavenging Activity of Olive Seed Hydrolysates by ABTS Assay

To further confirm the direct antioxidant property, the ABTS free scavenging activity of olive seed hydrolysates was determined at 0.01, 0.05, and 1.0 mg/mL. As indicated in Figure 7, FA, LA, and MA scavenged the ABTS radical by 17.8 ± 1.3%, 14.7 ± 4.3%, and 16.0 ± 0.9% at 0.01 mg/mL, respectively, and they scavenged the ABTS radical by 55.8 ± 0.5%, 55.1 ± 2.6%, and 55.8 ± 1.9% at 0.05 mg/mL, respectively. Finally, FA, LA, and MA scavenged the ABTS radical by 64.3 ± 0.8%, 64.6 ± 0.9%, and 65.3 ± 1.6% at 0.5 mg/mL, respectively. Hydrolysates with papain show a similar trend. FP, LP, and MP scavenged the ABTS radical by 14.5 ± 1.3%, 17.3 ± 1.4%, and 11.9 ± 0.9% at 0.01 mg/mL, respectively; they scavenged the same radical by 53.0 ± 0.5%, 51.7 ± 0.9%, and 54.5 ± 1.8% at 0.05 mg/mL, respectively. Lastly FP, LP, and MP scavenged the ABTS radical by 65.1 ± 1.2%, 64.8 ± 0.5%, and 65.3 ± 0.8% at 1.0 mg/mL, respectively.

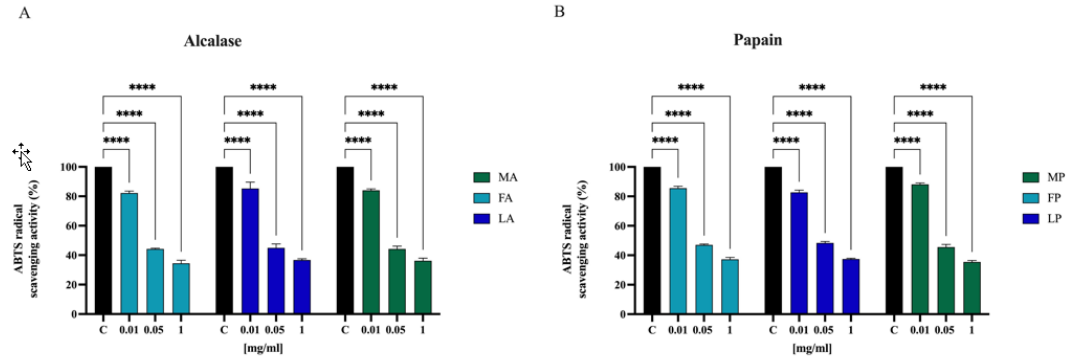

Figure 7. Direct radical scavenging activity of olive seed hydrolysates rom *Frantoio* (F), *Leccino* (L), and *Moraiolo* (M) obtained using Alcalase (A) (**A**) and Papain (P) (**B**) by ABTS assay. Data represent the mean ± s.d. of six independent experiments and each experiment was performed in triplicate. All the data sets have been analyzed by Two-way ANOVA. (****) $p < 0.0001$.

8.3.6.3 Ferric-Reducing Antioxidant Power (FRAP) Activity

Results showed that FA, LA, and MA increased the FRAP by radical by 1850.0 ± 1.8%, 1612.5 ± 62.9%, and 1750.5 ± 2.0% at 0.1 mg/mL, respectively. For 0.5 mg/mL, the FRAP levels are increased by 6387.5 ± 160.0%, 5125.0 ± 104.0%, and 6787.5 ± 118.1% for FA, LA, and MA, respectively. Finally, FA, LA, and MA tested at 1.0 mg/mL improved the FRAP by 13,025.0 ± 429.1%, 9037.5 ± 143.6%, and 13,025.0 ± 241.5%, respectively (Figure 8A). Papain hydrolysates also showed a significant increased the FRAP levels. In Figure 8B, results show that FP, LP, and MP tested at 0.1 mg/mL improved the FRAP by 1750.0 ± 70.7%, 1612.5 ± 25.0%, and 1825.0 ± 50.0%, respectively. For 0.5 mg/mL, the FRAP levels are increased by 6212.5 ± 131.4%, 5375.0 ± 64.5%, and 6787.5 ± 118.1% for FP, LP, and MP, respectively. Finally, FP, LP, and MP tested at 1.0 mg/mL improved the FRAP by 11,712.5 ± 149.3%, 8512.5 ± 495.6%, and 12,462.5 ± 311.9%, respectively.

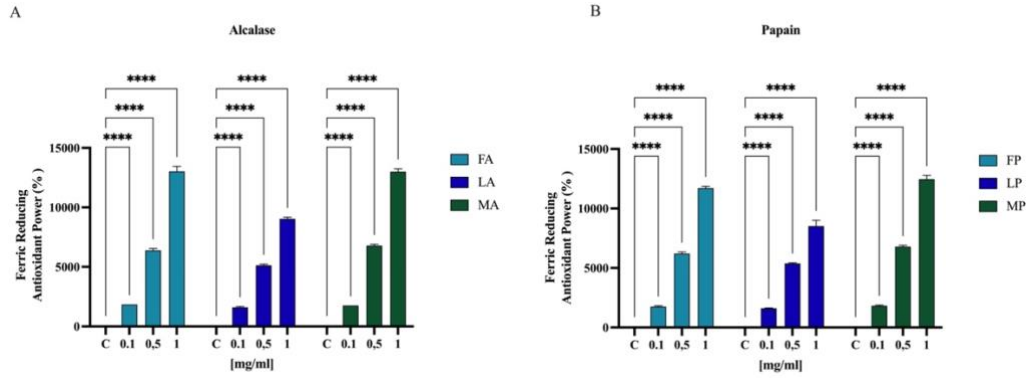

Figure 8. Antioxidant power evaluation by ferric reducing antioxidant power (FRAP) of olive seed hydrolysates from *Frantoio* (F), *Leccino* (L), and *Moraiolo* (M) obtained using Alcalase (A) (**A**) and Papain (P) (**B**). Data represent the mean ± s.d. of six determinations performed in triplicate. All the data sets have been analyzed by Two-way ANOVA. (****) $p < 0.0001$.

8.3.6.4 PH and AH Hydrolysates Decrease the H_2O_2-Induced ROS and Lipid Peroxidation Levels in Intestinal Caco-2 Cells

Considering the comparable ability of each peptide hydrolysate from the three different cultivars obtained with the two enzymes, PH and AH samples were prepared mixing peptides from *Frantoio*, *Leccino*, and *Moraiolo* obtained using papain (PH) and alcalase (AH), respectively. PH and AH were used for evaluating their antioxidant activity on human intestinal Caco-2 cells. To achieve this objective, the fluorometric intracellular ROS assay was performed. Preliminary MTT experiments were carried out for investigating the concentrations of the olive seed hydrolysates obtained using alcalase or papain that may possibly impair the Caco-2 cell viability. After a 48h treatment, no significant cell mortality was detected up to 5 mg/mL versus untreated cells (C) (Figure S1). Figure 9 clearly shows that the H_2O_2 treatment leads to an increase of intracellular ROS levels by 161.0 ± 9.10% versus the control cells, which were mitigated by pre-treatment with PH and AH hydrolysates that restore the ROS up 130.4 ± 4.24% and 128.5 ± 3.60%, respectively, at 0.1 mg/mL (Figure 9A). In addition, the capacity of PH and AH hydrolysates to modulate the H_2O_2-induced lipid peroxidation in human intestinal Caco-2 cells was assessed by the MDA measurement. In accordance with the observed increase ROS after the H_2O_2 treatment, a noticeable increase of the lipid peroxidation was observed up to 143.2 ± 5.44% versus the control cells. Moreover, our results showed that the pretreatment with PH and AH hydrolysates (1 mg/mL) resulted in a reduction in MDA levels up to 109.2 ± 7.95% and 73.0 ± 7.64%, respectively, restoring the lipid peroxidation baseline levels (Figure 9B).

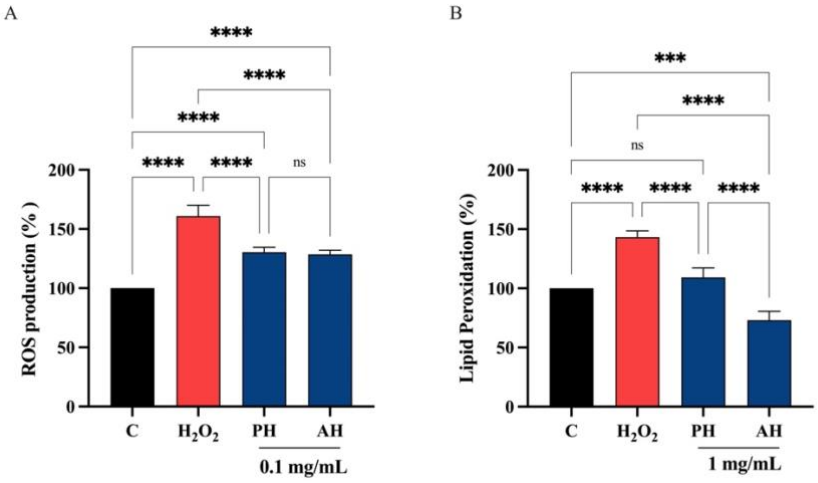

Figure 9. (**A**) Modulation of intracellular H_2O_2-induced ROS levels after the pretreatment with PH and AH hydrolysates. Modulation of H_2O_2-induced lipid peroxidation after the pretreatment with PH and AH hydrolysates (**B**). Data represent the mean ± s.d. of six independent experiments, each experiment was

performed in triplicate. All data sets were analyzed by One-way ANOVA followed by Tukey's post-hoc test. C: control sample; ns: not significant; (***) $p < 0.001$; (****) $p < 0.0001$.

8.3.7 Antidiabetic Activity of Olive Seed Hydrolysates

8.3.7.1 In Vitro and Cellular DPP-IV Inhibitory Activity of Olive Seed Hydrolysates

Biochemical experiments were realized to assess the inhibitory activity of olive seed hydrolysates against human recombinant DPP-IV enzyme. The enzymatic reaction was monitored by measuring the fluorescence signals at 465 nm after excitation at 350 nm due to the release of the free-AMC group after the cleavage of the fluorescent substrate H-Gly-Pro-AMC by DPP-IV. The activity of separate olive seed hydrolysates obtained from the three cultivars using alcalase was screened at the final concentrations of 0.1, 0.5, 1.0, and 1.5 mg/mL. Figure 10A suggests that the FA sample reduced the DPP-IV activity by 9.8 ± 1.8%, 37.8 ± 1.5%, 55.7 ± 3.7%, and 72.1 ± 3.1%. The LA sample lowered the DPP-IV activity by 7.1 ± 1.6%, 38.2 ± 1.3%, 57.9 ± 2.2%, and 75.8 ± 0.8%. Finally, the MA sample decreased the DPP-IV activity by 8.6 ± 1.3%, 37.5 ± 2.4%, 65.7 ± 4.3%, and 76.7 ± 1.9%. Similarly, the activity of separate olive seed hydrolysates obtained from the three cultivars using papain was screened at the final concentrations of 0.1, 0.5, and 1.0 mg/mL. Figure 10B indicates that the FP sample reduced the DPP-IV activity by 12.9 ± 1.0%, 51.0 ± 2.6%, and 75.7 ± 3.7%. The LP sample reduced the DPP-IV activity by 12.4 ± 2.3%, 50.1 ± 2.3%, and 76.6 ± 2.2%. Lastly, the MP sample inhibited the DPP-IV activity by 4.9 ± 2.4%, 45.7 ± 2.1%, and 73.6 ± 1.6%, respectively.

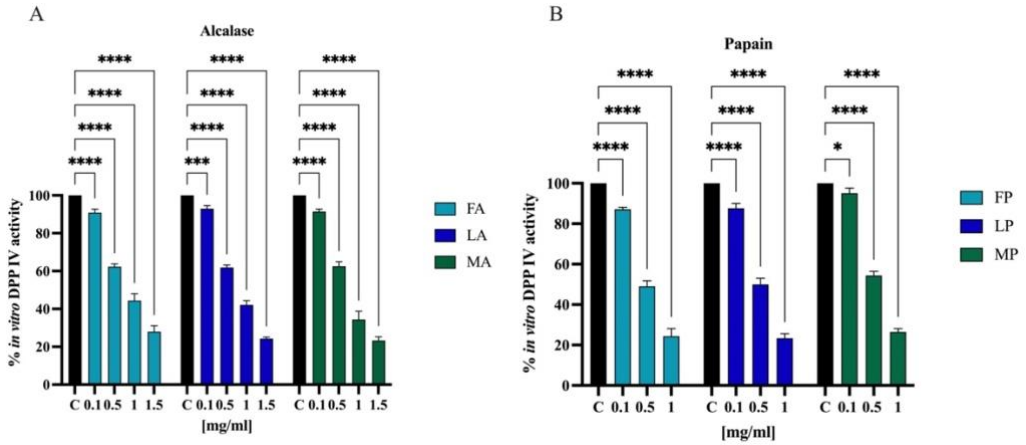

Figure 10. Effect of olive seed hydrolysates obtained from *Frantoio* (F), *Leccino* (L), and *Moraiolo* (M) using Alcalse (A) (**A**) and Papain (P) (**B**) on the *in vitro* DPP-IV activity, respectively. The data points represent the averages ± s.d. of 4 independent experiments and each experiment was performed in triplicate. All data sets were analyzed by 2-way ANOVA followed by Tukey's post-hoc test. ns: not significant; C: control sample (H_2O). (*) $p < 0.5$; (***) $p < 0.001$; (****) $p < 0.0001$.

The most frequently used model of human intestinal enterocytes is the human intestinal Caco-2 cell line. Numerous intestinal enzymes engaged in food digestion are expressed on the surface of Caco-2 cells, including DPP-IV Since both alcalase- and papain-derived hydrolysates have shown to express DPP-IV inhibitory activity *in vitro*, the validated Caco-2 cell-based DPP-IV activity assay was used to test the effects of both each sample on DPP-IV activity at cellular levels. Their activity was screened at the final concentration of 1.5 and 5.0 mg/mL. Figure 11A shows that FA inhibited the cellular DPP-IV activity by 10.7 ± 0.6% and 42.9 ± 6.5%, LA by 11.4 ± 2.8% and 36.2 ± 6.4%, and MA by 13.7 ± 4.5% and 36.4 ± 6.8% at 1.5 and 5.0 mg/mL, respectively. Regarding hydrolysates obtained using papain, FP inhibited cellular DPP-IV activity by 17.5 ± 2.7% and 35.3 ± 4.2%, LP by 16.4 ± 2.0% and 38.7 ± 7.2%, and MA by 17.0 ± 2.0% and 36.5 ± 4.6% at 1.5 and 5.0 mg/mL, respectively (Figure 11B).

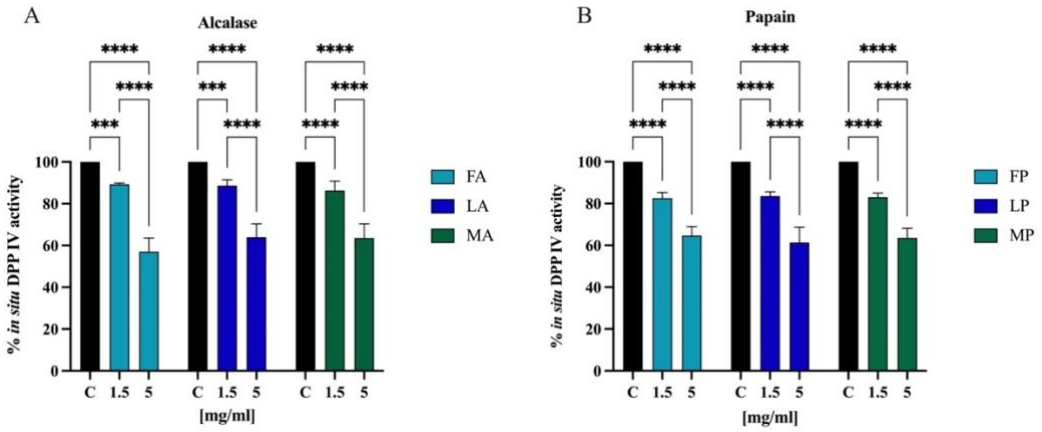

Figure 11. Effect of olive seed hydrolysates obtained from *Frantoio* (F), *Leccino* (L), and *Moraiolo* (M) using Alcalse (A) (**A**) and Papain (P) (**B**) on DPP-IV activity expressed by Caco-2 cells. The data points represent the averages ± s.d. of 4 independent experiments and each experiment was performed in triplicate. All data sets were analyzed by 2-way ANOVA followed by Tukey's post-hoc test. (***) $p < 0.001$; (****) $p < 0.0001$.

Comparing the DPP-IV inhibitory activity of the hydrolysates obtained from different *cultivars* but hydrolyzed with the same enzyme, no statistically significant differences were observed (Figure 12A,B). However, regarding the same *cultivar* but hydrolyzed with different enzymes, alcalase and papain, comparison revealed significative differences (Figure 12C), and in all the cases, the papain hydrolysates showed stronger inhibitory activity than alcalase samples ($p < 0.0001$ for *Frantoio* and *Leccino* and $p < 0.01$ for *Moraiolo*). Thus, PH and AH prepared mixing the peptides from *Frantoio*, *Leccino*, and *Moraiolo* obtained using papain and

alcalase, respectively, were used for deeper evaluation of their *in vitro* anti-diabetic effects.

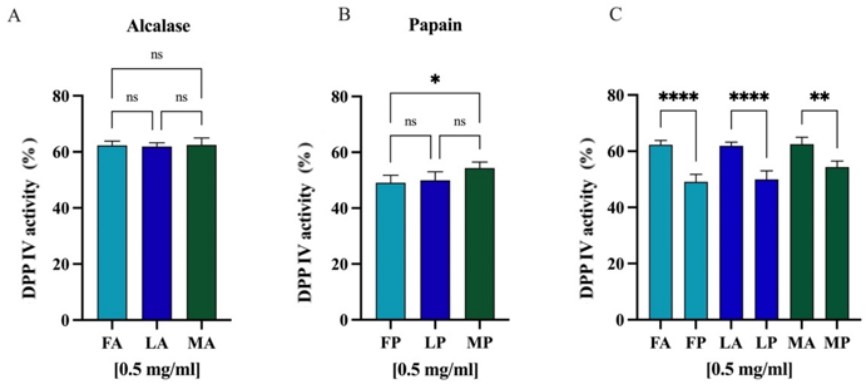

Figure 12. (**A**) Comparison between the *cultivars* hydrolyzed by Alcalase, (**B**) the *cultivars* hydrolyzed by Papain and (**C**) the same cultivars hydrolyzed with different enzymes. ns: not significant; (*) $p < 0.5$; (**) $p < 0.01$; (****) $p < 0.0001$.

8.3.7.2 STC-1/Caco-2 Co-Culture System and Assessment of Olive Seed Hydrolysates Capacity to Modulate Stability and Secretion of GLP-1 Hormone

A co-culture system was developed using Caco-2 enterocytes cells and STC-1 enteroendocrine cells to evaluate whether the treatment with potential DPP-IV inhibitors increased the stability of the GLP-1 hormone and whether they increased GLP-1 secretion (Figure 13A). Given the complexity of the cellular system and considering their similar ability in inhabiting the DPP-IV enzymes in both cell-free and cell-based conditions, we decided to directly test PH and AH samples, respectively. Therefore, both the co-culture and the STC-1 cells were treated with 5 mg/mL of each mixture (the concentration that determined the highest DPP-IV inhibition on Caco-2 cells, as highlighted in Figure 11) or sitagliptin 1 µM for 1 h, and the supernatant was collected to proceed with the GLP-1 detection. Before proceeding with the treatments, the cell viability of the co-culture was verified. After a 48h treatment, no significant impairment of cellular viability was detected versus untreated cells (C) (Figure S2). Figure 13B indicates that PH inhibited the cellular DPP-IV activity by 44.1 ± 5.6% and AH by 48.3 ± 5.2% in the co-culture system, respectively, and 71.6 ± 1.2% for sitagliptin. Moreover, PH inhibited the cellular DPP-IV activity by 38.6 ± 4.3% and AH by 42.4 ± 5.4% in Caco-2 cells alone and 70.3 ± 1.4% for sitagliptin. The treatment with sitagliptin (1 µM) and PH and AH hydrolysates led to an increase of GLP-1 levels versus the control cells (Figure 13C). In detail, after 1 h treatment with PH and AH

hydrolysates, the GLP-1 levels in the co-culture system reached 154.9 ± 9.6 pM and 226.7 ± 0.3 pM, respectively, at 5 mg/mL and 92.26 ± 1.1 pM for sitagliptin (Figure 13C). Statistical analysis clearly revealed that any significant differences were observed in the GLP-1 level modulation between sitagliptin and untreated cells, indicating that the reference compound through the inhibition of DPP-IV improves the GLP-1 stability, but it is unable to modulate its production in the co-culture system. On the contrary, both PH and AH improved the GLP-1 secretion in both cellular systems, suggesting a hypoglycemic activity occurring with a mechanism of action that is different than that of sitagliptin. Indeed, together with inhibition of DPP-IV, PH is more effective than AH in increasing the GLP-1 stability and secretion in the co-culture STC1/Caco-2 system (Figure 13C). This result is also confirmed when STC-1 alone was treated with both PH and AH (Figure 13C). In fact, results clearly show that, similarly, both olive seed hydrolysates increase the GLP-1 secretion by STC-1 cells. In detail, PH and AH hydrolysates lead to an increase of GLP-1 levels up to 660.7 ± 21.9 pM and 613.4 ± 39.1 pM, respectively (Figure 13C).

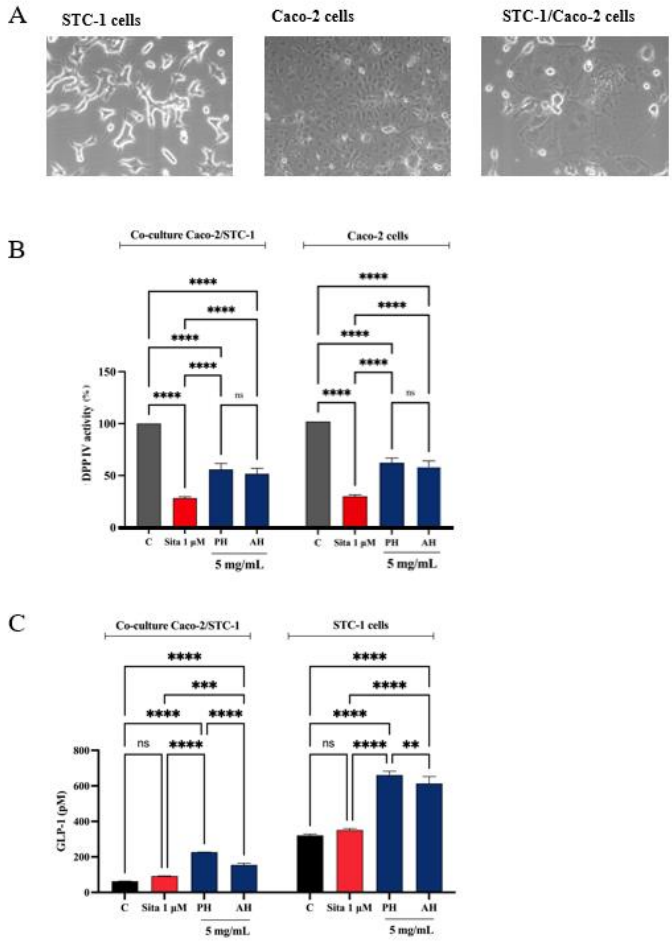

Figure 13. (**A**) Microscope cells images obtained by AxioCam MRc 5 Zeiss after 48h from seeding. (B) Effect of PH and AH on the *in situ* DPP-IV activity in both co-culture Caco-2/STC-1 and Caco-2 alone cells, respectively. **(C)** Effect of PH and AH on the GLP-1 concentration levels (expressed as pM) in both co-culture Caco-2/STC-1 and STC1-alone cells, respectively. Data points represent averages ± s.d. of three independent experiments in duplicate. All data sets were analyzed by two-way ANOVA followed by Tukey's post-hoc test. C: control sample; Sita: Sitagliptin; ns: not significant (**) $p < 0.01$, (***) $p < 0.001$ and (****) $p < 0.0001$ vs. control (C).

8.4 Discussion

Nowadays, food bioactive peptides represent a hot and challenging topic of research, and a great deal of evidence clearly underlines that food side-streams and/or by-products may be considered valuable sources of bioactive peptides with health-promoting properties. In this particular context, this study provides new evidences that olive seed proteins could be recovered and successfully exploited for the production of food bioactive peptides. To take into account the compositional variability, each seed sample was designed and built as a mix of several batches of olive fruits. With this approach, it was possible to study the protein composition of an average sample for each of the three cultivars. Furthermore, according to the time of collection, the sample was also suitable to reflect the composition of the seeds of the olive fruits used for the milling process to produce virgin olive oils. To our knowledge, such a study has never been performed on the seeds of the olive fruit, particularly on the seeds of these typical Tuscan cultivars. Indeed, starting from three different cultivars of olive seed, *Frantoio*, *Moraiolo*, and *Leccino*, proteins have been isolated using optimized conditions and characterized from physico-chemical and functional point of views. Hence, protein hydrolysates have been produced by enzymatic hydrolysis, which has become a widely used biotechnological process to obtain food protein hydrolysates endowed with biological activities (Cruz-Casas *et al.*, 2021). Alcalase and papain, two commercially and well-known food-grade enzymes, have been employed to hydrolysate these proteins. Comparing the DH %, alcalase was about 2-fold more efficient than papain in hydrolyzing the olive seed proteins extracted from *Frantoio* and *Leccino*. The more efficient ability of alcalase than papain to hydrolyze plant-derived proteins is in complete agreement with previous study (Ahmadifard *et al.*, 2016). On the contrary, both enzymes displayed the same ability to hydrolyze the *Moraiolo* proteins, indicating that alcalase was less efficient in digesting these proteins than those extracted from *Frantoio* and *Leccino*. Since the biological activity of a specific protein hydrolysate is strictly associated to its chemical composition, the identification of olive seed peptide sequences was assessed by

applying the most updated analytical techniques. Hence, the characterization of the medium-sized peptide revealed the presence of 104 peptides within the hydrolysates belonging to several parent proteins, i.e., protein TIC 214, a protein involved in protein precursor import into chloroplasts (13%), phosphopyruvate hydratase (10%), aquaporin PIP26 (8%), polyubiquitin OUB1 (8%), and superoxide dismutase (Cu-Zn) (7%). Unlike medium-sized, the short-sized peptides identification is a challenging topic for several reasons (Piovesana *et al.*, 2019). Standard proteomics database search engines cannot efficiently annotate short-sized peptides since their short sequence cannot be confidently associated with single proteins (Kopskinen *et al.*, 2011). Moreover, the short sequences generate mostly singly charged ions, which are non-compatible with proteomics workflows and generate noisier MS/MS spectra. Finally, the fragmentation pathways of short peptide sequences are more strongly affected by the nature of the single amino acid that constitutes the sequences (Cerrato et al., 2020). Nevertheless, applying a high-resolution mass spectrometry-based suspect screening approach, these particular issues were overcome and used to identify, for the first time, the sequence of short peptides within olive seed protein hydrolysates (Table S1). Notably, the olive seed hydrolysates contain 491 different short-sized peptides containing 2–4 amino acid residues. The parallel analysis of medium and short peptide sequences using the BIOPEP database allowed us to identify many sequences containing some known antioxidant and anti-diabetic characteristics (Table 4), respectively.

8.4.1 Olive Seed Hydrolysates Exert Direct and Cellular Antioxidant Activity

To evaluate the radical scavenging activity of olive seed hydrolysates, DPPH, ABTS, and FRAP assays were employed since these tests are widely applied to screen and evaluate the ability of natural compounds to act as free radical scavengers or hydrogen donors. Results clearly indicate that all the olive seed hydrolysates produced using both alcalase and papain exert a direct antioxidant activity being able to scavenge DPPH radicals in the range 1–5 mg/mL (Figure 6) and ABTS radicals in the range 0.01–1 mg/mL (Figure 7). Thus, olive seed hydrolysates are more active as ABTS than DPPH radical scavengers. This result may be explained considering that ABTS assay is based on the generation of a blue/green ABTS·+, which is applicable to both hydrophilic and lipophilic antioxidant systems, whereas DPPH assay uses a radical dissolved in organic media and is, therefore, applicable to hydrophobic systems (Kim *et al.*, 2002). Hence, using ABTS assay, the antioxidant contribution of total hydrophobic and hydrophilic

peptides was measured, whereas using DPPH test, the antioxidant contribution of only hydrophobic peptides was detected. In addition, the same peptide mixtures improve the ability to reduce the Fe(III) at Fe(II) in the range 0.1–1 mg/mL (Figure 8). Many physical-chemical factors may influence the ability of peptides to exert antioxidant activity. In fact, although certain aspects of the structure–function relationship of antioxidant peptides are still poorly understood (Harnedy *et al*., 2017), it has been suggested that chain length, amino acid type, amino acid composition, and amino acid sequence, which is the location of specific amino acids in a peptide chain, may be critical issues for exerting the antioxidant property (Nwachukwu *et al.*, 2018 and 2019, Bollati *et al*., 2022). In this peculiar context, all the tested olive seed hydrolysates are enriched of short peptides, which are often considered potent antioxidants, and they contain hydrophobic amino acids (such as Leu or Val) in their N-terminal regions, nucleophilic sulfur-containing amino acid residues (Cys and Met), or aromatic amino acid residues (Phe, Trp, and Tyr) and/or the imidazole ring-containing His, which are generally found to possess strong antioxidant properties (Nwachukwu *et al.*, 2019). The direct antioxidant ability of olive seed hydrolysates is in agreement with previous investigation in which it has been shown that olive seed hydrolysate obtained using alcalase displayed the highest antioxidant capacity compared to the hydrolysates obtained using neutrase, thermolysin, flaovourzyme, and PTN (Esteve *et al.*, 2015). In addition, olive seed hydrolysates show a similar ability to soybean (obtained using pepsin and trypsin) and hempseed (produced using pepsin) hydrolysates, respectively, to scavenge DPPH radicals (Nwachukwu *et al.*, 2018-2019), whereas they are more active than that of a hempseed protein hydrolysate obtained by co-digesting the proteins with pepsin and pancreatin, which has shown to be a poor scavenger of DPPH, i.e., about 4% (Lammi *et al.*, 2019). Instead, rice bran protein hydrolysates obtained after the hydrolysis of the proteins with alcalase displayed a DPPH radical scavenging activity of about 32% at 20 mg/mL (Girgih et al., 2011). Finally, fish and chicken bone hydrolysates obtained using trypsin showed an antioxidant activity of approximately 15 and 10%, respectively, at 5.0 mg/mL (Wattanasiritham *et al.*, 2015). To validate and confirm the antioxidant activity of olive seed hydrolysates, their effects were assessed at cellular level using human intestinal Caco-2 cells. Considering that *Frantoio*, *Leccino*, and *Moraiolo* protein-derived hydrolysates obtained using alcalase show the same direct antioxidant activity, a mixture of the three hydrolysates (1:1:1) was prepared and named as alcalase hydrolysate (AH) (Figure 6A, Figure 7A

and Figure 8). Similarly, a mixture of the three hydrolysate powders obtained using papain (1:1:1) was prepared and named as papain hydrolysate (PH) (Figure 6B, Figure 7B and Figure 8B). Indeed, our findings underline a dramatic increase of intracellular ROS when Caco-2 cells are treated with H_2O_2 ($p < 0.0001$), but the pre-treatment with AH and PH significantly and equally protected the human intestinal cells, thus restoring the ROS level to basal conditions and confirming their good ability to act as natural antioxidants (Figure 9A). High oxidative stress results in significant damage to human cells by altering proteins, lipids, and DNA, leading to several simultaneous processes that may culminate in pathological conditions involved in the progression of cardiovascular disease. Lipid of cellular membranes are susceptible to oxidative attack, typically by ROS, resulting in a well-defined chain reaction with the production of end products such as malondialdehyde (MDA) and related compounds known as TBA reactive substances (TBARS). Notably, in agreement with the observed increase of ROS after the H_2O_2 treatment, a significant increase of the lipid peroxidation at cellular level was observed ($p < 0.0001$). In addition, the pre-treatment of Caco-2 cells with both AH and PH hydrolysates determine a significant reduction of lipid peroxidation, and statistical analysis revealed that AH is more efficient than PH ($p < 0.0001$), being able to reduce the lipid peroxidation even under basal condition ($p < 0.001$). These results are totally in line with the effect of soybean and hempseed hydrolysates in the modulation of intracellular ROS and lipid peroxidation levels after the H_2O_2 stimulation of human intestinal Caco-2 and human hepatic HepG2 cells, respectively (Nwachukwu *et al.*, 2018, 2019).

8.4.2 Olive Seed Hydrolysates Inhibit DPP-IV Activity and Improve the Stability and Secretion of GLP-1

Protein hydrolysate, which is characterized by a high heterogeneous composition, may possess more than one biological activity, therefore exerting a multifunctional behavior. Indeed, beside their antioxidant property, olive seed hydrolysates inhibit the DPP-IV activity in a cell-free system in which human recombinant enzyme was applied (Figure 10) and in a cell-based assay in which human intestinal Caco-2 cells were employed (Figure 11). Flaxseed, rapeseed, sunflower, sesame, soybean, hempseed, whey, and casein hydrolysates generated using alcalase showed the capacity to reduce the DPP-IV activity using a cell-free *in vitro* system (Centenaro *et al.*, 2015). Specifically, whey hydrolysates showed inhibition by 42%, followed by the rapeseed hydrolysates that

reached a value of 30%, while the other hydrolysates inhibited the DPP-IV activity by around 20% at a concentration of 10 mg/mL. In addition, chickpea and collagen hydrolysates obtained using papain reached *in vitro* DPP-IV inhibition by 45.5% at 0.1 mg/mL and by 55.2% at 1 mg/mL, respectively (Centenaro *et al.*, 2011, Han *et al.*, 2021). In agreement with evidence from the literature, this study confirms that papain-derived hydrolysate is more active than alcalase-derived peptide mixture in decreasing the DPP-IV activity (Figure 12). Our results clearly indicate that olive seed hydrolysates are about 10-fold more active in a cell-free conditions than in cell-based system. This difference may be explained considering that when the peptide mixtures encounter human intestinal Caco-2 cells, they may be further hydrolysated by active peptidase, which are expressed on their cellular membranes (Xu *et al.*, 2022), and/or they are concomitantly up-taken at intracellular levels. Overall, this behavior is in agreement with previous studies on hydrolysates from *Arthrospira platensis* (spirulina) and *Chlorella pyrenoidosa* proteins (Xu *et al.*, 2022, Mentlein *et al.*, 2004). In particular, spirulina hydrolysate obtained with pepsin inhibited DPP-IV activity by 64% in a cell-free system and 34% in Caco-2 cells, while the inhibition of hydrolysates obtained with trypsin reached 72% and 41% in a cell-free system and Caco-2 cells at a dose of 5.0 mg/mL, respectively (Mentlein *et al.*, 2004, Li *et al.*, 2020). Other studies have also shown the capacity of hempseed and soybean protein hydrolysates to inhibit DPP-IV activity. In particular, 1.0 mg/mL of peptic hempseed hydrolysates inhibited the DPP-IV activity by 32% *in vitro* and 22% in Caco-2 cells (Lammi *et al.*, 2019), while DPP-IV activity was inhibited by 2.5 mg/mL of peptic soybean hydrolysates by 31% and 11% *in vitro* and in Caco-2 cells, respectively. The possibility to establish a reasonable structure–function relationship of the DPP-IV inhibitory property of olive seed peptide mixtures is impaired by the fact that the bioactivity of a protein hydrolysate depends strictly on its total composition, including inactive and active species and possible synergistic or antagonist effects. In this peculiar context, olive seed hydrolysates are rich in hydrophobic short-chain peptides sequences containing a Pro residue within their sequences, which is located at the first, second, third, or fourth N-terminal position. Moreover, the Pro residue is flanked by Leu, Val, Phe, Ala, and Gly (Table 4 and Table S1). It is doubtless that in the field of food bioactive peptides, DPP-IV inhibitory activity is among the most studied health-promoting effects. Notwithstanding, the evaluation of GLP-1 stability as a consequence of DPP-IV inhibition is completely underestimated. In order to fill this gap, in this study, a co-

culture system employing Caco-2 enterocytes cells and intestinal STC-1 endocrine cells was developed (Figure 13A). Notably, intestinal Caco-2 cells express DPP-IV enzymes on their surfaces (Lammi *et al.*, 2018), whereas STC-1 cells produce and secrete GLP-1 hormone, which is the physiological DPP-IV substrate (Aiello *et al.*, 2019). Thus, combining both cellular systems, it was possible to dynamically and directly assess the effect of DPP-IV inhibition exerted by olive seed hydrolysates on the GLP-1 stability and production. The experiments were performed using sitagliptin as reference compound. Moreover, in comparing the activity of the same cultivar but hydrolyzed with the two different enzymes (alcalase and papain), significative differences were observed (Figure 12), and in all the cases, the papain hydrolysates showed stronger inhibitory activity compared with the alcalase derived peptide mixtures ($p < 0.0001$ for *Frantoio* and *Leccino* and $p < 0.01$ for *Moraiolo*); the total PH and AH samples were investigated in the co-culture systems. In more detail, findings confirmed that similarly to sitagliptin, both PH and AH reduced the DPP-IV activity in both Caco-2 cells alone and Caco-2/STC-1 cells, respectively (Figure 12B). Hence, in agreement with DPP-IV inhibition in the co-culture Caco-2/STC-1 cells, sitagliptin slightly increases the GLP-1 levels even though this augmentation is not statically significative (Figure 13C). Interestingly, both AH and PH greatly increase the production of GLP-1 in the same co-culture systems, and PH is more effective than AH peptides ($p< 0.0001$, Figure 13C). These results clearly suggest an additional and different mechanism of action of olive seed peptides of sitagliptin through which they may exert the potential anti-diabetic effects. In order to better address this peculiar issue, sitagliptin and both AH and PH were tested on STC-1 alone. As shown in Figure 13C, it is clear that sitagliptin is ineffective on GLP-1 levels, whereas both AH and PH greatly improve the GLP-1 production and secretion, and also in these cells, PH is confirmed more active than AH in the modulation of GLP-1 levels ($p < 0.1$). Taking together these results, it is certainly important to underline that similarly to olive seed hydrolysates, other food bioactive peptides may display anti-diabetic activity with a complementary mechanism of action targeting, therefore not only impacting DPP-IV activity but directly modulating the GLP-1 production.

8.5 Conclusions

Combining biochemical and cellular techniques, our findings demonstrated that the olive seed hydrolysates obtained digesting olive seed proteins with both alcalase (AH)

and papain (PH) show multifunctional activities, as they are able to exert both antioxidant and DPP-IV inhibitory activity and to increase the GLP-1 production. In addition, combining both intestinal Caco-2 and STC-1 cells through the development of the co-culture systems, we have clearly demonstrated how the dynamic DPP-IV inhibition (expressed by Caco-2 cells) by both AH and PH peptides positively reflects on the stability of GLP-1 expressed by STC-1 cells. Surprisingly, we have also demonstrated that both AH and PH peptides enhance the GLP-1 production by STC-1 cells with a mechanism of action that is different from that of sitagliptin. Indeed, this study provides new evidences that besides their exploitation as energy source (biomass) production, olive seed peptides obtained from residual materials of table olive and olive oil production could be recovered and exploited as valuable ingredients for upgrade application, i.e., functional foods and/or dietary supplement developments. In addition, for a large-scale production of these hydrolysates, the hydrolysis process might be performed using immobilized enzymes. This technique that is used in the food, chemical, pharmaceutical, cosmetic, and medical device industries provides many advantages in term of costs, reproducibility, and also sustainability. Another important issue that need to be elucidated further regard the potential use of pectinolytic enzyme mixtures as a pretreatment approach for improving the extraction yields of proteins from olive seeds. In conclusion, this study can be considered the first step through which *in vitro* and cellular screening allow to assess and molecular characterize the mechanism through which olive seed peptides may exert antioxidant and anti-diabetic activity; certainly, other *in vivo* studies on suitable animal models are needed to obtain the "*proof of concept*" regarding the health promoting activity of both hydrolysates. Notably, upon the administration of hydrolysates on an animal model, the ability of peptides to exert antioxidant and anti-diabetic effects targeting DPP-IV and GLP-1 will be evaluated. These results can be useful for the development of nutraceutical and functional foods for preventing diabetic condition and oxidative stress.

8.6 Supporting information

Chemical and samples

All chemicals and reagents were of analytical grade and from commercial sources. Tris(hydroxymethyl)aminomethane (Tris), hydrochloric acid (HCl), Sodium chloride (NaCl), 1,4-dithiothreitol (DTT), hexane, Papain and Alcalase enzyme, sodium dodecyl sulfate (SDS), 3-(4,5-dimethylthiazol-2-yl)-2,5- diphenyltetrazolium bromide (MTT),

ROS and lipid peroxidantion (MDA) assay kits were from Sigma- Aldrich (St. Louis, MO, USA). Bovine serum albumin (BSA), Bradford reagent, and Coomassie Blue G-250 were purchased from Bio-Rad (Hercules, CA, USA). The DPP-IV enzyme and the substrate solution [5 mM H- Gly-Pro conjugated to aminomethylcoumarin (H-Gly-Pro-AMC)] were provided by Cayman Chemicals (Michigan, USA). Dulbecco's modified Eagle medium (DMEM), fetal bovine serum (FBS), L- glutamine, phosphate buffered saline (PBS), penicillin/streptomycin, 24 and 96- well plates were from Euroclone (Milan, Italy).

Protein extraction from olive seed

Olive seed were grounded with a domestic mill. Olive seed powder was defatted with hexane for 1h (ratio 1:20 w/v) under magnetic stirring. After drying, the defatted powder was subjected to protein extraction. In details, 1,5 g of defatted powder were mixed with 30 mL of extracting solution containing UREA 6M, 0.1 M Tris-HCl (pH 8), 0.5 M NaCl, 0.5% SDS, 0.1% DTT. The mixture has been stirred for 2h at 4 °C and centrifuged at 4000g for 20 min at 4 °C. The supernatant was collected and dialyzed against 1 M Tris-HCl (pH 8) and stored at -20 °C until use. The protein concentration was determined by the colorimetric Bradford using BSA as a standard curve. The protein extraction protocol was evaluated by SDS- PAGE (12% polyacrylamide gel), with Tris–glycine buffer (pH 8.3, 0.1% SDS). Staining was performed with Coomassie Blue and destaining with 7% (v/v) acetic acid in water.

Protein Solubility (PS), Water Binding Capacity (WBC) and Oil Binding Capacity (OBC)

Each sample 0,2 g was dispersed into 4 mL of 0.1 M phosphate buffer solutions (at pH 2.0 to 12.0), stirred for 20 min. After the pH adjustment the samples were stirred 30 min at RT and then centrifuged at 14,000 rpm for 30 min. The protein concentration in the samples was determined according to the Bradford assay using BSA as a standard. PS was expressed as percentage ratio of supernatant protein content to the total protein content. All determinations were conducted in triplicate. For WBC, 1 g of sample was dispersed in 10 mL distilled water in a 15 mL pre-weighed centrifuge tube. The dispersions were stirred for 30 min and then centrifuged at 7000 g for 25 min at room temperature (RT). The supernatant was discarded, and the tubes was weighed to

determine the amount of retained water per gram of sample. The OBC, 1 g of sample was dispersed in 10 mL sunflower oil.

Free Sulfhydryl Group Determination

Ellman's reagent (DTNB) is a compound used for quantifying free sulfhydryl groups in solution observing the production of a yellow-colored product when it reacts with sulfhydryl groups. Briefly, the Ellman's reagent was prepared as follows: 4 mg of DTNB reagent was added to 1 mL of Tris-glycine buffer (0.086 M Tris, 0.09 M glycine, 4 mM EDTA, pH 7.0). Each solution was diluted in Tris-glycine buffer (w/v 0.15%). Then, 5 μL of Ellman's reagent was added to 200 μL of protein suspension. The resulting protein suspensions were incubated at RT for 15 min under shaking and then centrifuged at 10,000 g for 10 min at RT. The absorbance was measured at 412 nm.

Intrinsic Fluorescence Spectroscopy

The intrinsic fluorescence spectrum of each sample was obtained using a fluorescence spectrophotometer (Synergy H1, Biotek, Bad Friedrichshall, Germany). The samples were diluted in phosphate-buffered saline (PBS, 10 mM, pH 7.0) in order to reach the equal concentration of 0.05 mg/mL and transferred in Greiner UV- Star® 96 well plates flat bottom clear cyclic olefin copolymer (COC) wells (cycloolefine). The excitation wavelength was set as 280 nm, while the excitation and emission slit widths were each set as 5 nm. The emission wavelength range was set up from 300 to 450 nm, and the scanning speed was 10 nm/s.

Raman Spectroscopy

Raman analysis was conducted using ProgenyTM spectrophotometer (Rigaku Corporation, Japan) with a 1,064 nm laser source, and selectable laser output set at 490 mW. The spectral range is 200–2,500 cm−1 with transmission-type volume phase grating. The spectral resolution is 15–18 cm−1 and the detector is a thermoelectrically cooled indium gallium arsenide (InGaAs). The samples were analyzed with 60 cumulative scans with optimized laser power, aperture size, and duration (7 s) per exposure in order to achieve the best signal to noise ratio. All of the obtained spectra were reported using OriginTM 8 software.

Olive seed protein hydrolysis for releasing bioactive peptides

The enzymatic hydrolysis of olive seed proteins was performed using Alcalase and Papain enzymes using optimal hydrolysis conditions (Table 1). After incubation, all reactions were blocked by heating at 95 °C for 5 min. The supernatants were taken for subsequent determination of the degree of hydrolysis (% DH). For the kinetics study, 40 μL of each hydrolysis solution was pipetted out for blocking the reaction at 0, 15, 30, 60, 90, 120, 150, 180, 210, 240 min incubation time points. Each hydrolysate was passed through ultrafiltration (UF) membranes with a 3 kDa cut-off, using a Millipore UF system (Millipore, Bedford, MA, USA). All recovered peptides were lyophilized and store -80 °C until use. The %DH for each hydrolysate was identified by the o-phthaldialdehyde (OPA) method.

Short peptide purification and analysis by high-performance liquid chromatography-high resolution mass spectrometry

Before analysis, short-sized peptides were purified from longer peptides and other macromolecules using a solid-phase extraction cartridge packed with 500 mg of Carbograph 4. The purified samples were then subject to HPLC-HRMS analysis using a Vanquish binary pump H (Thermo Fisher Scientific) coupled through a heated electrospray (ESI) source to a hybrid quadrupole-Orbitrap mass spectrometer Q Exactive (Thermo Fisher Scientific). The separation of 10 μL of each sample was carried out on a Kinetex XB-C18 (100 × 2.1 mm, 2.6 μm particle size, Phenomenex, Torrance, USA) with chosen flow rate, column temperature, gradient and ESI source parameters as previously reported without any modification. An untargeted suspect screening approach was chosen for the mass spectrometric method, based on the implementation of an inclusion list of m/z derived from all unique masses of short peptides. Data acquisition was performed in the range 150-750 with a resolution of 70,000 (FWHM, m/z 200). HCD fragmentation was performed at 40% normalized collision energy at resolution of 35,000 (FWHM @m/z 200) in top 5 DDA mode. All samples were run in triplicate analysis and raw data files were acquired by Xcalibur software (version 2.2, Thermo Fisher Scientific). Short peptide identification was aided by the Compound Discoverer software (v 3.1, Thermo Fisher Scientific) with a dedicated data processing workflow that was based on the use of a local mass list with IDs, molecular weights, and molecular formulas of all the combination of the 20 natural amino acids in short-sized peptide (the same list was also employed as an inclusion list in the mass spectrometric method). Raw data files of each sample and a blank sample

were simultaneously processed for peak alignment and remotion of all compounds that were present in the blank sample, that were not associated to one of the IDs in the mass list, or that were not associated to an MS/MS spectrum. Manual validation of the short peptide sequences was aided by mMass 5.5, that allows generating in-silico MS/MS spectra.

Profile of Potential Biological Activities and Peptide Ranking

The open access tool PeptideRanker (http://bioware.ucd.ie/~compass/biowareweb/Server_pages/peptideranker.php), a web-based tool used to predict the eventuality of biological activity of peptide sequences, was used to forecast the potential bioactivities of olive seed peptides. Using N-to-1 neural network probability, PeptideRanker provides peptide scores in the range of 0-1. The peptides with a score higher than 0.6 were considered as potentially "bioactive". Subsequently, the lists of best-ranked peptides were submitted to the web-available database BIOPEP (http://www.uwm.edu.pl/biochemia/index.php/pl/biopep/).

Cell Culture

Caco-2 cells, obtained from INSERM (Paris, France) and STC-1, bought from ATCC (HB- 8065, ATCC from LGC Standards, Milan, Italy) were routinely sub-cultured following a previously optimized protocol [9] and maintained at 37°C in a 90% air/10% CO_2 atmosphere in DMEM containing 25 mM of glucose, 3.7 g/L of NaHCO3, 4 mM of stable L-glutamine, 1% non-essential amino acids, 100 U/L of penicillin and 100 μg/L of streptomycin (complete medium), supplemented with 10% heat-inactivated FBS. For the co-culture, the STC- 1 and Caco-2 cells were cultured in a 1:5 ratio for 48h before proceeding with treatments.

3-(4,5-Dimethylthiazol-2-yl)-2,5-Diphenyltetrazolium Bromide (MTT) Assay

A total of 3×10^4 Caco-2 cells/well were seeded in 96-well plates and treated with 0.1, 0.5, 1.5, and 5 mg mL-1 of hydrolysates and/or vehicle (H_2O) in complete growth medium for 48 h at 37 °C under a 5% CO_2 atmosphere, following the procedure previously reported [10]. For the co-culture system a total of 3×10^4 Caco- 2 cells-STC-1 /well cells were seeded in 96-well plates and treated with 0.1, 0.5, and 5 mg mL-1 of hydrolysates and/or vehicle (H_2O) following the same conditions described above.

Antioxidant activity of olive seed hydrolysates

Diphenyl-2-picrylhydrazyl radical (DPPH) assay

The DPPH assay was performed by a standard method with a slight modification. Briefly, 45 μL of 0.0125 mM DPPH solution (dissolved in methanol) was added to 15 μL of the OA and OP hydrolysates at the final concentrations of 1.0, 2.5 and 5.0 mg/mL. The reaction for scavenging the DPPH radicals was performed in the dark at room temperature and the absorbance was measured at 520 nm after 30 min incubation.

2,2′ -Azino-bis(3-ethylbenzothiazoline-6-sulfonic) acid diammonium salt assay

The Trolox equivalent antioxidant capacity (TEAC) assay is based on the reduction of the 2,2-azino-bis-(3- ethylbenzothiazoline-6-sulfonic) acid (ABTS) radical induced by antioxidants. The ABTS radical cation (ABTS+•) was prepared by mixing a 7 mM ABTS solution (Sigma- Aldrich, Milan, Italy) with 2.45 mM potassium persulfate (1:1) and stored for 16 h at room temperature and in dark. To prepare the ABTS reagent, the ABTS+• was diluted in 5 mM phosphate buffer (pH 7.4) to obtain a stable absorbance of 0.700 (±0.02) at 730 nm. For the assay, 10 μL of OA and OP hydrolysates at the final concentrations of 0.01, 0.05 and 1 mg/mL were added to 140 μL of diluted the ABTS+•. The microplate was incubated for 30 min at 30 ◦C and the absorbance was read at 730 nm using a microplate reader Synergy H1 (Biotek). The TEAC values were calculated using a Trolox (Sigma-Aldrich, Milan, Italy) calibration curve (60-320 μM).

FRAP assay

The FRAP assay evaluates the ability of a sample to reduce ferric ion (Fe^{3+}) into ferrous ion (Fe^{2+}). Thus, 10 μL of OA and OP hydrolysates at the final concentrations of 0.01, 0.05 and 1 mg/mL were mixed with 140 μL of FRAP reagent. The FRAP reagent was prepared by mixing 1.3 mL of a 10 mM TPTZ (Sigma-Aldrich, Milan, Italy) solution in 40 mM HCl, 1.3 mL of 20 mM $FeCl_3 \times 6\ H_2O$ and 13 mL of 0.3 M acetate buffer (pH 3.6). The microplate was incubated for 30 min at 37°C and the absorbance was read at 595 nm. Absorbances were recorded on a microplate reader Synergy H1 (Biotek).

Fluorometric intracellular ROS assay

For cells preparation, 3×10^4 Caco-2 cells/well were seeded on a black 96-well plate overnight in growth medium. The day after, the medium was removed, 50 μL/well of Master Reaction Mix was added and the cells were incubated at 5% CO_2, 37 °C for 1 h

in the dark. Then, the PH and AH hydrolysates were added to reach the final concentrations of 0.1 mg/mL and incubated at 37 °C for 24 h. To induce ROS, cells were treated with H_2O_2 at a final concentration of 1.0 mM for 30 min a 37 °C in the dark and fluorescence signals (ex./em. 490/525 nm) were recorded using a microplate reader Synergy H1 (Biotek).

Lipid peroxidation (MDA) assay

Caco-2 cells (2.5×10^5 cells/well) were seeded in a 24 well plate and, the following day, they were treated the PH and AH hydrolysates for 24 h at 37 °C under 5% CO_2 atmosphere. The day after, cells were incubated with H_2O_2 1 mM or vehicle (H_2O) for 1 h, then collected and homogenized in 150 µL ice-cold MDA lysis buffer containing 3 µL of butylated hydroxytoluene (BHT). Samples were centrifuged at 13,000 g for 10 min, then were filtered through a 0.2 µm filter to remove insoluble material. To form the MDA-TBA adduct, 300 µL of the TBA solution were added into each vial containing 100 µL samples and incubated at 95 ◦C for 60 min, then cooled to RT for 10 min in an ice bath. For analysis, 100 µL of each reaction mixture were pipetted into a clear 96 well plate and the absorbance were measured at 532 nm using the microplate reader Synergy H1 (Biotek). To normalize the data, total proteins for each sample were quantified by Bradford method.

Antidiabetic activity of olive seed hydrolysates

***In vitro* measurement of the DPP-IV inhibitory activity**

The experiments were carried out in triplicate in a half volume 96 well solid plate (white) using conditions previously optimized. A total of 50.0 µL of each reaction was prepared in a microcentrifuge tube adding 30.0 µL of 1 × assay buffer [20mM Tris-HCl, pH 8.0, containing 100 mM NaCl, and 1 mM EDTA], 10.0 µL of each sample (at the final concentration of 0.1, 0.5, 1.0, and 1.5 mg/mL), sitagliptin at 1.0 µM (positive control) and 10.0 µL of purified human recombinant DPP-IV enzyme. Next, reagents were transferred in each well of the plate and each reaction was started by adding 50.0 µL of substrate solution (5mM H-Gly-Pro-AMC) and incubated at 37 °C for 30 min. Fluorescence signals were measured using the Synergy H1 fluorescent plate reader from Biotek (excitation/emission wavelength 360/465 nm).

Evaluation of the Inhibitory Effect of olive seed hydrolysates on Cellular DPP-IV Activity

A total of 3 x 10^4 Caco-2 cells/well were seeded in black 96-well plates with clear bottom. The second day after seeding, the spent medium was discarded and cells were treated with 100 µL/well of OA and OP at the concentration of 1.5 and 5 mg/mL or vehicle (C) in growth medium for 3 h at 37°C. Afterwards, treatments were removed and Caco-2 cells were washed once with 100 µL of PBS without Ca^{2+} and Mg^{2+}, before the addition to each well of 100 µL of Gly-Pro-AMC substrate at the concentration of 50.0 µM in PBS without Ca^{2+} and Mg^{2+}. Fluorescence signals deriving from the release of free AMC were measured using a Synergy H1 fluorescence microplate reader from BioTek (excitation/emission wavelength 350/465 nm respectively) every 1 min for up to 10 minutes.

Evaluation of the GLP-1 stability and secretion at cellular level

STC-1 GLP-1 secretion was measured by an active GLP-1 ELISA kit (catalog no. EGLP-35K; Millipore, Watford, UK). In details, a total of 2.4 x 10^4 Caco-2 cells and 6 x 10^3 STC-1 cells/well or 6 x 103 STC-1 cells/well were seeded in 96-well plates. After 48h cells were treated with Sitagliptin (1 µM), PH and AH (5 mg/mL) or vehicle (C) in growth medium for 1h. After the treatment, the supernatant was collected and centrifugated at 500 G, 4°C for 5 min and incubated in 96-well microplates coated with a monoclonal antibody for overnight (20 to 24 hours) at 4°C. After washing the wells, the detection conjugated was added for 2h. The wells were washed, and then the substrate solution was added for 20 min. The reaction was stopped by a stop solution, and then the plate was read to with an excitation/emission wavelength of 355 nm/460 nm with a Synergy H1 microplate reader (Biotek Instruments, Winooski, VT, USA).

Statically Analysis

All measurements were performed in triplicate and results were expressed as the mean ± standard deviation (s.d.), where p-values < 0.05 were considered to be significant. Statistical analyses were performed by ONE and 2way ANOVA followed by Dunnett's and Tukey's post-test (Graphpad Prism 9, GraphPad Software, La Jolla, CA, USA).

Results

Effect of the olive seed protein hydrolysates on cell vitality

MTT experiments were conducted for sorting out those concentrations of the hydrolysates that may potentially determine cytotoxic effects on Caco-2 cells. Notably, no cytotoxic effect was observed up to 5.0 mg/mL, after 48 h treatment. MTT experiments were conducted also on the co-culture system to determine potentially cytotoxic effects. Notably, no cytotoxic effect was observed up to 5.0 mg/mL, after 48h treatment.

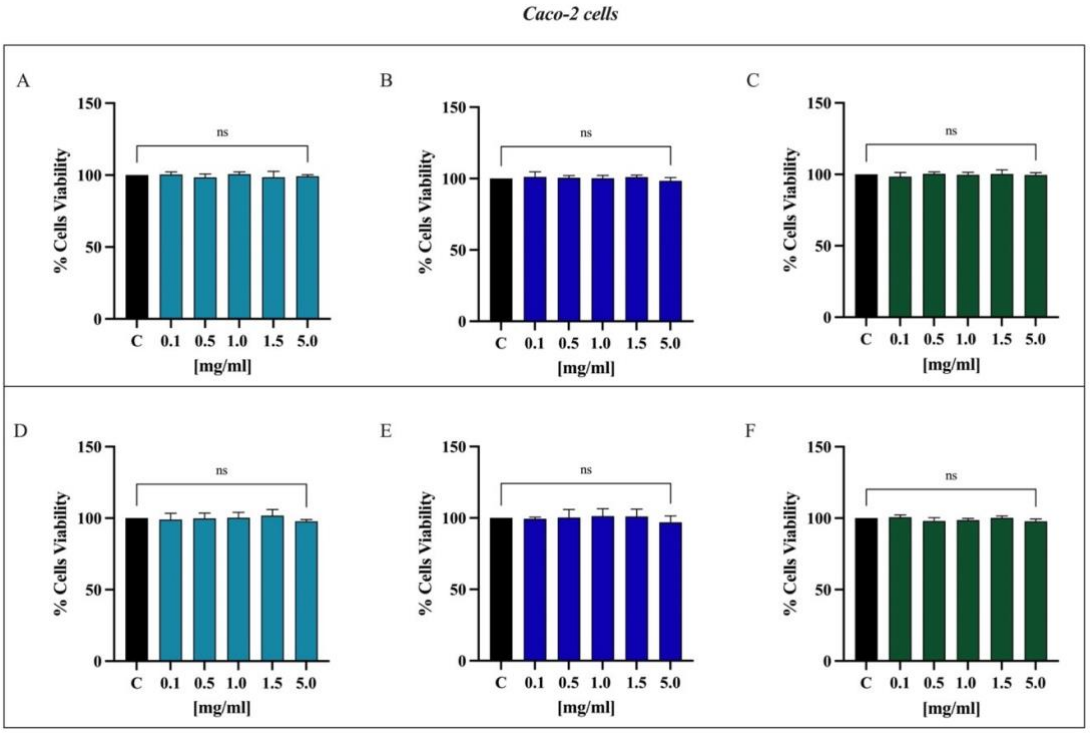

Figure S1. MTT assay - Effect of *Frantoio* (a, d), *Leccino* (b, e) and *Moraiolo* (c, f), samples hydrolyzed with Alcalase (top) and Papain (bottom) on the Caco-2 cells viability. Data represent the mean ± s.d. of three independent experiments performed in triplicate. ns: not significant.

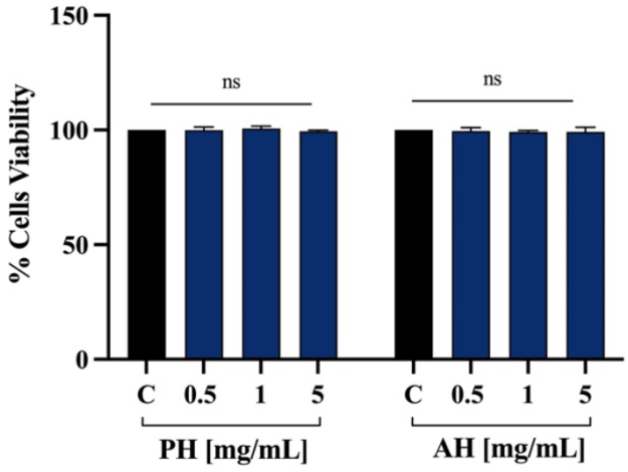

Figure S2. MTT assay. Effect of PH and AH on the co-culture Caco-2/STC-1 cells viability. Data represent the mean ± s.d of three independent experiments performed in triplicate. ns: not significant.

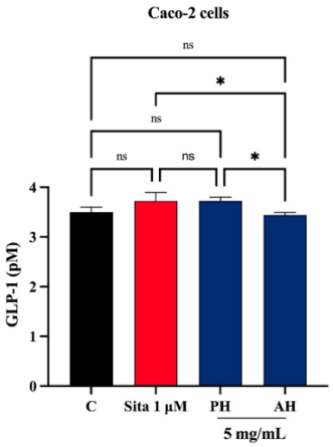

Figure S3. Effect of PH and AH on the GLP-1 concentration levels (expressed as pM) in Caco-2-alone cells. Data points represent averages ± s.d. of three independent experiments in duplicate. All data sets were analyzed by one-way ANOVA followed by Tukey's post-hoc test. C: control sample; Sita: Sitagliptin; ns: not significant (*) $p < 0.005$ vs. control (C).

8.7 References

Aguilar-Toalá, J.E.; Santiago-López, L.; Peres, C.M.; Peres, C.; Garcia, H.S.; Vallejo-Cordoba, B.; González-Córdova, A.F.; Hernández-Mendoza, A. Assessment of Multifunctional Activity of Bioactive Peptides Derived from Fermented Milk by Specific Lactobacillus Plantarum Strains. J. Dairy Sci. 2017, 100, 65–75.

Ahmadifard, N.; Murueta, J.H.C.; Abedian-Kenari, A.; Motamedzadegan, A.; Jamali, H. Comparison the Effect of Three Commercial Enzymes for Enzymatic Hydrolysis of Two Substrates (Rice Bran Protein Concentrate and Soy-Been Protein) with SDS-PAGE. J. Food Sci. Technol. 2016, 53, 1279–1284.

Aiello, G.; Ferruzza, S.; Ranaldi, G.; Sambuy, Y.; Arnoldi, A.; Vistoli, G.; Lammi, C. Behavior of Three Hypocholesterolemic Peptides from Soy Protein in an Intestinal Model Based on Differentiated Caco-2 Cell. J. Funct. Foods 2018, 45, 363–370.

Aiello, G.; Lammi, C.; Boschin, G.; Zanoni, C.; Arnoldi, A. Exploration of Potentially Bioactive Peptides Generated from the Enzymatic Hydrolysis of Hempseed Proteins. J. Agric. Food Chem. 2017, 65, 10174–10184.

Aiello, G.; Li, Y.; Boschin, G.; Bollati, C.; Arnoldi, A.; Lammi, C. Chemical and Biological Characterization of Spirulina Protein Hydrolysates: Focus on ACE and DPP-IV Activities Modulation. J. Funct. Foods 2019, 63, 103592.

Aiello, G.; Pugliese, R.; Rueller, L.; Bollati, C.; Bartolomei, M.; Li, Y.; Robert, J.; Arnoldi, A.; Lammi, C. Assessment of the Physicochemical and Conformational Changes of Ultrasound-Driven Proteins Extracted from Soybean Okara Byproduct. Foods 2021, 10, 562.

Barnett, A. DPP-4 Inhibitors and Their Potential Role in the Management of Type 2 Diabetes. Int. J. Clin. Pract.2006, 60, 1454–1470.

Bertelli, M.; Kiani, A.K.; Paolacci, S.; Manara, E.; Kurti, D.; Dhuli, K.; Bushati, V.; Miertus, J.; Pangallo, D.; Baglivo, M.; et al. Hydroxytyrosol: A Natural Compound with Promising Pharmacological Activities. J. Biotechnol. 2020, 309, 29–33.

Bollati, C.; Cruz-Chamorro, I.; Aiello, G.; Li, J.; Bartolomei, M.; Santos-Sánchez, G.; Ranaldi, G.; Ferruzza, S.; Sambuy, Y.; Arnoldi, A.; et al. Investigation of the Intestinal Trans-Epithelial Transport and Antioxidant Activity of Two Hempseed Peptides WVSPLAGRT (H2) and IGFLIIWV (H3). Food Res. Int. 2022, 152, 110720.

Cabizza, R.; Fancello, F.; Petretto, G.L.; Addis, R.; Pisanu, S.; Pagnozzi, D.; Piga, A.; Urgeghe, P.P. Exploring the DPP-IV Inhibitory, Antioxidant and Antibacterial Potential of Ovine “Scotta” Hydrolysates. Foods 2021, 10, 3137.

Centenaro, G.S.; Mellado, M.S.; Prentice-Hernández, C. Antioxidant Activity of Protein Hydrolysates of Fish and Chicken Bones. Adv. J. Food Sci. Technol. 2011, 3, 282–288.

Ceriello, A.; Testa, R.; Genovese, S. Clinical Implications of Oxidative Stress and Potential Role of Natural Antioxidants in Diabetic Vascular Complications. Nutr. Metab. Cardiovasc. Dis. 2016, 26, 285–292.

Cerrato, A.; Aita, S.E.; Capriotti, A.L.; Cavaliere, C.; Montone, C.M.; Laganà, A.; Piovesana, S. A New Opening for the Tricky Untargeted Investigation of Natural and Modified Short Peptides. Talanta 2020, 219, 121262.

Choksawangkarn, W.; Phiphattananukoon, S.; Jaresitthikunchai, J.; Roytrakul, S. Antioxidative Peptides from Fish Sauce By-Product: Isolation and Characterization. Agric. Nat. Resour. 2018, 52, 460–466.

Cruz-Casas, D.E.; Aguilar, C.N.; Ascacio-Valdés, J.A.; Rodríguez-Herrera, R.; Chávez-González, M.L.; Flores-Gallegos, A.C. Enzymatic Hydrolysis and Microbial Fermentation: The Most Favorable Biotechnological Methods for the Release of Bioactive Peptides. Food Chem. Mol. Sci. 2021, 3, 1000047.

De Campos Zani, S.C.; Wu, J.; Chan, C.B. Egg and Soy-Derived Peptides and Hydrolysates: A Review of Their Physiological Actions against Diabetes and Obesity. Nutrients 2018, 10, 549.

De Dios Alché, J.; Jiménez-López, J.C.; Wang, W.; Castro-López, A.J.; Rodríguez-García, M.I. Biochemical Characterization and Cellular Localization of 11S Type Storage Proteins in Olive (Olea Europaea L.) Seeds. J. Agric. Food Chem. 2006, 54, 5562–5570.

Dicker, D. DPP-4 Inhibitors: Impact on Glycemic Control and Cardiovascular Risk Factors. Diabetes Care 2011, 34, S276–S278.

Eckert, E.; Zambrowicz, A.; Pokora, M.; Setner, B.; Dabrowska, A.; Szołtysik, M.; Szewczuk, Z.; Polanowski, A.; Trziszka, T.; Chrzanowska, J. Egg-Yolk Protein by-Product as a Source of ACE-Inhibitory Peptides Obtained with Using Unconventional Proteinase from Asian Pumpkin (Cucurbita Ficifolia). J. Proteom. 2014, 110, 107–116.

Esteve, C.; Marina, M.L.; García, M.C. Novel Strategy for the Revalorization of Olive (Olea Europaea) Residues Based on the Extraction of Bioactive Peptides. Food Chem. 2015, 167, 272–280.

Ferri, M.; Graen-Heedfeld, J.; Bretz, K.; Guillon, F.; Michelini, E.; Calabretta, M.M.; Lamborghini, M.; Gruarin, N.; Roda, A.; Kraft, A.; et al. Peptide Fractions Obtained from Rice By-Products by Means of an Environment-Friendly Process Show in Vitro Health-Related Bioactivities. PLoS ONE 2017, 12, 1–14.

Girgih, A.T.; Udenigwe, C.C.; Aluko, R.E. In Vitro Antioxidant Properties of Hemp Seed (Cannabis Sativa L.) Protein Hydrolysate Fractions. JAOCS, J. Am. Oil Chem. Soc. 2011, 88, 381–389.

Han, R.; Hernández Álvarez, A.J.; Maycock, J.; Murray, B.S.; Boesch, C. Comparison of Alcalase- and Pepsin-Treated Oilseed Protein Hydrolysates—Experimental Validation of Predicted Antioxidant, Antihypertensive and Antidiabetic Properties. Curr. Res. Food Sci. 2021, 4, 141–149.

Haque, M.A.; Timilsena, Y.P.; Adhikari, B. Food Proteins, Structure, and Function. In Reference Module in Food Science; Elsevier: Amsterdam, The Netherlands, 2016.

Harding, J.L.; Pavkov, M.E.; Magliano, D.J.; Shaw, J.E.; Gregg, E.W. Global Trends in Diabetes Complications: A Review of Current Evidence. Diabetologia 2019, 62, 3–16.

Harnedy, P.A.; O'Keeffe, M.B.; FitzGerald, R.J. Fractionation and Identification of Antioxidant Peptides from an Enzymatically Hydrolysed Palmaria Palmata Protein Isolate. Food Res. Int. 2017, 100, 416–422.

Ibáñez, E.; Palacios, J.; Señoráns, F.J.; Santa-María, G.; Tabera, J.; Reglero, G. Isolation and Separation of Tocopherols from Olive By-Products with Supercritical Fluids. JAOCS J. Am. Oil Chem. Soc. 2000, 77, 187–190.

Ishibashi, Y.; Matsui, T.; Maeda, S.; Higashimoto, Y.; Yamagishi, S. ichi Advanced Glycation End Products Evoke Endothelial Cell Damage by Stimulating Soluble Dipeptidyl Peptidase-4 Production and Its Interaction with Mannose 6-Phosphate/Insulin-like Growth Factor II Receptor. Cardiovasc. Diabetol. 2013, 12, 125.

Jin, R.; Teng, X.; Shang, J.; Wang, D.; Liu, N. Identification of Novel DPP–IV Inhibitory Peptides from Atlantic Salmon (Salmo Salar) Skin. Food Res. Int. 2020, 133, 109161.

Kanu, P.J.; Kanu, J.B.; Sandy, E.H.; Kandeh, J.B.A.; Mornya, P.M.P.; Huiming, Z. Optimization of Enzymatic Hydrolysis of Defatted Sesame Flour by Different Proteases and Their Effect on the Functional Properties of the Resulting Protein Hydrolysate. Am. J. Food Technol. 2009, 4, 226–240

Kim, D.O.; Lee, K.W.; Lee, H.J.; Lee, C.Y. Vitamin C Equivalent Antioxidant Capacity (VCEAC) of Phenolic Phytochemicals. J. Agric. Food Chem. 2002, 50, 3713–3717.

Koskinen, V.R.; Emery, P.A.; Creasy, D.M.; Cottrell, J.S. Hierarchical Clustering of Shotgun Proteomics Data. Mol. Cell. Proteomics 2011, 10, 1–12.

Lammi, C.; Bollati, C.; Arnoldi, A. Antioxidant Activity of Soybean Peptides on Human Hepatic HepG2 Cells. J. Food Bioact. 2019.

Lammi, C.; Bollati, C.; Ferruzza, S.; Ranaldi, G.; Sambuy, Y.; Arnoldi, A. Soybean-and Lupin-Derived Peptides Inhibit DPP-IV Activity on in Situ Human Intestinal Caco-2 Cells and Ex Vivo Human Serum. Nutrients 2018, 10, 1082.

Lammi, C.; Bollati, C.; Gelain, F.; Arnoldi, A.; Pugliese, R. Enhancement of the Stability and Anti-DPPIV Activity of Hempseed Hydrolysates through Self-Assembling Peptide-Based Hydrogels. Front. Chem. 2019, 6, 670.

Lammi, C.; Zanoni, C.; Arnoldi, A.; Vistoli, G. Peptides Derived from Soy and Lupin Protein as Dipeptidyl-Peptidase IV Inhibitors: In Vitro Biochemical Screening and in Silico Molecular Modeling Study. J. Agric. Food Chem. 2016, 64, 9601–9606.

Lammi, C.; Zanoni, C.; Scigliuolo, G.M.; D'Amato, A.; Arnoldi, A. Lupin Peptides Lower Low-Density Lipoprotein (LDL) Cholesterol through an up-Regulation of the LDL Receptor/Sterol Regulatory Element Binding Protein 2 (SREBP2) Pathway at HepG2 Cell Line. J. Agric. Food Chem. 2014, 62, 7151–7159.

Li, Y.; Aiello, G.; Bollati, C.; Bartolomei, M.; Arnoldi, A.; Lammi, C. Phycobiliproteins from Arthrospira Platensis (Spirulina): A New Source of Peptides with Dipeptidyl Peptidase-IV Inhibitory Activity. Nutrients 2020, 13, 1624.

Lima, R.D.C.L.; Berg, R.S.; Rønning, S.B.; Afseth, N.K.; Knutsen, S.H.; Staerk, D.; Wubshet, S.G. Peptides from Chicken Processing By-Product Inhibit DPP-IV and Promote Cellular Glucose Uptake: Potential Ingredients for T2D Management. Food Funct. 2019, 10, 1619–1628.

Liu, J.; Jin, Y.; Lin, S.; Jones, G.S.; Chen, F. Purification and Identification of Novel Antioxidant Peptides from Egg White Protein and Their Antioxidant Activities. Food Chem. 2015, 175, 258–266.

Maddux, B.A.; See, W.; Lawrence, J.C.; Goldfine, A.L.; Goldfine, I.D.; Evans, J.L. Protection against Oxidative Stress-Induced Insulin Resistance in Rat L6 Muscle Cells by Micromolar Concentrations of α-Lipoic Acid. Diabetes 2001, 50, 404–410.

Malomo, S.A.; He, R.; Aluko, R.E. Structural and Functional Properties of Hemp Seed Protein Products. J. Food Sci. 2014, 79, 1512–1521.

Mentlein, R. Cell-Surface Peptidases. Int. Rev. Cytol. 2004, 235, 165–213.

Mishra, K.; Ojha, H.; Chaudhury, N.K. Estimation of Antiradical Properties of Antioxidants Using DPPH- Assay: A Critical Review and Results. Food Chem. 2012, 130, 1036–1043.

Nwachukwu, I.D.; Aluko, R.E. Antioxidant Properties of Flaxseed Protein Hydrolysates: Influence of Hydrolytic Enzyme Concentration and Peptide Size. JAOCS, J. Am. Oil Chem. Soc. 2018, 95, 1105–1118.

Nwachukwu, I.D.; Aluko, R.E. Structural and Functional Properties of Food Protein-derived Antioxidant Peptides. J. Food Biochem. 2019, 43, e12761.

Pedroza, M.A.; Amendola, D.; Maggi, L.; Zalacain, A.; De Faveri, D.M.; Spigno, G. Microwave-Assisted Extraction of Phenolic Compounds from Dried Waste Grape Skins. Int. J. Food Eng. 2015, 11, 359–370.

Piovesana, R.; Faroni, A.; Magnaghi, V.; Reid, A.J.; Tata, A.M. M2 Receptors Activation Modulates Cell Growth, Migration and Differentiation of Rat Schwann-like Adipose-Derived Stem Cells. Cell Death Discov. 2019, 5, 92.

Piovesana, S.; Montone, C.M.; Cavaliere, C.; Crescenzi, C.; La Barbera, G.; Laganà, A.; Capriotti, A.L. Sensitive Untargeted Identification of Short Hydrophilic Peptides by High Performance Liquid

Chromatography on Porous Graphitic Carbon Coupled to High Resolution Mass Spectrometry. J. Chromatogr. A 2019, 1590, 73–79.

Power, O.; Jakeman, P.; Fitzgerald, R.J. Antioxidative Peptides: Enzymatic Production, in Vitro and in Vivo Antioxidant Activity and Potential Applications of Milk-Derived Antioxidative Peptides. Amino Acids 2013, 44, 797–820.

Rivero-Pino, F.; Espejo-Carpio, F.J.; Guadix, E.M. Production and Identification of Dipeptidyl Peptidase IV (DPP-IV) Inhibitory Peptides from Discarded Sardine Pilchardus Protein. Food Chem. 2020, 328, 127096.

Rudich, A.; Tlrosh, A.; Potashnik, R.; Hemi, R.; Kanety, H.; Bashan, N. Prolonged Oxidative Stress Impairs Insulin-Induced GLUT4 Translocation in 3T3-L1 Adipocytes. Diabetes 1998, 47, 1562–1569.

Saidi, S.; Saoudi, M.; Ben Amar, R. Valorisation of Tuna Processing Waste Biomass: Isolation, Purification and Characterisation of Four Novel Antioxidant Peptides from Tuna by-Product Hydrolysate. Environ. Sci. Pollut. Res. 2018, 25, 17383–17392.

Shewry, P.R.; Napier, J.A.; Tatham, A.S. Seed Storage Proteins: Structures and Biosynthesis. Plant Cell 1995, 7, 945–956.

Socas-Rodríguez, B.; Álvarez-Rivera, G.; Valdés, A.; Ibáñez, E.; Cifuentes, A. Food By-Products and Food Wastes: Are They Safe Enough for Their Valorization? Trends Food Sci. Technol. 2021, 114, 133–147.

Stathopoulos, P.; Koutra, C.; Bata, E.; Skaltsounis, A.-L. Optimization of Oleuropein Extraction from Olive Leaves. Alternative Approaches for the Recovery of Olive Bioactive Secoiridoids. Planta Med. 2021, 87, PC4–PC35.

Suda, C.N.K.; Giorgini, J.F. Seed Reserve Composition and Mobilization during Germination and Initial Seedling Development of Euphorbia Heterophylla. Rev. Bras. Fisiol. Veg. 2000, 12, 226–244.

Ulloa, J.A.; Villalobos Barbosa, M.C.; Resendiz Vazquez, J.A.; Rosas Ulloa, P.; Ramírez Ramírez, J.C.; Silva Carrillo, Y.; González Torres, L. Producción y Caracterización Fisico-Química y Functional de Un Aislado Proteínico de Semillas de Jaca (Artocarpus Heterophyllus). CYTA - J. Food 2017, 15, 497–507

Vilaplana-Pérez, C.; Auñón, D.; García-Flores, L.A.; Gil-Izquierdo, A. Hydroxytyrosol and Potential Uses in Cardiovascular Diseases, Cancer, and AIDS. Front. Nutr. 2014, 1, 18.

Wang, B.; Qu, J.; Luo, S.; Feng, S.; Li, T.; Yuan, M.; Huang, Y.; Liao, J.; Yang, R.; Ding, C. Optimization of Ultrasound-Assisted Extraction of Flavonoids from Olive (Olea Europaea) Leaves, and Evaluation of Their Antioxidant and Anticancer Activities. Molecules 2018, 23, 2513.

Wang, W.; De Dios Alché, J.; Rodríguez-García, M.I. Characterization of Olive Seed Storage Proteins. Acta Physiol. Plant. 2007, 29, 439–444.

Wattanasiritham, L.; Kubglomsong, S.; Theerakulkait, C. Antioxidant Activity of Rice Bran Protein Extract, Its Enzymatic Hydrolysates and Its Combination with Commercial Antioxidants. Pakistan J. Nutr. 2015, 14, 647–652.

Wu, M.; Li, Z.; Wei, R.; Luan, Y.; Hu, J.; Wang, Q.; Liu, R.; Ge, Q.; Yu, H. Role of Disulfide Bonds and Sulfhydryl Blocked by N-Ethylmaleimide on the Properties of Different Protein-Stabilized Emulsions. Foods 2021, 10, 3079.

Xu, Q.; Zheng, L.; Huang, M.; Zhao, M. Exploring Structural Features of Potent Dipeptidyl Peptidase IV (DPP-IV) Inhibitory Peptides Derived from Tilapia (Oreochromis Niloticus) Skin Gelatin by an Integrated Approach of Multivariate Analysis and Gly-Pro-Based Peptide Library. Food Chem. 2022, 397, 133821.

Zambrowicz, A.; Eckert, E.; Pokora, M.; Bobak, Ł.; Da˛browska, A.; Szołtysik, M.; Trziszka, T.; Chrzanowska, J. Antioxidant and Antidiabetic Activities of Peptides Isolated from a Hydrolysate of an Egg-Yolk Protein by-Product Prepared with a Proteinase from Asian Pumpkin (Cucurbita Ficifolia). RSC Adv. 2015, 5, 10460–10467.

Zamora-sillero, J.; Gharsallaoui, A.; Prentice, C.; Prentice, C. Peptides From Fish By-Product Protein Hydrolysates and Its Functional Properties: An Overview. Mar. Biotechnol. 2018, 20, 118–130.

MANUSCRIPT 6

OLIVE (Olea europaea L.) SEED AS NEW SOURCE OF CHOLESTEROL-LOWERING BIOACTIVE PEPTIDES: ELUCIDATION OF THEIR MECHANISM OF ACTION IN HEPG2 CELLS AND THEIR TRANS-EPITHELIAL TRANSPORT IN DIFFERENTIATED CACO-2 CELLS

Martina Bartolomei [1], Jianqiang Li [1], Anna Laura Capriotti [2], Melissa Fanzaga [1], Lorenza d'Adduzio [1], Aldo Laganà [2], Andrea Cerrato [2], Nadia Mulinacci [3], Lorenzo Cecchi [4], Carlotta Bollati [1], Carmen Lammi [1*]

[1] Department of Pharmaceutical Sciences, University of Milan, 20133 Milan, Italy.

[2] Department of Chemistry, Sapienza University of Rome, Piazzale Aldo Moro 5, 00185 Rome, Italy

[3] Department of Neuroscience, Psychology, Drug and Child Health, Pharmaceutical and Nutraceutical Section, University of Florence, 50019 Florence, Italy.

[4] Department of Agricultural, Food, Environmental and Forestry Sciences and Technologies, University of Florence,Via Donizetti, 50144, Florence, Italy

[*] Author to whom correspondence should be addressed.

9. Abstract

The production of olive oil has important economic repercussions in Mediterranean countries but also a considerable impact on the environment. This production generates enormous quantities of waste and by-products, which can be exploited as new raw materials to obtain innovative ingredients and therefore make the olive production more sustainable. In a previous study, we decided to foster olive seeds by generating two protein hydrolysates using food-grade enzymes, alcalase (AH) and papain (PH). These hydrolysates have shown, both *in vitro* and at the cellular level, antioxidant and antidiabetic activities, being able to inhibit the activity of the DPP-IV enzyme and modulate the secretion of GLP-1. Given the multifunctional behavior of peptides, both hydrolysates displayed dual hypocholesterolemic activity, inhibiting the activity of HMGCoAR and impairing the PPI of PCSK9/LDLR, with an IC50 equal to 0.61 mg/mL and 0.31 mg/mL for AH and PH, respectively. Furthermore, both samples restored LDLR protein levels on the membrane of human hepatic HepG2 cells, increasing the uptake of LDL from the extracellular environment. Since intestinal bioavailability is a key component of bioactive peptides, the second objective of this work is to evaluate the capacity of AH and PH peptides to be transported by differentiated human intestinal Caco-2 cells. The peptides transported by intestinal cells have been analyzed using mass spectrometry analysis, identifying a mixture of stable peptides that may represent new ingredients with multifunctional qualities for the development of nutraceuticals and functional foods to delay the onset of metabolic syndrome, promoting the principles of environmental sustainability.

9.1 Introduction

The Mediterranean basin's countries greatly benefit economically from the production of olive oil. However, its production is associated with a serious environmental impact due to resource depletion, soil degradation and the generation of enormous quantities of waste and by-products. These negative effects can vary depending on the practices and techniques used both during cultivation and during the extraction of oil from olives (Salomone *et al*., 2012, Arvanitoyannis *et al*., 2007). Therefore, the use of innovative cultivation and oil extraction techniques can bring about economic, environmental, and

social transformations. For instance, the pitting phase could be a simple but effective answer from both an economic and environmental point of view. The pitting step makes it possible to obtain a paste (oil pomace) from which the oil extraction yield is higher, and the by-product, the olive stone, is recovered and is easily accessible, as it does not require any additional processing to be used (Romaniello *et al*., 2017). This by-product is highly appreciated for energy use and has a better combustion efficiency and a low ash content, when compared to the pomace (Cappelletti *et al*., 2017). In a previous work, we decided to valorize this by-product to obtain new and higher value-added products, to achieve a more sustainable and profitable production in the olive oil sector. In detail, we targeted the extraction and characterization of the proteins present in the olive seeds, derived from *Frantoio* cultivar of *Olea europaea L,.* to generate hydrolysates rich in bioactive peptides, using two food-grade enzymes, i.e., Alcalase and Papain obtaining AH and PH samples, respectively. About 104 medium and 491 short peptides were identified within the hydrolysates and it was also demonstrated, their antioxidant and antidiabetic property by investigating the inhibition of the Dipeptidyl Peptidase IV (DPP-IV) enzyme and modulation of incretin hormone Glucagon Like peptide-1 (GLP-1) levels, using a combination of *in vitro* and cellular assays (Bartolomei *et al*., 2022). Considering that protein hydrolysates often show a multifunctional behavior, due to their heterogeneous composition and the ability of peptides to interact with two or more biological pathways (Lammi *et al.*, 2019, Bollati *et al.*, 2022, Peighambardoust *et al*., 2021), the first objective of this work was to study new possible biological activities of AH and PH focusing on the hypocholesterolemic one and evaluate their effects in modulating the cholesterol metabolism. Notably, the rate-limiting enzyme involved in the intracellular generation of cholesterol is 3-hydroxy-3-methylglutaryl coenzyme A reductase (HMGCoAR) (Sharpe *et al.*, 2013). When this enzyme is inhibited, a

reduction in intracellular cholesterol biosynthesis occurs, leading to the activation of the sterol regulatory element-binding protein (SREBP)-2 transcription factor, which, in order to maintain cholesterol homeostasis, improves the low-density lipoprotein receptor (LDLR) and HMGCoAR (its two main target) protein levels. The improved LDLR on the surface of hepatocytes is correlated with an improved ability of hepatic cells to clear plasmatic LDL-cholesterol, which ultimately results in a hypocholesterolemic effect (Kumar *et al*., 2019; Horton *et al*., 2002; Go *et al*. 2012). Given the constant increase in the incidence of cardiovascular diseases (CD), there has been a growing interest in strategies capable of reducing their onset by modifying lifestyle and diet (Lopez *et al.*, 2020). Peptides, especially derived from soy and lupin, which show hypocholesterolemic effects have been reported in the literature. The mechanisms of action involved are multiple, such as increasing the expression of the low density lipoprotein receptor (LDLR), reducing the absorption of sterols at the intestinal level and increasing the secretion of bile acids (Boachie *et al.*, 2018, Lammi *et al*., 2014, Lammi *et al*., 2015, Lin *et al.*, 2015). Over the last decade, peptides capable of inhibiting the proprotein convertase subtilisin/kexin type 9 (PCSK9), responsible for LDLR degradation in the liver, have also been identified (Tombling *et al.*, 2021). PCSK9 is regulated by its N-terminal prodomain, which is enzymatically cleaved for protein activation and act by binding to the EGF-A domain of LDLR on the cell surface. Dietary peptides with structural similarity to the prodomain, or EGF-A domain of LDLR, may be explored as PCSK9 ligands and inhibitors (Lin *et al*., 2015, Horton *et al*., 2009). Peptides with inhibitory activity on the PCSK9 protein stimulate the absorption of cholesterol by the LDLR with consequent increase in its degradation in hepatocytes. The current work assesses the AH and PH hypocholesterolemic activity through the modulation of HMGCoAR enzyme and PCSK9/LDLR protein-protein

interaction (PPI) in human hepatic HepG2. A problem that many proteins hydrolysates present is the lack of stability in the extensive metabolism phase that occurs in the gastrointestinal tract and therefore poor bioavailability. Therefore, bioavailability is the limiting factor for the application of protein hydrolysates. Peptides that show resistance to the action of digestive enzymes of the gastrointestinal tract and to peptidases present in the brush border membrane have a greater chance of being absorbed through the intestine (Xu *et al.*, 2019). Indeed, although several peptides have been identified as having multiple beneficial effects on human health, there is little evidence of their bioavailability (Udenigwe *et al.*, 2017). A widely used model to simulate the human intestine in terms of biological functions and structure is the Caco-2 cell monolayer obtained from human intestinal carcinoma. In fact, this monolayer is widely used to study drug absorption across the epithelium since differentiated cells express all the major digestive enzymes and transport proteins present in the human small intestine, providing metabolism as well as active and passive transport to be examined (Ungell *et al*., 2008, Hilgendorf *et al*., 2007). The absorption of peptides derived from olive seeds has never been evaluated, hence, the second aim of this work was to investigate the AH and PH *in vitro* trans-epithelial transport across differentiated human intestinal Caco-2 cell monolayers.

9.2 Material and methods

9.2.1 Chemicals

All chemicals and reagents were commercially available, and additional information is reported in the Supplementary Materials.

9.2.2 Sample preparation

Alcalase and papain olive seed hydrolysates were prepared as previously described (Bartolomei *et al*. 2022). Briefly, after extraction from the olive seed, proteins were hydrolyzed with Alcalase (50°C, 4h, 0.15 UA/g, pH 8.5) and Papain (65°C, 8h, 100 UA/g, pH 7) enzymes. Both hydrolysates were ultrafiltrated with 3 kDa cut-off Millipore UF System ultrafiltration membrane using optimized conditions (Bollati *et al.*, 2022).

9.2.3 Cell Culture

Human intestinal Caco-2 cells INSERM (Paris, France) and human hepatic HepG2 cells (ATCC, HB-8065, ATCC from LGC Standards, Milan, Italy) were cultured in DMEM high glucose with stable L-glutamine, supplemented with 10% FBS, 100 U/mL penicillin, 100 μg/mL streptomycin (complete growth medium) with incubation at 37 °C under 5% CO_2 atmosphere.

9.2.4 3-(4,5-Dimethylthiazol-2-yl)-2,5-Diphenyltetrazolium Bromide (MTT) Assay

A total of 3×10^4 HepG2 cells/well were seeded in 96-well plates and treated with 0.1, 0.5, 1.0, 1.5 and 5.0 mg/mL of AH and PH samples, or vehicle (H_2O) in complete growth media for 48h at 37 °C under 5% CO_2 atmosphere. MTT experiments have been performed following conditions already optimized (Lammi *et al.,* 2020). More details are available in Supplementary Materials.

9.2.5 In Vitro PCSK9-LDLR Binding Assay

The *in vitro* PCSK9-LDLR binding assay (CycLex Co., Nagano, Japan) was used to test AH and PH (1 mg/mL) in accordance with the manufacturer's instructions and under pre-optimized conditions (Lammi *et al*., 2016).

9.2.6 In-Cell Western (ICW) Assay

The ICW assay was performed using the same previously optimized procedure (Lammi *et al.*, 2015). Briefly, a total of 3×10^4 HepG2 cells/well were seeded in 96-well plate and, the following day, they were treated with 4.0 µg/mL PCSK9-WT, 1 mg/mL of Alcalase and Papain hydrolysates, 4.0 µg/mL PCSK9 + 1 mg/mL of Alcalase and Papain hydrolysates and vehicle (H_2O) for 2 h at 37 °C under 5% CO_2 atmosphere. Subsequently, ICW assay was carried out following the protocol that is available on Supplementary Materials.

9.2.7 Fluorescent LDL Uptake

The LDL Uptake assay was carried out following condition already described (Zanoni *et al.*, 2017). Shortly, a total of 3×10^4 HepG2 cells/well were seeded in 96-well plates and then kept in complete growth medium for 2 d before treatment. On the third day, cells were treated with 4.0 µg/mL PCSK9-WT, 1 mg/mL of Alcalase and Papain hydrolysates, 4.0 µg/mL PCSK9 + 1 mg/mL of Alcalase and Papain hydrolysates and vehicle (H_2O) for 2 h at 37 °C under 5% CO_2 atmosphere and LDL-Uptake was carried out following protocol that is detailed described in the Supplementary Materials.

9.2.8 Western Blot Analysis

Immunoblotting experiments were carried out with an optimized technique (Aiello *et al.*, 2017). 1.5×10^5 HepG2 cells/well (24-well plate) were treated with 1 mg/mL of AH and PH for 24 h. More details are available in the Supplementary Materials.

9.2.9 HMGCoAR A activity Assay

The experiments were carried out in accordance with the manufacturer's guidelines and the recommended protocol (Aiello *et al.*, 2017). More details are available in the Supplementary Materials.

9.2.10 Caco-2 Cell Culture and Differentiation

Caco-2 cells were cultured as reported by a previous protocol (Natoli *et al.*, 2012). Additional information is provided in the Supplementary Materials.

9.2.11 Trans-Epithelial Transport Experiments

TEER measurement was used to verify the integrity and differentiation of the cell monolayer prior to investigations. Hydrolysate trans-epithelial passage was assayed in differentiated Caco-2 cells in transport buffer solution (137 mM NaCl, 5.36 mM KCl, 1.26 mM CaCl2, and 1.1 mM MgCl2, 5.5 mM glucose) in accordance with previously described conditions (Bartolomei *et al.*, 2021). More details are reported in the Supplementary Materials.

9.2.12 UHPLC-HRMS analysis and short-sized peptide identification

Short peptides were analyzed by Vanquish binary pump H (Thermo Fisher Scientific, Str. Rivoltana—Rodano, Milan, Italy) coupled to a hybrid quadrupole—Orbitrap mass spectrometer Q Exactive (Thermo Fisher Scientific, Str. Rivoltana—Rodano, Milan, Italy) using a heated ESI source operating in positive ion mode. The mass-spectrometric strategy was developed as previously documented (Cerrato *et al*., 2020). More details are reported in the Supplementary Materials.

9.2.13 In Silico Toxicity prediction of the Bioavailable fraction of AH and PH hydrolysates

The peptides, which were identified as the most abundant in the BL side of the Transwell system exploited for the absorption studies for both AH and PH hydrolysates, were analyzed using a web-based server Toxinpred (https://webs.iiitd.edu.in/raghava/toxinpred/multi_submit.php (accessed on 3 January 2024)), which is useful to identify and predict highly toxic or non-toxic peptides from a large number of submitted sequences in FASTA format (Zaky *et al*., 2022).

9.2.14. Statistical Analysis

All measurements were performed in triplicate, and results were expressed as the mean ± standard deviation (s.d.), where p-values < 0.05 were considered to be significant. Statistical analyses were performed by one-way ANOVA followed by Dunnett's and Tukey's post-test (Graphpad Prism 9, GraphPad Software, La Jolla, CA, USA).

9.3 Results

9.3.1 Olive seed peptides target PCSK9/LDLR PPI and HMGCoAR Activity with a dual inhibitory effect.

9.3.1.1 Alcalase (AH) and Papain (PH) hydrolysates impairs the PCSK9/LDLR PPI.

The LDL receptor interacts with a protein produced in several organs such as the liver, kidneys, and intestines, named PCSK9. This interaction causes the activation of the catabolism of the receptor leading to its degradation especially in the liver (Péč *et al.*, 2023). We therefore evaluated whether the hydrolysates were able to inhibit this interaction. Both AH and PH can reduce PCSK9-LDLR binding with a dose-response trend (Figure 1A-B) with a IC_{50} of 0.61 mg/mL and 0.31 mg/mL, respectively (Figure 1C).

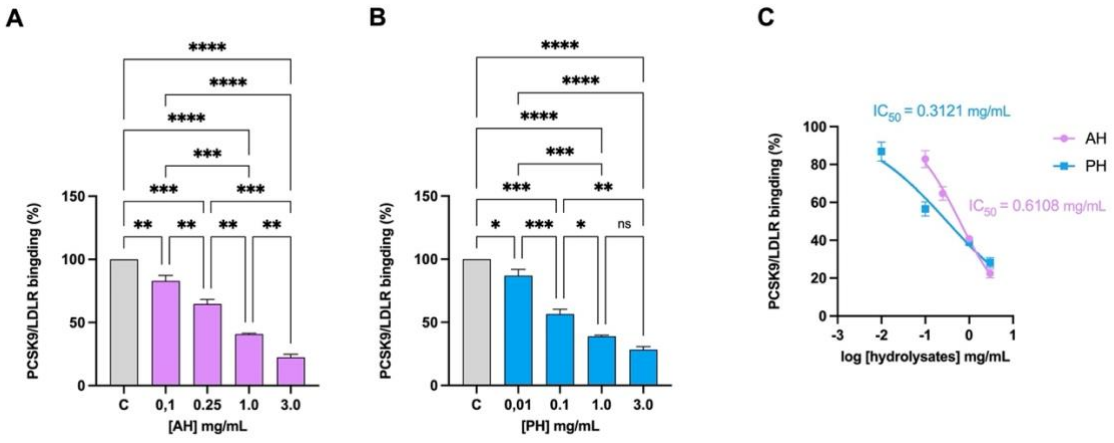

Figure 1. Inhibition of the PPI between PCSK9 and LDLR. AH (A) and PH (B) impairment of the protein–protein interaction between PCSK9 and LDLR with a dose-dependent trend. PCSK9/LDLR

binding and IC_{50} assessment (C). Data represent the mean ± s.d. of three independent experiments performed in triplicate. Data were analyzed by One-Way ANOVA followed by Tukey's post-hoc test; (*) $p < 0.05$; (****) $p < 0.0001$. ns: not significant. C: control sample.

9.3.1.2 Olive seed Hydrolysates Drop In Vitro the HMGCoAR Activity.

The HMGCoAR enzyme is considered the rate-limiting enzyme in the intracellular biosynthesis of cholesterol, and it is the target of statins, the primary drugs used to treat hypercholesterolemia (Madison *et al*., 2016). Hence, the potential HMGCoAR inhibitory activity of each hydrolysate was assessed by further biochemical investigation. The data presented in Figure 2 unequivocally imply that both hydrolysates decrease enzyme activity with dose–response trends. At the concentrations of 0.5 and 1 mg/mL, the AH hydrolysate the residual activity is 82.7 ± 1.2%, and 51.3 ± 1.5%, respectively (Figure 2A), whereas for the PH hydrolysates is 77.65 ± 2.3% and 53.7 ± 2.7%, respectively (Figure 2B). Comparing hydrolysates produced with different enzymes, no significant difference is observed at a concentration of 1 mg/mL (Figure 2C).

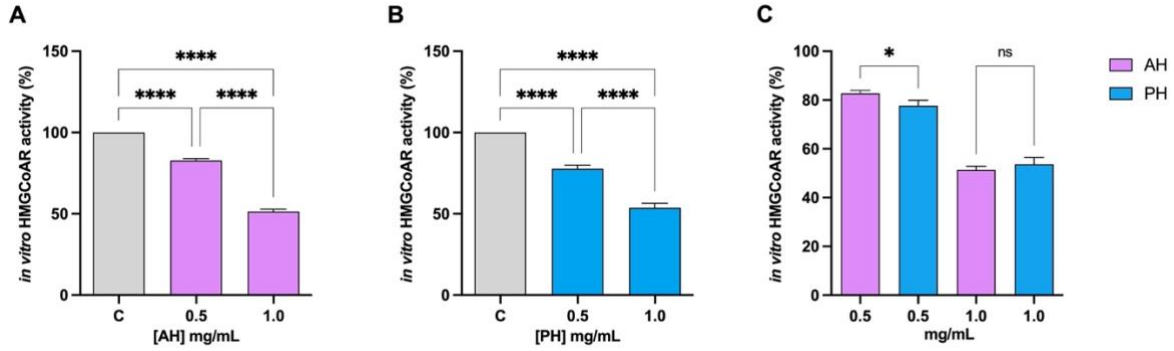

Figure 2. Effect of AH and PH on the modulation of the *in vitro* HMGCoAR activity. Both AH (A) and PH (B) hydrolysates drop HMGCoAR with dose-response trends. Comparison between the enzymes (C). Data represent the mean ± s.d. of six independent experiments performed in triplicate. Data were analyzed by One-Way ANOVA followed by Tukey's post-hoc test; (*) $p < 0.05$; (****) $p < 0.0001$. ns: not significant. C: control sample.

9.3.2 Assessment of Olive seed peptide ability to modulate the cholesterol metabolism in HepG2 cells

9.3.2.1 Alcalase (AH) and Papain (PH) hydrolysates do not show any cytotoxic effect on HepG2.

The possible cytotoxic effect of Alcalase (AH) and Papain (PH) hydrolysates on intestinal cells Caco-2 had already been evaluated in a previous work. Treatment up to 5 mg/mL did not show any toxicity (Bartolomei *et al*.,2023). Before proceeding with

the experiments on hepatic HepG2 cells, an MTT was conducted to exclude potential cytotoxic effects also in this cell line. As shown in Figure 3. Increasing concentrations of AH and PH (0.1, 0.5, 1, 1.5 and 5 mg/mL) were tested and no significant cell mortality was noticed at all doses tested after 48 hours of treatment compared to vehicle (H_2O).

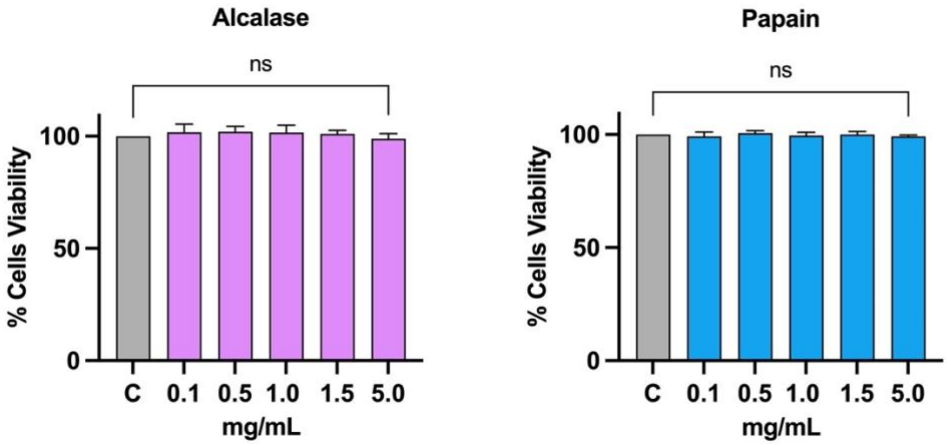

Figure 3. Cell vitality after treatment with AH and PH. Both hydrolysates do not affect the HepG2 vitality after 48 h of incubation up to 5 mg/mL. Data represent the mean ± s.d. of six independent experiments performed in triplicate. Data were analyzed by One-Way ANOVA followed by Dunnett post-hoc test. ns: not significant. C: control sample.

9.3.2.2 Alcalase (AH) and Papain (PH) hydrolysates modulate the hepatic LDLR Pathway in human hepatic HepG2 cells

The ICW assay is a quantitative colorimetric cell-based assay that allows the identification of target proteins in fixed cultured cells. It was used to evaluate the ability of AH and PH to modulate the protein level of LDLR on the HepG2 cell surface (Bartolomei *et al*., 2021). As seen in Figure 4A, there is an improvement in the level of LDLR specifically localized on the cell membrane of hepatocytes, up to 163.4 ± 13.1% for and up to 153.1 ± 6.1%. The results are also confirmed by repeating the experiment in presence of PCSK9 (Lammi *et al*., 2015). In fact, treatment with PCSK9 alone leads to a significant reduction of 45.17 ± 4.1%, in the receptor levels, while we only have a reduction of 21.8 ± 5.7% and 14.24 ± 8.6% compared to untreaded cells, for AH and PH, respectively (Figure 4C). In both experiments no significant difference was observed between AH and PH. The increase of membrane LDLR protein levels resulted in an improved functional ability of HepG2 cells to absorb the extracellular LDL by 157.3 ± 15.4% and 167.2 ± 20.7% after the treatment with AH and PH at the same concentration of 1 mg/mL (Figure 4B). Following the treatment with PCSK9 alone, the

capacity of HepG2 cells to uptake fluorescent LDL was lower by 35.66 ± 0.8% versus untreated cells and, the treatment with AH and PH reversed this effect up to 78.59 ± 5.2% and 85.8 ± 8.0% as shown in Figure 4D. Also in this case, we did not observe significant differences between the two hydrolysates.

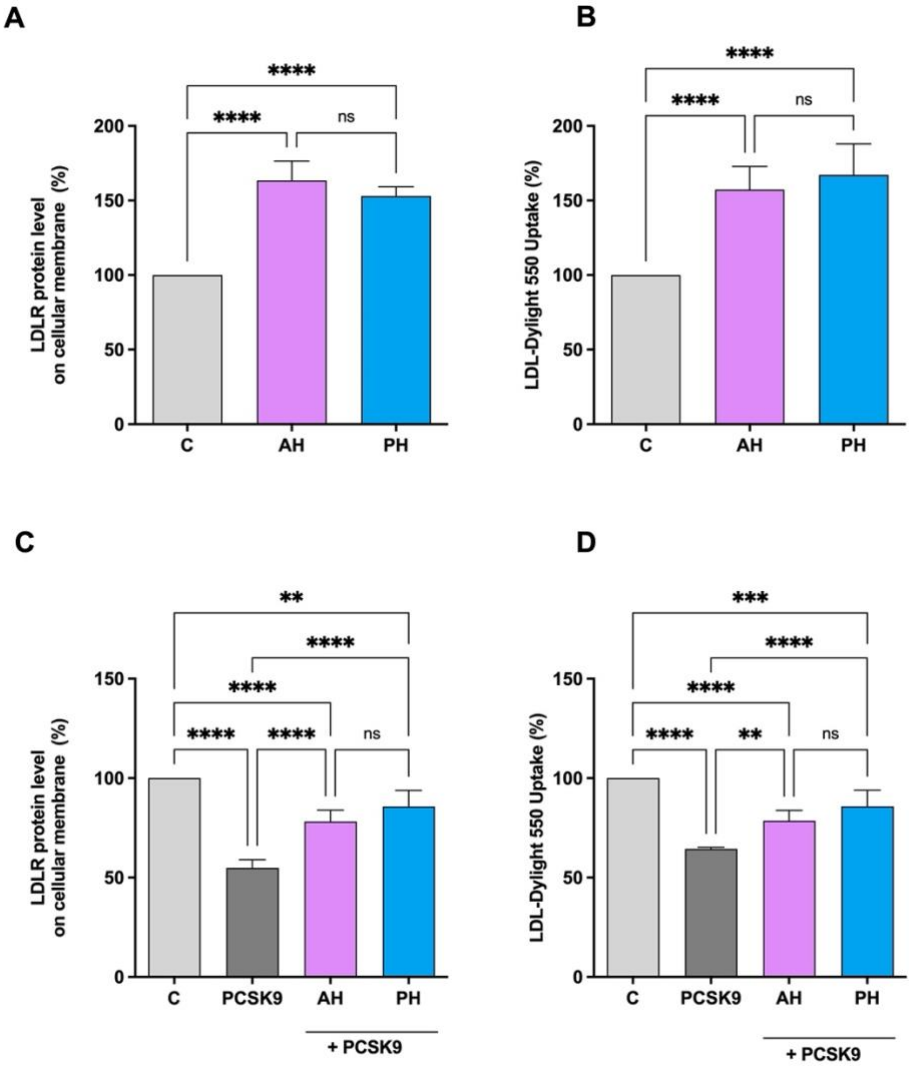

Figure 4. Effects of PH and AH on LDLR protein level and activity specifically located on the surface of hepatic cells. HepG2 cells were treated with AH and PH (1 mg/mL) for 24 h. The percentage of LDLR protein level was measured by ICW assay (A). The treatment of HepG2 cells with PCSK9 (4 µg/mL) reduced active LDLR protein levels localized on the surface of cells, which were restored by both AH and PH (B). Effect of AH and PH (1 mg/mL) on the HepG2 cell ability to uptake LDL from extracellular environment (C). The decreased functional ability of HepG2 cells to absorb LDL from the extracellular space observed after incubation with PCSK9 (4 µg/mL) is improved after treatment with both hydrolysates (D). Data represent the mean ± s.d. of three independent experiments performed in triplicate. Data were analyzed by One-Way ANOVA followed by Tukey's post-hoc test; (**) $p < 0.01$; (***) $p < 0.001$, (****) $p < 0.0001$. ns: not significant. C: control sample.

The activation of the receptor was also confirmed by immunoblotting experiments where HepG2 cells were treated for 24h with AH and PH at a concentration of 1 mg/mL. More in details, AH and PH hydrolysates up-regulate the protein levels of SREBP-2

transcription factor by 132.9 ± 19.8% and 146.0 ± 24.8%, respectively (Figure 5A). The rise of SREBP-2 protein level result in an advancement of total LDLR protein levels up to 137.1 ± 20.4% and 131.1 ± 25.1%, respectively (Figure 5B).

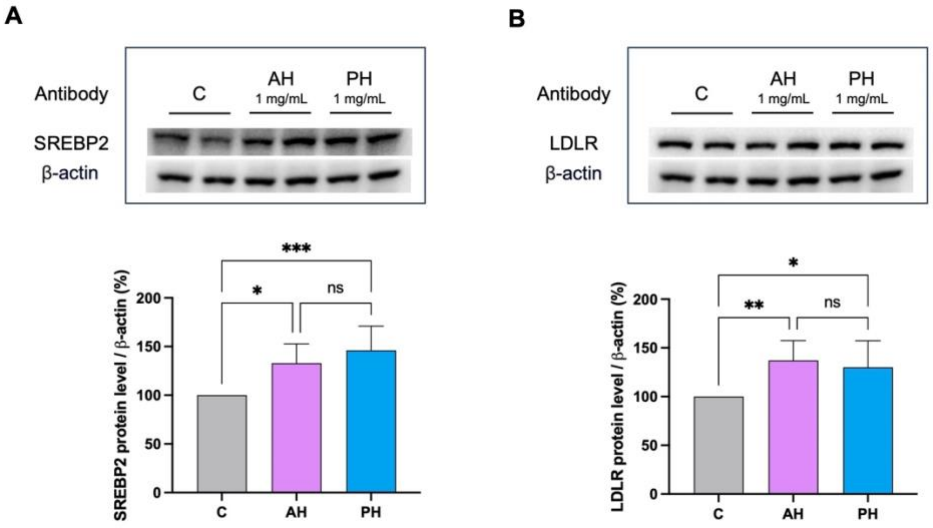

Figure 5. In HepG2 cells treated with AH and PH, the LDLR pathway is modulated. After the treatment of HepG2 cells with AH and PH, the SREBP-2 protein level was increased (A), as well as (B) the. Data points represent the averages ± SD of four independent experiments performed in duplicate. Data were analyzed by One-Way ANOVA followed by Tukey's post-hoc test; (*) $p<0.05$; (**) $p < 0.01$ (***) $p < 0.001$. ns: not significant. C: untreated HepG2 cells.

No significant difference was found comparing the two hydrolysates. Both hydrolysates were also unable of modulating the mature PCSK9 protein levels and they were also ineffective on the activation of HNF1-α, the PCSK9 transcription factor (Figure 6).

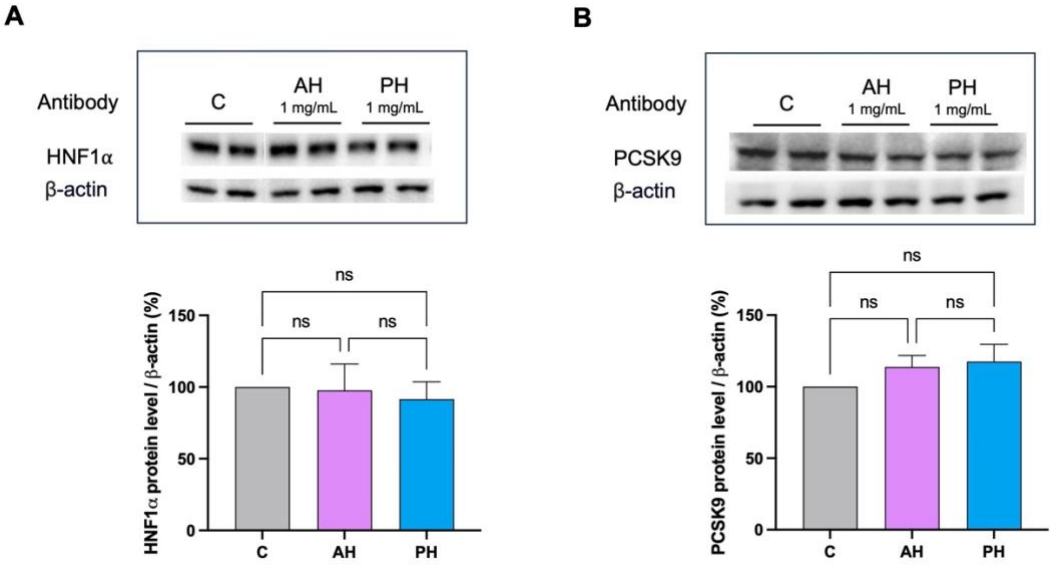

Figure 6. Effects of AH and PH hydrolysates on the PCSK9 pathway. AH and PH extracts did not produce any effect on the modulation of HNF1-α protein levels (A) and did not modulate PCSK9 (B). Data represent the mean ± s.d. of three independent experiments performed in duplicate. ns: not significant. C: untreated HepG2 cells.

9.3.3 Intestinal Transport of Alcalase (AH) and Papain (AH) hydrolysates across Caco-2 Cells

Peptides must be absorbed to carry out their biological activity and, furthermore, they must be resistant to proteolytic hydrolysis given by the action of intestinal proteases and peptidases (Sun *et al*., 2020). Indeed, an absorption study has been conducted to characterize the ability of AH and PH to be transported across differentiated human intestinal Caco-2 cells. During the experiments, TEER values were monitored. Results indicated that both AH and PH did not alter the intestinal monolayer permeability as depicted in the Figure 1S. For AH, 360 peptides in the AP and 199 in BL, whereas for PH, 358 peptides in AP and 252 in BL were identified, respectively. Compared to the original peptide mixture, 316 peptides in AP and 135 peptides in BL were identified for AH sample. Of these, 134 stable peptides present in both AP and BL were identified for the hydrolysate with Alcalase. Regarding the PH sample, 316 peptides in AP and 219 in BL were identified compared to the original mixture. Moreover, the peptides present in both AP and BL were 218 for the Papain hydrolysates (Figure 7).

Figure 7. Transport of AH and PH across differentiated Caco-2 cells. Distribution of short-sized peptides in AP and BL compartments for AH (A) and PH (B) where on the x axis are shown the peptide sequences and on the y axis signal intensity. Schematic description of the peptides absorbed and stable for intestinal absorption (C).

Based on these results, we can state that the sample hydrolyzed with Papain contains a greater number of peptides stable for intestinal absorption. The list of peptides absorbed in AP and BL for each hydrolysate and the analysis of stable peptides can be consulted in Supplementary Information. For the AP and BL samples, the percentage of the different peptide species was characterized (Table 1).

peptide length (AA)	abundance (%)	sample
2	16,1	AH AP
	31,7	AH BL
	17,0	PH AP
	22,2	PH BL
3	42,5	AH AP
	37,9	AH BL
	42,1	PH AP
	41,3	PH BL
4	38,0	AH AP
	28,0	AH BL
	37,6	PH AP
	33,3	PH BL
5	3,4	AH AP
	2,5	AH BL
	3,3	PH AP
	3,2	PH BL

Table 1. Percentage of the different peptide species.

In detail we observed an abundance of di- and tri-peptides in both samples. It is in fact known that small peptides (< 3 kDa) are those that show greater biological activity (Yang *et al*., 2021). Furthermore, of the most abundant species in the BL portion in both AH and PH, an analysis was done to evaluate their possible toxicity using an *in silico* method, which is developed to predict and design toxic/non-toxic peptides. No toxicity was predicted for any of the most abundant peptides (Table S.1).

9.4 Discussion

9.4.1. Cholesterol Lowering Activity of Olive Seed Hydrolysates

Food bioactive peptides represent a very dynamic and challenging field of research. It is quite well established that food peptides may exert a plethora of biological effects, being antioxidant, hypocholesterolemic, anti-inflammatory, anti-diabetic, anti-microbial, and hypotensive (Zaky *et al.*, 2022 Jakubczyk *et al.*, 2020). In this scenario, many efforts have been pursued by the scientific community for fostering their health promoting application, however, it appears clear that some biological effects have been more extensively investigated than some other ones. In this context, cholesterol-lowering peptides are much less studied than antioxidant, anti-diabetic (DPP-IV inhibitory), and/or hypotensive (ACE inhibitory) peptides, respectively (Zaky *et al.*, 2022). In light with this observation and with the aim at filling this gap, since ever, our

research activity is mainly focused on the identification and characterization of plant food hydrolysate/peptides with hypocholesterolemic effects. In this study, with the aim at improving a more responsible and sustainable use of food resources, we have focused our interested in valorizing olive seed protein as a new source of food bioactive peptides with ability to modulate the cholesterol metabolism through the elucidation of their mechanism of action. Olive seed hydrolysates produced with Alcalase (AH) and Papain (PH) target the activity of both PCSK9 and HMGCoAR, which are two pivotal enzymes involved in the modulation of cholesterol pathway in hepatic cell (Gupta, 2015). Notably, PCSK9 recognizes and binds LDLR located on the surfaces of hepatic cells activating the receptor catabolism, whereases HMGCoAR, the main target of statins, is involved in the endogenous synthesis of cholesterol (Boachie *et al*., 2018, Gupta, 2015) by hepatic cells. Findings clearly demonstrated that both AH and PH successes in the *in vitro* impairment of the PCSK9/LDLR PPI with and IC_{50} equals to 0.61 mg/mL and 0.31 mg/mL, respectively (Figure 1C), suggesting that PH is more active than AH. In addition, both hydrolysates inhibited the *in vitro* HMGCoAR activity with a dose response behavior, reaching about the 50% of inhibition at 1 mg/mL. Unlike to the effects exerted on the PCK9/LDLR PPI, comparing hydrolysates produced with the two different enzymes, no significant difference was observed at the concentration of 1 mg/mL, whereas PH confirmed to be more active than AH at 0.5 mg/mL (Figure 2C). These results agree with literature evidence according to which similarly to AH and PH, lupin protein hydrolysates exert hypocholesterolemic effects targeting *in vitro* both PCSK9/LDLR PPI and HMGCoAR activity, respectively (Lammi *et al.*, 2014, 2016). More in details, lupin hydrolysates obtained hydrolyzing the total *L. albus* protein with pepsin and trypsin reduced the PCSK9-LDLR binding by 25% and 23% at 1.0 mg/ml, respectively. In addition, unlike the peptides obtained using pepsin, only tryptic derived lupin hydrolysate was capable to reduce the *in vitro* HMGCoAR activity with a dose response trend (Lammi *et al.*, 2016). Literature evidence suggest that *L. angustifolius* hydrolysate (obtained using Alcalase) displayed a similar activity of a *L. albus* protein hydrolysate generated using trypsin (Santos-Sánchez *et al*., 2022). In addition, a recent study has reported the preparation of different hydrolysates from hempseed protein produced using pepsin, trypsin, pancreatin, or a mixture of these enzymes. The extensive protein cleavage exerted by pancreatin alone or in combination with pepsin leads to the generation of hempseed hydrolysates with a scarce capacity of modulating the HMGCoAR activity *in vitro*, whereas pepsin and trypsin generate hydrolysates with

enhanced activity (Aiello *et al*., 2017). In addition, our results are in line with other literature evidence. Recently, it was demonstrated that cowpea and amaranth hydrolysates drop the HMGCoAR activity (Marques *et al*., 2015, Soares *et al.*, 2015). Notably, *in vitro* experiments using the catalytic domain of HMGCoAR demonstrated that the peptides GGV, IVG, and VGVL from amaranth, reduced the HMGCoAR activity (Soares *et al.*, 2015). These findings suggest that these peptides act as HMGCoAR competitive inhibitors, similarly to some peptides from soybean (IAVPGEVA, IAVPTGVA, LPYP, YVVNPDNDEN and YVVNPDNNEN) and lupin (P5 and P7) (Zanoni *et* al., 2017, Lammi *et al*., 2022). However, more detailed studies should be performed to better characterize the hypocholesterolemic mechanism of action at cellular level and to assess the potential bioavailability of these peptides.

Overall, it appears clear that AH and PH exert HMGCoAR inhibitory activity similarly to hydrolysates from other sources, but they are more active in the impairment of the PCSK9 ability to bind the LDLR than lupin hydrolysates. This enhanced dual inhibitory activity makes AH and PH, two innovative cholesterol lowering peptide mixtures that trough the inhibition of both PCSK9 and HMGCoAR activity modulate intracellular cholesterol metabolism at cellular level. More in details, it was demonstrated that both AH and PH increased the LDLR protein levels located on the surface of human hepatic cells, which led from a functional point of view to an improved ability of HepG2 cells to uptake LDL from the extracellular environment (Figure 4A,B). Dedicate experiments confirmed that both AH and PH restored the PCSK9 reduced membrane LDLR protein level and functionality, renewing the ability of HepG2 to improve the PCSK9 reduced LDLR absorption (Figure 4C and D). To better elucidate the molecular mechanism of action through which these peptides exert *in vitro* hypocholesterolemic effect, it was demonstrated by western blotting analysis that both AH and PH increased the total LDLR protein levels through the activation of SREBP-2 transcription factor (Figure 5A-B). Interestingly, AH and PH were not able to modulate the HNF1-α being therefore ineffective in the modulation of PCSK9 protein levels. These results are in line with the behavior of hempseed hydrolysates obtained using pepsin and it is different from that of lupin hydrolysate obtained using pepsin as well. Indeed, unlike lupin peptides, AH and PH, hempseed peptide mixture improved the PCSK9 protein level trough the modulation of HNF1-α, displaying a statin-like mechanism of action (Zanoni *et al.*, 2017).

9.4.2 Assessment of trans-epithelial transport of AH and PH peptide mixtures using differentiated Caco-2 cells

In the field of food bioactive peptides, a significant challenge to their rapid utilization as nutraceuticals and functional foods is their limited metabolic stability and bioavailability at intestinal level (Amigo *et al*., 2020). The intestinal brush border is the main physiological barrier encountered by food peptides and hydrolysates. When these substances come into contact with human enterocytes, two main phenomena may occur: some peptides are transported by the cells, while others are metabolized within the cellular environment. It is important to underline that the metabolic degradation of bioactive peptides does not necessarily imply a loss of bioactivity (Bollati *et* al, 2022). Due to its direct impacts on the chemical compositions and peptidomic profiles of protein hydrolysates and peptides, the highly complex intestinal environment actively regulates their bioactivity. Consequently, conducting *in vitro* experiments to simulate the intestinal transport of food protein hydrolysates is crucial before proceeding with expensive *in vivo* experiments to confirm their health-promoting activities. In this context, human intestinal Caco-2 cells are commonly used as an effective model for *in vitro* evaluation of the propensity of food bioactive peptides to be transported by intestinal cells. In this study, differentiated Caco-2 cells were incubated with both AH and PH (at a concentration of 1 mg/mL) on the apical side for 2 h. The apical (AP) and basolateral (BL) solutions were then collected and analyzed by UHPLC-HRMS. The analysis of short-sized peptides clearly indicated a different peptidomic profile in the AP and BL samples (Figure 7A,B). In more details, first, different peptides were determined in the AH and PH, confirming that the enzyme activity is crucial for the determination of peptide mixture composition. Thus, when these two mixtures encountered the brush border level, intestinal cells selectively modulate the transport of specific peptides rather than other ones. This is clearly highlighted in the Figure 7 A and B where it is doubtless depicted that all the short-sized peptides display lower signal intensity in the BL solution than in the AP one, however peptides from PH are higher transported by Caco-2 cells than AH peptides. Notably, RFI, VI, RIA, and IG from AH mixture, and RI, RFI, RE, RI, SFVI, and VIA from PH mixture are the peptides mainly transported by differentiated Caco- 2, interestingly suggesting that the R residue in the N-terminus of the short peptides play an important role in the *in vitro* bioavailability.

Mature enterocytes develop microvilli that act as the primary surface for nutrient absorption in the gastrointestinal tract. These microvilli membranes contain enzymes that facilitate the breakdown of complex nutrients into simpler compounds that can be absorbed more easily. The dynamic equilibrium between the degradation and transport of bioactive peptides is crucial from a physiological perspective. Differentiated Caco-2 models are reliable tools for studying the proteolytic activity of the brush border barrier, as they express a wide range of membrane peptidases, including DPP-IV and ACE, on the apical side of enterocytes (Lammi *et al.*, 2021). Under this hypothesis, our results indicate that out of the total 491 short peptides identified in the AH and PH hydrolysates, 316 are present in the AP solutions, suggesting that about 64.4% of peptides, which were present in the original AH sample, are stable at the metabolic degradation exerted by the apical side of intestinal cells, and less than 40% are metabolized by active intestinal peptidases (Figure 7C). In addition, out of the 199 and 258 AH and PH peptides identified in the BL solution, 135 and 219 peptides were in common with total AH and PH, respectively (Figure 7C). This results clearly suggested that 27.5% and 44.6% of short-sized peptides identified in the AH and PH sample, respectively, were intactly transported by intestinal cells (Figure 7C). For both AH and PH samples, tripeptides are the most abundant moiety. In detail, in the AP portion they correspond to 42,5% in AP and 38% in BL for the AH sample and, they correspond to 42,1% in AP and 41,3% in BL for the PH sample (Table 1). In general, food-derived peptides can be transported across the intestinal brush-border membrane into the bloodstream through several routes: (i) peptide transport 1 (PepT1)-mediated route, (ii) paracellular route via tight junctions (TJs), (iii) transcytosis route, and (iv) passive transcellular diffusion. The absorption of peptides through these routes is influenced by factors such as peptide size, charge, hydrophobicity, and degradation by peptidases. Short peptides, such as dipeptides and tripeptides, are preferentially transported by PepT1, which is highly expressed in the intestinal epithelium. On the other hand, highly hydrophobic peptides are transported through passive transcellular diffusion or transcytosis. During the experiments the TEER of intestinal monolayer were measured and no effect on cell permeability was detected, suggesting that both AH and PH do not affect the monolayer permeability. In addition, using the ToxinPred database, it was confirmed that the most abundant species in the BL portion in both AH and PH do not display a toxic effect using this in silico system (Table S1). Overall, this in silico output is in agreement with

the MTT experiments on HepG2 and Caco-2 cells (Bartolomei *et al*., 2023) and with functional TERR measurement.

9.5 Conclusion

In conclusion, using our multidisciplinary approach, we have provided new insights that reinforce the evidence supporting the multifunctional behavior of food bioactive hydrolysates from a new plant source, clearly suggesting that they might be beneficially utilized as novel ingredients in the creation of dietary supplements intended to prevent metabolic syndrome. In addition, based on our findings, the general critical issues related to the low bioavailability and intestinal stability of food peptides were successfully faced, providing the peptidomic profile of short-sized peptides able to be stably transported by *in vitro* human intestinal cells. This study may be considered an important starting point for further investigation of their health-promoting effects using an animal model.

9.6 Supporting information

Chemical and samples

Dulbecco's modified Eagle's medium (DMEM), stable L-glutamine, fetal bovine serum (FBS), phosphate buffered saline (PBS), penicillin/streptomycin, chemiluminescent reagent, 24 and 96-well plates were purchased from Euroclone (Milan, Italy). The Transwell, polycarbonate filters (12 mm diameter, 0.4 μ m pore diameter) were purchased from Corning Inc. (Lowell, MA, US). 3 kDa cut-off Millipore UF System ultrafiltration was purchased from membrane (Millipore, Bedford, MA, USA). The HMGCoAR assay kit, bovine serum albumin (BSA), MTT [3-(4,5-dimethylthiazol-2-yl)-2,5-diphenyltetrazolium bromide], Janus Green B, formaldehyde, HCl and H_2SO_4 were from Sigma-Aldrich (St. Louis, MO, USA). Antibody against LDLR and the 3,3′, 5,5′ -tetramethylbenzidine (TMB) substrate were bought from Thermo Fisher Scientific (Waltham, MA, USA). The LDL-DyLightTM 550 was from Cayman Chemical (Ann Arbor, MI, USA). The CircuLex PCSK9 *in vitro* binding Assay Kit was from CircuLex (CycLex Co., Nagano, Japan). Phenylmethanesulfonyl fluoride (PMSF), Na-orthovanadate inhibitors, and the antibodies against rabbit Ig- horseradish peroxidase (HRP), mouse Ig-HRP, and SREBP-2 were purchased from Santa Cruz Biotechnology Inc. (Santa Cruz, CA, USA). The antibodies against hepatocyte nuclear factor 1-alpha (HNF1-alpha) and PCSK9 were bought from GeneTex (Irvine, CA, USA). The

inhibitor cocktail Complete Midi was from Roche (Basel, Switzerland). Mini protean TGX pre-cast gel 7.5% and Mini nitrocellulose Transfer Packs were purchased from BioRad (Hercules, CA, USA).

Sample Preparation

Alcalase and papain olive seed hydrolysates were prepared as previously described (Bartolomei *et al.*, 2022). Briefly, olive seeds were grounded with a domestic mill and hexane (ratio 1:20 w/v) was used to defatten olive seed powder for 1h while magnetic stirring was in place. After drying, the defatted powder was subjected to protein extraction. In detail, 1.5 g of defatted powder were mixed with 30 mL of extracting solution containing UREA 6 M, 0.1 M Tris-HCl (pH 8), 0.5 M NaCl, 0.5% SDS, and 0.1% DTT. After extraction from the olive seed, proteins were hydrolyzed with Alcalase (50°C, 4h, 0.15 UA/g, pH 8.5) and Papain (65°C, 8h, 100 UA/g, pH 7) enzymes. Both hydrolysates were ultrafiltrated with 3 kDa cut-off Millipore UF System ultrafiltration membrane using optimized conditions (Bollati *et al.*, 2022).

Cell Culture

Human hepatic HepG2 cells (ATCC, HB-8065, ATCC from LGC Standards, Milan, Italy) and human intestinal Caco-2 cells INSERM (Paris, France) were cultured in DMEM high glucose with stable L-glutamine, supplemented with 10% FBS, 100 U/mL penicillin, 100 µg/mL streptomycin (complete growth medium) with incubation at 37 °C under 5% CO_2 atmosphere.

3-(4,5-Dimethylthiazol-2-yl)-2,5-Diphenyltetrazolium Bromide (MTT) Assay

A total of 3×10^4 HepG2 cells/well were seeded in 96-well plates and treated with 0.1, 0.5, 1.0, 1.5 and 5.0 mg/mL of AH and PH samples, or vehicle (H_2O) in complete growth media for 48 h at 37 °C under 5% CO_2 atmosphere. MTT experiments have been performed following conditions already optimized (Udenigwe *et al.*, 2021). Subsequently, the treatment solvent was aspirated and 100 µL/well of 3-(4,5-dimethylthiazol-2-yl)-2,5- diphenyltetrazolium bromide (MTT) filtered solution added. After 2 h of incubation at 37 °C under 5% CO_2 atmosphere, 0.5 mg/mL solution was aspirated and 100 µL/well of the lysis buffer (8 mM HCl + 0.5% NP-40 in DMSO) added. After 5 min of slow shaking, the absorbance at 575 nm was read on the Synergy H1 fluorescence plate reader (Biotek, Bad Friedrichshall, Germany).

In Vitro PCSK9-LDLR Binding Assay

Alcalase and Papain hydrolysates (1 mg/mL) were tested using the *in vitro* PCSK9-LDLR binding assay (CycLex Co., Nagano, Japan) following the manufacture instructions and conditions already optimized (Ungell *et al*., 2008). Briefly, plates are pre-coated with a recombinant LDLR-AB domain, which contains the binding site for PCSK9. The vehicle and/or tested peptides were added to microcentrifuge tubes and diluted in reaction buffer prior to the experiment commencing. Afterwards, the reaction mixtures were added in each well of the microplate and the reaction was started by adding His-tagged PCSK9 wild type solution (3 µl). The microplate was allowed to incubate for 2h at RT shaking at 300 rpm on an orbital microplate shaker. The biotinylated anti-His-tag monoclonal antibody (100 µl) was added and incubated at RT for 1h shaking at 300 rpm. After incubation, wells were washed for 4 times with wash buffer. After the last wash, 100 µl of HRP-conjugated streptavidin were added and the plate was incubated for 20 min at RT. After incubation, wells were washed 4 times with wash buffer. Finally, the substrate reagent was added and the plate was incubated for 10 min at RT shaking at ca. 300 rpm. The reaction was stopped with 2.0 N sulfuric acid and the absorbance at 450 nm was measured using the Synergy H1 (Biotek, Bad Friedrichshall, Germany).

In-Cell Western (ICW) Assay

The ICW assay was performed using the same previously optimized procedure (Hilgendorf *et al*., 2007). Briefly, a total of 3×10^4 HepG2 cells/well were seeded in 96-well plate and, the following day, they were treated with 4.0 µg/mL PCSK9-WT, 1 mg/mL of Alcalase and Papain hydrolysates, 4.0 µg/mL PCSK9 + 1 mg/mL of Alcalase and Papain hydrolysates and vehicle (H_2O) for 2 h at 37 °C under 5% CO_2 atmosphere. Subsequently, they were fixed in 4% paraformaldehyde for 20 min at RT. Cells were washed 5 times with 100 µL of PBS/well and the endogenous peroxides activity quenched adding 3% H_2O_2 for 20 min at RT. Non-specific sites were blocked with 100 µL/well of 5% BSA in PBS for 1.5h at RT. LDLR primary antibody solution (Abcam) (1:3000 in 5% BSA in PBS, 25 µL/well) was incubated O/N at +4 °C. Afterwards, the primary antibody solution was discarded, and each sample was washed 5 times with 100 µL/well of PBS. Goat anti-rabbit Ig-HRP secondary antibody (Santa Cruz) solution (1:6000 in 5% BSA in PBS, 50µL/well) was added and incubated 1h at RT. The secondary antibody solution was washed 5 times with 100 µL/well of PBS (each wash

for 5 min at RT). Fresh prepared TMB Substrate (Pierce, 100 µL/well) was added, and the plate was incubated at RT until the desired color was developed. The reaction was stopped with 2 M H_2SO_4 and then the absorbance at 450 nm was measured using a microplate reader Synergy H1 from Biotek. Cells were stained by adding 1 × Janus green stain, incubating for 5 min at RT. The dye was removed, and the sample washed 5 times with water. Afterward, 0.1 mL 0.5 M HCl per well were added and incubated for 10 min. After 10 s shaking, the OD at 595 nm was measured using the Synergy H1 fluorescent plate reader from Biotek.

Fluorescent LDL Uptake

LDL Uptake assay was carried out following condition already described (Lammi *et al.*, 2020). Shortly, a total of 3×10^4 HepG2 cells/well were seeded in 96-well plates and then kept in complete growth medium for 2 d before treatment. On the third day, cells were treated with 4.0 µg/mL PCSK9-WT, 1 mg/mL of Alcalase and Papain hydrolysates, 4.0 µg/mL PCSK9 + 1 mg/mL of Alcalase and Papain hydrolysates and vehicle (H_2O) for 2 h at 37 °C under 5% CO_2 atmosphere. At the end of the treatment periods, the culture medium was replaced with 75 µL/well LDL-DyLight 549 working solution. The cells were additionally incubated for 2 h at 37 °C, and then the culture medium was aspirated and replaced with PBS 100 µL/well. The degree of LDL uptake was measured using the Synergy H1 fluorescent plate reader from Biotek (excitation and emission wavelengths 540 and 570 nm, respectively).

Western Blot Analysis

Immunoblotting experiments were performed using optimized protocol (Lammi et al., 2020). A total of 1.5×10^5 HepG2 cells/well (24-well plate) were treated with 1 mg/mL of AH and PH for 24 h. After each treatment, the supernatants were collected and stored at -80 °C. After cell lysis the protein concentration was evaluated by the Bradford's method and 50 µg of total proteins loaded on a precast 7.5% Sodium Dodecyl Sulfate-Polyacrylamide (SDS-PAGE) gel at 130 V for 45 min. Subsequently, the gel was pre-equilibrated in H_2O for 5 min at room temperature (RT) and transferred to a nitrocellulose membrane (Mini nitrocellulose Transfer Packs,) using a Trans-Blot Turbo at 1.3 A, 25 V for 7 min. Target proteins, on milk or BSA blocked membrane, were detected by primary antibodies as follows: anti-SREBP-2, anti-LDLR, anti-

HNF1a, anti-PCSK9 and anti- β-actin. Secondary antibodies conjugated with HRP and a chemiluminescent reagent were used to visualize target proteins and their signal was quantified using the Image Lab Software (Biorad, Hercules, CA, USA). The internal control β-actin was used to normalize loading variations.

HMGCoAR A activity Assay

The experiments were conducted following the manufacturer instructions and optimized protocol (Lammi et al., 2015). The assay buffer, NADPH, substrate solution, and HMGCoAR were provided in the HMGCoAR Assay Kit. Specifically, each reaction (200 μL) was set up adding the reagents accordance with the following procedure: 1× assay buffer, a 0.1 and 0.5 mg/mL of Alcalase and Papain hydrolysate or vehicle (C), the NADPH (4 μL), the substrate solution (12 μL), and lastly the HMGCoAR (catalytic domain) (2 μL). Eventually, the samples were mixed and the absorbance at 340 nm read by the microplate reader Synergy H1 at time 0 and 10 min. The HMGCoAR-dependent oxidation of NADPH and the inhibition properties of peptides were measured by absorbance reduction, which is directly proportional to enzyme activity.

Caco-2 Cell Culture and Differentiation

Caco-2 cells were cultured as reported by a previous protocol (Zanoni *et al*., 2017). For differentiation, cells were seeded on a Transwell at 3.5×10^5 cells/cm^2 density in complete medium supplemented with 10% FBS in both AP and BL compartments for 2 d to allow the formation of a confluent cell monolayer. Starting from day three after seeding, cells were transferred to FBS-free medium in the AP compartment and allowed to differentiate for 18-21 days with regular medium changes three times weekly (Zanoni *et al*., 2017). To monitor the cell monolayers integrity, the transepithelial electrical resistance (TEER) of differentiated Caco-2 cells was estimated at 37 °C using the voltmeter apparatus Millicell (Millipore Co., Billerica, MA, USA), promptly before and at the end of the transport tests.

Trans-Epithelial Transport Experiments

Prior to experiments, the cell monolayer integrity and differentiation were checked by TEER measurement. Hydrolysates trans-epithelial passage was assayed in

differentiated Caco-2 cells in transport buffer solution (137 mM NaCl, 5.36 mM KCl, 1.26 mM CaCl2, and 1.1 mM MgCl2, 5.5 mM glucose) according to previously described conditions (Aiello *et al.,* 2017). With the purpose of reproduce the pH conditions existing *in vivo* in the small intestinal mucosa, the apical (AP) solutions were maintained at pH 6.0 (buffered with 10 mM morpholinoethane sulfonic acid), and the basolateral (BL) solutions were maintained at pH 7.4 (buffered with 10 mM N-2-hydroxyethylpiperazine-N-4-butanesulfonic acid). Prior to transport experiments, cells were washed twice with 500 µL PBS containing Ca++ and Mg++. Alcalase and papain hydrolysates (1 mg/mL) where added in the AP compartment in the AP transport solution (500 µL) and the BL compartment with the BL transport solution (700 µL). After 2h at 37°C, all BL and AP solutions were collected and were stored at -80 °C prior to analysis. Three independent transport experiments were performed, each in duplicate.

UHPLC-HRMS Analysis and Short-Sized Peptide Identification

Short peptides were analyzed by Vanquish binary pump H (Thermo Fisher Scientific) coupled to a hybrid quadrupole- Orbitrap mass spectrometer Q Exactive (Thermo Fisher Scientific) using a heated ESI source operating in positive ion mode. The mass-spectrometric strategy was set up as previously reported (Natoli *et al.,* 2012). Each sample (20 µL) was injected onto a Kinetex XB-C18 (100 × 2.1 mm, 2.6 µm particle size, Phenomenex, Torrance, USA). Chosen flow, column temperature, and gradient parameters are reported in our previous work without any modification (Bartolomei *et al.,* 2021). Untargeted suspect screening analysis was performed in the top 5 data-dependent acquisition mode in the range m/z 150-750 with a resolution (full width at half maximum, FWHM, m/z 200) of 70,000. Higher-energy collisional dissociation fragmentation was performed at 40% normalized collision energy at the resolution of 35,000 (FWHM, m/z 200). An inclusion list, in which all precursor ions deriving from the combination of the 20 amino acids in di-, tri-, and tetrapeptides were listed, was included in the method (Natoli *et al.,* 2012). Raw data files from three experimental replicates and a blank sample were processed by Compound Discoverer using a workflow specifically dedicated to short peptide analysis. The database of short peptide sequences with IDs, masses, and molecular formulas, was implemented for the automatic matching of the extracted m/z ratios. Extracted masses from the chromatograms were aligned and filtered to remove background compounds present in

the blank sample, features whose masses were not present in the databases, and those not fragmented. Filtered features were manually validated, matching experimental spectra to those generated in silico by mMass 5.5 (Cerrato *et al.*, 2020).

In Silico Toxicity Prediction of the Bioavailable Fraction of AH and PH Hydrolysates

The peptides which were identified as the most abundant in the BL side of the Transwell system exploited for the absorption studies for both AH and PH hydrolysates, were analyzed using a web-based server Toxinpred (https://webs.iiitd.edu.in/raghava/toxinpred/multi_submit.php), useful to identify and predict highly toxic or non-toxic peptides from large number of submitted sequences in FASTA format (Zaky *et al*., 2022).

Statistical Analysis

All measurements were performed in triplicate, and results were expressed as the mean ± standard deviation (s.d.), where p-values < 0.05 were considered to be significant. Statistical analyses were performed by one-way ANOVA followed by Dunnett's and Tukey's post-test (Graphpad Prism 9, GraphPad Software, La Jolla, CA, USA).

SAMPLE	PEPTIDE SEQUENCE	PREDICTION	BIOPEP
AH	AI	Non-Toxin	ACE inhibitor
	APA	Non-Toxin	ACE and DPPIV inhibitor
	IGEE	Non-Toxin	ACE and DPPIV inhibitor
	IVR	Non-Toxin	ACE and DPPIV inhibitor
	RF	Non-Toxin	ACE and DPPIV inhibitor
	RFI	Non-Toxin	ACE and DPPIV inhibitor
	IV	Non-Toxin	Glucose Uptake stimulating
	RI	Non-Toxin	DPP-IV inhibitor
	SFI	Non-Toxin	ACE, renin, and DPPIV inhibitor
	SVIY	Non-Toxin	ACE and DPPIV inhibitor and antiox
	VI	Non-Toxin	DPPIV inhibitor
	VVPQ	Non-Toxin	ACE and DPPIV inhibitor
	VY	Non-Toxin	ACE and DPPIV inhibitor and antiox

PH	RF	Non-Toxin	ACE and DPPIV inhibitor
	RI	Non-Toxin	DPP-IV inhibitor
	IVR	Non-Toxin	ACE and DPPIV inhibitor
	RFI	Non-Toxin	ACE and DPPIV inhibitor
	IGEE	Non-Toxin	ACE and DPP-IV and III inhibitor
	IAPE	Non-Toxin	ACE and DPP-IV and III, and alpha glucosidase inhibitor
	SVIY	Non-Toxin	ACE and DPPIV inhibitor and antiox
	VY	Non-Toxin	ACE and DPPIV inhibitor and antiox
	AIPA	Non-Toxin	ACE and DPPIV inhibitor and antiox
	SFI	Non-Toxin	ACE, renin, and DPPIV inhibitor
	VA	Non-Toxin	DPP-IV inhibitor
	AI	Non-Toxin	ACE inhibitor
	IA	Non-Toxin	ACE inhibitor
	IAF	Non-Toxin	HMGCoAR, ACE and DPP-IV inhibitor
	VV	Non-Toxin	DPPIV inhibitor
	VI	Non-Toxin	DPPIV inhibitor

Table S1: Representation of the toxicity prediction obtain using ToxinPred and of the potential activity using BioPep. ACE: angiotensin-convertin enzyme; DPP: dypeptidil-dipeptidase; HMGCoAR: 3-hydroxy-3-methylglutaryl coenzyme A Reductase.

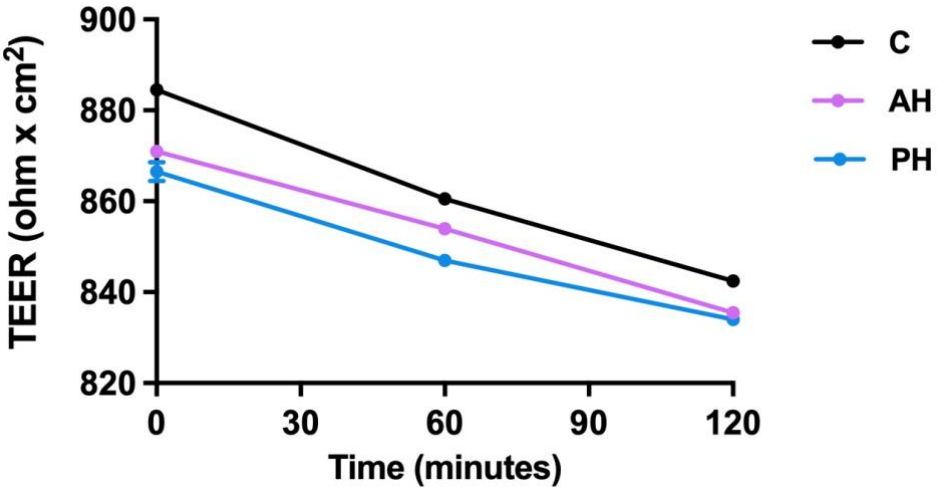

Figure S1: Time course of TEER changes recorded in untreated (control), AH, and PH-treated Caco-2 cells.

9.7 References

Aiello, G.; Lammi, C.; Boschin, G.; Zanoni, C.; Arnoldi, A. Exploration of Potentially Bioactive Peptides Generated from the Enzymatic Hydrolysis of Hempseed Proteins. J. Agric. Food Chem. 2017, 65, 10174–10184.

Amigo, L.; Hernández-Ledesma, B. Current Evidence on the Bioavailability of Food Bioactive Peptides. Molecules 2020, 25, 4479.

Arvanitoyannis, I.S.; Kassaveti, A.; Stefanatos, S. Olive Oil Waste Treatment: A Comparative and Critical Presentation of Methods, Advantages Disadvantages. Crit. Rev. Food Sci. Nutr. 2007, 47, 187–229.

Bartolomei, M.; Bollati, C.; Bellumori, M.; Cecchi, L.; Cruz-Chamorro, I.; Santos-Sánchez, G.; Ranaldi, G.; Ferruzza, S.; Sambuy, Y.; Arnoldi, A.; et al. Extra Virgin Olive Oil Phenolic Extract on Human Hepatic HepG2 and Intestinal Caco-2 Cells: Assessment of the Antioxidant Activity and Intestinal Trans-Epithelial Transport. Antioxidants 2021, 10, 118.

Bartolomei, M.; Capriotti, A.L.; Li, Y.; Bollati, C.; Li, J.; Cerrato, A.; Cecchi, L.; Pugliese, R.; Bellumori, M.; Mulinacci, N.; et al. Exploitation of Olive (Olea europaea L.) Seed Proteins as Upgraded Source of Bioactive Peptides with Multifunctional Properties: Focus on Antioxidant and Dipeptidyl-Dipeptidase & Mdash; IV Inhibitory Activities, and Glucagon-like Peptide 1 Improved Modulatio. Antioxidants 2022, 11, 1730.

Boachie, R.; Yao, S.; Udenigwe, C.C. Molecular Mechanisms of Cholesterol-Lowering Peptides Derived from Food Proteins. Curr. Opin. Food Sci. 2018, 20, 58–63.

Bollati, C.; Xu, R.; Boschin, G.; Bartolomei, M.; Rivardo, F.; Li, J.; Arnoldi, A.; Lammi, C. Integrated Evaluation of the Multifunctional DPP-IV and ACE Inhibitory Effect of Soybean and Pea Protein Hydrolysates. Nutrients 2022, 14, 2379.

Cappelletti, G.M.; Grilli, L.; Nicoletti, G.M.; Russo, C. Innovations in the Olive Oil Sector: A Fuzzy Multicriteria Approach. J. Clean. Prod. 2017, 159, 95–105.

Cerrato, A.; Aita, S.E.; Capriotti, A.L.; Cavaliere, C.; Montone, C.M.; Laganà, A.; Piovesana, S. A New Opening for the Tricky Untargeted Investigation of Natural and Modified Short Peptides. Talanta 2020, 219, 121262.

Go, G.-W.; Mani, A. Low-Density Lipoprotein Receptor (LDLR) Family Orchestrates Cholesterol Homeostasis. Yale J. Biol. Med. 2012, 85, 19–28.

Gupta, S. LDL Cholesterol, Statins And PCSK 9 Inhibitors. Indian Heart J. 2015, 67, 419–424.

Hilgendorf, C.; Ahlin, G.; Seithel, A.; Artursson, P.; Ungell, A.-L.; Karlsson, J. Expression of Thirty-Six Drug Transporter Genes in Human Intestine, Liver, Kidney, and Organotypic Cell Lines. Drug Metab. Dispos. 2007, 35, 1333–1340.

Horton, J.D.; Cohen, J.C.; Hobbs, H.H. PCSK9: A Convertase That Coordinates LDL Catabolism. J. Lipid Res. 2009, 50, S172–S177.

Horton, J.D.; Goldstein, J.L.; Brown, M.S. SREBPs: Activators of the Complete Program of Cholesterol and Fatty Acid Synthesis in the Liver. J. Clin. Investig. 2002, 109, 1125–1131.

Jakubczyk, A.; Karaś, M.; Rybczyńska-Tkaczyk, K.; Zielińska, E.; Zieliński, D. Current Trends of Bioactive Peptides—New Sources and Therapeutic Effect. Foods 2020, 9, 846.

Kumar, V.; Sharma, P.; Bairagya, H.R.; Sharma, S.; Singh, T.P.; Tiku, P.K. Inhibition of Human 3-Hydroxy-3-Methylglutaryl CoA Reductase by Peptides Leading to Cholesterol Homeostasis through SREBP2 Pathway in HepG2 Cells. Biochim. Biophys. Acta-Proteins Proteom. 2019, 1867, 604–615.

Lammi, C.; Aiello, G.; Boschin, G.; Arnoldi, A. Multifunctional Peptides for the Prevention of Cardiovascular Disease: A New Concept in the Area of Bioactive Food-Derived Peptides. J. Funct. Foods 2019, 55, 135–145.

Lammi, C.; Bellumori, M.; Cecchi, L.; Bartolomei, M.; Bollati, C.; Clodoveo, M.L.; Corbo, F.; Arnoldi, A.; Mulinacci, N. Extra Virgin Olive Oil Phenol Extracts Exert Hypocholesterolemic Effects through the Modulation of the LDLR Pathway: In Vitro and Cellular Mechanism of Action Elucidation. Nutrients 2020, 12, 1723.

Lammi, C.; Fassi, E.M.A.; Li, J.; Bartolomei, M.; Benigno, G.; Roda, G.; Arnoldi, A.; Grazioso, G. Computational Design and Biological Evaluation of Analogs of Lupin Peptide P5 Endowed with Dual PCSK9/HMG-CoAR Inhibiting Activity. Pharmaceutics 2022, 14, 665.

Lammi, C.; Zanoni, C.; Aiello, G.; Arnoldi, A.; Grazioso, G. Lupin Peptides Modulate the Protein-Protein Interaction of PCSK9 with the Low Density Lipoprotein Receptor in HepG2 Cells. Sci. Rep. 2016, 6, 29931.

Lammi, C.; Zanoni, C.; Arnoldi, A. A Simple and High-Throughput in-Cell Western Assay Using HepG2 Cell Line for Investigating the Potential Hypocholesterolemic Effects of Food Components and Nutraceutics. Food Chem. 2015, 169, 59–64.

Lammi, C.; Zanoni, C.; Arnoldi, A. IAVPGEVA, IAVPTGVA, and LPYP, Three Peptides from Soy Glycinin, Modulate Cholesterol Metabolism in HepG2 Cells through the Activation of the LDLR-SREBP2 Pathway. J. Funct. Foods 2015, 14, 469–478.

Lammi, C.; Zanoni, C.; Scigliuolo, G.M.; D'Amato, A.; Arnoldi, A. Lupin Peptides Lower Low-Density Lipoprotein (LDL) Cholesterol through an Up-Regulation of the LDL Receptor/Sterol Regulatory Element Binding Protein 2 (SREBP2) Pathway at HepG2 Cell Line. J. Agric. Food Chem. 2014, 62, 7151–7159.

Lin, S.-H.; Chang, D.-K.; Chou, M.-J.; Huang, K.-J.; Shiuan, D. Peptide Inhibitors of Human HMG-CoA Reductase as Potential Hypocholesterolemia Agents. Biochem. Biophys. Res. Commun. 2015, 456, 104–109.

Lopez, A.D.; Murray, C.C.J.L. The Global Burden of Disease, 1990–2020. Nat. Med. 1998, 4, 1241–1243.

Madison, B.B. Srebp2: A Master Regulator of Sterol and Fatty Acid Synthesis. J. Lipid Res. 2016, 57, 333–335.

Marques, M.R.; Fontanari, G.G.; Pimenta, D.C.; Soares-Freitas, R.M.; Arêas, J.A.G. Proteolytic Hydrolysis of Cowpea Proteins Is Able to Release Peptides with Hypocholesterolemic Activity. Food Res. Int. 2015, 77, 43–48.

Natoli, M.; Leoni, B.D.; D'Agnano, I.; Zucco, F.; Felsani, A. Good Caco-2 Cell Culture Practices. Toxicol. In Vitro 2012, 26, 1243–1246.

Péč, M.J.; Benko, J.; Jurica, J.; Péčová, M.; Samec, M.; Hurtová, T.; Bolek, T.; Galajda, P.; Péč, M.; Samoš, M.; et al. The Anti-Thrombotic Effects of PCSK9 Inhibitors. Pharmaceuticals 2023, 16, 1197.

Peighambardoust, S.H.; Karami, Z.; Pateiro, M.; Lorenzo, J.M. A Review on Health-Promoting, Biological, and Functional Aspects of Bioactive Peptides in Food Applications. Biomolecules 2021, 11, 631.

Romaniello, R.; Leone, A.; Tamborrino, A. Specification of a New De-Stoner Machine: Evaluation of Machining Effects on Olive Paste's Rheology and Olive Oil Yield and Quality. J. Sci. Food Agric. 2017, 97, 115–121.

Salomone, R.; Ioppolo, G. Environmental Impacts of Olive Oil Production: A Life Cycle Assessment Case Study in the Province of Messina (Sicily). J. Clean. Prod. 2012, 28, 88–100.

Santos-Sánchez, G.; Cruz-Chamorro, I.; Bollati, C.; Bartolomei, M.; Pedroche, J.; Millán Rodríguez, F.; del Carmen Millán-Linares, M.; Capriotti, A.L.; Cerrato, A.; Laganà, A.; et al. A Lupinus Angustifolius Protein Hydrolysate Exerts Hypocholesterolemic Effect in Western Diet-Fed-ApoE−/− Mice through the Modulation of LDLR and PCSK9 Pathways. Food Funct. 2022, 13, 4158–4170.

Sharpe, L.J.; Brown, A.J. Controlling Cholesterol Synthesis beyond 3-Hydroxy-3-Methylglutaryl-CoA Reductase (HMGCR). J. Biol. Chem. 2013, 288, 18707–18715. [Google Scholar] [CrossRef]

Soares, R.A.M.; Mendonça, S.; De Castro, L.Í.A.; Menezes, A.C.C.C.C.; Arêas, J.A.G. Major Peptides from Amaranth (Amaranthus cruentus) Protein Inhibit HMG-CoA Reductase Activity. Int. J. Mol. Sci. 2015, 16, 4150–4160.

Sun, X.; Acquah, C.; Aluko, R.E.; Udenigwe, C.C. Considering Food Matrix and Gastrointestinal Effects in Enhancing Bioactive Peptide Absorption and Bioavailability. J. Funct. Foods 2020, 64, 103680.

Tombling, B.J.; Zhang, Y.; Huang, Y.-H.; Craik, D.J.; Wang, C.K. The Emerging Landscape of Peptide-Based Inhibitors of PCSK9. Atherosclerosis 2021, 330, 52–60.

Udenigwe, C.C.; Fogliano, V. Food Matrix Interaction and Bioavailability of Bioactive Peptides: Two Faces of the Same Coin? J. Funct. Foods 2017, 35, 9–12.

Ungell, A.-L.; Artursson, P. An Overview of Caco-2 and Alternatives for Prediction of Intestinal Drug Transport and Absorption. In Drug Bioavailability; John Wiley & Sons Ltd.: Hoboken, NJ, USA, 2008; pp. 133–159. ISBN 9783527623860.

Xu, Q.; Yan, X.; Zhang, Y.; Wu, J. Current Understanding of Transport and Bioavailability of Bioactive Peptides Derived from Dairy Proteins: A Review. Int. J. Food Sci. Technol. 2019, 54, 1930–1941.

Yang, F.; Chen, X.; Huang, M.; Yang, Q.; Cai, X.; Chen, X.; Du, M.; Huang, J.; Wang, S. Molecular Characteristics and Structure–Activity Relationships of Food-Derived Bioactive Peptides. J. Integr. Agric. 2021, 20, 2313–2332.

Zaky, A.A.; Simal-Gandara, J.; Eun, J.-B.; Shim, J.-H.; Abd El-Aty, A.M. Bioactivities, Applications, Safety, and Health Benefits of Bioactive Peptides From Food and By-Products: A Review. Front. Nutr. 2022, 8, 815640.

Zanoni, C.; Aiello, G.; Arnoldi, A.; Lammi, C. Hempseed Peptides Exert Hypocholesterolemic Effects with a Statin-Like Mechanism. J. Agric. Food Chem. 2017, 50, 8829–8838.

Zanoni, C.; Aiello, G.; Arnoldi, A.; Lammi, C. Investigations on the Hypocholesterolaemic Activity of LILPKHSDAD and LTFPGSAED, Two Peptides from Lupin β-Conglutin: Focus on LDLR and PCSK9 Pathways. J. Funct. Foods 2017, 32, 1–8.

10. Abroad Experience

During the third year of my doctorate program, I spent a period of five months in Seville (Spain) at the Institute of Biomedicine of Seville (IBiS), a multidisciplinary center whose objective is to carry out research on the causes and mechanisms of the most widespread pathologies in the population and the development of new methods of diagnosis and treatment for them. The institute collaborates with the University of Seville and the university hospitals present in the city and my experience took place in the laboratory of Professor Antonio Carrillo Vico. Over the course of five months, I was trained and obtained certification to work with laboratory animals. First, I took part in a course where I studied the ethics of using laboratory animals, the various techniques applied to reduce the suffering of animals and finally how to handle them. Under the supervision of Doctor Ivan Cruz Chamorro, I learned the main techniques for administering treatments (i.e. oral gavage, intraperitoneal administration) and sacrificing animals. This certification allowed me to take part in the *in vivo* study that is being carried out which aims to demonstrate the safety and effectiveness of the protein hydrolysates derived from olive seeds that I generated during my first years of PhD. The laboratory also has an in-depth background regarding the study of anti-inflammatory effects, allowing me to study the effect of hydrolysates using both *in vitro* and cellular approaches. I assessed the anti-inflammatory properties of both hydrolysates in primary human monocytes (PBMC) and in macrophage cell line (RAW 264.7), learned new techniques such as RNA extraction and the use of PCR. Overall, the experience was very educational as it allowed me to acquire new skills and follow lectures held within the institute specifically designed for doctoral students. Moreover, it allowed me to experience a very different cultural environment and grow as a person by adapting to a new lifestyle and learning a new language.

11. Conclusion and future prospective

In conclusion by performing biochemical, cellular, and *in vivo* investigations, the antioxidant and hypocholesterolemic properties of phenols extracted from EVOO and derived from olive oil supply chain by-products, were demonstrated. The results suggest a role played not only by single phenolic compounds, but by the entire pool of secoiridoids molecules. Furthermore, the results demonstrated that Ole derivatives are selectively transported by differentiated Caco-2 cells. Moreover, the results suggest that olive seed peptides, which are extracted from side-stream materials of the production of table olives and olive oil, can be recovered, and used as valuable components for the development of functional foods and/or dietary supplements, in addition to being used as an energy source. The hydrolysates shown multifunctional activities, as they can exert antioxidant, anti-diabetic, hypocholesterolemic and anti-inflammatory effects, however the animal study will allow to obtain the "*proof of concept*" regarding the health promoting activity of both hydrolysates.

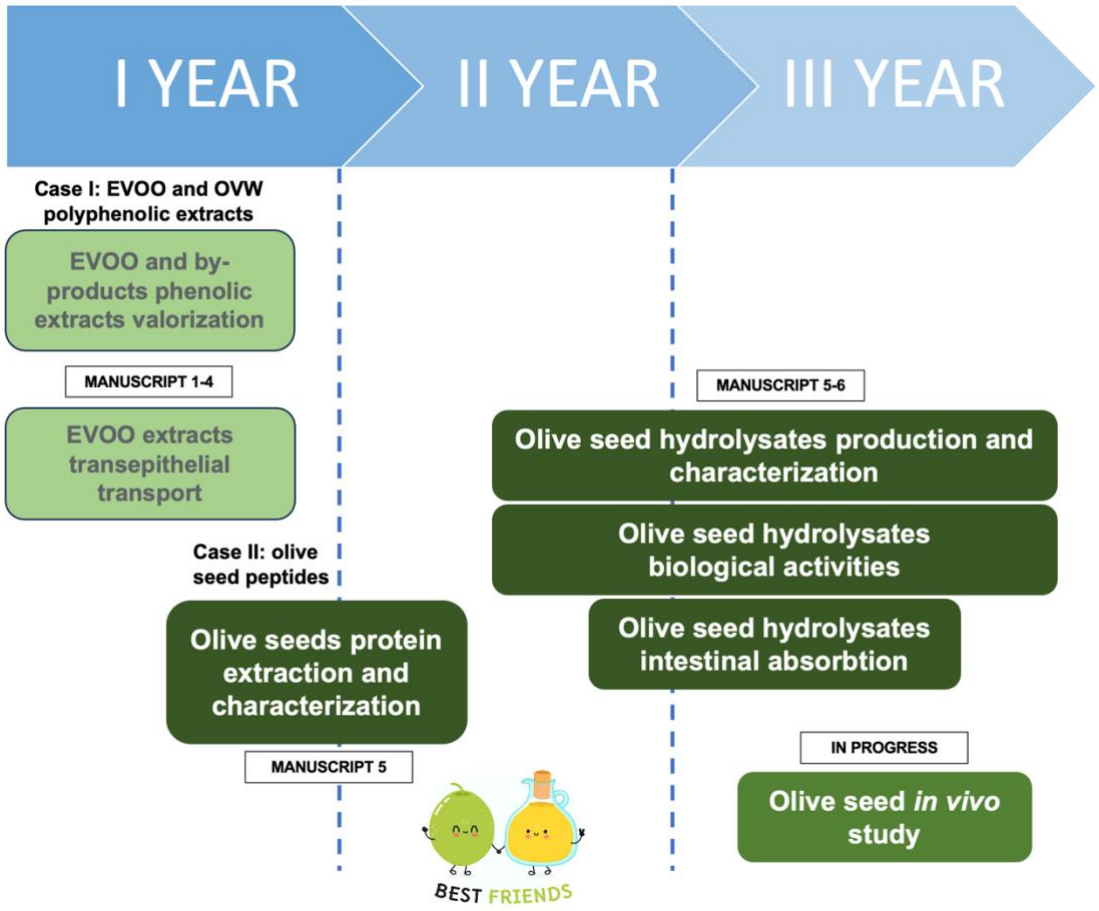

Figure 8. Time flow representation of my doctorate research project.

Based on the extensive characterization of the hydrolysates and the results obtained from the animal study, the next step is the human intervention study which could allow us to make a EFSA request for novel foods and a delivery of health claims. In addition, the hydrolysates can be valorized thanks to a synergy with companies. Specifically, a collaboration can arise with olive oil companies that are interested in producing, with an innovative approach, to obtain a superior quality olive oil by introducing the depicting process. Indeed, the depicting step removes the stones from the paste so that they do not take part in the malaxation and separation operations. It is known that the stones transfer oxidative enzymes to the pulp (phenoloxidase and lipoxygenase) and an increase in the phenol concentration was observed when a depicter was used. Additionally, a synergy with companies that can enhance these ingredients as functional foods or food supplements can be establish. This project could therefore be a mediator between two important industrial players, those who are rich in wastes and by-products that can be valorized into new resources and those who produce finished products which need innovative and sustainable ingredients.

The aim of my research focused on the extraction and characterization of the proteins present in olive seeds to obtain the best hydrolysates rich in bioactive peptides. This approach required the use of solvents and detergents that were not environmentally sustainable but necessary to obtain a good protein extraction yield. However, sustainability has always been taken into consideration in such a way as to enhance every part of the of the olive stone. The woody endocarp, which was removed to obtain the seeds, can still be used as pellets. The seed-oil, rich in OH-Tyr, which is obtained before the protein extraction step, is widely used in the cosmetic field thanks to its antioxidant and antimicrobial effects. Finally, the fiber that is removed in the protein extraction process can be recovered and used for the preparation of gluten-free products.

However, thinking about a possible scale-up of the protein extraction and hydrolysis process, several innovative technologies can be applied. These technologies involve the use of equipment that mixes the ground raw material with water and uses methods such as alkaline or acid extraction, or enzyme-assisted extraction to release the proteins into the water. The proteins in solution are then separated using centrifugation technologies such as decanters, hydro-cyclones and separators. Once brought into solution, the proteins are generally precipitated (often using very acidic pH) and then separated again

using decanters or separators. These processes have proven to be very efficient with matrices of different plant origins such as cereals, legumes, oil-rich seeds, and aquatic plants. Thanks to the development of a pilot-plan, the best conditions can be developed so that the process is potentially capable of producing large quantities of extracted proteins. Finally, the number of companies specialized in the hydrolysis of proteins is increasing, given that the market for hydrolysates is constantly growing. Thanks to the selection of the best hydrolysis conditions, hydrolysates rich in bioactive peptides can be obtained.

12. Scientific Publications & Communications

12.1 Scientific Publications

I had the opportunity to participate in other projects relating to the valorization of protein hydrolysates, such as the Era-Net BlueBio project "IMPRESSIVE- Improved Processing to Enhance Seafood Sidestream Valorization and Exploration project, where I valorized waste from the fish supply chain. Thanks to this collaboration I wrote a paper in which I am the first name and I contributed to the writing of other scientific papers.

1. **Bartolomei, M.**; Li, J.; Capriotti, A.L.; Fanzaga, M.; d'Adduzio, L.; Laganà, sA.; Cerrato, A.; Mulinacci, N.; Cecchi, L.; Bollati, C.; et al. Olive (Olea Europaea L.) Seed as New Source of Cholesterol-Lowering Bioactive Peptides: Elucidation of Their Mechanism of Action in HepG2 Cells and Their Trans-Epithelial Transport in Differentiated Caco-2 Cells. Nutrients 2024, 16, doi:10.3390/nu16030371.
2. Cruz-Chamorro, I.; Santos-Sánchez, G.; Ponce-España, E.; Bollati, C.; d'Adduzio, L.; **Bartolomei, M.**; Li, J.; Carrillo-Vico, A.; Lammi, C. MOMAST(®) Reduces the Plasmatic Lipid Profile and Oxidative Stress and Regulates Cholesterol Metabolism in a Hypercholesterolemic Mouse Model: The Proof of Concept of a Sustainable and Innovative Antioxidant and Hypocholesterolemic Ingredient. Antioxidants (Basel, Switzerland) 2023, 12, doi:10.3390/antiox12071335.
3. Cruz-Chamorro, I.; Santos-Sánchez, G.; Bollati, C.; **Bartolomei, M.**; Capriotti, A.L.; Cerrato, A.; Laganà, A.; Pedroche, J.; Millán, F.; del Carmen Millán-Linares, M.; et al. Chemical and Biological Characterization of the DPP-IV Inhibitory Activity Exerted by Lupin (Lupinus Angustifolius) Peptides: From the Bench to the Bedside Investigation. Food Chem. 2023, 426, 136458, doi:https://doi.org/10.1016/j.foodchem.2023.136458.
4. **Bartolomei, M.**; Cropotova, J.; Bollati, C.; Kvangarsnes, K.; d'Adduzio, L.; Li, J.; Boschin, G.; Lammi, C. Rainbow Trout (Oncorhynchus Mykiss) as Source of Multifunctional Peptides with Antioxidant, ACE and DPP-IV Inhibitory Activities. Nutrients 2023, 15, doi:10.3390/nu15040829.

5. Li, J.; Bollati, C.; Aiello, G.; **Bartolomei, M.**; Rivardo, F.; Boschin, G.; Arnoldi, A.; Lammi, C. Evaluation of the Multifunctional Dipeptidyl-Peptidase IV and Angiotensin Converting Enzyme Inhibitory Properties of a Casein Hydrolysate Using Cell-Free and Cell-Based Assays. Front. Nutr. 2023, 10, doi:10.3389/fnut.2023.1198258.
6. Santos-Sánchez, G.; Aiello, G.; Rivardo, F.; **Bartolomei, M.**; Bollati, C.; Arnoldi, A.; Cruz-Chamorro, I.; Lammi, C. Antioxidant Effect Assessment and Trans Epithelial Analysis of New Hempseed Protein Hydrolysates. Antioxidants 2023, 12, doi:10.3390/antiox12051099.
7. Kvangarsnes, K.; Dauksas, E.; Tolstorebrov, I.; Rustad, T.; **Bartolomei, M.**; Xu, R.; Lammi, C.; Cropotova, J. Physicochemical and Functional Properties of Rainbow Trout (Oncorhynchus Mykiss) Hydrolysate. Heliyon 2023, 9, e17979, doi:10.1016/j.heliyon.2023.e17979.
8. Cerrato, A.; Lammi, C.; Laura Capriotti, A.; Bollati, C.; Cavaliere, C.; Maria Montone, C.; **Bartolomei, M.**; Boschin, G.; Li, J.; Piovesana, S.; et al. Isolation and Functional Characterization of Hemp Seed Protein-Derived Short- and Medium-Chain Peptide Mixtures with Multifunctional Properties for Metabolic Syndrome Prevention. Food Res. Int. 2023, 163, 112219, doi:10.1016/j.foodres.2022.112219.
9. Bollati, C.; Marzorati, S.; Cecchi, L.; **Bartolomei, M.**; Li, J.; Bellumori, M.; d'Adduzio, L.; Verotta, L.; Piazza, L.; Arnoldi, A.; et al. Valorization of the Antioxidant Effect of Mantua PGI Pear By-Product Extracts: Preparation, Analysis and Biological Investigation. Antioxidants (Basel, Switzerland) 2023, 12, doi:10.3390/antiox12010144.
10. Bollati, C.; Cruz-Chamorro, I.; Aiello, G.; Li, J.; **Bartolomei, M.**; Santos-Sánchez, G.; Ranaldi, G.; Ferruzza, S.; Sambuy, Y.; Arnoldi, A.; et al. Investigation of the Intestinal Trans-Epithelial Transport and Antioxidant Activity of Two Hempseed Peptides WVSPLAGRT (H2) and IGFLIIWV (H3). Food Res. Int. 2022, doi:10.1016/j.foodres.2021.110720.
11. Zhang, Y.; Wang, L.; Tombling, B.J.; Lammi, C.; Huang, Y.-H.; Li, Y.; **Bartolomei, M.**; Hong, B.; Craik, D.J.; Wang, C.K. Improving Stability Enhances In Vivo Efficacy of a PCSK9 Inhibitory Peptide. J. Am. Chem. Soc. 2022, 144, 19485–19498, doi:10.1021/jacs.2c08029.

12. **Bartolomei, M.**; Capriotti, A.L.; Li, Y.; Bollati, C.; Li, J.; Cerrato, A.; Cecchi, L.; Pugliese, R.; Bellumori, M.; Mulinacci, N.; et al. Exploitation of Olive (Olea Europaea L.) Seed Proteins as Upgraded Source of Bioactive Peptides with Multifunctional Properties: Focus on Antioxidant and Dipeptidyl-Dipeptidase—IV Inhibitory Activities, and Glucagon-like Peptide 1 Improved Modulatio. Antioxidants 2022, 11, doi:10.3390/antiox11091730.
13. **Bartolomei, M.**; Bollati, C.; Li, J.; Arnoldi, A.; Lammi, C. Assessment of the Cholesterol-Lowering Effect of MOMAST®: Biochemical and Cellular Studies. Nutrients 2022, 14, doi:10.3390/nu14030493.
14. Cruz-Chamorro, I.; Santos-Sánchez, G.; Bollati, C.; **Bartolomei, M.**; Li, J.; Arnoldi, A.; Lammi, C. Hempseed (Cannabis Sativa) Peptides WVSPLAGRT and IGFLIIWV Exert Anti-Inflammatory Activity in the LPS-Stimulated Human Hepatic Cell Line. J. Agric. Food Chem. 2022, doi:10.1021/acs.jafc.1c07520.
15. Santos-Sánchez, G.; Álvarez-López, A.I.; Ponce-España, E.; Carrillo-Vico, A.; Bollati, C.; **Bartolomei, M.**; Lammi, C.; Cruz-Chamorro, I. Hempseed (Cannabis Sativa) Protein Hydrolysates: A Valuable Source of Bioactive Peptides with Pleiotropic Health-Promoting Effects. Trends Food Sci. Technol. 2022, 127, 303–318, doi:https://doi.org/10.1016/j.tifs.2022.06.005.
16. Bollati, C.; Xu, R.; Boschin, G.; **Bartolomei, M.**; Rivardo, F.; Li, J.; Arnoldi, A.; Lammi, C. Integrated Evaluation of the Multifunctional DPP-IV and ACE Inhibitory Effect of Soybean and Pea Protein Hydrolysates. Nutrients 2022, 14, doi:10.3390/nu14122379.
17. Lammi, C.; Boschin, G.; **Bartolomei, M.**; Arnoldi, A.; Galaverna, G.; Dellafiora, L. Mechanistic Insights into Angiotensin I-Converting Enzyme Inhibitory Tripeptides to Decipher the Chemical Basis of Their Activity. J. Agric. Food Chem. 2022, 70, 11572–11578, doi:10.1021/acs.jafc.2c04755.
18. Pugliese, R.; **Bartolomei, M.**; Bollati, C.; Boschin, G.; Arnoldi, A.; Lammi, C. Gel-Forming of Self-Assembling Peptides Functionalized with Food Bioactive Motifs Modulate DPP-IV and ACE Inhibitory Activity in Human Intestinal Caco-2 Cells. Biomedicines 2022, 10, doi:10.3390/biomedicines10020330.

19. Aiello, G.; Xu, R.; Pugliese, R.; **Bartolomei, M.**; Li, J.; Bollati, C.; Rueller, L.; Robert, J.; Arnoldi, A.; Lammi, C. Quality Assessment of the Protein Ingredients Recovered by Ultrasound-Assisted Extraction from the Press Cakes of Coconut and Almond Beverage Preparation. Foods 2022, 11, doi:10.3390/foods11223693.
20. Lammi, C.; Fassi, E.M.A.; Li, J.; **Bartolomei, M.**; Benigno, G.; Roda, G.; Arnoldi, A.; Grazioso, G. Computational Design and Biological Evaluation of Analogs of Lupin Peptide P5 Endowed with Dual PCSK9/HMG-CoAR Inhibiting Activity. Pharmaceutics 2022, 14, 665, doi:10.3390/pharmaceutics14030665.
21. Li, J.; Bollati, C.; **Bartolomei, M.**; Mazzolari, A.; Arnoldi, A.; Vistoli, G.; Lammi, C. Hempseed (Cannabis Sativa) Peptide H3 (IGFLIIWV) Exerts Cholesterol-Lowering Effects in Human Hepatic Cell Line. Nutrients 2022, 14, doi:10.3390/nu14091804.
22. Santos-Sánchez, G.; Cruz-Chamorro, I.; Bollati, C.; **Bartolomei, M.**; Pedroche, J.; Millán Rodríguez, F.; Millán-Linares, M. del C.; Capriotti, A.L.; Cerrato, A.; Laganà, A.; et al. A Lupinus Angustifolius Protein Hydrolysate Exerts Hypocholesterolemic Effect in Western Diet-Fed-ApoE−/− Mice through the Modulation of LDLR and PCSK9 Pathways. Food Funct. 2022, doi:10.1039/d1fo03847h.
23. **Bartolomei, M.**; Bollati, C.; Bellumori, M.; Cecchi, L.; Cruz-Chamorro, I.; Santos-Sánchez, G.; Ranaldi, G.; Ferruzza, S.; Sambuy, Y.; Arnoldi, A.; et al. Extra Virgin Olive Oil Phenolic Extract on Human Hepatic HEPG2 and Intestinal CACO-2 Cells: Assessment of the Antioxidant Activity and Intestinal Trans-Epithelial Transport. Antioxidants 2021, 10, 1–20, doi:10.3390/antiox10010118.
24. Lammi, C.; Aiello, G.; Bollati, C.; Li, J.; **Bartolomei, M.**; Ranaldi, G.; Ferruzza, S.; Fassi, E.M.A.; Grazioso, G.; Sambuy, Y.; et al. Trans-Epithelial Transport, Metabolism, and Biological Activity Assessment of the Multi-Target Lupin Peptide LILPKHSDAD (P5) and Its Metabolite LPKHSDAD (P5-Met). Nutrients 2021, 13, doi:10.3390/nu13030863
25. Aiello, G.; Pugliese, R.; Rueller, L.; Bollati, C.; **Bartolomei, M**.; Li, Y.; Robert, J.; Arnoldi, A.; Lammi, C. Assessment of the Physicochemical and

Conformational Changes of Ultrasound-Driven Proteins Extracted from Soybean Okara Byproduct. Foods 2021, 10, doi:10.3390/foods10030562.

26. Li, Y.; Aiello, G.; Fassi, E.M.A.; Boschin, G.; **Bartolomei, M.**; Bollati, C.; Roda, G.; Arnoldi, A.; Grazioso, G.; Lammi, C. Investigation of Chlorella Pyrenoidosa Protein as a Source of Novel Angiotensin I-Converting Enzyme (Ace) and Dipeptidyl Peptidase-Iv (Dpp-Iv) Inhibitory Peptides. Nutrients 2021, doi:10.3390/nu13051624.
27. Lammi, C.; **Bartolomei, M**.; Bollati, C.; Cecchi, L.; Bellumori, M.; Sabato, E.; Vistoli, G.; Mulinacci, N.; Arnoldi, A. Phenolic Extracts from Extra Virgin Olive Oils Inhibit Dipeptidyl Peptidase Iv Activity: In Vitro, Cellular, and in Silico Molecular Modeling Investigations. Antioxidants 2021, 10, doi:10.3390/antiox10071133.
28. Lammi, C.; Mulinacci, N.; Cecchi, L.; Bellumori, M.; Bollati, C.; **Bartolomei, M**.; Franchini, C.; Clodoveo, M.L.; Corbo, F.; Arnoldi, A. Virgin Olive Oil Extracts Reduce Oxidative Stress and Modulate Cholesterol Metabolism: Comparison between Oils Obtained with Traditional and Innovative Processes. Antioxidants 2020, 9, 1–17, doi:10.3390/antiox9090798.
29. Li, Y.; Aiello, G.; Bollati, C.; **Bartolomei, M**.; Arnoldi, A.; Lammi, C. Phycobiliproteins from Arthrospira Platensis (Spirulina): A New Source of Peptides with Dipeptidyl Peptidase-IV Inhibitory Activity. Nutrients 2020, doi:10.3390/nu12030794.

12.2 Communications

Project COMPETiTiVE (Claims of Olive oil to iMProvE The market ValuE of the product). Webinar 24 Sep 2021 attended as a speaker: Cholesterol-lowering activity of polyphenolic extracts of Extra Virgin Olive Oil.

IV Giornata della Ricerca del Centro Enrica Grossi Paoletti – "La prevenzione cardiovascolare nell'era post-COVID" – Milano, 26 Nov 2021- Presented as speaker "Valutazione delle proprietà benefiche-salutistiche e del trasporto trans-epiteliale di estratti fenolici di olio extra vergine di oliva".

V Giornata della Ricerca del Centro Enrica Grossi Paoletti – "Il colesterolo oltre il cuore, oltre i farmaci" – Milano, 17 Jun 2022 - Presented as speaker "Valutazione dell'effetto ipocolesterolemizzante del complesso polifenolico ottenuto dalle acque di vegetazione dell'oliva: studi biochimici e cellulari".

1st edition of Autumn School in Food Chemistry. Flash Communication: "Integrated and sustainable strategy for the investigation and valorization of extra virgin olive oil extracts". Pavia, 17-18th October 2022.

Congresso nazionale di chimica degli alimenti "CHIMALI". Oral presentation, "Integrated and sustainable strategy for the investigation and valorization of Extra Virgin Olive Oil extracts and by-products". XIII°, Marsala, 29-31th May 2023.

12.3 Data Management Plan Pilot Project

I was involved in a pilot project promoted by the University relating to the drafting of a Data Management Plan, a document that describes how the data used or generated by the research will be managed during and after the life of the project, to make the data generated during my PhD course Findable - Accessible - Interoperable – Reusable (FAIR). I followed a short training on the management of research data and on the organization of FAIR data. I then draft the plan, explaining the type of data generated, which approaches were used to make the data FAIR and ensure its security. This means standardizing the metadata that allows data to be found, depositing the data themselves in secure repositories, ensuring that they are interoperable, and that the interpretation software is available, and finally providing them with open licenses of the creative commons type.

13. Bibliography

1. Zeb, A.; Murkovic, M. Olive (Olea Europaea L.) Seeds, From Chemistry to Health Benefits. In Nuts and Seeds in Health and Disease Prevention; 2011 ISBN 9780123756886.
2. Skodra, C.; Titeli, V.S.; Michailidis, M.; Bazakos, C.; Ganopoulos, I.; Molassiotis, A.; Tanou, G. Olive Fruit Development and Ripening: Break on through to the "-omics" Side. Int. J. Mol. Sci. 2021.
3. Cruz, F.; Julca, I.; Gómez-Garrido, J.; Loska, D.; Marcet-Houben, M.; Cano, E.; Galán, B.; Frias, L.; Ribeca, P.; Derdak, S.; et al. Genome Sequence of the Olive Tree, Olea Europaea. Gigascience 2016, doi:10.1186/s13742-016-0134-5.
4. Reale, L.; Sgromo, C.; Ederli, L.; Pasqualini, S.; Orlandi, F.; Fornaciari, M.; Ferranti, F.; Romano, B. Morphological and Cytological Development and Starch Accumulation in Hermaphrodite and Staminate Flowers of Olive (Olea Europaea L.). Sex. Plant Reprod. 2009, doi:10.1007/s00497-009-0096-1.
5. Erel, R.; Yermiyahu, U.; Van Opstal, J.; Ben-Gal, A.; Schwartz, A.; Dag, A. The Importance of Olive (Olea Europaea L.) Tree Nutritional Status on Its Productivity. Sci. Hortic. (Amsterdam). 2013, doi:10.1016/j.scienta.2013.04.036.
6. Calabriso, N.; Scoditti, E.; Pellegrino, M.; Annunziata Carluccio, M. Olive Oil. In The Mediterranean Diet: An Evidence-Based Approach; 2015 ISBN 9780124079427.
7. Langgut, D.; Cheddadi, R.; Carrión, J.S.; Cavanagh, M.; Colombaroli, D.; Eastwood, W.J.; Greenberg, R.; Litt, T.; Mercuri, A.M.; Miebach, A.; et al. The Origin and Spread of Olive Cultivation in the Mediterranean Basin: The Fossil Pollen Evidence. Holocene 2019, doi:10.1177/0959683619826654.
8. Avidan, B.; Meni, Y.; Tsur, N. Composition and Morphology Changes in Olive Fruit as Indication of Maturation. Adv. Hortic. Sci. 2007.
9. Esteves Da Silva, J.C.G. Chemometric Classification of Cultivars of Olives: Perspectives on Portuguese Olives. In Olives and Olive Oil in Health and Disease Prevention; 2010 ISBN 9780123744203.
10. Conde, C.; Delrot, S.; Gerós, H. Physiological, Biochemical and Molecular Changes Occurring during Olive Development and Ripening. J. Plant Physiol. 2008.
11. Connor, D.J.; Fereres, E. The Physiology of Adaptation and Yield Expression in Olive. In Horticultural Reviews; 2010 ISBN 9780470650882.
12. Proietti, P.; Famiani, F.; Tombesi, A. Gas Exchange in Olive Fruit. Photosynthetica 1999, doi:10.1023/A:1007028220042.
13. Rotondi, A.; Bendini, A.; Cerretani, L.; Mari, M.; Lercker, G.; Toschi, T.G. Effect of Olive Ripening Degree on the Oxidative Stability and Organoleptic Properties of Cv. Nostrana Di Brisighella Extra Virgin Olive Oil. J. Agric. Food Chem. 2004, doi:10.1021/jf049845a.
14. Cano, M.; Roales, J.; Castillero, P.; Mendoza, P.; Calero, A.M.; Jiménez-Ot, C.; Pedrosa, J.M. Improving the Training and Data Processing of an Electronic Olfactory System for the Classification of Virgin Olive Oil into Quality Categories. Sensors Actuators, B Chem. 2011, doi:10.1016/j.snb.2011.09.002.
15. Garcia, R.; Martins, N.; Cabrita, M.J. Putative Markers of Adulteration of Extra Virgin Olive Oil with Refined Olive Oil: Prospects and Limitations. Food Res. Int. 2013, doi:10.1016/j.foodres.2013.05.008.
16. García-González, D.L.; Aparicio, R. Classification of Different Quality Virgin Olive Oils by Metal-Oxide Sensors. Eur. Food Res. Technol. 2004, doi:10.1007/s00217-003-0855-4.
17. Blekas, G.; Tsimidou, M.; Boskou, D. Olive Oil Composition. In Olive Oil; 2006.
18. Cimato, A. Effect of Agronomic Factors on Virgin Olive Oil Quality. Olivae 1991.
19. Criado, M.N.; Morelló, J.R.; Motilva, M.J.; Romero, M.P. Effect of Growing Area on Pigment and Phenolic Fractions of Virgin Olive Oils of the Arbequina Variety in Spain. JAOCS, J. Am. Oil Chem. Soc. 2004, doi:10.1007/s11746-004-954-z.
20. Owen, R.W.; Giacosa, A.; Hull, W.E.; Haubner, R.; Würtele, G.; Spiegelhalder, B.; Bartsch, H. Olive-Oil Consumption and Health: The Possible Role of Antioxidants. Lancet Oncol. 2000.
21. Aparicio-Soto, M.; Sánchez-Hidalgo, M.; Rosillo, M.Á.; Castejón, M.L.; Alarcón-De-La-Lastra, C. Extra Virgin Olive Oil: A Key Functional Food for Prevention of Immune-Inflammatory Diseases. Food Funct. 2016.
22. Aguilera, Y.; Dorado, M.E.; Prada, F.A.; Martínez, J.J.; Quesada, A.; Ruiz-Gutiérrez, V. The Protective Role of Squalene in Alcohol Damage in the Chick Embryo Retina. Exp. Eye Res. 2005, doi:10.1016/j.exer.2004.11.003.

23. Saudek, C.D.; Frier, B.M.; Liu, G.C.K. Plasma Squalene: Lipoprotein Distribution and Kinetic Analysis. J. Lipid Res. 1978, doi:10.1016/s0022-2275(20)40695-9.
24. Warleta, F.; Campos, M.; Allouche, Y.; Sánchez-Quesada, C.; Ruiz-Mora, J.; Beltrán, G.; Gaforio, J.J. Squalene Protects against Oxidative DNA Damage in MCF10A Human Mammary Epithelial Cells but Not in MCF7 and MDA-MB-231 Human Breast Cancer Cells. Food Chem. Toxicol. 2010, doi:10.1016/j.fct.2010.01.031.
25. Smith, T.J. Squalene: Potential Chemopreventive Agent. Expert Opin. Investig. Drugs 2000.
26. Jiang, L.; Yamaguchi, T.; Takamura, H.; Matoba, T. Characteristics of Shodo Island Olive Oils in Japan: Fatty Acid Composition and Antioxidative Compounds. Food Sci. Technol. Res. 2005, doi:10.3136/fstr.11.254.
27. Szymańska, R.; Nowicka, B.; Kruk, J. Vitamin E - Occurrence, Biosynthesis by Plants and Functions in Human Nutrition. Mini-Reviews Med. Chem. 2016, doi:10.2174/1389557516666160725094819.
28. Berger, A.; Jones, P.J.H.; Abumweis, S.S. Plant Sterols: Factors Affecting Their Efficacy and Safety as Functional Food Ingredients. Lipids Health Dis. 2004.
29. Rudkowska, I.; AbuMweis, S.S.; Jones, P.J.H.; Nicolle, C. Cholesterol-Lowering Efficacy of Plant Sterols in Low-Fat Yogurt Consumed as a Snack or with a Meal. J. Am. Coll. Nutr. 2008, doi:10.1080/07315724.2008.10719742.
30. Vivancos, M.; Moreno, J.J. β-Sitosterol Modulates Antioxidant Enzyme Response in RAW 264.7 Macrophages. Free Radic. Biol. Med. 2005, doi:10.1016/j.freeradbiomed.2005.02.025.
31. Li, J.H.; Awad, A.B.; Fink, C.S.; Wu, Y.W.B.; Trevisan, M.; Muti, P. Measurement Variability of Plasma β-Sitosterol and Campesterol, Two New Biomarkers for Cancer Prevention. Eur. J. Cancer Prev. 2001, doi:10.1097/00008469-200106000-00007.
32. Donner, M.; Radić, I.; Erraach, Y.; El Hadad-Gauthier, F. Implementation of Circular Business Models for Olive Oil Waste and By-Product Valorization. Resources 2022, 11, doi:10.3390/resources11070068.
33. Galili, E.; Langgut, D.; Terral, J.F.; Barazani, O.; Dag, A.; Kolska Horwitz, L.; Ogloblin Ramirez, I.; Rosen, B.; Weinstein-Evron, M.; Chaim, S.; et al. Early Production of Table Olives at a Mid-7th Millennium BP Submerged Site off the Carmel Coast (Israel). Sci. Rep. 2021, 11, 2218, doi:10.1038/s41598-020-80772-6.
34. Kapellakis, I.E.; Tsagarakis, K.P.; Crowther, J.C. Olive Oil History, Production and by-Product Management. Rev. Environ. Sci. Bio/Technology 2008, 7, 1–26, doi:10.1007/s11157-007-9120-9.
35. Hitchner, R.B. 4 Olive Production and the Roman Economy: The Case for Intensive Growth in the Roman Empire. In The Ancient Economy; Edinburgh University Press: Edinburgh, 2002; pp. 71–84 ISBN 9781474472326.
36. Strohalm, M.; Hassman, M.; Košata, B.; Kodíček, M. MMass Data Miner: An Open Source Alternative for Mass Spectrometric Data Analysis. Rapid Commun. Mass Spectrom. 2008, 22, 905–908, doi:https://doi.org/10.1002/rcm.3444.
37. Abu Tayeh, H.N.; Azaizeh, H.; Gerchman, Y. Circular Economy in Olive Oil Production – Olive Mill Solid Waste to Ethanol and Heavy Metal Sorbent Using Microwave Pretreatment. Waste Manag. 2020, 113, 321–328, doi:https://doi.org/10.1016/j.wasman.2020.06.017.
38. Inarejos-García, A.M.; Fregapane, G.; Salvador, M.D. Effect of Crushing on Olive Paste and Virgin Olive Oil Minor Components. Eur. Food Res. Technol. 2011, 232, 441–451, doi:10.1007/s00217-010-1406-4.
39. Calabriso, N.; Massaro, M.; Scoditti, E.; D'Amore, S.; Gnoni, A.; Pellegrino, M.; Storelli, C.; De Caterina, R.; Palasciano, G.; Carluccio, M.A. Extra Virgin Olive Oil Rich in Polyphenols Modulates VEGF-Induced Angiogenic Responses by Preventing NADPH Oxidase Activity and Expression. J. Nutr. Biochem. 2016, 28, 19–29, doi:https://doi.org/10.1016/j.jnutbio.2015.09.026.
40. Clodoveo, M.L. Malaxation: Influence on Virgin Olive Oil Quality. Past, Present and Future – An Overview. Trends Food Sci. Technol. 2012, 25, 13–23, doi:https://doi.org/10.1016/j.tifs.2011.11.004.
41. Salvador, M.D.; Aranda, F.; Gómez-Alonso, S.; Fregapane, G. Influence of Extraction System, Production Year and Area on Cornicabra Virgin Olive Oil: A Study of Five Crop Seasons. Food Chem. 2003, 80, 359–366, doi:https://doi.org/10.1016/S0308-8146(02)00273-X.
42. Artajo, L.-S.; Romero, M.-P.; Suárez, M.; Motilva, M.-J. Partition of Phenolic Compounds during the Virgin Olive Oil Industrial Extraction Process. Eur. Food Res. Technol. 2007, 225, 617–625, doi:10.1007/s00217-006-0456-0.
43. Rubio-Senent, F.; Rodríguez-Gutíerrez, G.; Lama-Muñoz, A.; Fernández-Bolaños, J. New Phenolic Compounds Hydrothermally Extracted from the Olive Oil Byproduct Alperujo and Their Antioxidative Activities. J. Agric. Food Chem. 2012, 60, 1175–1186, doi:10.1021/jf204223w.

44. Molina Alcaide, E.; Nefzaoui, A. Recycling of Olive Oil By-Products: Possibilities of Utilization in Animal Nutrition. Int. Biodeterior. Biodegradation 1996, 38, 227–235, doi:https://doi.org/10.1016/S0964-8305(96)00055-8.
45. Stempfle, S.; Carlucci, D.; de Gennaro, B.C.; Roselli, L.; Giannoccaro, G. Available Pathways for Operationalizing Circular Economy into the Olive Oil Supply Chain: Mapping Evidence from a Scoping Literature Review. Sustainability 2021, 13, doi:10.3390/su13179789.
46. Garcia-Maraver, A.; Perez-Jimenez, J.A.; Serrano-Bernardo, F.; Zamorano, M. Determination and Comparison of Combustion Kinetics Parameters of Agricultural Biomass from Olive Trees. Renew. Energy 2015, 83, 897–904, doi:https://doi.org/10.1016/j.renene.2015.05.049.
47. Romero-García, J.M.; Niño, L.; Martínez-Patiño, C.; Álvarez, C.; Castro, E.; Negro, M.J. Biorefinery Based on Olive Biomass. State of the Art and Future Trends. Bioresour. Technol. 2014, 159, 421–432, doi:10.1016/j.biortech.2014.03.062.
48. Darjazi, H.; Bottoni, L.; Moazami, H.R.; Rezvani, S.J.; Balducci, L.; Sbrascini, L.; Staffolani, A.; Tombesi, A.; Nobili, F. From Waste to Resources: Transforming Olive Leaves to Hard Carbon as Sustainable and Versatile Electrode Material for Li/Na-Ion Batteries and Supercapacitors. Mater. Today Sustain. 2023, 21, 100313, doi:https://doi.org/10.1016/j.mtsust.2022.100313.
49. Mediavilla, I.; Barro, R.; Borjabad, E.; Peña, D.; Fernández, M.J. Quality of Olive Stone as a Fuel: Influence of Oil Content on Combustion Process. Renew. Energy 2020, 160, 374–384, doi:https://doi.org/10.1016/j.renene.2020.07.001.
50. Roig, A.; Cayuela, M.L.; Sánchez-Monedero, M.A. An Overview on Olive Mill Wastes and Their Valorisation Methods. Waste Manag. 2006, 26, 960–969, doi:https://doi.org/10.1016/j.wasman.2005.07.024.
51. Paredes, C.; Cegarra, J.; Roig, A.; Sánchez-Monedero, M.A.; Bernal, M.P. Characterization of Olive Mill Wastewater (Alpechin) and Its Sludge for Agricultural Purposes. Bioresour. Technol. 1999, 67, 111–115, doi:https://doi.org/10.1016/S0960-8524(98)00106-0.
52. Jail, A.; Boukhoubza, F.; Nejmeddine, A.; Sayadi, S.; Hassani, L. Co-Treatment of Olive-Mill and Urban Wastewaters by Experimental Stabilization Ponds. J. Hazard. Mater. 2010, 176, 893–900, doi:https://doi.org/10.1016/j.jhazmat.2009.11.120.
53. Jarboui, R.; Sellami, F.; Azri, C.; Gharsallah, N.; Ammar, E. Olive Mill Wastewater Evaporation Management Using PCA Method: Case Study of Natural Degradation in Stabilization Ponds (Sfax, Tunisia). J. Hazard. Mater. 2010, 176, 992–1005, doi:https://doi.org/10.1016/j.jhazmat.2009.11.140.
54. Otero, P.; Garcia-Oliveira, P.; Carpena, M.; Barral-Martinez, M.; Chamorro, F.; Echave, J.; Garcia-Perez, P.; Cao, H.; Xiao, J.; Simal-Gandara, J.; et al. Applications of By-Products from the Olive Oil Processing: Revalorization Strategies Based on Target Molecules and Green Extraction Technologies. Trends Food Sci. Technol. 2021, 116, 1084–1104, doi:https://doi.org/10.1016/j.tifs.2021.09.007.
55. Morillo, J.A.; Antizar-Ladislao, B.; Monteoliva-Sánchez, M.; Ramos-Cormenzana, A.; Russell, N.J. Bioremediation and Biovalorisation of Olive-Mill Wastes. Appl. Microbiol. Biotechnol. 2009, 82, 25–39, doi:10.1007/s00253-008-1801-y.
56. El Gnaoui, Y.; Sounni, F.; Bakraoui, M.; Karouach, F.; Benlemlih, M.; Barz, M.; El Bari, H. Anaerobic Co-Digestion Assessment of Olive Mill Wastewater and Food Waste: Effect of Mixture Ratio on Methane Production and Process Stability. J. Environ. Chem. Eng. 2020, 8, 103874, doi:https://doi.org/10.1016/j.jece.2020.103874.
57. Miranda, I.; Simões, R.; Medeiros, B.; Nampoothiri, K.M.; Sukumaran, R.K.; Rajan, D.; Pereira, H.; Ferreira-Dias, S. Valorization of Lignocellulosic Residues from the Olive Oil Industry by Production of Lignin, Glucose and Functional Sugars. Bioresour. Technol. 2019, 292, 121936, doi:10.1016/j.biortech.2019.121936.
58. Lama-Muñoz, A.; Álvarez-Mateos, P.; Rodríguez-Gutiérrez, G.; Durán-Barrantes, M.M.; Fernández-Bolaños, J. Biodiesel Production from Olive–Pomace Oil of Steam-Treated Alperujo. Biomass and Bioenergy 2014, 67, 443–450, doi:https://doi.org/10.1016/j.biombioe.2014.05.023.
59. Pereira, A.P.; Ferreira, I.C.F.R.; Marcelino, F.; Valentão, P.; Andrade, P.B.; Seabra, R.; Estevinho, L.; Bento, A.; Pereira, J.A. Phenolic Compounds and Antimicrobial Activity of Olive (Olea Europaea L. Cv. Cobrançosa) Leaves. Molecules 2007, 12, 1153–1162, doi:10.3390/12051153.
60. Guinda, Á.; Pérez-Camino, M.C.; Lanzón, A. Supplementation of Oils with Oleanolic Acid from the Olive Leaf (Olea Europaea). Eur. J. Lipid Sci. Technol. 2004, 106, 22–26, doi:https://doi.org/10.1002/ejlt.200300769.
61. Sudjana, A.N.; D'Orazio, C.; Ryan, V.; Rasool, N.; Ng, J.; Islam, N.; Riley, T. V; Hammer, K.A. Antimicrobial Activity of Commercial Olea Europaea (Olive) Leaf Extract. Int. J. Antimicrob. Agents 2009, 33, 461–463, doi:https://doi.org/10.1016/j.ijantimicag.2008.10.026.

62. Wainstein, J.; Ganz, T.; Boaz, M.; Bar Dayan, Y.; Dolev, E.; Kerem, Z.; Madar, Z. Olive Leaf Extract as a Hypoglycemic Agent in Both Human Diabetic Subjects and in Rats. J. Med. Food 2012, 15, 605–610, doi:10.1089/jmf.2011.0243.
63. Şahin, S.; Şamlı, R. Optimization of Olive Leaf Extract Obtained by Ultrasound-Assisted Extraction with Response Surface Methodology. Ultrason. Sonochem. 2013, 20, 595–602, doi:https://doi.org/10.1016/j.ultsonch.2012.07.029.
64. Stramarkou, M.; Missirli, T.-V.; Kyriakopoulou, K.; Papadaki, S.; Angelis-Dimakis, A.; Krokida, M. The Recovery of Bioactive Compounds from Olive Pomace Using Green Extraction Processes. Resources 2023, 12, doi:10.3390/resources12070077.
65. Roselló-Soto, E.; Galanakis, C.M.; Brnčić, M.; Orlien, V.; Trujillo, F.J.; Mawson, R.; Knoerzer, K.; Tiwari, B.K.; Barba, F.J. Clean Recovery of Antioxidant Compounds from Plant Foods, by-Products and Algae Assisted by Ultrasounds Processing. Modeling Approaches to Optimize Processing Conditions. Trends Food Sci. Technol. 2015, 42, 134–149, doi:https://doi.org/10.1016/j.tifs.2015.01.002.
66. Dobrinčić, A.; Repajić, M.; Garofulić, I.E.; Tuđen, L.; Dragović-Uzelac, V.; Levaj, B. Comparison of Different Extraction Methods for the Recovery of Olive Leaves Polyphenols. Processes 2020, 8, doi:10.3390/pr8091008.
67. Macedo, G.A.; Santana, Á.L.; Crawford, L.M.; Wang, S.C.; Dias, F.F.G.; de Moura Bell, J.M.L.N. Integrated Microwave- and Enzyme-Assisted Extraction of Phenolic Compounds from Olive Pomace. LWT 2021, 138, 110621, doi:https://doi.org/10.1016/j.lwt.2020.110621.
68. Mallamaci, R.; Budriesi, R.; Clodoveo, M.L.; Biotti, G.; Micucci, M.; Ragusa, A.; Curci, F.; Muraglia, M.; Corbo, F.; Franchini, C. Olive Tree in Circular Economy as a Source of Secondary Metabolites Active for Human and Animal Health Beyond Oxidative Stress and Inflammation. Molecules 2021, 26, doi:10.3390/molecules26041072.
69. Álvarez, A.; Pizarro, C.; García, R.; Bueno, J.L. Spanish Biofuels Heating Value Estimation Based on Structural Analysis. Ind. Crops Prod. 2015, 77, 983–991, doi:https://doi.org/10.1016/j.indcrop.2015.09.078.
70. Saleem, J.; Shahid, U. Bin; Hijab, M.; Mackey, H.; McKay, G. Production and Applications of Activated Carbons as Adsorbents from Olive Stones. Biomass Convers. Biorefinery 2019, 9, 775–802, doi:10.1007/s13399-019-00473-7.
71. Blázquez, G.; Hernáinz, F.; Calero, M.; Ruiz-Núñez, L.F. Removal of Cadmium Ions with Olive Stones: The Effect of Somes Parameters. Process Biochem. 2005, 40, 2649–2654, doi:https://doi.org/10.1016/j.procbio.2004.11.007.
72. Fiol, N.; Villaescusa, I.; Martínez, M.; Miralles, N.; Poch, J.; Serarols, J. Sorption of Pb(II), Ni(II), Cu(II) and Cd(II) from Aqueous Solution by Olive Stone Waste. Sep. Purif. Technol. 2006, 50, 132–140, doi:https://doi.org/10.1016/j.seppur.2005.11.016.
73. Valvez, S.; Maceiras, A.; Santos, P.; Reis, P.N.B. Olive Stones as Filler for Polymer-Based Composites: A Review. Mater. (Basel, Switzerland) 2021, 14, doi:10.3390/ma14040845.
74. Rodríguez, G.; Lama, A.; Rodríguez, R.; Jiménez, A.; Guillén, R.; Fernández-Bolaños, J. Olive Stone an Attractive Source of Bioactive and Valuable Compounds. Bioresour. Technol. 2008, 99, 5261–5269, doi:https://doi.org/10.1016/j.biortech.2007.11.027.
75. Lama-Muñoz, A.; Romero-García, J.M.; Cara, C.; Moya, M.; Castro, E. Low Energy-Demanding Recovery of Antioxidants and Sugars from Olive Stones as Preliminary Steps in the Biorefinery Context. Ind. Crops Prod. 2014, 60, 30–38, doi:https://doi.org/10.1016/j.indcrop.2014.05.051.
76. Ranalli, A.; Pollastri, L.; Contento, S.; Di Loreto, G.; Iannucci, E.; Lucera, L.; Russi, F. Acylglycerol and Fatty Acid Components of Pulp, Seed, and Whole Olive Fruit Oils. Their Use to Characterize Fruit Variety by Chemometrics. J. Agric. Food Chem. 2002, 50, 3775–3779, doi:10.1021/jf011506j.
77. Padilla-Rascón, C.; Ruiz, E.; Romero, I.; Castro, E.; Oliva, J.M.; Ballesteros, I.; Manzanares, P. Valorisation of Olive Stone By-Product for Sugar Production Using a Sequential Acid/Steam Explosion Pretreatment. Ind. Crops Prod. 2020, 148, 112279, doi:https://doi.org/10.1016/j.indcrop.2020.112279.
78. De Dios Alché, J.; Jiménez-López, J.C.; Wang, W.; Castro-López, A.J.; Rodríguez-García, M.I. Biochemical Characterization and Cellular Localization of 11S Type Storage Proteins in Olive (Olea Europaea L.) Seeds. J. Agric. Food Chem. 2006, 54, 5562–5570, doi:10.1021/jf060203s.
79. Manach, C.; Scalbert, A.; Morand, C.; Rémésy, C.; Jiménez, L. Polyphenols: Food Sources and Bioavailability. Am. J. Clin. Nutr. 2004.
80. Quideau, S.; Deffieux, D.; Douat-Casassus, C.; Pouységu, L. Plant Polyphenols: Chemical Properties, Biological Activities, and Synthesis. Angew. Chemie - Int. Ed. 2011.
81. Fogliano, V.; Sacchi, R. Oleocanthal in Olive Oil: Between Myth and Reality. Mol. Nutr. Food Res. 2006.

82. Servili, M.; Esposto, S.; Fabiani, R.; Urbani, S.; Taticchi, A.; Mariucci, F.; Selvaggini, R.; Montedoro, G.F. Phenolic Compounds in Olive Oil: Antioxidant, Health and Organoleptic Activities According to Their Chemical Structure. Inflammopharmacology 2009.
83. Dias, L.G.; Rodrigues, N.; Veloso, A.C.A.; Pereira, J.A.; Peres, A.M. Monovarietal Extra-Virgin Olive Oil Classification: A Fusion of Human Sensory Attributes and an Electronic Tongue. Eur. Food Res. Technol. 2016, doi:10.1007/s00217-015-2537-4.
84. Brenes, M.; García, A.; García, P.; Garrido, A. Acid Hydrolysis of Secoiridoid Aglycons during Storage of Virgin Olive Oil. J. Agric. Food Chem. 2001, doi:10.1021/jf0107860.
85. Cecchi, L.; Migliorini, M.; Zanoni, B.; Breschi, C.; Mulinacci, N. An Effective HPLC-Based Approach for the Evaluation of the Content of Total Phenolic Compounds Transferred from Olives to Virgin Olive Oil during the Olive Milling Process. J. Sci. Food Agric. 2018, 98, 3636–3643, doi:https://doi.org/10.1002/jsfa.8841.
86. Amiot, M.J.; Fleuriet, A.; Macheix, J.J. Importance and Evolution of Phenolic Compounds in Olive during Growth and Maturation. J. Agric. Food Chem. 1986, doi:10.1021/jf00071a014.
87. Omar, S.H. Oleuropein in Olive and Its Pharmacological Effects. Sci. Pharm. 2010.
88. Cifá, D.; Skrt, M.; Pittia, P.; Di Mattia, C.; Poklar Ulrih, N. Enhanced Yield of Oleuropein from Olive Leaves Using Ultrasound-Assisted Extraction. Food Sci. \& Nutr. 2018, 6, 1128–1137, doi:https://doi.org/10.1002/fsn3.654.
89. Nediani, C.; Ruzzolini, J.; Romani, A.; Calorini, L. Oleuropein, a Bioactive Compound from Olea Europaea l., as a Potential Preventive and Therapeutic Agent in Non-Communicable Diseases. Antioxidants 2019.
90. Visioli, F.; Bellosta, S.; Galli, C. Oleuropein, the Bitter Principle of Olives, Enhances Nitric Oxide Production by Mouse Macrophages. Life Sci. 1998, doi:10.1016/S0024-3205(97)01150-8.
91. Marković, A.K.; Torić, J.; Barbarić, M.; Brala, C.J. Hydroxytyrosol, Tyrosol and Derivatives and Their Potential Effects on Human Health. Molecules 2019.
92. Wang, M.; Ramasamy, V.S.; Kang, H.K.; Jo, J. Oleuropein Promotes Hippocampal LTP via Intracellular Calcium Mobilization and Ca2+-Permeable AMPA Receptor Surface Recruitment. Neuropharmacology 2020, 176, 108196, doi:https://doi.org/10.1016/j.neuropharm.2020.108196.
93. Kucukgul, A.; Isgor, M.M.; Duzguner, V.; Atabay, N.M.; Kucukgul, A. Antioxidant Effects of Oleuropein on Hydrogen Peroxide-Induced Neuronal Stress- An In Vitro Study. Antiinflamm. Antiallergy. Agents Med. Chem. 2020, 19, 74–84.
94. Han, J.; Talorete, T.P.N.; Yamada, P.; Isoda, H. Anti-Proliferative and Apoptotic Effects of Oleuropein and Hydroxytyrosol on Human Breast Cancer MCF-7 Cells. Cytotechnology 2009, doi:10.1007/s10616-009-9191-2.
95. Hamdi, H.K.; Castellon, R. Oleuropein, a Non-Toxic Olive Iridoid, Is an Anti-Tumor Agent and Cytoskeleton Disruptor. Biochem. Biophys. Res. Commun. 2005, doi:10.1016/j.bbrc.2005.06.161.
96. Guo, W.; Xu, Y.; Yang, Y.; Xiang, J.; Chen, J.; Luo, D.; Xie, Q. Antibiofilm Effects of Oleuropein against Staphylococcus Aureus: An In Vitro Study. Foods 2023, 12, doi:10.3390/foods12234301.
97. Zorić, N.; Kopjar, N.; Bobnjarić, I.; Horvat, I.; Tomić, S.; Kosalec, I. Antifungal Activity of Oleuropein against Candida Albicans—The In Vitro Study. Molecules 2016, 21, doi:10.3390/molecules21121631.
98. Topuz, S.; Bayram, M. Oleuropein Extraction from Leaves of Three Olive Varieties (Olea Europaea L.): Antioxidant and Antimicrobial Properties of Purified Oleuropein and Oleuropein Extracts. J. Food Process. Preserv. 2022, 46, e15697, doi:https://doi.org/10.1111/jfpp.15697.
99. Andreadou, I.; Sigala, F.; Iliodromitis, E.K.; Papaefthimiou, M.; Sigalas, C.; Aligiannis, N.; Savvari, P.; Gorgoulis, V.; Papalabros, E.; Kremastinos, D.T. Acute Doxorubicin Cardiotoxicity Is Successfully Treated with the Phytochemical Oleuropein through Suppression of Oxidative and Nitrosative Stress. J. Mol. Cell. Cardiol. 2007, 42, 549–558, doi:https://doi.org/10.1016/j.yjmcc.2006.11.016.
100. Omar, S.H. Cardioprotective and Neuroprotective Roles of Oleuropein in Olive. Saudi Pharm. J. 2010.
101. Hadrich, F.; Garcia, M.; Maalej, A.; Moldes, M.; Isoda, H.; Feve, B.; Sayadi, S. Oleuropein Activated AMPK and Induced Insulin Sensitivity in C2C12 Muscle Cells. Life Sci. 2016, 151, 167–173, doi:https://doi.org/10.1016/j.lfs.2016.02.027.
102. Zheng, S.; Huang, K.; Tong, T. Efficacy and Mechanisms of Oleuropein in Mitigating Diabetes and Diabetes Complications. J. Agric. Food Chem. 2021.
103. Del Ben, M.; Nocella, C.; Loffredo, L.; Bartimoccia, S.; Cammisotto, V.; Mancinella, M.; Angelico, F.; Valenti, V.; Cavarretta, E.; Carnevale, R.; et al. Oleuropein-Enriched Chocolate by Extra Virgin Olive Oil Blunts Hyperglycaemia in Diabetic Patients: Results from a One-Time 2-

Hour Post-Prandial Cross over Study. Clin. Nutr. 2020, 39, 2187–2191, doi:https://doi.org/10.1016/j.clnu.2019.09.006.
104. Hermans, M.P.; Lempereur, P.; Salembier, J.P.; Maes, N.; Albert, A.; Jansen, O.; Pincemail, J. Supplementation Effect of a Combination of Olive (Olea Europea L.) Leaf and Fruit Extracts in the Clinical Management of Hypertension and Metabolic Syndrome. Antioxidants 2020, doi:10.3390/antiox9090872.
105. Petkov, V.; Manolov, P. Pharmacological Analysis of the Iridoid Oleuropein. Arzneimittelforschung. 1972, 22, 1476–1486.
106. Susalit, E.; Agus, N.; Effendi, I.; Tjandrawinata, R.R.; Nofiarny, D.; Perrinjaquet-Moccetti, T.; Verbruggen, M. Olive (Olea Europaea) Leaf Extract Effective in Patients with Stage-1 Hypertension: Comparison with Captopril. Phytomedicine 2011, 18, 251–258, doi:https://doi.org/10.1016/j.phymed.2010.08.016.
107. Beauchamp, G.K.; Keast, R.S.J.; Morel, D.; Lin, J.; Pika, J.; Han, Q.; Lee, C.H.; Smith, A.B.; Breslin, P.A.S. Ibuprofen-like Activity in Extra-Virgin Olive Oil. Nature 2005, doi:10.1038/437045a.
108. Scotece, M.; Gómez, R.; Conde, J.; Lopez, V.; Gómez-Reino, J.J.; Lago, F.; Smith, A.B.; Gualillo, O. Further Evidence for the Anti-Inflammatory Activity of Oleocanthal: Inhibition of MIP-1α and IL-6 in J774 Macrophages and in ATDC5 Chondrocytes. Life Sci. 2012, doi:10.1016/j.lfs.2012.09.012.
109. Iacono, A.; Gómez, R.; Sperry, J.; Conde, J.; Bianco, G.; Meli, R.; Gómez-Reino, J.J.; Smith, A.B.; Gualillo, O. Effect of Oleocanthal and Its Derivatives on Inflammatory Response Induced by Lipopolysaccharide in a Murine Chondrocyte Cell Line. Arthritis Rheum. 2010, doi:10.1002/art.27437.
110. Montoya, T.; Sánchez-Hidalgo, M.; Castejón, M.L.; Rosillo, M.Á.; González-Benjumea, A.; Alarcón-De-la-lastra, C. Dietary Oleocanthal Supplementation Prevents Inflammation and Oxidative Stress in Collagen-Induced Arthritis in Mice. Antioxidants 2021, doi:10.3390/antiox10050650.
111. Emma, M.R.; Augello, G.; Di Stefano, V.; Azzolina, A.; Giannitrapani, L.; Montalto, G.; Cervello, M.; Cusimano, A. Potential Uses of Olive Oil Secoiridoids for the Prevention and Treatment of Cancer: A Narrative Review of Preclinical Studies. Int. J. Mol. Sci. 2021.
112. Patti, A.M.; Carruba, G.; Cicero, A.F.G.; Banach, M.; Nikolic, D.; Giglio, R. V.; Terranova, A.; Soresi, M.; Giannitrapani, L.; Montalto, G.; et al. Daily Use of Extra Virgin Olive Oil with High Oleocanthal Concentration Reduced Body Weight, Waist Circumference, Alanine Transaminase, Inflammatory Cytokines and Hepatic Steatosis in Subjects with the Metabolic Syndrome: A 2-Month Intervention Study. Metabolites 2020, doi:10.3390/metabo10100392.
113. Agrawal, K.; Melliou, E.; Li, X.; Pedersen, T.L.; Wang, S.C.; Magiatis, P.; Newman, J.W.; Holt, R.R. Oleocanthal-Rich Extra Virgin Olive Oil Demonstrates Acute Anti-Platelet Effects in Healthy Men in a Randomized Trial. J. Funct. Foods 2017, doi:10.1016/j.jff.2017.06.046.
114. Pang, K.L.; Chin, K.Y. The Biological Activities of Oleocanthal from a Molecular Perspective. Nutrients 2018.
115. Gutiérrez-Miranda, B.; Gallardo, I.; Melliou, E.; Cabero, I.; Álvarez, Y.; Magiatis, P.; Hernández, M.; Nieto, M.L. Oleacein Attenuates the Pathogenesis of Experimental Autoimmune Encephalomyelitis through Both Antioxidant and Anti-Inflammatory Effects. Antioxidants 2020, doi:10.3390/antiox9111161.
116. Dinda, B.; Debnath, S.; Harigaya, Y. Naturally Occurring Secoiridoids and Bioactivity of Naturally Occurring Iridoids and Secoiridoids. A Review, Part 2. Chem. Pharm. Bull. 2007.
117. Nikou, T.; Liaki, V.; Stathopoulos, P.; Sklirou, A.D.; Tsakiri, E.N.; Jakschitz, T.; Bonn, G.; Trougakos, I.P.; Halabalaki, M.; Skaltsounis, L.A. Comparison Survey of EVOO Polyphenols and Exploration of Healthy Aging-Promoting Properties of Oleocanthal and Oleacein. Food Chem. Toxicol. 2019, 125, 403–412, doi:https://doi.org/10.1016/j.fct.2019.01.016.
118. Lepore, S.M.; Maggisano, V.; Bulotta, S.; Mignogna, C.; Arcidiacono, B.; Procopio, A.; Brunetti, A.; Russo, D.; Celano, M. Oleacein Prevents High Fat Diet-Induced a Diposity and Ameliorates Some Biochemical Parameters of Insulin Sensitivity in Mice. Nutrients 2019, doi:10.3390/nu11081829.
119. Lombardo, G.E.; Lepore, S.M.; Morittu, V.M.; Arcidiacono, B.; Colica, C.; Procopio, A.; Maggisano, V.; Bulotta, S.; Costa, N.; Mignogna, C.; et al. Effects of Oleacein on High-Fat Diet-Dependent Steatosis, Weight Gain, and Insulin Resistance in Mice. Front. Endocrinol. (Lausanne). 2018, doi:10.3389/fendo.2018.00116.

120. Filipek, A.; Gierlikowska, B. Oleacein May Intensify the Efflux of OxLDL from Human Macrophages by Increasing the Expression of the SRB1 Receptor, as Well as ABCA1 and ABCG1 Transporters. J. Funct. Foods 2021, 78, 104373, doi:https://doi.org/10.1016/j.jff.2021.104373.
121. Bonetti, A.; Venturini, S.; Ena, A.; Faraloni, C. Innovative Method for Recovery and Valorization of Hydroxytyrosol from Olive Mill Wastewaters. Water Sci. Technol. 2016, 74, 73–86, doi:10.2166/wst.2016.181.
122. Gorzynik-Debicka, M.; Przychodzen, P.; Cappello, F.; Kuban-Jankowska, A.; Gammazza, A.M.; Knap, N.; Wozniak, M.; Gorska-Ponikowska, M. Potential Health Benefits of Olive Oil and Plant Polyphenols. Int. J. Mol. Sci. 2018, 19, doi:10.3390/ijms19030686.
123. Zhang, X.; Cao, J.; Zhong, L. Hydroxytyrosol Inhibits Pro-Inflammatory Cytokines, INOS, and COX-2 Expression in Human Monocytic Cells. Naunyn. Schmiedebergs. Arch. Pharmacol. 2009, doi:10.1007/s00210-009-0399-7.
124. Fuccelli, R.; Fabiani, R.; Rosignoli, P. Hydroxytyrosol Exerts Anti-Inflammatory and Anti-Oxidant Activities in a Mouse Model of Systemic Inflammation. Molecules 2018, doi:10.3390/molecules23123212.
125. Vázquez-Velasco, M.; Esperanza Daz, L.; Lucas, R.; Gómez-Martínez, S.; Bastida, S.; Marcos, A.; Sánchez-Muniz, F.J. Effects of Hydroxytyrosol-Enriched Sunflower Oil Consumption on CVD Risk Factors. Br. J. Nutr. 2011, doi:10.1017/S0007114510005015.
126. Ruano, J.; Lopez-Miranda, J.; Fuentes, F.; Moreno, J.A.; Bellido, C.; Perez-Martinez, P.; Lozano, A.; Gómez, P.; Jiménez, Y.; Pérez Jiménez, F. Phenolic Content of Virgin Olive Oil Improves Ischemic Reactive Hyperemia in Hypercholesterolemic Patients. J. Am. Coll. Cardiol. 2005, doi:10.1016/j.jacc.2005.06.078.
127. Bellumori, M.; Cecchi, L.; Innocenti, M.; Clodoveo, M.L.; Corbo, F.; Mulinacci, N. The EFSA Health Claim on Olive Oil Polyphenols: Acid Hydrolysis Validation and Total Hydroxytyrosol and Tyrosol Determination in Italian Virgin Olive Oils. Molecules 2019, doi:10.3390/molecules24112179.
128. EFSA Panel on Dietetic Products Scientific Opinion on the Substantiation of Health Claims Related to Polyphenols in Olive and Protection of LDL Particles from Oxidative Damage (ID 1333, 1638, 1639, 1696, 2865).; 2011;
129. Priore, P.; Siculella, L.; Gnoni, G.V. Extra Virgin Olive Oil Phenols Down-Regulate Lipid Synthesis in Primary-Cultured Rat-Hepatocytes. J. Nutr. Biochem. 2014, doi:10.1016/j.jnutbio.2014.01.009.
130. Hamden, K.; Allouche, N.; Damak, M.; Elfeki, A. Hypoglycemic and Antioxidant Effects of Phenolic Extracts and Purified Hydroxytyrosol from Olive Mill Waste in Vitro and in Rats. Chem. Biol. Interact. 2009, doi:10.1016/j.cbi.2009.04.002.
131. Hamden, K.; Allouche, N.; Jouadi, B.; El-Fazaa, S.; Gharbi, N.; Carreau, S.; Damak, M.; Elfeki, A. Inhibitory Action of Purified Hydroxytyrosol from Stored Olive Mill Waste on Intestinal Disaccharidases and Lipase Activities and Pancreatic Toxicity in Diabetic Rats. Food Sci. Biotechnol. 2010, doi:10.1007/s10068-010-0062-6.
132. Calahorra, J.; Martínez-Lara, E.; Granadino-Roldán, J.M.; Martí, J.M.; Cañuelo, A.; Blanco, S.; Oliver, F.J.; Siles, E. Crosstalk between Hydroxytyrosol, a Major Olive Oil Phenol, and HIF-1 in MCF-7 Breast Cancer Cells. Sci. Rep. 2020, doi:10.1038/s41598-020-63417-6.
133. Zubair, H.; Bhardwaj, A.; Ahmad, A.; Srivastava, S.K.; Khan, M.A.; Patel, G.K.; Singh, S.; Singh, A.P. Hydroxytyrosol Induces Apoptosis and Cell Cycle Arrest and Suppresses Multiple Oncogenic Signaling Pathways in Prostate Cancer Cells. Nutr. Cancer 2017, doi:10.1080/01635581.2017.1339818.
134. Goldstein, D.S.; Jinsmaa, Y.; Sullivan, P.; Holmes, C.; Kopin, I.J.; Sharabi, Y. 3,4-Dihydroxyphenylethanol (Hydroxytyrosol) Mitigates the Increase in Spontaneous Oxidation of Dopamine During Monoamine Oxidase Inhibition in PC12 Cells. Neurochem. Res. 2016, 41, 2173–2178, doi:10.1007/s11064-016-1959-0.
135. Perona, J.S.; Cabello-Moruno, R.; Ruiz-Gutierrez, V. The Role of Virgin Olive Oil Components in the Modulation of Endothelial Function. J. Nutr. Biochem. 2006.
136. Giovannini, C.; Straface, E.; Modesti, D.; Coni, E.; Cantafora, A.; De Vincenzi, M.; Malorni, W.; Masella, R. Tyrosol, the Major Olive Oil Biophenol, Protects against Oxidized-LDL- Induced Injury in Caco-2 Cells. J. Nutr. 1999, doi:10.1093/jn/129.7.1269.
137. Berrougui, H.; Ikhlef, S.; Khalil, A. Extra Virgin Olive Oil Polyphenols Promote Cholesterol Efflux and Improve HDL Functionality. Evidence-based Complement. Altern. Med. 2015, doi:10.1155/2015/208062.

138. Sarna, L.K.; Sid, V.; Wang, P.; Siow, Y.L.; House, J.D.; O, K. Tyrosol Attenuates High Fat Diet-Induced Hepatic Oxidative Stress: Potential Involvement of Cystathionine β-Synthase and Cystathionine γ-Lyase. Lipids 2016, doi:10.1007/s11745-015-4084-y.
139. De La Puerta, R.; Domínguez, M.E.M.; Ruíz-Gutíerrez, V.; Flavill, J.A.; Hoult, J.R.S. Effects of Virgin Olive Oil Phenolics on Scavenging of Reactive Nitrogen Species and upon Nitrergic Neurotransmission. Life Sci. 2001, doi:10.1016/S0024-3205(01)01218-8.
140. Chandramohan, R.; Pari, L. Anti-Inflammatory Effects of Tyrosol in Streptozotocin-Induced Diabetic Wistar Rats. J. Funct. Foods 2016, doi:10.1016/j.jff.2016.08.043.
141. De La Torre, R. Bioavailability of Olive Oil Phenolic Compounds in Humans. Inflammopharmacology 2008.
142. Scalbert, A.; Morand, C.; Manach, C.; Rémésy, C. Absorption and Metabolism of Polyphenols in the Gut and Impact on Health. Biomed. Pharmacother. 2002, 56, 276–282, doi:https://doi.org/10.1016/S0753-3322(02)00205-6.
143. Visioli, F.; Galli, C.; Grande, S.; Colonnelli, K.; Patelli, C.; Galli, G.; Caruso, D. Hydroxytyrosol Excretion Differs between Rats and Humans and Depends on the Vehicle of Administration. J. Nutr. 2003, doi:10.1093/jn/133.8.2612.
144. Miro-Casas, E.; Covas, M.I.; Farre, M.; Fito, M.; Ortuño, J.; Weinbrenner, T.; Roset, P.; De La Torre, R. Hydroxytyrosol Disposition in Humans. Clin. Chem. 2003, doi:10.1373/49.6.945.
145. Corona, G.; Tzounis, X.; Dessì, M.A.; Deiana, M.; Debnam, E.S.; Visioli, F.; Spencer, J.P.E. The Fate of Olive Oil Polyphenols in the Gastrointestinal Tract: Implications of Gastric and Colonic Microflora-Dependent Biotransformation. Free Radic. Res. 2006, doi:10.1080/10715760500373000.
146. Granados-Principal, S.; Quiles, J.L.; Ramirez-Tortosa, C.L.; Sanchez-Rovira, P.; Ramirez-Tortosa, M.C. Hydroxytyrosol: From Laboratory Investigations to Future Clinical Trials. Nutr. Rev. 2010.
147. Margalef, M.; Pons, Z.; Iglesias-Carres, L.; Bravo, F.I.; Muguerza, B.; Arola-Arnal, A. Flavanol Plasma Bioavailability Is Affected by Metabolic Syndrome in Rats. Food Chem. 2017, doi:10.1016/j.foodchem.2017.03.141.
148. Rodríguez-López, P.; Lozano-Sanchez, J.; Borrás-Linares, I.; Emanuelli, T.; Menéndez, J.A.; Segura-Carretero, A. Structure–Biological Activity Relationships of Extra-Virgin Olive Oil Phenolic Compounds: Health Properties and Bioavailability. Antioxidants 2020.
149. D'Archivio, M.; Filesi, C.; Di Benedetto, R.; Gargiulo, R.; Giovannini, C.; Masella, R. Polyphenols, Dietary Sources and Bioavailability. Ann. Ist. Super. Sanita 2007.
150. Nicholls, G.; Flynn, H.; Woodhouse, N. Chapter 6: The Role of in Vivo Imaging in the Study of Transporter Interactions in Animals and Humans. In RSC Drug Discovery Series; 2016.
151. Cicerale, S.; Lucas, L.; Keast, R. Biological Activities of Phenolic Compounds Present in Virgin Olive Oil. Int. J. Mol. Sci. 2010.
152. D'Angelo, S.; Manna, C.; Migliardi, V.; Mazzoni, O.; Morrica, P.; Capasso, G.; Pontoni, G.; Galletti, P.; Zappia, V. Pharmacokinetics and Metabolism of Hydroxytyrosol, a Natural Antioxidant from Olive Oil. Drug Metab. Dispos. 2001.
153. Maria-José Motilva, A.S.; Rubió, L. Nutrikinetic Studies of Food Bioactive Compounds: From in Vitro to in Vivo Approaches. Int. J. Food Sci. Nutr. 2015, 66, S41–S52, doi:10.3109/09637486.2015.1025721.
154. Rutherfurd-Markwick, K.J. Food Proteins as a Source of Bioactive Peptides with Diverse Functions. Br. J. Nutr. 2012, 108, S149–S157, doi:DOI: 10.1017/S000711451200253X.
155. CHOI, J.; SABIKHI, L.; HASSAN, A.; ANAND, S. Bioactive Peptides in Dairy Products. Int. J. Dairy Technol. 2012, 65, 1–12, doi:https://doi.org/10.1111/j.1471-0307.2011.00725.x.
156. Capriotti, A.L.; Cavaliere, C.; Piovesana, S.; Samperi, R.; Laganà, A. Recent Trends in the Analysis of Bioactive Peptides in Milk and Dairy Products. Anal. Bioanal. Chem. 2016, 408, 2677–2685, doi:10.1007/s00216-016-9303-8.
157. Karr-Lilienthal, L.K.; Grieshop, C.M.; Merchen, N.R.; Mahan, D.C.; Fahey, G.C. Chemical Composition and Protein Quality Comparisons of Soybeans and Soybean Meals from Five Leading Soybean-Producing Countries. J. Agric. Food Chem. 2004, 52, 6193–6199, doi:10.1021/jf049795+.
158. Dozier, W.A.; III; Hess, J.B. Soybean Meal Quality and Analytical Techniques. In Soybean and Nutrition; El-Shemy, H., Ed.; IntechOpen: Rijeka, 2011.
159. Papageorgiou, M.; Skendi, A. 1 - Introduction to Cereal Processing and by-Products. In Sustainable Recovery and Reutilization of Cereal Processing By-Products; Galanakis, C.M., Ed.; Woodhead Publishing Series in Food Science, Technology and Nutrition; Woodhead Publishing, 2018; pp. 1–25 ISBN 978-0-08-102162-0.

160. Meshginfar, N.; Mahoonak, A.S.; Hosseinian, F.; Tsopmo, A. Physicochemical, Antioxidant, Calcium Binding, and Angiotensin Converting Enzyme Inhibitory Properties of Hydrolyzed Tomato Seed Proteins. J. Food Biochem. 2019, 43, e12721, doi:10.1111/jfbc.12721.
161. Chauhan, V.; Kanwar, S.S. Chapter 4 - Bioactive Peptides: Synthesis, Functions and Biotechnological Applications. In Biotechnological Production of Bioactive Compounds; Verma, M.L., Chandel, A.K., Eds.; Elsevier, 2020; pp. 107–137 ISBN 978-0-444-64323-0.
162. Mora, L.; Gallego, M.; Aristoy, M.-C.; Reig, M.; Toldrá, F. 12 - Bioactive Peptides. In Innovative Thermal and Non-Thermal Processing, Bioaccessibility and Bioavailability of Nutrients and Bioactive Compounds; Barba, F.J., Saraiva, J.M.A., Cravotto, G., Lorenzo, J.M., Eds.; Woodhead Publishing Series in Food Science, Technology and Nutrition; Woodhead Publishing, 2019; pp. 333–345 ISBN 978-0-12-814174-8.
163. Mandalari, G.; Rigby, N.M.; Bisignano, C.; Lo Curto, R.B.; Mulholland, F.; Su, M.; Venkatachalam, M.; Robotham, J.M.; Willison, L.N.; Lapsley, K.; et al. Effect of Food Matrix and Processing on Release of Almond Protein during Simulated Digestion. LWT - Food Sci. Technol. 2014, 59, 439–447, doi:https://doi.org/10.1016/j.lwt.2014.05.005.
164. McDonald, J.K. An Overview of Protease Specificity and Catalytic Mechanisms: Aspects Related to Nomenclature and Classification. Histochem. J. 1985, 17, 773–785, doi:10.1007/BF01003313.
165. Toldrá, F.; Reig, M.; Aristoy, M.-C.; Mora, L. Generation of Bioactive Peptides during Food Processing. Food Chem. 2018, 267, 395–404, doi:https://doi.org/10.1016/j.foodchem.2017.06.119.
166. Fernández-Tomé, S.; Hernández-Ledesma, B. Gastrointestinal Digestion of Food Proteins under the Effects of Released Bioactive Peptides on Digestive Health. Mol. Nutr. \& Food Res. 2020, 64, 2000401, doi:https://doi.org/10.1002/mnfr.202000401.
167. Sanjukta, S.; Rai, A.K. Production of Bioactive Peptides during Soybean Fermentation and Their Potential Health Benefits. Trends Food Sci. Technol. 2016, 50, 1–10, doi:https://doi.org/10.1016/j.tifs.2016.01.010.
168. Chai, K.F.; Voo, A.Y.H.; Chen, W.N. Bioactive Peptides from Food Fermentation: A Comprehensive Review of Their Sources, Bioactivities, Applications, and Future Development. Compr. Rev. Food Sci. Food Saf. 2020, 19, 3825–3885, doi:https://doi.org/10.1111/1541-4337.12651.
169. Taniguchi, M.; Aida, R.; Saito, K.; Ochiai, A.; Takesono, S.; Saitoh, E.; Tanaka, T. Identification and Characterization of Multifunctional Cationic Peptides from Traditional Japanese Fermented Soybean Natto Extracts. J. Biosci. Bioeng. 2019, 127, 472–478, doi:https://doi.org/10.1016/j.jbiosc.2018.09.016.
170. Olagunju, A.I.; Omoba, O.S.; Enujiugha, V.N.; Alashi, A.M.; Aluko, R.E. Pigeon Pea Enzymatic Protein Hydrolysates and Ultrafiltration Peptide Fractions as Potential Sources of Antioxidant Peptides: An in Vitro Study. LWT 2018, 97, 269–278, doi:https://doi.org/10.1016/j.lwt.2018.07.003.
171. Butylina, S.; Luque, S.; Nyström, M. Fractionation of Whey-Derived Peptides Using a Combination of Ultrafiltration and Nanofiltration. J. Memb. Sci. 2006, 280, 418–426, doi:https://doi.org/10.1016/j.memsci.2006.01.046.
172. Aondona, M.M.; Ikya, J.K.; Ukeyima, M.T.; Gborigo, T.J.A.; Aluko, R.E.; Girgih, A.T. In Vitro Antioxidant and Antihypertensive Properties of Sesame Seed Enzymatic Protein Hydrolysate and Ultrafiltration Peptide Fractions. J. Food Biochem. 2021, 45, e13587, doi:https://doi.org/10.1111/jfbc.13587.
173. Liu, H.; Guo, L.; Xing, J.; Li, P.; Sang, H.; Hu, X.; Du, Y.; Zhao, L.; Song, R.; Gu, H. The Protective Role of DPP4 Inhibitors in Atherosclerosis. Eur. J. Pharmacol. 2020, 875, 173037, doi:https://doi.org/10.1016/j.ejphar.2020.173037.
174. Tu, M.; Liu, H.; Cheng, S.; Mao, F.; Chen, H.; Fan, F.; Lu, W.; Du, M. Identification and Characterization of a Novel Casein Anticoagulant Peptide Derived from in Vivo Digestion. Food Funct. 2019, 10, 2552–2559, doi:10.1039/C8FO02546K.
175. Möller, N.P.; Scholz-Ahrens, K.E.; Roos, N.; Schrezenmeir, J. Bioactive Peptides and Proteins from Foods: Indication for Health Effects. Eur. J. Nutr. 2008, 47, 171–182, doi:10.1007/s00394-008-0710-2.
176. Minkiewicz, P.; Iwaniak, A.; Darewicz, M. BIOPEP-UWM Database of Bioactive Peptides: Current Opportunities. Int. J. Mol. Sci. 2019, 20, doi:10.3390/ijms20235978.
177. Rivero-Pino, F.; Espejo-Carpio, F.J.; Guadix, E.M. Production and Identification of Dipeptidyl Peptidase IV (DPP-IV) Inhibitory Peptides from Discarded Sardine Pilchardus Protein. Food Chem. 2020, 328, 127096, doi:10.1016/j.foodchem.2020.127096.

178. Nasri, R.; Nasri, M. Marine-Derived Bioactive Peptides as New Anticoagulant Agents: A Review. Curr. Protein Pept. Sci. 2013, doi:10.2174/13892037113149990042.
179. Tian, Q.; Li, S.-M.; Li, B. The Pro-Gly or Hyp-Gly Containing Peptides from Absorbates of Fish Skin Collagen Hydrolysates Inhibit Platelet Aggregation and Target P(2)Y(12) Receptor by Molecular Docking. Foods (Basel, Switzerland) 2021, 10, doi:10.3390/foods10071553.
180. Harnedy, P.A.; FitzGerald, R.J. Bioactive Peptides from Marine Processing Waste and Shellfish: A Review. J. Funct. Foods 2012.
181. Gibbs, B.F.; Zougman, A.; Masse, R.; Mulligan, C. Production and Characterization of Bioactive Peptides from Soy Hydrolysate and Soy-Fermented Food. Food Res. Int. 2004, 37, 123–131, doi:https://doi.org/10.1016/j.foodres.2003.09.010.
182. Zou, Z.; Wang, M.; Wang, Z.; Aluko, R.E.; He, R. Antihypertensive and Antioxidant Activities of Enzymatic Wheat Bran Protein Hydrolysates. J. Food Biochem. 2020, 44, e13090, doi:10.1111/jfbc.13090.
183. Shobako, N.; Ohinata, K. Anti-Hypertensive Effects of Peptides Derived from Rice Bran Protein. Nutrients 2020, 12, doi:10.3390/nu12103060.
184. Ketnawa, S.; Wickramathilaka, M.; Liceaga, A.M. Changes on Antioxidant Activity of Microwave-Treated Protein Hydrolysates after Simulated Gastrointestinal Digestion: Purification and Identification. Food Chem. 2018, 254, 36–46, doi:https://doi.org/10.1016/j.foodchem.2018.01.133.
185. Lee, S.Y.; Hur, S.J. Antihypertensive Peptides from Animal Products, Marine Organisms, and Plants. Food Chem. 2017, 228, 506–517, doi:https://doi.org/10.1016/j.foodchem.2017.02.039.
186. Ramakrishnan, V.V.; Hossain, A.; Dave, D.; Shahidi, F. Salmon Processing Discards: A Potential Source of Bioactive Peptides – a Review. Food Prod. Process. Nutr. 2024, 6, 22, doi:10.1186/s43014-023-00197-2.
187. Bartolomei, M.; Cropotova, J.; Bollati, C.; Kvangarsnes, K.; d'Adduzio, L.; Li, J.; Boschin, G.; Lammi, C. Rainbow Trout (Oncorhynchus Mykiss) as Source of Multifunctional Peptides with Antioxidant, ACE and DPP-IV Inhibitory Activities. Nutrients 2023, 15, doi:10.3390/nu15040829.
188. Gregory, K.S.; Cozier, G.E.; Schwager, S.L.U.; Sturrock, E.D.; Acharya, K.R. Structural Insights into the Inhibitory Mechanism of Angiotensin-I-Converting Enzyme by the Lactotripeptides IPP and VPP. FEBS Lett. 2023, doi:10.1002/1873-3468.14768.
189. Wu, N.; Wuhanqimuge; Shuang, Q. Screening, Characterization, and Mechanistic Evaluation of Angiotensin Converting Enzyme Inhibitory Peptides Derived from Milk Fermented with Lactobacillus Delbrueckii QS306 with and without Ultrahigh-Pressure Treatment. J. Agric. Food Chem. 2023, doi:10.1021/acs.jafc.3c03752.
190. López-Fandiño, R.; Otte, J.; van Camp, J. Physiological, Chemical and Technological Aspects of Milk-Protein-Derived Peptides with Antihypertensive and ACE-Inhibitory Activity. Int. Dairy J. 2006, 16, 1277–1293, doi:https://doi.org/10.1016/j.idairyj.2006.06.004.
191. Pihlanto-Leppälä, A. Bioactive Peptides Derived from Bovine Whey Proteins: Opioid and Ace-Inhibitory Peptides. Trends Food Sci. Technol. 2000, 11, 347–356, doi:https://doi.org/10.1016/S0924-2244(01)00003-6.
192. Adams, C.; Sawh, F.; Green-Johnson, J.M.; Jones Taggart, H.; Strap, J.L. Characterization of Casein-Derived Peptide Bioactivity: Differential Effects on Angiotensin-Converting Enzyme Inhibition and Cytokine and Nitric Oxide Production. J. Dairy Sci. 2020, 103, 5805–5815, doi:https://doi.org/10.3168/jds.2019-17976.
193. Nishibori, N.; Kishibuchi, R.; Morita, K. Soy Pulp Extract Inhibits Angiotensin I-Converting Enzyme (ACE) Activity In Vitro: Evidence for Its Potential Hypertension-Improving Action. J. Diet. Suppl. 2017, 14, 241–251, doi:10.1080/19390211.2016.1207744.
194. Pokora, M.; Zambrowicz, A.; Dąbrowska, A.; Eckert, E.; Setner, B.; Szołtysik, M.; Szewczuk, Z.; Zabłocka, A.; Polanowski, A.; Trziszka, T.; et al. An Attractive Way of Egg White Protein By-Product Use for Producing of Novel Anti-Hypertensive Peptides. Food Chem. 2014, 151, 500–505, doi:https://doi.org/10.1016/j.foodchem.2013.11.111.
195. Montone, C.M.; Zenezini Chiozzi, R.; Marchetti, N.; Cerrato, A.; Antonelli, M.; Capriotti, A.L.; Cavaliere, C.; Piovesana, S.; Laganà, A. Peptidomic Approach for the Identification of Peptides with Potential Antioxidant and Anti-Hyperthensive Effects Derived From Asparagus By-Products. Molecules 2019, 24, doi:10.3390/molecules24193627.
196. Elitsur, Y.; Luk, G.D. Beta-Casomorphin (BCM) and Human Colonic Lamina Propria Lymphocyte Proliferation. Clin. Exp. Immunol. 1991, 85, 493–497, doi:10.1111/j.1365-2249.1991.tb05755.x.
197. Cruz-Chamorro, I.; Santos-Sánchez, G.; Bollati, C.; Bartolomei, M.; Li, J.; Arnoldi, A.; Lammi, C. Hempseed (Cannabis Sativa) Peptides WVSPLAGRT and IGFLIIWV Exert Anti-Inflammatory

Activity in the LPS-Stimulated Human Hepatic Cell Line. J. Agric. Food Chem. 2022, doi:10.1021/acs.jafc.1c07520.
198. Montserrat-de la Paz, S.; Villanueva-Lazo, A.; Millan, F.; Martin-Santiago, V.; Rivero-Pino, F.; Millan-Linares, M.C. Production and Identification of Immunomodulatory Peptides in Intestine Cells Obtained from Hemp Industrial By-Products. Food Res. Int. 2023, 174, 113616, doi:10.1016/j.foodres.2023.113616.
199. Ahn, C.-B.; Cho, Y.-S.; Je, J.-Y. Purification and Anti-Inflammatory Action of Tripeptide from Salmon Pectoral Fin Byproduct Protein Hydrolysate. Food Chem. 2015, 168, 151–156, doi:https://doi.org/10.1016/j.foodchem.2014.05.112.
200. Ozogul, F.; Cagalj, M.; Šimat, V.; Ozogul, Y.; Tkaczewska, J.; Hassoun, A.; Kaddour, A.A.; Kuley, E.; Rathod, N.B.; Phadke, G.G. Recent Developments in Valorisation of Bioactive Ingredients in Discard/Seafood Processing by-Products. Trends Food Sci. Technol. 2021, 116, 559–582, doi:https://doi.org/10.1016/j.tifs.2021.08.007.
201. Wilson, J.; Hayes, M.; Carney, B. Angiotensin-I-Converting Enzyme and Prolyl Endopeptidase Inhibitory Peptides from Natural Sources with a Focus on Marine Processing by-Products. Food Chem. 2011, 129, 235–244, doi:https://doi.org/10.1016/j.foodchem.2011.04.081.
202. Damian Crowley Yvonne O'Callaghan, A.M.A.C.C.O.P.R.J.F.; O'Brien, N.M. Immunomodulatory Potential of a Brewers' Spent Grain Protein Hydrolysate Incorporated into Low-Fat Milk Following in Vitro Gastrointestinal Digestion. Int. J. Food Sci. Nutr. 2015, 66, 672–676, doi:10.3109/09637486.2015.1077788.
203. Ribeiro-Oliveira, R.; Martins, Z.E.; Sousa, J.B.; Ferreira, I.M.P.L.V.O.; Diniz, C. The Health-Promoting Potential of Peptides from Brewing by-Products: An up-to-Date Review. Trends Food Sci. Technol. 2021, 118, 143–153, doi:https://doi.org/10.1016/j.tifs.2021.09.019.
204. Mollea, C.; Marmo, L.; Bosco, F. Valorisation of Cheese Whey, a By-Product from the Dairy Industry. In Food Industry; Muzzalupo, I., Ed.; IntechOpen: Rijeka, 2013.
205. Zhong, F.; Liu, J.; Ma, J.; Shoemaker, C.F. Preparation of Hypocholesterol Peptides from Soy Protein and Their Hypocholesterolemic Effect in Mice. Food Res. Int. 2007, 40, 661–667, doi:https://doi.org/10.1016/j.foodres.2006.11.011.
206. Lammi, C.; Zanoni, C.; Scigliuolo, G.M.; D'Amato, A.; Arnoldi, A. Lupin Peptides Lower Low-Density Lipoprotein (LDL) Cholesterol through an up-Regulation of the LDL Receptor/Sterol Regulatory Element Binding Protein 2 (SREBP2) Pathway at HepG2 Cell Line. J. Agric. Food Chem. 2014, 62, 7151–7159, doi:10.1021/jf500795b.
207. Li, J.; Bollati, C.; Bartolomei, M.; Mazzolari, A.; Arnoldi, A.; Vistoli, G.; Lammi, C. Hempseed (Cannabis Sativa) Peptide H3 (IGFLIIWV) Exerts Cholesterol-Lowering Effects in Human Hepatic Cell Line. Nutrients 2022, 14, doi:10.3390/nu14091804.
208. Colombo, R.; Pellicorio, V.; Barberis, M.; Frosi, I.; Papetti, A. Recent Advances in the Valorization of Seed Wastes as Source of Bioactive Peptides with Multifunctional Properties. Trends Food Sci. Technol. 2024, 144, 104322, doi:https://doi.org/10.1016/j.tifs.2023.104322.
209. Hernández-Corroto, E.; Plaza, M.; Marina, M.L.; García, M.C. Sustainable Extraction of Proteins and Bioactive Substances from Pomegranate Peel (Punica Granatum L.) Using Pressurized Liquids and Deep Eutectic Solvents. Innov. Food Sci. Emerg. Technol. 2020, 60, 102314, doi:https://doi.org/10.1016/j.ifset.2020.102314.
210. Zanoni, C.; Aiello, G.; Arnoldi, A.; Lammi, C. Hempseed Peptides Exert Hypocholesterolemic Effects with a Statin-Like Mechanism. J. Agric. Food Chem. 2017, doi:10.1021/acs.jafc.7b02742.
211. Kumar, V.; Tiku, P.K. A Cholesterol Homeostasis by Bioactive Peptide Fraction from Pigeon Pea By-Product: An In-Vitro Study. Int. J. Pept. Res. Ther. 2021, 27, 977–985, doi:10.1007/s10989-020-10143-2.
212. Vijayan, D.K.; Perumcherry Raman, S.; Dara, P.K.; Jacob, R.M.; Mathew, S.; Rangasamy, A.; Chandragiri Nagarajarao, R. In Vivo Anti-Lipidemic and Antioxidant Potential of Collagen Peptides Obtained from Great Hammerhead Shark Skin Waste. J. Food Sci. Technol. 2022, 59, 1140–1151, doi:10.1007/s13197-021-05118-0.
213. Harnedy, P.A.; Fitzgerald, R.J. Bioactive Proteins and Peptides from Macroalgae, Fish, Shellfish and Marine Processing Waste. In Marine Proteins and Peptides; John Wiley & Sons, Ltd, 2013; pp. 5–39 ISBN 9781118375082.
214. Kumar, V.; Kurup, L. V; Tiku, P.K. The Modulatory Effect of Cholesterol Synthesis by Oryza Sativa Derived Bioactive Peptide Fractions: An In Vitro Investigation. Int. J. Pept. Res. Ther. 2021, 27, 245–251, doi:10.1007/s10989-020-10079-7.
215. Ngoh, Y.-Y.; Gan, C.-Y. Enzyme-Assisted Extraction and Identification of Antioxidative and α-Amylase Inhibitory Peptides from Pinto Beans (Phaseolus Vulgaris Cv. Pinto). Food Chem. 2016, 190, 331–337, doi:10.1016/j.foodchem.2015.05.120.

216. Nongonierma, A.B.; FitzGerald, R.J. Features of Dipeptidyl Peptidase IV (DPP-IV) Inhibitory Peptides from Dietary Proteins. J. Food Biochem. 2019, 43, e12451, doi:10.1111/jfbc.12451.
217. Nongonierma, A.B.; Mazzocchi, C.; Paolella, S.; FitzGerald, R.J. Release of Dipeptidyl Peptidase IV (DPP-IV) Inhibitory Peptides from Milk Protein Isolate (MPI) during Enzymatic Hydrolysis. Food Res. Int. 2017, doi:10.1016/j.foodres.2017.02.004.
218. Udenigwe, C.C. Towards Rice Bran Protein Utilization: In Silico Insight on the Role of Oryzacystatins in Biologically-Active Peptide Production. Food Chem. 2016, 191, 135–138, doi:https://doi.org/10.1016/j.foodchem.2015.01.043.
219. Ngo, N.T.T.; Senadheera, T.R.L.; Shahidi, F. Antioxidant Properties and Prediction of Bioactive Peptides Produced from Flixweed (Sophia, Descurainis Sophia L.) and Camelina (Camelina Sativa (L.) Crantz) Seed Meal: Integrated In Vitro and In Silico Studies. Plants (Basel, Switzerland) 2023, 12, doi:10.3390/plants12203575.
220. Lammi, C.; Bollati, C.; Ferruzza, S.; Ranaldi, G.; Sambuy, Y.; Arnoldi, A. Soybean-and Lupin-Derived Peptides Inhibit DPP-IV Activity on in Situ Human Intestinal Caco-2 Cells and Ex Vivo Human Serum. Nutrients 2018, 10, 1–11, doi:10.3390/nu10081082.
221. Jia, C.; Hussain, N.; Joy Ujiroghene, O.; Pang, X.; Zhang, S.; Lu, J.; Liu, L.; Lv, J. Generation and Characterization of Dipeptidyl Peptidase-IV Inhibitory Peptides from Trypsin-Hydrolyzed α-Lactalbumin-Rich Whey Proteins. Food Chem. 2020, 318, 126333, doi:https://doi.org/10.1016/j.foodchem.2020.126333.
222. Le Gouic, A. V; Harnedy, P.A.; FitzGerald, R.J. Bioactive Peptides from Fish Protein By-Products. In Bioactive Molecules in Food; Mérillon, J.-M., Ramawat, K.G., Eds.; Springer International Publishing: Cham, 2019; pp. 355–388 ISBN 978-3-319-78030-6.
223. Colletti, A.; Favari, E.; Grandi, E.; Cicero, A.F.G. Pharmacodynamics and Clinical Implications of the Main Bioactive Peptides: A Review. Nutraceuticals 2022, 2, 404–419, doi:10.3390/nutraceuticals2040030.
224. Jahan-Mihan, A.; Luhovyy, B.L.; El Khoury, D.; Anderson, G.H. Dietary Proteins as Determinants of Metabolic and Physiologic Functions of the Gastrointestinal Tract. Nutrients 2011, 3, 574–603, doi:10.3390/nu3050574.
225. Greenwood-Van Meerveld, B.; Johnson, A.C.; Grundy, D. Gastrointestinal Physiology and Function BT - Gastrointestinal Pharmacology. In; Greenwood-Van Meerveld, B., Ed.; Springer International Publishing: Cham, 2017; pp. 1–16 ISBN 978-3-319-56360-2.
226. Xu, Q.; Yan, X.; Zhang, Y.; Wu, J. Current Understanding of Transport and Bioavailability of Bioactive Peptides Derived from Dairy Proteins: A Review. Int. J. Food Sci. \& Technol. 2019, 54, 1930–1941, doi:https://doi.org/10.1111/ijfs.14055.
227. Vermeirssen, V.; Camp, J. Van; Verstraete, W. Bioavailability of Angiotensin I Converting Enzyme Inhibitory Peptides. Br. J. Nutr. 2004, 92, 357–366, doi:DOI: 10.1079/BJN20041189.
228. Brodin, B.; Nielsen, C.U.; Steffansen, B.; Frøkjær, S. Transport of Peptidomimetic Drugs by the Intestinal Di/Tri-Peptide Transporter, PepT1. Pharmacol. Toxicol. 2002, 90, 285–296, doi:https://doi.org/10.1034/j.1600-0773.2002.900601.x.
229. Bornhorst, G.M.; Paul Singh, R. Gastric Digestion In Vivo and In Vitro: How the Structural Aspects of Food Influence the Digestion Process. Annu. Rev. Food Sci. Technol. 2014, 5, 111–132, doi:10.1146/annurev-food-030713-092346.
230. Przybylla, R.; Mullins, C.S.; Krohn, M.; Oswald, S.; Linnebacher, M. Establishment and Characterization of Novel Human Intestinal In Vitro Models for Absorption and First-Pass Metabolism Studies. Int. J. Mol. Sci. 2022, 23, doi:10.3390/ijms23179861.
231. Walter, E.; Kissel, T. Heterogeneity in the Human Intestinal Cell Line Caco-2 Leads to Differences in Transepithelial Transport. Eur. J. Pharm. Sci. 1995, 3, 215–230, doi:https://doi.org/10.1016/0928-0987(95)00010-B.
232. Artursson, P. Cell Cultures as Models for Drug Absorption across the Intestinal Mucosa. Crit. Rev. Ther. Drug Carrier Syst. 1991, 8, 305–330.
233. Ungell, A.-L.; Artursson, P. An Overview of Caco-2 and Alternatives for Prediction of Intestinal Drug Transport and Absorption. In Drug Bioavailability; John Wiley & Sons, Ltd, 2008; pp. 133–159 ISBN 9783527623860.
234. Vieira, E.F.; das Neves, J.; Ferreira, I.M.P.L.V.O. Bioactive Protein Hydrolysate Obtained from Canned Sardine and Brewing By-Products: Impact of Gastrointestinal Digestion and Transepithelial Absorption. Waste and Biomass Valorization 2021, 12, 1281–1292, doi:10.1007/s12649-020-01113-2.
235. Vásquez, P.; Zapata, J.E.; Chamorro, V.C.; García Fillería, S.F.; Tironi, V.A. Antioxidant and Angiotensin I-Converting Enzyme (ACE) Inhibitory Peptides of Rainbow Trout (Oncorhynchus

Mykiss) Viscera Hydrolysates Subjected to Simulated Gastrointestinal Digestion and Intestinal Absorption. LWT 2022, 154, 112834, doi:https://doi.org/10.1016/j.lwt.2021.112834.
236. Wang, K.; Han, L.; Tan, Y.; Hong, H.; Luo, Y. Generation of Novel Antioxidant Peptides from Silver Carp Muscle Hydrolysate: Gastrointestinal Digestion Stability and Transepithelial Absorption Property. Food Chem. 2023, 403, 134136, doi:https://doi.org/10.1016/j.foodchem.2022.134136.
237. Taroncher, M.; Rodríguez-Carrasco, Y.; Aspevik, T.; Kousoulaki, K.; Barba, F.J.; Ruiz, M.-J. Cytoprotective Effects of Fish Protein Hydrolysates against H2O2-Induced Oxidative Stress and Mycotoxins in Caco-2/TC7 Cells. Antioxidants 2021, 10, doi:10.3390/antiox10060975.
238. Gallego, M.; Grootaert, C.; Mora, L.; Aristoy, M.C.; Van Camp, J.; Toldrá, F. Transepithelial Transport of Dry-Cured Ham Peptides with ACE Inhibitory Activity through a Caco-2 Cell Monolayer. J. Funct. Foods 2016, 21, 388–395, doi:https://doi.org/10.1016/j.jff.2015.11.046.
239. Feng, M.; Betti, M. Transepithelial Transport Efficiency of Bovine Collagen Hydrolysates in a Human Caco-2 Cell Line Model. Food Chem. 2017, 224, 242–250, doi:https://doi.org/10.1016/j.foodchem.2016.12.044.
240. Xing, L.; Li, G.; Toldrá, F.; Zhang, W. Chapter Four - The Physiological Activity of Bioactive Peptides Obtained from Meat and Meat by-Products. In; Toldrá, F., Ed.; Advances in Food and Nutrition Research; Academic Press, 2021; Vol. 97, pp. 147–185.
241. Ding, L.; Wang, L.; Zhang, T.; Yu, Z.; Liu, J. Hydrolysis and Transepithelial Transport of Two Corn Gluten Derived Bioactive Peptides in Human Caco-2 Cell Monolayers. Food Res. Int. 2018, 106, 475–480, doi:https://doi.org/10.1016/j.foodres.2017.12.080.
242. Vieira, E.F.; das Neves, J.; Vitorino, R.; Dias da Silva, D.; Carmo, H.; Ferreira, I.M.P.L.V.O. Impact of in Vitro Gastrointestinal Digestion and Transepithelial Transport on Antioxidant and ACE-Inhibitory Activities of Brewer's Spent Yeast Autolysate. J. Agric. Food Chem. 2016, 64, 7335–7341, doi:10.1021/acs.jafc.6b02719.
243. Monente, C.; Ludwig, I.A.; Stalmach, A.; de Peña, M.P.; Cid, C.; Crozier, A. In Vitro Studies on the Stability in the Proximal Gastrointestinal Tract and Bioaccessibility in Caco-2 Cells of Chlorogenic Acids from Spent Coffee Grounds. Int. J. Food Sci. Nutr. 2015, 66, 657–664, doi:10.3109/09637486.2015.1064874.
244. Ribeiro-Oliveira, R.; Martins, Z.E.; Faria, M.Â.; Sousa, J.B.; Ferreira, I.M.P.L.V.O.; Diniz, C. Protein Hydrolysates from Brewing By-Products as Natural Alternatives to ACE-Inhibitory Drugs for Hypertension Management. Life 2022, 12, doi:10.3390/life12101554.
245. Nunes, A.R.; Gonçalves, A.C.; Alves, G.; Falcão, A.; Garcia-Viguera, C.; A. Moreno, D.; Silva, L.R. Valorisation of Prunus Avium L. By-Products: Phenolic Composition and Effect on Caco-2 Cells Viability. Foods 2021, 10, doi:10.3390/foods10061185.
246. Cai, L.; Wu, S.; Jia, C.; Cui, C. Hydrolysates of Hemp (Cannabis Sativa L.) Seed Meal: Characterization and Their Inhibitory Effect on α-Glucosidase Activity and Glucose Transport in Caco-2 Cells. Ind. Crops Prod. 2023, 205, 117559, doi:https://doi.org/10.1016/j.indcrop.2023.117559.